Journal of the OPTICAL SOCIETY *of* AMERICA

VOLUME 38
No. 12

DECEMBER
1948

Xerography: A New Principle of Photography and Graphic Reproduction . . . . . R. M. SCHAFFERT AND C. D. OUGHTON 991

Theory of Electron Retrapping in Phosphors . . . . . ROBERT C. HERMAN, CHARLES F. MEYER, AND HELEN S. HOPFIELD 999

Optical Properties of Zinc Fluoride Phosphors . . GORTON R. FONDA AND FRANK J. STUDER 1007

Theory of the Corner-Cube Interferometer . . . . . EDSON R. PECK 1015

Effect of Chromatic Adaptation on Achromaticity . HARRY HELSON AND WALTER C. MICHELS 1025

Design of Triplet Anastigmat Lenses of the Taylor Type . . . . . ROBERT E. STEPHENS 1032

Photographic Sharpness and Resolving Power. I. The Design and Performance of an Apochromatic Resolving-Power Camera Objective . FRED H. PERRIN AND H. ORLO HOADLEY 1040

Mechanism of Latent Image Formation in a Photographic Emulsion by Mechanical Pressure . . . . . K. B. MATHER 1054

Applications of the Photographic Pressure Effect . . . . . K. B. MATHER 1065

Errata: New Contributions to the Optics of Intensely Light-Scattering Materials. Part I . . . . . PAUL KUBELKA 1067

Fabrication of Boric Acid Glass for Luminescence Studies . . . . . M. KASHA 1068

Optical Determination of Thin Films on Reflecting Bases in Transparent Environments . . . . . A. B. WINTERBOTTOM 1074

Photometer for Measurement of Sky Brightness near the Sun . . . . . JOHN W. EVANS 1083

Fourth Annual Analytical Symposium and Exposition of New Analytical Tools 1085

Infra-Red Chopped-Radiation Analyzer . . . . . GILBERT KIVENSON, RALPH T. STEINBACK, AND MYRTLE RIDER 1086

Proceedings of the Thirty-Third Annual Meeting of the Optical Society of America 1092

Minutes of the Thirty-Second Meeting of the Board of Directors of the Optical Society of America, Incorporated 1107

Author Index to Volume 38 1108

Analytic Subject Index to Volume 38 1114

Volume Table of Contents III

Published monthly
at Prince and Lemon Sts., Lancaster, Pa.
by the
AMERICAN INSTITUTE OF PHYSICS
Incorporated
57 East 55 Street, New York 22, New York
FOR AND UNDER THE EDITORIAL SUPERVISION OF THE
OPTICAL SOCIETY OF AMERICA

THE OPTICAL SOCIETY OF AMERICA

Officers of the Society

RUDOLF KINGSLAKE, *President*
Eastman Kodak Company
Rochester, New York

WILLIAM F. MEGGERS, *Vice President*
National Bureau of Standards
Washington 25, D. C.

ARTHUR C. HARDY, *Secretary*
Massachusetts Institute of Technology
Cambridge 39, Massachusetts

W. W. GRAEPER, *Treasurer*
Bausch & Lomb Optical Company
Rochester 2, New York

The Board of Directors consists of the above officers; the Editor of the Journal; the Past President; and five directors-at-large.

G. R. HARRISON, *Editor and Past President*
Massachusetts Institute of Technology
Cambridge 39, Massachusetts

Directors-at-Large

FRANK BENFORD
General Electric Company
Schenectady, New York

F. M. BISHOP
Eastman Kodak Company
Rochester 4, New York

WALLACE R. BRODE
Ohio State University
Columbus 10, Ohio

A. H. BENNETT
American Optical Company
Buffalo 11, New York

E. H. LAND
Polaroid Corporation
Cambridge, Massachusetts

Local Sections

STANLEY S. BALLARD, *Secretary for the Local Sections*, Tufts College, Medford 55, Massachusetts

Rochester Section

JOHN H. MCLEOD, *President*
HARRY D. POLSTER, *Vice President*
JAMES R. BENFORD, *Secretary*
LUVILLE T. STEADMAN, *Treasurer*

Detroit Section

DAVID L. FRY, *Chairman*
KARL W. BEYER, *Vice Chairman*
DANIEL L. HARMON, *Secretary*
W. R. O'NEILL, *Treasurer*

Niagara Frontier Section

GALEN PORTER, *President*
LELAND E. HAVENS, *Secretary*
CLAIR M. BIRDSALL, *Treasurer*

Ohio Valley Section

M. E. MERCHANT, *Chairman*
J. F. WOODRUFF, *Chairman-elect*
C. S. MILLS, *Secretary-Treasurer*

Patrons

AMERICAN OPTICAL COMPANY — BAUSCH & LOMB OPTICAL COMPANY
EASTMAN KODAK COMPANY

Corporation Members

ALLIED CHEMICAL AND DYE CORPORATION, NATIONAL ANILINE DIVISION, Buffalo, New York
AMERICAN CYSTOSCOPE MAKERS, INC., New York, New York
AMERICAN OPTICAL COMPANY, Southbridge, Massachusetts
ARGUS, INCORPORATED, Ann Arbor, Michigan
BAUSCH & LOMB OPTICAL COMPANY, Rochester, New York
BELL & HOWELL COMPANY, Chicago, Illinois
BELL TELEPHONE LABORATORIES, INC., New York, New York
CENTURY LIGHTING, INC., New York, New York
CORNING GLASS WORKS, Corning, New York
R. R. DONNELLEY & SONS COMPANY, Chicago, Illinois
E. I. DUPONT DE NEMOURS & COMPANY, INC., Chemical Department, Experimental Station, Wilmington, Delaware
EASTMAN KODAK COMPANY, Rochester, New York
EDMUND SALVAGE COMPANY, Oaklyn-Audubon, New Jersey
FAIRCHILD AVIATION CORPORATION, Jamaica, New York
FARRAND OPTICAL COMPANY, INC., New York, New York
FISH-SCHURMAN CORPORATION, New York, New York
GAERTNER SCIENTIFIC CORPORATION, Chicago, Illinois
GENERAL ELECTRIC COMPANY, Schnectady, New York
W. & L. E. GURLEY, Troy, New York
INTERCHEMICAL CORPORATION, New York, New York
KEUFFEL & ESSER COMPANY, Hoboken, New Jersey
KOLLSMAN INSTRUMENT DIVISION OF SQUARE D COMPANY, Elmhurst, New York
NATIONAL CARBON COMPANY, Cleveland, Ohio
NATIONAL TECHNICAL LABORATORIES, South Pasadena, California
PERKIN-ELMER CORPORATION, Glenbrook, Connecticut
POLAROID CORPORATION, Cambridge, Massachusetts
PORTMAN MACHINE TOOL COMPANY, New Rochelle, New York
SIMPSON OPTICAL MANUFACTURING COMPANY, Chicago, Illinois
SOCONY-VACUUM LABORATORIES, Paulsboro, New Jersey
ARTHUR H. THOMAS COMPANY, Philadelphia, Pennsylvania
UNIVIS LENS COMPANY, Dayton, Ohio
ZENITH OPTICAL COMPANY, Huntington, West Virginia

THE OPTICAL SOCIETY OF AMERICA was organized in 1916 "*to increase and diffuse the knowledge of optics in all its branches, pure and applied, to promote the mutual interests of investigators of optical problems, of designers, manufacturers and users of optical instruments and apparatus of all kinds and to encourage cooperation among them.*" It aims to serve the interests of all who are engaged in any branch of optics from fundamental research to the manufacture of optical goods.

MEMBERSHIP

Regular Members: "Any person who has contributed materially to the advancement of optics is eligible for regular membership."

Associate Members: "Any person who is interested in optics is eligible for associate membership."

Corporate Members: "Any corporation desirous of encouraging the work of the Society is eligible for corporation membership."

Patrons: The payment, within any one year, of $1000 or more toward the expenses of the Society by any corporation or individual entitles such corporation or individual to the rank of patron.

The Society cordially invites to membership all who are interested in any branch of optics, either in research, in instruction, in optical or illuminating engineering, in the manufacture and distribution of optical goods of all kinds, or in physiological and medical optics.

ANNUAL DUES

Regular members, $8.50; Associate members, $6.00; Corporate members, $50.00. These dues include subscription to the Society's official journal, the *Journal of the Optical Society of America.*

CHANGES OF ADDRESS

All changes of address of members of the Optical Society of America should be communicated to the Secretary, Professor Arthur C. Hardy, Massachusetts Institute of Technology, Cambridge 39, Massachusetts.

Journal of the
OPTICAL SOCIETY
of AMERICA

VOLUME 38, NUMBER 12 DECEMBER, 1948

Xerography: A New Principle of Photography and Graphic Reproduction

R. M. SCHAFFERT AND C. D. OUGHTON
Battelle Memorial Institute, Columbus, Ohio

(Received August 20, 1948)

A new process of graphic reproduction and photography has been developed. The basic process, known as xerography, is dry, direct positive-to-positive, rapid, and has a number of potential applications in graphic arts and related fields. As a photographic process, xerography employs a re-usable plate consisting of a thin layer of a photo-conductive material on an electrically conductive base. The plate is sensitized by electrostatic charging immediately before use. After exposure, the image is developed by dusting the plate with a micronized powder. Prints are made by transferring and fixing the powder image to paper or other materials. The plate can be used many times to produce additional images. Xerography also provides a unique and simplified process of graphic reproduction, particularly in printing and duplicating.

INTRODUCTION

THE object of this paper is to introduce the subject of xerography and to present a general explanation of the basic principles and techniques involved in the process.

Xerography was originated by Chester F. Carlson[1] in 1938, and first publicized by Nicholas Langer[2] in 1944. Since 1944, the process has been a subject of research and development in the Graphic Arts Research Laboratories of Battelle Memorial Institute, Columbus, Ohio, under projects sponsored initially by Battelle, and since January 1, 1947, by Battelle and the Haloid Company of Rochester, New York.

Xerography has a number of characteristics which distinguish it as being an entirely new process. The process is completely dry. No chemical reactions are involved. It is a direct positive-to-positive operation. The plates or films are not destroyed by exposure and may be re-used many times. The process is economical and versatile; prints may be prepared on almost any type of paper or on any other material having a reasonably smooth surface. Finished, permanent prints may be completed in a matter of seconds.

PHOTOGRAPHIC ASPECTS OF XEROGRAPHY

Description of Process

The application of xerography to photography involves the formation of an electrostatic latent image on a layer of photo-conductive insulating material and the development of the image with a finely divided powder, which adheres to the electrically charged areas of the plate. The plate is sensitized by applying an electrostatic charge to the surface of the photo-conductive coating. The sensitized plate is then exposed to the light image which it is desired to reproduce. Impinge-

[1] U. S. Patents No. 2,297,691 and No. 2,357,809.
[2] Nicholas Langer, "Electrophotography," Radio News, Eng. Dept. **32**, 22 (1944).

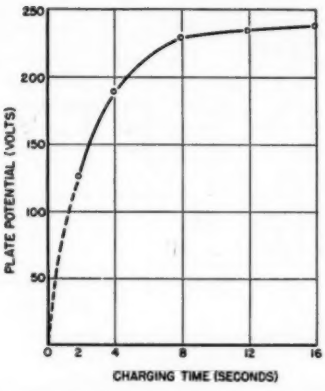

FIG. 1. Plate potential as a function of charging time.

ment of light on the photo-conductive coating causes electrical charges to leak away or to be reduced in quantity in proportion to the amount of light falling on the particular area, thus leaving an electrostatic latent image. The image is developed by dusting the plate with a finely divided powder which adheres only to the electrically charged areas in proportion to the amount of charge remaining on the plate after exposure to light. Prints are made by transferring and fixing the powder image to paper.

The photosensitive plate consists of a photo-conductive coating on a conductive supporting medium, such as metal. The developer consists of a finely divided powder, mixed with a coarser powder. The coarser powder serves to generate an electrostatic charge on the fine powder. The charged powder is then used to develop a latent electrostatic image on the photo-conductive coating.

The process involves photo-conductivity and electrostatics. Photoconductivity has received considerable attention from both physicists and chemists. Images have been formed inside of crystals as discolorations directly associated with photoconductivity,[3] and an image has been observed by Selenyi[4] on selenium-coated plates as a result of exposure to light. Also, pictures have been produced by electrolytic reaction on the surface of a photoelectrically sensitive layer.[5]

[3] A. L. Hughes, "Photo-conductivity in crystals," Rev. Mod. Phys. **8**, 312 (1936).

[4] P. Selenyi, "Photography on selenium," Nature **161**, 522 (1948).

[5] Goldman, German Patent No. 674999.

Various electrical and electrolytic photo-processes have been reviewed by Yates.[6] Selenyi[7,8] reported a process of forming an electrostatic image on insulating plates by various methods of scanning and of developing that image by dusting it with a finely divided powder. Various observations have been published concerning the generation of an electrical charge on powder particles from frictional or tribo effects.[9–11] The reaction of the powder particles in electrical fields is well known and is the basis of processes for the removal of dust particles from the air for electrostatic separation of powders[12] and for the deposition of powders in a pattern form.[13]

Carlson[14] introduced the method of forming an electrostatic image on a photo-conducting material and developing the latent electrostatic image with a finely divided powder.

Five steps are involved in making a photographic print by xerography: (1) Sensitizing the plate with an electrostatic charge, (2) exposing the plate to form an electrostatic image, (3) developing the latent image with fine powder, (4) transferring the powder image to paper or other materials, and (5) fixing the image by fusing the powder. The plate can then be cleaned, after which it can be used again for taking additional photographs.

Preparation of the Plates

Xerographic plates for use in photography are prepared by depositing a smooth layer of a photo-conductive material on a supporting medium. Evaporation is a suitable method for preparing such layers. The supporting medium is suspended in a bell jar, the air evacuated, and the photo-conductive material evaporated by conventional methods. Photo-conductive coat-

[6] R. F. Yates, "Photo-electrography—tomorrow's miracle," Radio-Craft, p. 334 (March, 1943).

[7] P. Selenyi, "On the electrographic recording of fast electrical phenomena," J. App. Phys. **9**, 637 (1938).

[8] P. Seleyni, "Methoden, Ergebnisse und Aussichten des elektrostatischen Aufzeichungsverfahrens (Elektrographie)," Zeits. f. tech. Physik **16**, 607 (1935).

[9] Leonard B. Loeb, "The basic mechanisms of static electrification," Science **102**, 573 (1945).

[10] H. F. Richards, "The contact electricity of solid dielectrics," Phys. Rev. **22**, 122 (1923).

[11] F. E. Shaw, "Experiments in tribo-electricity," Proc. Roy. Soc., **A94**, 16 (1917).

[12] F. Fraas and O. C. Ralston, "Electrostatic separation of solids," Ind. Eng. Chem. **32**, 600 (1940).

[13] U. S. Patents Nos. 2,097,233 and 2,152,077.

[14] U. S. Patents No. 2,297,691 and No. 2,357,809.

ings of materials such as anthracene, sulphur, and selenium have been prepared by this technique.

Studies of the electrical properties of the photo-conductive layers indicate that they must have specific dark resistances of approximately 10^{15} ohm-centimeters to retain electrical charges on their surfaces. When the photo-conductive materials are illuminated, this specific resistance must be reduced to something like 10^{10} or 10^{12} ohm-centimeters to account for observed exposure times. Photo-conductivity is not an effect which lends itself to expression in terms of ohmic resistances so that the above values are to be used only in expressing qualitatively the characteristics involved.

Numerous materials have been used successfully as the supporting media for the photo-conductive coatings. To serve as a conductive backing for the plates, it is only necessary for a material to have a specific electrical resistance below the equivalent resistance of the illuminated photo-conductive layer. Thus, materials having specific resistances of approximately 10^{10} ohm-centimeters can serve as backing materials. Such materials might ordinarily be considered to be electrical insulators. Plates functioned satisfactorily when the photo-conductive material was deposited on various types of paper, glass, and plastics having electrical resistances below that of the photo-conductive material.

Sensitization of the Plates

Before the plate can be used, it must be sensitized by depositing an electrostatic charge on the photo-conductive surface. Plates were originally sensitized by rubbing with materials such as fur and cloth. When a swab of fur is brushed across the surface of the plate, an electrostatic charge is generated on the surface. A more convenient method of sensitizing the plate, and one which gives higher plate potentials, is the application of a corona discharge from a row of needles or from fine wires. The plate is passed under the wires in the field of the corona discharge. Reversing the polarity of the voltage applied to the wires reverses the sign of the electrical charge on the plate. Electrical potentials from 4000 to 7000 volts are ordinarily used to produce the corona discharge with one to three 0,004-inch

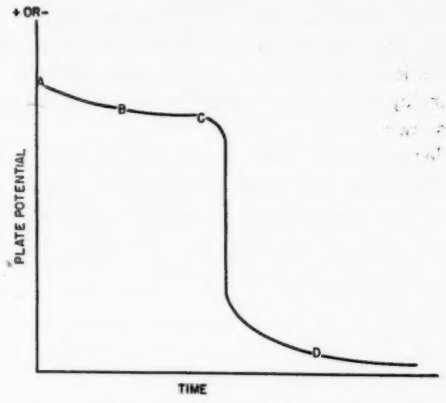

FIG. 2. Graph showing decay of plate potential under varying conditions of illumination.

wires suspended approximately one centimeter above the photo-conductive surface of the plate. Half-wave, rectified, unfiltered power sources are convenient, but electrostatic generators can be used.

The magnitude of the electrical charge on the plate resulting from the sensitization is measured by the potential to which the surface of the plate is raised. In the laboratory this potential is measured by an electrometer of the Lindemann type. The plate is brought to a definite position in relation to a probe connected to the electrometer, and the deflection of the electrometer is read and interpreted in terms of a calibration made with an electrically conducting plate in the same position. The maximum quantity of

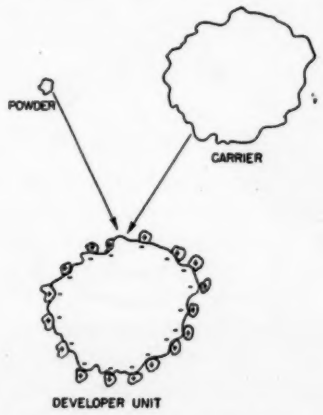

FIG. 3. Schematic diagram of xerophotographic developer unit,

charge, which a plate will acquire during the sensitizing operation, is dependent on several variables. One of these variables is the time of charging of the plate under the corona discharge, as shown in Fig. 1.

Because of the light-sensitivity characteristics of the plate, the sensitizing operation must be performed in the dark or under a suitable safe light. After one use, the plate can be resensitized and used over again. The primary limitation on the use-life of a plate appears to be the mechanical abrasion to which the plate might be subjected. If handled carefully, the plate may be re-used many times. Some plates in the laboratory have been used over 500 times and still yield satisfactory reproductions.

Exposure of the Plates

The sensitized plate may be exposed by any of the conventional techniques. The plate may be mounted in a standard plate holder and exposed in a camera; images may be projected onto the plate by an enlarger; or the plate may be exposed by passing light through copy held in close contact with the plate. In the area where light strikes the plate, the photo-conductive coating acts as a conductor for the electrostatic charge and disperses the charge into the supporting medium, leaving a latent electrostatic image on the plate surface. The light transmission of most papers is sufficient to permit the reproduction by contact exposure of such items as typed letter, drawings, ink or pencil memoranda, and printed matter.

A summary of what has happened to the plate during the sensitizing and exposing operations is shown in Fig. 2. The plate was sensitized to an initial potential (*A*). Laboratory measurements show that a slow decay of the charge takes place in the dark. This is indicated by section (*B*) on

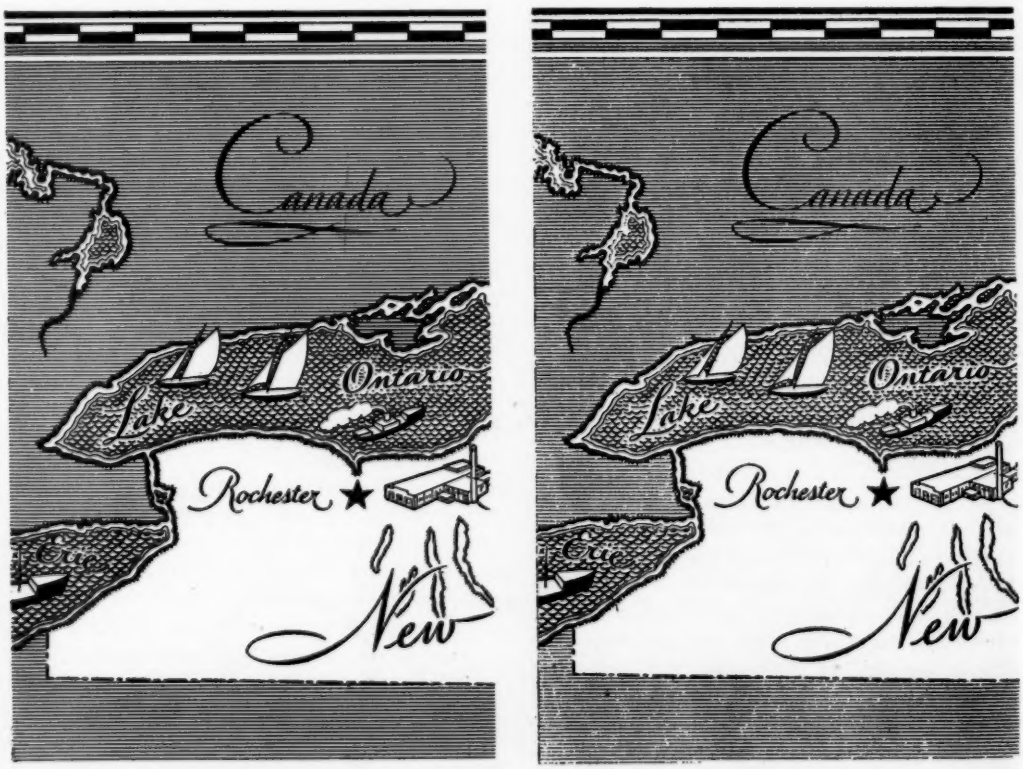

Original Xerographic copy

FIG. 4.

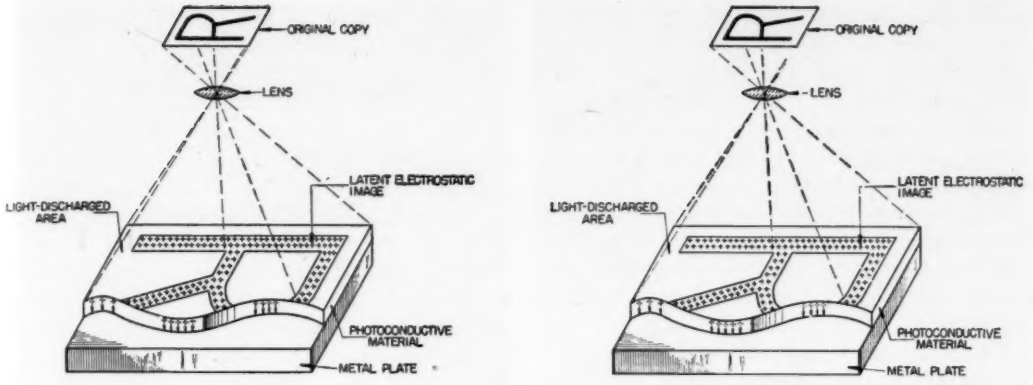

FIG. 5.

the curve. At (*C*) the plate is exposed to the light image. The potential of the areas of the plate exposed to light drops to a low value as the charge is conducted from the plate in those areas. The potential appears to decrease in proportion to the intensity of the light striking the photo-conductive surface though the relationship is not exactly a linear one. At point (*D*) the decay of potential ceases, leaving a minimum charge on the plate. Thus, the latent electrostatic image may have a potential which varies from near zero to a maximum over different parts of the plate. Indications are that tone gradations can be reproduced and that the process has fair photoregressive properties. The latent electrostatic image can be retained on the plate for several days without losing the image quality.

Image Development

The developer, used to develop the latent electrostatic image on the plate, is a mixture of a micronized resinous powder and a relatively large particle size granular carrier (Fig. 3). The micronized resin particles, which are used to develop the image, are referred to as the powder, the larger granular particles as the carrier. The sizes of powder particles now used are from 0.1 to 20 microns for the powder and approximately 300 microns for the carrier. These sizes may be varied over wide ranges. In the developing operation, the granular particles of carrier serve to generate an electrostatic charge on the powder particles, thus causing the finer powder particles to cling to the coarser carrier particles. As a result of this mutual electrical attraction between the two powders, the carrier is able to sweep the finer developer powder across the plate surface. The electrification of the two materials is caused by triboelectricity. Formulation of the proper developer for use on a plate is determined by the relationship of various materials in the triboelectric series. An illustrative and abbreviated series is as follows:

Corn meal—positive end of series
Cork
Calcium carbonate
Pigmented lycopodium
Rosin
Sand
Cupric sulphide
Tartaric acid—negative end of series

A triboelectric series consists of a list of materials arranged in such a way that each material will acquire a positive electrical charge when contacted or rubbed against any material below it in the list. In general, the magnitude of the electrical charge generated on each of two materials on contact will depend on the relative positions of the two materials in the series. If the materials are close together in the series, the magnitude of the charge will be small; if the materials are far apart in the series, the magnitude

of the charge will be large. Thus, by combining the proper materials, one in the form of a micronized resin powder and the other in the form of a granular carrier, it is possible to control the magnitude and the sign of the electrostatic charge generated on the powder. Two developers suitable for reproducing high contrast line copy are: (1) micronized tartaric acid powder and corn meal carrier, and (2) pigmented lycopodium and sand carrier. The former is for positively charged images, the latter for negatively charged images.

The image on the plate is developed by flowing the powder over the surface of the plate. In the laboratory, the plate bearing the latent image is placed in a tray and developer cascaded back and forth over the surface of the plate by tilting the tray.

Transfer of Image

The resulting powder image on the plate must be transferred to some other material to form a permanent record. To transfer the powder to some medium such as paper, the sheet of paper is placed in contact with the powder image on the plate and the paper is charged with an electrostatic charge of opposite sign to the charge on the powder. The powder is attracted from the plate to the paper and adheres to the paper when it is removed from the plate. The transfer operation can be accomplished with the same equipment used in the plate sensitizing operation. With this technique the powder image may be transferred to almost any type of material (wood, plastic, metal, cloth, paper, glass, etc.).

Fixing the Image

The powder image may be made permanent on the paper (or other media) by exposing the powder to heat. The micronized powder is usually a low fusing-temperature resin. When the medium bearing the powder image is placed between heated platens, the resin is quickly fused to form a permanent image. Powder images have been transferred and fixed to over 70 different types of paper in the laboratory. With a few exceptions, all produced equally satisfactory results. Illustrations of the original and the finished xerographic copy are shown in Figures 4, 5, and 6. Figures 1, 2, and 3 are reproductions of xerographic prints.

Cleaning the Plate for Re-Use

The residual powder remaining after the transfer operation must be removed before the plate can be re-used. Rubbing techniques cannot be employed because of the resulting abrasion. The plate is cleaned by placing the plate in a tilting tray and cascading a coarse granular powder, such as sodium chloride, across the plate surface. This operation removes the remaining micronized powder particles. The same results may be obtained by dipping the plate vertically into a box of the material.

Resolving Power

Present plates and powders have a resolving power of between 7.5 and 10 lines per millimeter. Because the latent image on the plate is of an electrostatic nature, it is believed that the resolving power of the process will be limited only by the size of the powder particles used to develop the image.

Photo-Regression

Experiments to determine the photo-regression on various photo-conductive surfaces have indicated that some photo-conductors will retain the latent electrostatic image before developing for a period of 100 hours without appreciable loss of contrast in the image and for 240 hours without loss of resolution.

Spectral Sensitivity and Photographic Speed

The spectral sensitivity of the plates, using selenium as the photoconductor, is approximately equivalent to orthochromatic film. The speed of such a coating is about 0.3 ASA (Tungsten).

Multiple-Copy Reproduction by Xerography

The cycle of operations for obtaining a photographic print by xerography can be repeated over and over again to obtain as many copies of a particular design or subject as might be desired. Since the process is positive-to-positive, any printed sheet drawing in which the printing or writing is on one side of the paper, could be used as a positive for contact exposure with a

Original

Paramount Pictures, Inc.
Xerographic copy

FIG. 6.

xerographic plate. If the subject matter to be reproduced is printed on both sides, such as literature or pages from books, the subject can be photographed by the xerographic procedure, using a camera. However, after the first copy has been prepared additional copies can be produced by contact methods.

Where a large number of copies of the same subject material is desired, the developed powder image can be fixed onto the plate, either by spraying with a solvent or by fusing the resinous powder with heat. Multiple copies can then be made by simply subjecting the plate under light to the electrostatic discharge which places a charge on the fused image, dusting with powder, and then transferring to paper. This cycle can be repeated indefinitely for as many copies as might be required, since the plate with the fixed image can be used as the master plate. When the plate is to be used again for another subject or design, the resin image can be washed off with a solvent. Thus, in this process of making multiple copies the exposure step is eliminated except in the initial preparation of the master plate.

Another application of xerography to multiple-copy production involves the use of a plate which consists of an insulating image layer on a conductive surface. Such a plate can be prepared by a number of different methods. For instance, the design or image can be drawn or painted on the surface of a metal sheet with an insulating lacquer. However, a more practical way of producing an insulating image on such a plate is to use the established photomechanical methods used in preparing lithographic printing plates and photoengravings, in which a bichromated colloid is used as a sensitive coating on the plate. After exposure in contact with a negative or positive of the subject, the plate is treated by washing or developing to provide a sharp resist image on a metal surface. Such a plate might be

termed a dry planographic printing plate. The steps of obtaining printed copies of such a plate are simply to charge the image, dust with powder, and transfer to paper. This is the basis of a new method of printing. The method is unique in as much as it does not require pressure or liquid inks. The ink is replaced by dry powder and instead of mechanical pressure the impression is obtained by electrical transfer. This technique has been incorporated into a laboratory printing machine in which the printing plate is mounted on a rotating cylinder. The dusting and transfer operations are accomplished at convenient intervals around the cylinder. With this equipment, it has been possible to print at speeds up to 1200 linear feet per minute, the paper being fed to the cylinder from a roll.

CONCLUSIONS

Xerography constitutes a new and different approach to the recording of light images and the printing of multiple copies of original designs. The process has proven to be applicable to photo-copying—having the distinct advantages of rapid and dry processing. Continuous-tone subjects, and even live subjects, have been xerophotographed with fair results. Color prints have been made from transparencies by using filters and complementary colors in developing powders. The process shows promise of being applicable to the general field of color reproduction. Since images can be transferred to numerous materials, the process should have application in the field of surface decoration.

Potential applications to the fields of duplicating and printing are indicated, and applications to the photographic and photomechanical[15] branches of the graphic arts industry are possibilities.

ACKNOWLEDGMENTS

The authors wish to acknowledge the cooperation and support of the Haloid Company, Rochester, New York. Its permission to include results of research on its project is greatly appreciated and the guidance and counsel of Dr. John Dessauer, Haloid's Vice President in charge of Research and Product Development, have been particularly helpful.

Numerous members of the research staff of Battelle Memorial Institute have contributed to studies on xerography. Particular acknowledgment is due P. G. Andrus, W. E. Bixby, J. M. Chapman, H. E. Copley, R. L. Deubner, J. P. Ebert, D. L. Fauser, R. B. Landrigan, J. J. Rheinfrank, and L. E. Walkup.

The Army Signal Corps is sponsoring in part continued research on the process.

[15] R. M. Schaffert, "Plate making without film," Share Your Knowledge Review (Technical Digest) p. 33, Vol. **XXIX**, No. 5 (February, 1948).

Theory of Electron Retrapping in Phosphors*, **

ROBERT C. HERMAN, CHARLES F. MEYER, AND HELEN S. HOPFIELD
Applied Physics Laboratory, The Johns Hopkins University, Silver Spring, Maryland

(Received May 26, 1948)

The set of non-linear differential equations that generally have been employed to describe the electron transfer processes in infra-red phosphors has been solved by means of a differential analyzer in the general case, and approximate solutions have been obtained for cases of practical interest. It is shown that the simultaneous measurement of the brightness and instantaneous photo-current in a phosphor stimulated by infra-red light allows a determination to be made of the ratio of the cross sections for electron capture into empty trapping centers and into empty luminescent centers. This cross-section ratio can also be determined from measurements of the light sum and the maximum instantaneous photo-current.

I. INTRODUCTION

THE thermoluminescence of phosphors, as well as the brightness and conductivity of phosphors under infra-red stimulation, recently have been the subject of extensive investigations. The purpose of the present paper is to extend the theoretical aspects of this subject discussed by the authors some time ago.[1] While the phenomenon of thermoluminescence is of considerable interest, the present discussion is confined to the behavior of phorphors stimulated with infra-red light.[2]

It is now generally accepted that a phosphor is an insulating crystal which can be made luminescent by the addition of a small concentration of impurity or activator atoms. The infra-red sensitive phosphors, developed during the past few years by Urbach, Fonda, Ward, and others, exhibit a large increase in brightness when irradiated with infra-red light. This effect can be produced long after normal phosphorescence has decayed and is undoubtedly similar to the well-known storage of light at low temperatures which can be recovered by warming. Many of the properties of phosphors can be explained, at least qualitatively, by simple models based on the energy-band theory of solids.[3] On the basis of such concepts, Ellickson and Parker[4] have discussed the theory of the decay in brightness of infra-red sensitive phosphors, with special emphasis on the role of light absorption effects. From the experimental point of view brightness studies in phosphors are both simpler and of more practical importance than studies of photoconductivity which is associated with the brightness in certain types of phosphors. Nevertheless, a number of experiments have been performed on the conductivity of phosphors. Gisolf[5] performed a series of qualitative experiments with ZnS phosphors which showed that electrons in trapping states are raised to the conduction band by the absorption of infra-red light. A quantitative study by Reimann[6] showed that the resistance of a ZnS phosphor containing trapped electrons increases linearly with time when the phosphor is irradiated with infra-red light. A conduction current also has been observed in phosphors during thermoluminescence by Herman and Hofstadter[7] and Garlick.[8] Measurements of photo-conductivity in infra-red phosphors have been carried out more recently by Fine[9] and by Parker and Dropkin.[10]

An adequate theoretical description of phos-

* The work described in this paper has been supported by the Bureau of Ordnance, U. S. Navy, under Contract NOrd-7386.

** A preliminary account of this paper was reported at the meeting of the American Physical Society, Washington, D. C., April 29, 30–May 1, 1948.

[1] R. C. Herman and C. F. Meyer, J. App. Phys. **17**, 743 (1946); *ibid.* **18**, 258 (1947).

[2] For theoretical discussions of thermoluminescence in phosphors, see J. T. Randall and M. H. F. Wilkins, Proc. Roy. Soc. **A184**, 366 (1945); F. E. Williams and H. Eyring, J. Chem. Phys. **15**, 289 (1947), and reference 1.

[3] F. Seitz and R. P. Johnson, J. App. Phys. **8**, 186, 84, 246 (1937); N. F. Mott, Trans. Faraday Soc. **34**, 822 (1938); R. P. Johnson, J. Opt. Soc. Am. **29**, 387 (1939).

[4] R. T. Ellickson and W. L. Parker, Phys. Rev. **70**, 290 (1946).

[5] J. H. Gisolf, Ned. T. Natuurk **5**, 289 (1938).

[6] A. L. Reimann, Nature **140**, 501 (1937).

[7] R. C. Herman and R. Hofstadter, Phys. Rev. **57**, 936 (1940).

[8] G. F. J. Garlick and A. F. Gibson, Proc. Roy. Soc. **A188**, 485 (1947).

[9] S. Fine, M.S. Thesis (Polytechnic Institute of Brooklyn, 1946).

[10] W. L. Parker and J. J. Dropkin, Bull. Am. Phys. Soc. **23**, 48 (1948).

phor behavior must take into account the fact that variations of conductivity occur simultaneously with changes in brightness during stimulation with infra-red light. Thus, it is necessary to inquire as to the relative probabilities that a conduction electron will be trapped or return to an empty luminescent center. A set of non-linear differential equations, originally proposed and solved graphically for the case of phosphorescence by de Groot,[11] may be employed to describe the rates of electron transfer that occur between the conduction band, trapping states, and empty luminescent centers. These equations involve as a parameter the quantity ϵ, the ratio of the cross sections for electron capture into empty traps and into empty luminescent centers or holes. Most discussions have been confined to the cases $\epsilon=0$ or 1, except for the work of de Groot[11] and the authors.[1] As a matter of fact, it is of great interest to determine ϵ for infra-red phosphors from experiment. In the remaining sections of this paper the effect of electron retrapping in infra-red sensitive phosphors is discussed, and a method is described which permits the determination of ϵ from the simultaneous observation of the time variations in brightness and photo-conductivity.

II. THEORY

According to the energy-band theory of solids, the spectrum of energy states of electrons in a phosphor may be represented as in Fig. 1. During the excitation of an infra-red phosphor with ultraviolet light, electrons are raised from the uppermost filled band, A, to the conduction band, B, from which they fall into localized discrete traps, E, or empty luminescent centers via states $D\rightarrow C$. The electrons in states C will fill the holes in A during this process. When the excitation is stopped there will be phosphorescence with an intensity and decay rate depending upon the trap depth. In most infra-red sensitive phosphors the trap depth is large compared to kT, so that the normal phosphorescence is weak and decays rapidly. Subsequent irradiation with infra-red light which is absorbed by the trapping centers will raise electrons to the conduction band. The processes described above will take place in such a manner that there will be variations in the brightness and conductivity as functions of the time until the trapping states are exhausted of electrons. As given in a previous paper,[1] the description of the situation is simplified by considering only those electron transfer processes between conduction band, trapping states, and holes.[12] It is also assumed that there are discrete sets of trapping states; in fact, for the sake of simplicity it is assumed that there is only one set. Furthermore, the theory to be described is confined to very thin phosphors, unless otherwise stated. The effect of light absorption will be discussed briefly.

Let N_1 be the number of trapping states per cm^3 at an energy ϵ_1 below the conduction band, n_0 the number of empty luminescent centers per cm^3, n the number of electrons per cm^3 in the conduction band, and n_1 the number of electrons per cm^3 in the trapping states in $d\epsilon_1$ at ϵ_1. Consider a phosphor in which all the trapping states are at a single energy depth. If these states are filled with electrons, and if $\epsilon_1 \gg kT$, then the electron transfer processes that occur on irradiation with infra-red light can be represented by the following set of differential equations:

$$\begin{aligned}(dn_0/dt) &= -An_0n,\\ (dn/dt) &= -An_0n+c_0n_1-K[N_1-n_1]n,\\ (dn_1/dt) &= -c_0n_1+K[N_1-n_1]n,\end{aligned} \tag{1a}$$

and

$$n_0=n+n_1,$$

where $A(=\sigma_L v)$ is the probability that an electron in the conduction band recombines with an ionized luminescent center or positive hole, σ_L is the cross section for capture of an electron by a luminescent center with the emission of light, v is the velocity of the conduction electron, and $K(=\sigma_T v)$ is the probability that a conduction electron is captured into a trap, with σ_T the cross section for capture of an electron into an empty trap. The quantity c_0 is given by

$$c_0=\sigma_P I_0/h\nu, \tag{1b}$$

where σ_P is the cross section of a trapped elec-

[11] W. de Groot, Physica 6, 275 (1939).

[12] This removes the difficulty of taking into account two possible transitions for an electron in an upper state of a luminescent center, namely, luminescent transitions to the ground state and thermal transitions to the conduction band.

tron for a photon of energy $h\nu$ and I_0 is the intensity of the stimulating light.[13] Equations (1) can be stated in a more convenient form if the following substitutions are made:

$$\xi = n/N_1,$$
$$\eta = n_0/N_1,$$

and

$$\zeta = n_1/N_1.$$

The quantities ξ, η, and ζ are, therefore, fractions of the number of electrons originally trapped that are in the various states at time t. Substituting Eq. (2) into Eqs. (1), we obtain

$$(d\eta/d\tau) = -\xi\eta, \tag{3a}$$
$$(d\xi/d\tau) = -\xi\eta - \epsilon(1-\zeta)\xi + \gamma\zeta, \tag{3b}$$
$$(d\zeta/d\tau) = \epsilon(1-\zeta)\xi - \gamma\zeta, \tag{3c}$$

and

$$\eta = \xi + \zeta, \tag{3d}$$

where

$$\epsilon = k/a, \quad \tau = at,$$
$$a = AN_1, \quad k = KN_1,$$
$$\gamma = c_0/a,$$

and c_0 is given by Eq. (1a). The solutions of Eqs. (3a)–(3c) depend upon the choice of γ and ϵ, where it is to be noted that ϵ is the ratio of the cross sections for electron capture into empty traps and empty luminescent centers or holes. In order to obtain the solutions in terms of n_0, n, and n_1 as functions of the time t it is necessary to specify further the parameter a.

Solutions[1, 14] of Eqs. (3) have been obtained in the two special cases, $\epsilon = 0$ and $\epsilon = 1$. If the probability of trapping, K, is considered to be negligible compared to the probability for recombination, A, the parameter $\epsilon = k/a = 0$, and we have

$$\zeta = \zeta_0 \exp(-\gamma\tau), \tag{4a}$$

and

$$\eta^{-1} = \eta_0^{-1} e^{y} \exp(-\zeta_0/\gamma) - \gamma^{-1} e^{y}[Ei(-y) - Ei(-y_0)], \tag{4b}$$

where $y = \gamma^{-1} e^{-\gamma\tau}$ and ζ_0, η_0 are the values of ζ and η when $\tau = 0$. The value of ξ may be found from Eq. (3d). Recently, Klasens and Wise[14] solved Eqs. (3) for the special case $\epsilon = 1$, when the cross sections for capture of a conduction electron into an empty trap and empty luminescent center are equal. The results for this case may be found readily if ζ is eliminated from Eq. (3b) and a substitution is made for ξ/η. The solutions are the following:

$$\eta^{-1} = \eta_0^{-1} + \alpha\tau - \beta^{-2}[\gamma - \beta(\xi_0/\eta_0)] \times [1 - e^{-\beta\tau}], \tag{5a}$$

$$\xi = [\alpha - (\alpha - \xi_0/\eta_0)e^{-\beta\tau}]\eta, \tag{5b}$$

where

$$\alpha = \gamma/\beta, \quad \beta = 1+\gamma, \quad \gamma = c_0/a,$$

and ζ may be found from Eq. (3d).

The following is a discussion of the behavior of the solutions of Eqs. (3) when τ becomes large. Equations (3a) and (3b) can be combined in the form

$$(d\xi/d\eta) = (1-\epsilon) + \epsilon(\xi/\eta) + [(\epsilon+\gamma)\xi - \gamma\eta]/\xi\eta. \tag{6}$$

From Eq. (6) it can be seen that there is a singularity in $d\xi/d\eta$ at the origin. The physically important solutions for the curves $\xi = f(\eta)$ are those for which $d\xi/d\eta$ is finite at the origin. In order that $d\xi/d\eta \nrightarrow \infty$ when $\xi \to 0$ and $\eta \to 0$, we have[15]

$$\xi = [\gamma/(\epsilon+\gamma)]\eta, \tag{7a}$$

and

$$\zeta = (\epsilon/\gamma)\xi. \tag{7b}$$

The brightness, B, and instantaneous photocurrent, i, induced in a phosphor by infra-red stimulation, are given by[16]

$$B \propto (d\eta/d\tau), \tag{8a}$$

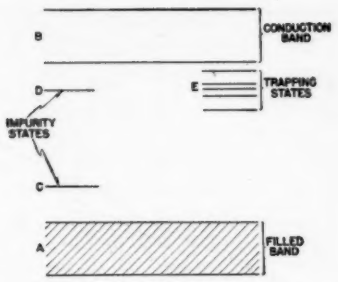

FIG. 1. Energy states of electron in phosphor.

[13] When these equations are used to discuss ordinary phosphorescence or thermoluminescence, the quantity c_0 would represent $s\exp(-\epsilon/kT)$, where s, the frequency factor, is the number of times per second an electron strikes the potential barrier of a trap.

[14] H. A. Klasens and M. E. Wise, Nature **158**, 483 (1946), have given the solutions for $\epsilon = 1$.

[15] This result has been stated by de Groot in reference 11.

[16] If non-optical transitions do not occur,

$$B = aN_1 h\nu(d\eta/d\tau) = h\nu(dn_0/dt).$$

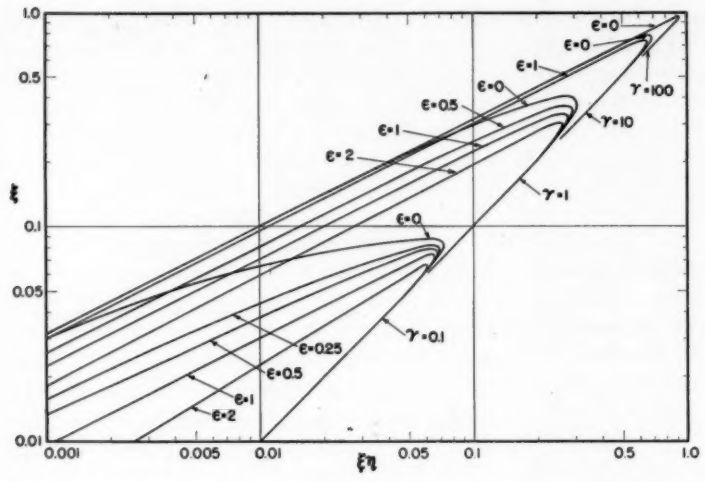

FIG. 2. Logarithmic plot of ξ *vs.* $\xi\eta$ (current *vs.* brightness) for a phosphor under infra-red stimulation in an electric field, for the cases $\gamma=100$, 10, 1, and 0.1 and for varying ϵ. For the case $\gamma=100$, only the curve for $\epsilon=0$ is plotted, since all the curves for $0\leqq\epsilon\leqq2$ are nearly coincident. For all other values of γ, curves are given for several values of ϵ.

and

$$i\propto\xi. \tag{8b}$$

The use of Eq. (7a) in Eq. (3a) shows that for large values of τ

$$B\propto[C_1+C_2\tau]^{-2}, \tag{9a}$$

and

$$i\propto[C_1+C_2\tau]^{-1}, \tag{9b}$$

for all values of the parameter ϵ. Equation (9b) shows that the resistance of a phosphor will increase linearly with time after sufficiently long times, a result found by Reimann[6] for ZnS.

III. DIFERENTIAL ANALYZER SOLUTIONS FOR $10^{-2}\leqq\gamma\leqq10^{2}$

Solutions for Eqs. (3) have been obtained by means of the differential analyzer at the Moore School of Electrical Engineering, University of Pennsylvania. Values of ξ, η, and ζ were tabulated by the analyzer as functions of τ for a number of values of the parameters γ and ϵ in the ranges, $10^{-2}\leqq\gamma\leqq10^{2}$ and $0\leqq\epsilon\leqq4$. While most of the solutions were obtained with initial conditions $\zeta_0=\eta_0=1$ and $\xi_0=0$, some information was obtained for the case $\zeta_0=\eta_0$, $0<\zeta_0\leqq1$, and $\xi_0=0$. The latter initial conditions apply to cases in which the trapping states are partially filled at $\tau=0$.

The values of $\xi=\eta-\zeta$ for the case $\gamma<1$ become quite small, so that there is considerable uncertainty in the analyzer results. In this case the variation of ξ with τ was obtained in the following manner. From Eq. (3a) we have $\xi=-\eta^{-1}(d\eta/d\tau)$, which serves to determine ξ

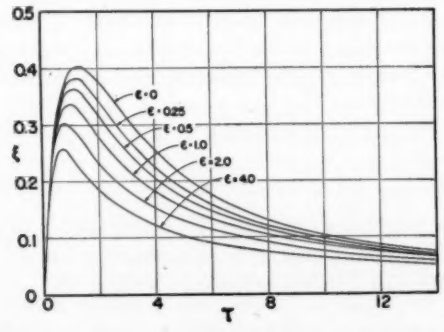

FIG. 3. Effect of varying ϵ on the time dependence of current for a phosphor under infra-red stimulation in an electric field, for the case $\gamma=1$ and for $\epsilon=0$, 0.25, 0.5, 1.0, 2.0, and 4.0.

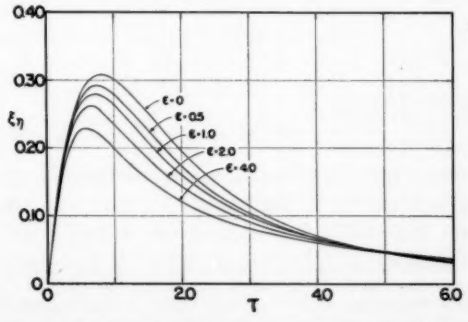

FIG. 4. Effect of varying ϵ on the time dependence of brightness for a phosphor under infra-red stimulation, for the case $\gamma=1$ and for $\epsilon=0$, 0.5, 1.0, 2.0, and 4.0.

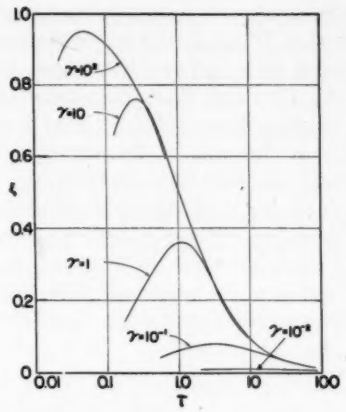

FIG. 5. Effect of varying γ on the time dependence of current (semilogarithmic plot) for a phosphor under infra-red stimulation in an electric field, for the case $\epsilon=0.5$ and for $\gamma=10^2$, 10, 1, 10^{-1}, 10^{-2}.

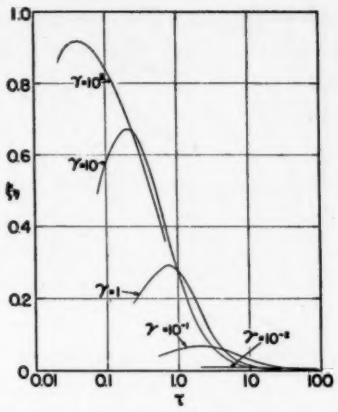

FIG. 6. Effect of varying γ on the time dependence of brightness (semilogarithmic plot) for a phosphor under infra-red stimulation, for the case $\epsilon=0.5$ and for $\gamma=10^2$, 10, 1, 10^{-1}, 10^{-2}.

if $d\eta/d\tau$ is known. The values of $d\eta/d\tau$ were found graphically from a plot of η *vs.* τ and then multiplied by the appropriate value of $(-1/\eta)$ for each value of τ. This procedure gives values of ξ which are good to about 2 percent based on a comparison with the calculated values of ξ for $\epsilon=0$. In general, the differential analyzer results presented have an accuracy of about 1 percent based on test runs for $\epsilon=0$, and 1. Another criterion used to determine the accuracy of the solutions is the positions of the peaks of the ξ *vs.* τ and $\xi\eta$ *vs.* τ curves. The peak of the curve ξ *vs.* τ occurs when $d\xi/d\tau=0$, which yields, according to Eq. (3b), the relation

$$(\epsilon-1)\xi_1\eta_1-(\epsilon+\gamma)\xi_1-\epsilon\xi_1^2+\gamma\eta_1=0, \quad (10a)$$

where ξ_1 is the maximum value of ξ and η_1 the corresponding value of η. Similarly, from $[d(\xi\eta)/d\tau]=0$, we obtain from Eqs. (3b) and (3c) the relation

$$(\epsilon-1)\xi_2\eta_2-(\epsilon-\gamma)\xi_2-(\epsilon+1)\xi_2^2+\gamma\eta_2=0, \quad (10b)$$

where ξ_2 and η_2 are the values of ξ and η when $\xi\eta$ is a maximum. The application of the conditions defined by Eqs. (10a) and (10b) shows that the solutions presented are self-consistent. Finally, one may also apply the criterion given in Eq. (7a) for large values of τ.

In Fig. 2, a logarithmic plot of ξ *vs.* $\xi\eta$ is given for various values of γ and ϵ. The results for small values of γ are given in Section IV. It is to be noted that the solutions start out with $[d(\ln\xi)/d\ln(\xi\eta)]_{\tau=0}=1$, and at large values of τ the slope approaches the value $\frac{1}{2}$. In Figs. 3 and 4 the curves for ξ *vs.* τ and $\xi\eta$ *vs.* τ are given for $\gamma=1$ and various values of ϵ, while in Figs. 5 and 6 similar curves are given for $\epsilon=0.5$ and various values of γ. Finally, the effect of the initial condition η_0 on the brightness is illustrated in Fig. 7.

IV. APPROXIMATE SOLUTIONS FOR $\gamma\ll1$

An examination of the size of the parameter γ in cases of practical interest shows that $\gamma\ll1$. This can be seen in the following manner. The cross section of a trapped electron for an infra-red photon may be estimated by an application

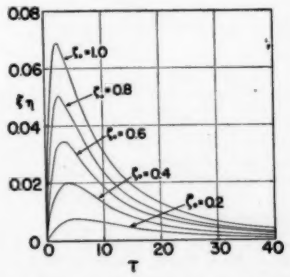

FIG. 7. Effect of varying initial conditions on brightness as a function of time for a phosphor under infra-red stimulation for the case $\gamma=0.1$ and $\epsilon=0.5$; $\xi_0=0$ for all curves, while $\eta_0=\zeta_0=1.0$, 0.8, 0.6, 0.4, and 0.2, respectively.

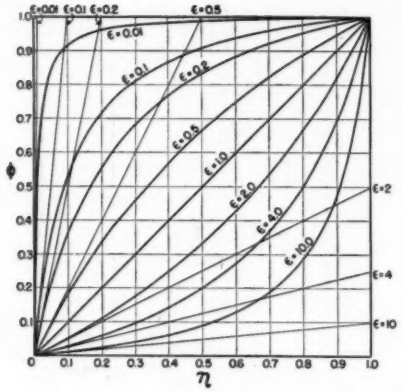

FIG. 8. Effect of varying ϵ on ϕ as a function of η at times beyond the maximum in ϕ, for $\gamma \ll 1$, for a phosphor under infra-red stimulation in an electric field; $\epsilon = 0.01$, 0.1, 0.2, 0.5, 1, 2, 4, and 10, respectively, [Eq. (13)]. As $\tau \to \infty$ the curves approach the indicated asymptotes.

of the theory proposed by Smakula[17] for F-center absorption. According to this theory, σ_P is given by the following expression:

$$\sigma_P = \alpha_m / N_1 = f/Q, \tag{11}$$

where

$$Q = 1.31 \times 10^{17} [n'/(n'^2+2)^2] W. \tag{11a}$$

In the above, α_m is the absorption coefficient at the center of the band, N_1 is the concentration of trapped electrons, f is the oscillator strength, n' is the index of refraction, and W is the width of the absorption band at half-maximum expressed in electron volts. Equation (11) is valid if the frequency at the peak of the band is large compared to $W/2$. From stimulation curves on strontium selenides[18] and strontium sulfides,[19] it is found that $W \cong 0.3-0.4$ ev. If we take $n' \cong 2$ and assume that $f \cong 1$, we have from Eq. (11), $\sigma_P \cong 10^{-15}-10^{-16}$ cm^2. For intensities of the infra-red stimulating light $I_0 \cong 10^{-3}$ watt/cm^2 and a frequency at the peak of the stimulation curve $\nu \cong 10^4$ cm^{-1}, so that $h\nu \cong 2 \times 10^{-12}$ erg, we find that $c_0 = \sigma_P I_0 / h\nu$ is of the order of unity. Since it has been shown[20] that $A \cong 10^{-8}$ cm^3/sec. and $N_1 \cong 10^{16}$ cm^{-3}, we find $\gamma \cong 10^{-8}$. It should be pointed out that the experiments of Parker and Dropkin[10] also show that $\gamma \ll 1$. If we now define $\phi = \xi/\gamma$, Eq. (6) becomes

$$d\phi/d\eta = (1-\epsilon)/\gamma + \epsilon(\phi/\eta) + [(\epsilon+\gamma)\phi - \eta]/(\gamma\phi\eta). \tag{12}$$

Since $\gamma \ll 1$, a plot of the vector field determined by Eq. (12) shows that all trajectories determined by this vector field run essentially parallel to the ϕ-axis except in the immediate neighborhood of the curve

$$\eta = \epsilon\phi/[1-(1-\epsilon)\phi]. \tag{13}$$

It is to be noted that Eq. (13) represents the solution from the point $\phi = \eta = 1$ to $\phi = \eta = 0$. Therefore a solution which starts at $\phi = 0$ and $\eta = 1$ rises almost along the line $\eta = 1$, turns in the immediate neighborhood of $\phi = \eta = 1$, and goes to the origin essentially along the curve given by Eq. (13). The relation given in Eq. (13) has been employed, together with Eqs. (3), by Randall and Wilkins[21] and Adirovich[22] to describe crystal phosphorescence. These investigators have not considered from a theoretical view-

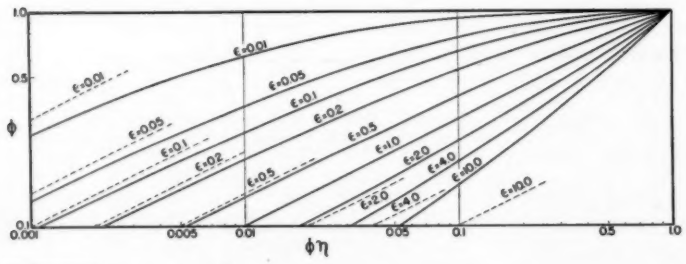

FIG. 9. Effect of varying ϵ on the logarithmic plot of ϕ *versus* $\phi\eta$ (current *versus* brightness) at times beyond the maximum in ϕ, for $\gamma \ll 1$, for a phosphor under infra-red stimulation in an electric field; for $\epsilon = 0.01$, 0.05, 0.1, 0.2, 0.5, 1.0, 2, 4, and 10. As $\tau \to \infty$ the curves approach the asymptotes of slope $\frac{1}{2}$, which are indicated by broken lines.

[17] A. Smakula, Zeits. f. Physik **59**, 603 (1930). Also see F. Seitz, *The Modern Theory of Solids* (McGraw-Hill Book Company, Inc., New York, 1940), p. 664.
[18] A. L. Smith, R. D. Rosenstein, and R. Ward, J. Am. Chem. Soc. **69**, 1725 (1947).
[19] F. Urbach, D. Pearlman, and H. Hemmendinger, J. Opt. Soc. Am. **36**, 372 (1946).
[20] N. F. Mott and R. W. Gurney, *Electronic Processes in Ionic Crystals* (Oxford University Press, New York, 1940), p. 217.
[21] J. T. Randall and M. H. F. Wilkins, Proc. Roy. Soc. **A184**, 390 (1945).
[22] E. I. Adirovich, Comptes Rendus (Doklady) U.R.S.S. **53**, 313 (1946).

point the problem of the associated photoconductivity. In Fig. 8 is shown a plot of ϕ *vs.* η for various values of ϵ, obtained from Eq. (13). From Eq. (13), or from the condition that $d\phi/d\tau=0$, it is seen that the maximum value of ϕ is approximately unity when $\eta_0=1$. The time required to reach this maximum value for the case $\epsilon=1$ is given by $e^{-\tau}=\gamma$, and the time required to reach the brightness peak is given by $e^{-\tau}=2\gamma$. Since $\gamma\ll1$, the rise time is extremely short. Referring to Eqs. (8), we note that Fig. 8 is, in fact, a plot of (i/i_{max}) *vs.* $(B/B_{max})/(i/i_{max})$, where i_{max} and B_{max} are the peak values of the photo-current and brightness *vs.* time curves obtained by simultaneous measurements during infra-red stimulation. The experimental data plotted in this fashion should give curves which are concave downward, upward, or linear, according to whether $\epsilon<1$, $\epsilon>1$, or $\epsilon=1$. Furthermore, ϵ may be determined by fitting the data to Eq. (13). This method gives a value of ϵ independent of the knowledge of γ, since γ is very small. Preliminary results of Parker and Dropkin[10] on the simultaneous determination of i and B in a type B-1 phosphor (strontium selenide+europium+samarium) have been analyzed in this fashion. They have shown that $\epsilon<1$ and probably has a value of about 0.2 for a 2-mm thick sample of this phosphor. While they have not employed extremely thin samples, they find better agreement with the theoretical curves for phosphors with smaller thickness. According to Randall and Wilkins,[21] ϵ lies between 0.5 and 1.0 for a ZnS-Cu phosphor as determined from a study of its fluorescence.

In the interpretation of these experimental measurements two difficulties arise which are first, the effects of polarization, which can be minimized by pulsing the stimulating infra-red light, and secondly, the fact that the above theory does not include the effects of absorption of both the stimulating infra-red and the emitted visible light. The latter question can be taken into account in the theory by writing

$$c_0=\sigma_P I'/h\nu,$$

where the intensity I' is now a function of the depth below the surface of the phosphor. It may be possible to avoid the difficulties mentioned above by another interpretation of Fig. 8. Up

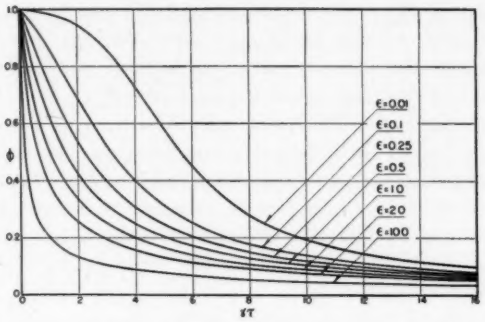

FIG. 10. Effect of varying ϵ on current as a function of time for $\gamma\ll1$, for a phosphor under infra-red stimulation in an electric field; $\epsilon=0.01$, 0.1, 0.25, 0.5, 1.0, 2.0 and 10.0, respectively. (This approximation is valid at times later than the maximum in ϕ.) No curve is shown for $\epsilon=0$, since in this case the shape of the curve is a function of γ.

to this point the discussion was based on $\eta_0=1$, i.e., completely filled trapping centers when $\tau=0$. In the event that $0\leqq\eta_0<1$, the solution $\phi=f(\eta)$ will start at $\eta=\eta_0$, $\phi=0$, rise almost vertically along the line $\eta=\eta_0$, turn in the immediate vicinity of the curve given by Eq. (13) for a particular value of ϵ, and then proceed to the origin along that curve. In this case the maximum value of ϕ is given by

$$\phi_{max}=\eta_0[\epsilon+(1-\epsilon)\eta_0]^{-1}. \qquad (14)$$

Now, the light sum, $\sum$, given by $\sum=\int Bdt$, is proportional to η_0. Thus, the curve given in Eq. (13) can be interpreted as a plot of $\phi_{max}/(\phi_{max})_0$

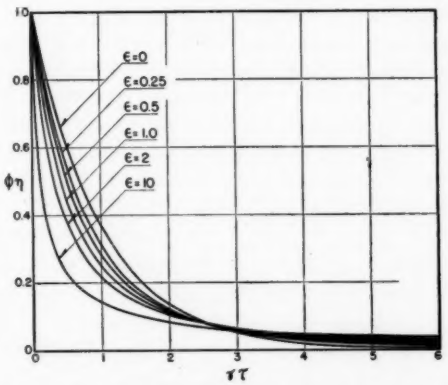

FIG. 11. Effect of varying ϵ on brightness as a function of time for $\gamma\ll1$, for a phosphor under infra-red stimulation; $\epsilon=0$, 0.25, 0.5, 1.0, 2 and 10, respectively. This approximation is valid at times later than the maximum in ϕ. Note that the curve for $\epsilon=0$ is valid only so long as $\phi\sim1$.

vs. $\sum/\sum_0$, where $(\phi_{max})_0$ and $\sum_0$ are proportional to the maximum photo-current for a fixed electric field, and to the light sum obtained when the traps are completely filled, i.e., $\eta_0=1$, respectively. The latter condition can be satisfied if kT is sufficiently smaller than the trap depth. This technique might reduce the effects of polarization and perhaps some of the effects caused by light absorption. Since the light sums $\sum$ and $\sum_0$ both contain the same geometrical factor, providing the absorption of infra-red and emitted light is caused chiefly by the crystal matrix, then the quantity $\sum/\sum_0$ will be relatively independent of absorption effects. It is believed that this latter technique should be less susceptible to thickness effects.

Another manner of presenting the experimental results is given in Fig. 9, which is a logarithmic plot of ϕ *vs.* $\phi\eta$. The solutions start with $\eta_0=1$, $\phi_0=0$, and slope unity, turn in the immediate neighborhood of $\eta=1$, $\phi=1$, and proceed along the curve given by

$$\ln\phi=\tfrac{1}{2}\ln\phi\eta+\tfrac{1}{2}\ln[1-(1-\epsilon)\phi]-\tfrac{1}{2}\ln\epsilon. \qquad (15)$$

As $\tau\to\infty$ the slope $d(\ln\phi)/d(\ln\phi\eta)\to\frac{1}{2}$. Thus, if $\epsilon<1$, the experimental data plotted in this manner will give a curve whose slopes lie between 0 and $\frac{1}{2}$, and which is concave downward.

As has been done previously,[21,22] Eq. (3a) can be integrated with the aid of Eq. (13) to yield

$$\epsilon(1-1/\eta)+(1-\epsilon)\ln\eta=\gamma\tau. \qquad (16)$$

From Eqs. (13) and (16) we obtain the dependence of ϕ and $\phi\eta$ on $\gamma\tau$ or c_0t, since $\gamma=c_0/a$ and $\tau=at$. Thus, the time dependence of the instantaneous photo-current and brightness can be found as functions of ϵ, and appropriate curves are shown in Figs. 10 and 11.

The photo-current curves in Fig. 10 do not include the curve for $\epsilon=0$. In the approximation discussed, the solution for $\epsilon=0$ is the line $\phi=1$, which is obviously incorrect. From Eqs. (4) it can be shown that $\phi\cong0.45$ when $\gamma\tau=1.577-\ln\gamma$. Thus, if $\gamma\cong10^{-8}$, we have $\phi\cong0.45$ when $\gamma\tau\cong20$. The quantity ϕ decreases quite slowly at first according to Eqs. (4). During this period the decay of the brightness for $\epsilon=0$ is approximately exponential.[23] However, at longer times $\phi\to0$ in such a manner that $\xi\to\eta$. This means, as stated earlier, that the brightness decay for thin samples according to this theory is hyperbolic after long times for all values of ϵ.

ACKNOWLEDGMENTS

We wish to acknowledge profitable discussion with Professor Frederick Seitz, of the Carnegie Institute of Technology, and Professor W. L. Parker, of the Brooklyn Polytechnic Institute. We express our appreciation to Drs. R. B. Kershner, G. C. Munro, and D. T. Sigley of the Applied Physics Laboratory of the Johns Hopkins University for their interest in this problem, and thank the differential analyzer staff of the Moore School of Electrical Engineering, University of Pennsylvania, for their cooperation.

[23] Adirovich in reference 22 states that the law of decay is exponential when $\epsilon=0$, but ignores the fact that the decay becomes a second-order hyperbola after long times.

JOURNAL OF THE OPTICAL SOCIETY OF AMERICA VOLUME 38, NUMBER 12 DECEMBER, 1948

Optical Properties of Zinc Fluoride Phosphors*

GORTON R. FONDA AND FRANK J. STUDER
Research Laboratory, General Electric Company, Schenectady, New York

(Received August 18, 1948)

When activated with manganese alone, zinc fluoride emits an orange fluorescence under excitation by 2537A whose brightness is very weak because its peak excitation lies at 2200A. Other activators, cerium, tungsten, and titanium, shift the peak excitation to 2500–2600A and produce a higher absorption in the range 2000–2600A. The emission of tungsten and titanium lies mainly in the visible; that of cerium consists of a series of bands in the ultraviolet.

Combinations of these elements with manganese produce greater fluorescence brightness. With tungsten or titanium, the normal orange emission of manganese is increased manifold with no change in the spectral distribution nor in the unique exponential decay of its afterglow except that the decay is raised to a higher brightness level. With cerium, the individual emission of each activator persists, with no reduction in intensity of the ultraviolet cerium bands and with only a slight increase in the intensity of the manganese band.

As explanation of this apparent discrepancy, evidence was found that only tungsten and titanium are present in the same phase as manganese, namely, zinc fluoride. Cerium combines to form a separate phase, an aggregate of zinc and cerium fluorides.

IN recent years, a zinc fluoride phosphor activated with manganese has received considerable attention because of its remarkably slow rate of exponential decay.[1,2] Its luminous efficiency is high under cathode-ray excitation. It is very low, however, under excitation by the low pressure mercury lamp which radiates predominantly the 2537A resonance line. Experiments were undertaken to find if more efficient excitation under 2537A could be obtained by the use of a secondary activator. This device had proved successful when applied to another similar phosphor, calcium silicate activated with manganese. Although this silicate was normally responsive to cathode-ray excitation only, Froelich showed that, in common with some other phosphors, it also becomes capable of excitation by 2537A when lead is incorporated in it as well as manganese.[3] Furthermore, he demonstrated that the presence of lead is accompanied by the introduction of an absorption band that comprises the region of 2537A. In the present experiments with zinc fluoride, it was therefore equally important to investigate changes in the absorption and excitation spectra.

Of the many secondary activators tried, the greatest increase in luminous efficiency resulted from the presence of titanium or tungsten. Cerium exercised a small but definite sensitizing action. Germanium was also effective but less so than cerium. Its presence sometimes led to peculiar distortions of the emission spectrum. Its effect was so erratic that the presence of another active factor was suspected. The effect of lead was insignificant, although it introduced an absorption band at 2537A and, by itself, gave rise to a weak emission in the yellow.

Each of the three most effective sensitizing elements, cerium, tungsten, and titanium, proved to emit a characteristic and interesting luminescence when present alone in zinc fluoride. These singly activated phosphors will be described before the doubly activated, because their characteristics are helpful in understanding the variable efficiency at which they sensitize the manganese emission.

First of all, however, a description will be given of the method of preparing the phosphors and of the measurements made to determine their characteristics.

PREPARATION OF PHOSPHORS

Pure zinc fluoride was prepared in a precipitation process by adding an ammonium fluoride solution to a boiling solution of zinc chloride.

* Presented at the Winter Meeting of the Optical Society of America in New York, New York, on March 6, 1948 [J. Opt. Soc. Am. **38**, 665(A) (1948)].

[1] H. W. Leverenz, *Final Report on Research and Development Leading to New and Improved Radar Indicators*, Report PB 25481, Office of the Publication Board, Dept. of Commerce, Washington, D. C. (1945). "Luminescence and tenebrescence as applied in radar," RCA Rev. **7**, 236 (1946).

[2] F. E. Williams and H. Eyring, J. Chem. Phys. **15**, 289 (1947).

[3] H. C. Froelich, Brit. Pat. 577,694 (May 28, 1946). J. Electrochem. Soc. **93**, 101 (1948).

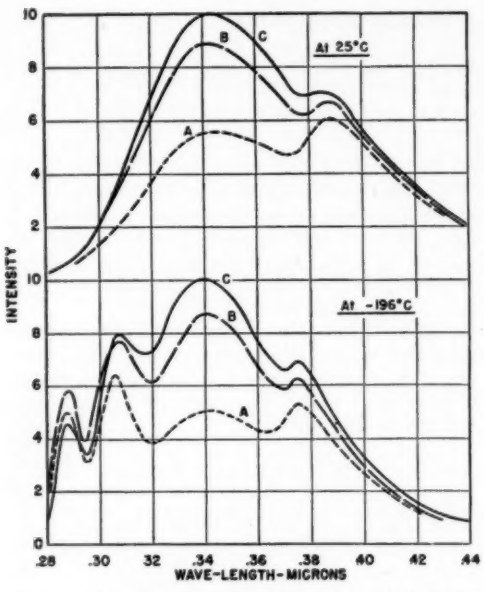

FIG. 1. Variation in spectral emission of ZnF_2:CeF_3 phosphors with composition at room temperature and in liquid nitrogen. *A*—0.7-molar percent CeF_3. *B*—7.6-molar percent CeF_3. *C*—25.0-molar percent CeF_3.

Reagent quality chemicals were used for the solutions. The solutions were further purified by cross precipitation. The precipitated fluoride was washed and dried at 115°C.

Phosphors were prepared by mixing dry the fluoride with compounds of the activators. Manganese was introduced as the chloride. Cerium was introduced as ceric oxide as well as cerous fluoride. The other secondary activators were introduced as oxides. The mixtures were fired in platinum containers at 800°C for 20 minutes. At this temperature it became apparent that the compound of the activator is converted into the fluoride. The resulting phosphor was a sintered pellet, rather hard. It was scraped free of whatever loose, extraneous material was present and was pulverized.

When air was used as the furnace atmosphere, the upper surface of the phosphor pellet was covered with a slight, pulverous coating of oxide. When tank nitrogen was introduced to the furnace, this coating was reduced to a thin film, discolored to an orange brown. In both cases, the pellet was white. In a moist hydrogen atmosphere, the pellet was light gray in color and there were further evidences of partial reduction, despite the presence of moisture. Dry hydrogen was not used, as this would have caused serious reduction. In the presence of steam, either alone or with hydrogen, a white pulverous mass was formed which was non-fluorescent, evidently the oxide.

In order to establish the identity of the compounds that were used as well as of those formed in the fired phosphors, their x-ray diffraction patterns were recorded with the North American Philips Geiger counter x-ray spectrometer. The lines in the pattern of the zinc fluoride, which had been precipitated and dried at 110°, were identical in location and in relative intensity with the reported pattern for ZnF_2.[4] This pattern persisted after firing in nitrogen and even in air, thus demonstrating that no alteration in composition or constitution resulted at 800°C. The pulverous coating which had been removed from the surface of the pellet was, of course, zinc oxide.

When the zinc fluoride was fired in moist hydrogen, the pattern of the resulting product showed basically the pattern for ZnF_2. In addition, however, there were seven lines of the ZnO pattern, whose intensity denoted that about one third of the fluoride had been converted into oxide by the moisture present in the hydrogen.

Nitrogen was therefore selected as the most favorable atmosphere for the firing operation.

MEASUREMENT OF OPTICAL CHARACTERISTICS

Emission Spectra

The emission, absorption, and excitation spectra of the phosphors were measured by means of the recording radiometer developed by Studer.[5] The phosphors were in the form of heavy deposits, about 1 mm thick, pressed into a circular recess, 2.5 cm in diameter, in a copper plate. All measurements were, of course, made on the surface irradiated with ultraviolet. In recording the emission curves, the source of excitation was a germicidal lamp, over 90 percent of whose radiant energy is concentrated in the 2537A resonance line of mercury.

---

[4] J. D. Hanawalt, H. W. Rinn, and L. K. Frevel, J. Ind. Eng. Chem. Anal. Ed. **10**, 457 (1938).
[5] Frank J. Studer, J. Opt. Soc. Am. **38**, 467 (1948).

Absorption Spectra

Absorption measurements on a powder are open to the danger of error imposed by the scattering of the incipient radiation. In transmission measurements, the error is large and variable because of the difficulty of attaining uniformity either in grain size or in the thickness of the phosphor layer. Reflectance measurements from a thick phosphor deposit seemed to offer much less possibility of error than measurements of transmission. Inasmuch as all preparations had had the same heat treatment, their grain size was necessarily of the same order. As a consequence, the extent of scattering should be uniform in all cases. The reflectance method was therefore chosen.

The radiation from a hydrogen arc lamp which gives a continuous spectrum from 4000A to below 2000A was first directed against a plaque of smoked magnesium oxide about 1 mm thick and the spectrum of the reflected light was recorded by an automatic grating spectrometer. The magnesium oxide was then replaced by a similar sample of the phosphor or other test material and the spectral reflectance curve recorded. From these two curves, the percentage reflectance of the phosphor was calculated on the assumption that the magnesium oxide is a perfect reflector. It was assumed that the difference between such values and 100 percent was representative of the relative absorption.

Excitation Spectra

The method of measurement was similar to that used in absorption except that the test material, which in this case was always a phosphor, was in the form of a thin coating on a glass slide. It was placed directly in front of the exit slit of the grating spectrometer, normal to the axis of the diffracted beam, with the phosphor-coated surface toward the incident light. The hydrogen spectrum was caused to move across it and the intensity of the emitted fluorescent light was recorded for variation in wave-length of the exciting beam. Inasmuch as the latter was confined to the ultraviolet, whatever portion of it was transmitted by the phosphor was effectively absorbed in the glass on which the phosphor was coated. The light emitted by the phosphor was consequently limited to the visible fluorescence.

CERIUM-ACTIVATED PHOSPHORS

Composition

The phosphors on whose measurements the most reliance was placed were made by admixture of cerous fluoride and by firing in a current of nitrogen at 800°C. The cerous fluoride was prepared by precipitation from a solution of cerous nitrate with an ammonium fluoride solution. The composition of the phosphors was studied by means of their x-ray diffraction patterns. The pattern of the precipitated cerous fluoride agreed with that reported by Offedal.[6] It was unaltered by firing at 800°C in nitrogen.

At all compositions, ranging from 0.3- to 50-molar percent cerous fluoride, the patterns of both zinc fluoride and cerous fluoride persisted independently and unaltered, denoting that these fluorides do not form solid solutions. As will appear from the emission data, however, there is evidently some type of association between them.

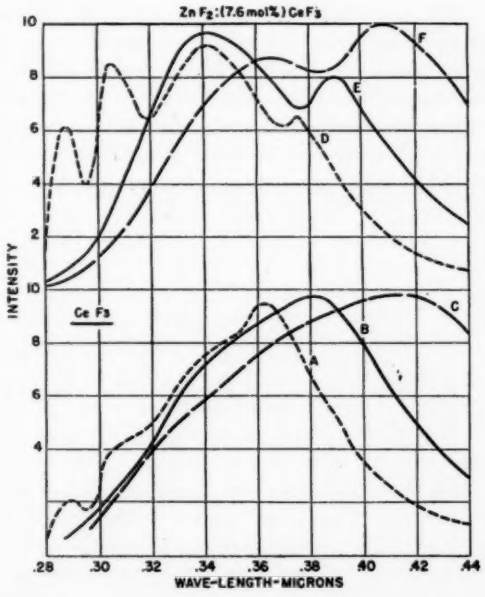

FIG. 2. Spectral emission at different temperatures of CeF_3 as compared with ZnF_2:CeF_3. CeF_3—*A* at −196°C, *B* at 25°C, *C* at 200°C, ZnF_2:(7.6-molar percent) CeF_3—*D* at −196°C, *E* at 25°C, *F* at 150°C.

[6] Ivar Offedal, Zeits. f. physik. Chemie **5B**, 277 (1929).

When ceric oxide rather than cerous fluoride was fired in mixtures with zinc fluoride at 800°C in nitrogen, x-ray patterns of the products showed that a reaction took place in which cerous fluoride was formed and an equivalent amount of zinc fluoride was converted into oxide. Ceric oxide appeared in the reaction product only when its initial concentration was in excess of that necessary to consume all of the zinc fluoride. This concentration was at about 33 molar percent cerium. The reaction can accordingly be represented by the following equation:

$$2ZnF_2+CeO_2\rightarrow CeF_3+2ZnO+\tfrac{1}{2}F_2. \quad (1)$$

Emission Spectra

The emission of all phosphors lay in the near ultraviolet and extended into the blue. Cerous fluoride, itself, as already observed by Kröger and Bakker,[7] proved to have a strong fluorescence, but its emission has a distinctive spectral distribution which is somewhat different from the emission of zinc fluoride phosphors containing cerous fluoride.

The latter were investigated up to a content of 50-molar percent CeF_3. Their emission spectrum, as shown in Fig. 1 for three widely different compositions, is made up of four constituent bands. These are best discerned in the measurements made at the temperature of liquid nitrogen. The higher resolution obtained at this low temperature demonstrates that the peaks of these bands lie at 2880A, 3060A, 3400A, and 3750A. Increase in concentration of cerium alters the relative intensities of the bands to an extent that changes with temperature but it does not affect their spectral location. The total energy of emission increases with cerium concentration up to about 25-molar percent CeF_3 and thereafter decreases slowly, up at least to 50-molar percent, the limit of our tests. In Fig. 1 the relative intensities for 7.6- and 25.0-molar percent CeF_3 are as drawn. Curve *A* for 0.7-molar percent is considerably amplified to give greater emphasis to its constituent bands.

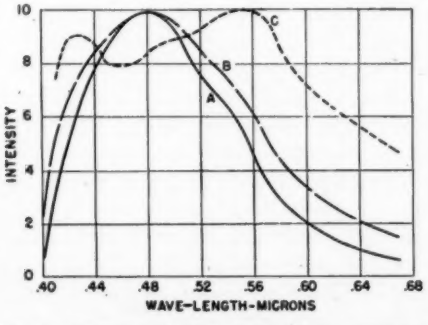

FIG. 3. Spectral emission of phosphors prepared from zinc fluoride containing variable amounts of tungstic acid. *A*—50-molar percent WO_3, *B*—3.7-molar percent WO_3, *C*—0.9-molar percent WO_3.

[7] F. A. Kröger and J. Bakker, Physika **8**, 628 (1941).

In phosphors prepared from mixtures of zinc fluoride with ceric oxide, the spectral locations of all four bands remained unchanged, but their intensities were seriously reduced. That these reductions were due to the presence of zinc oxide, formed as a reaction product in the firing, according to Eq. (1) above, was demonstrated by the conscious addition of zinc oxide, which had the same effect. The extent of the reduction in intensity produced in the various bands depended on temperature. The longest wave-length band was predominant at room temperature whereas, at liquid nitrogen temperature, the two bands at 2880A and 3060A were very strongly predominant.

As illustrated in Fig. 2, the emission spectrum of cerous fluoride occupies the same spectral region as that of the zinc fluoride phosphors and is made up likewise of four bands, but their spectral locations are different. From the measurements made in liquid nitrogen, they appear to be at 2900A, 3020A, 3300A, and 3630A. The spectrum is similar to that reported by Kröger and Bakker.[7] The energy content of the emission as a whole is about the same as for ZnF_2: (25-molar percent) CeF_3. An increase in temperature decreases the emission very considerably and has the apparent effect of shifting its relative distribution to longer wave-lengths. As a matter of fact, however, this effect is probably the result of a broadening of the bands combined with changes in their relative intensities.

The changes produced in the emission of cerous fluoride by the presence of zinc fluoride are of similar nature to the changes produced by the fluorides of lanthanum, calcium and strontium, as observed by Kröger and Bakker. They are sufficiently significant to denote that

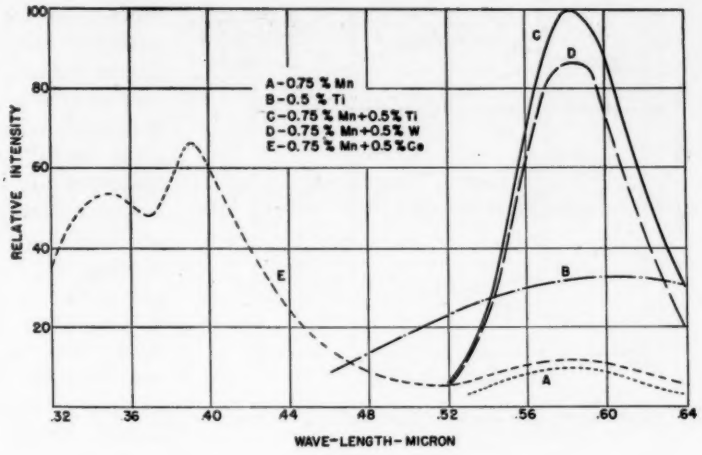

FIG. 4. Emission spectra of zinc fluoride phosphors under excitation by 2537A radiation.

some type of complex is formed between cerous fluoride and the added fluoride. The fact that no further change in emission occurs in ZnF_2:CeF_3 when the cerous fluoride is reduced to a very low concentration is in accord with the diffraction data and demonstrates again that cerous fluoride is insoluble in zinc fluoride.

TUNGSTEN-ACTIVATED PHOSPHORS

In phosphors made with additions of tungstic oxide, there was a weak, whitish emission, whose color suggested the formation of the phosphor, zinc tungstate, as the source. X-ray patterns confirmed this for those mixtures containing appreciable amounts of tungsten. In products made with smaller contents of tungsten, such as 3.7-molar percent, the $ZnWO_4$ pattern persisted at moderate intensity together with the pattern of ZnF_2.

The spectral emission is shown in Fig. 3. Curve *A*, for 50-molar percent WO_3, is identical with that of the normal phosphor, $ZnWO_4$, prepared at high temperature from a mixture of the oxides, except for the slight hump at 5500A. Curve *B*, for 3.7-molar percent, has the same general distribution but is somewhat broader.

At 0.9-molar percent WO_3, however, a distinctive emission appears, as illustrated in curve *C* of Fig. 3. The predominant emission is now at 5500A, the location of the weak hump observable at higher concentrations. There appear therefore to be two phosphors involved in the products obtained from reaction of ZnF_2 with WO_3. In addition to the $ZnWO_4$ formed at higher concentrations of tungsten, the distinctive emission found at low concentration denotes that a very small amount of tungsten is incorporated directly in the fluoride lattice and that its atoms function as fluorescence centers. Its solubility is probably very low, as this would account for the weak fluorescence observed.

The greater breadth of the emission band shown in curve *B* of Fig. 3 can therefore be regarded as due to the additive contributions made to it by the independent emission spectra of two phosphors, $ZnWO_4$ and ZnF_2:W.

TITANIUM-ACTIVATED PHOSPHORS

The emission of the product obtained by firing zinc fluoride with titanium oxide at 800°C is also very broad, just as in the case of tungsten. Its intensity however is considerably greater. It is shown in Fig. 4 as curve *B*. Its unusual breadth would indicate that it might be a multiple of several constituent, closely overlapping bands. Measurement in liquid nitrogen failed, however, to show any resolution into narrower bands. Its emission was not altered in spectral distribution by change in concentration of the titanium, but its intensity proved to be strongly dependent on concentration. It was strongest at an optimum concentration of 1 percent Ti by weight, 2-molar percent. At 8-molar percent, the intensity was reduced to about one-half. At 30-molar percent, the emission was completely suppressed. Mixtures of the oxides of zinc and ti-

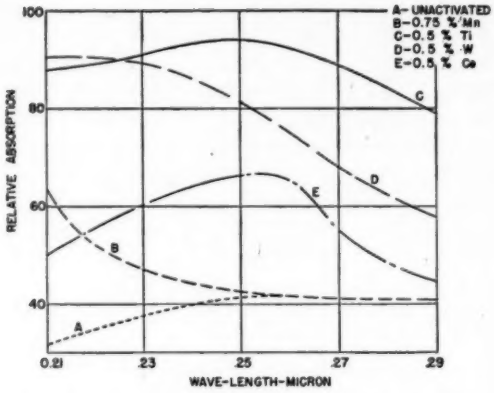

FIG. 5. Apparent relative absorption spectra of singly activated zinc fluoride phosphors.

tanium failed to give any appreciable emission after firing at 1180°C. It is presumable, therefore, that the luminescence from the phosphor ZnF_2: Ti is due to the presence of titanium atoms as activator centers, incorporated in the zinc fluoride lattice, just as assumed for the low concentration form of the tungsten phosphors.

SENSITIZATION OF MANGANESE EMISSION

The manganese emission consists of a single, rather narrow band, whose peak lies at about 5800A. The optimum concentration is 0.7 percent by weight. It is sensitized appreciably, though to varying degrees, by the three elements, cerium, tungsten and titanium, at an optimum concentration, in each case, of 0.5 percent by weight. A general survey of the emission spectra is given in Fig. 4. The shape and spectral location of the manganese emission band is not altered by the presence of any one of these foreign elements.

As is evident from Fig. 4, cerium, as a secondary activator, has only a slight effect in enhancing the manganese emission. The greater part of the excitation energy is evidently utilized in generating the ultraviolet emission of cerium rather than the visible emission of manganese. This is further evidence that the cerium and the manganese lie in different phases of the zinc fluoride. Whenever two activators are present in the same phase, the shorter wave emission band is reduced in favor of the longer wave band.

The most remarkable sensitizing effects were shown by titanium and by tungsten, as illustrated in curves *C* and *D* of Fig. 4. The bands of the secondary activators were completely suppressed. The intensity of the manganese band is increased manifold, more particularly by titanium. The intensity level of the phosphorescence decay is increased proportionately to the fluorescence by each of these secondary activators.

One further observation bearing on the emission characteristics associated with these activators should be recorded. In a phosphor con-

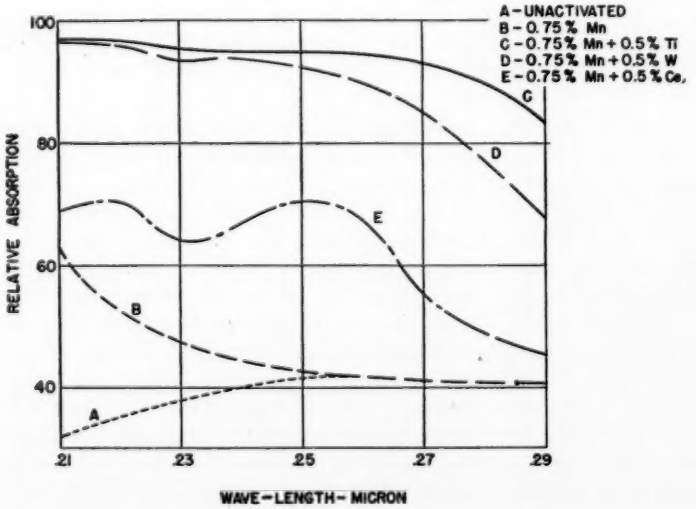

FIG. 6. Apparent relative absorption spectra of doubly activated zinc fluoride phosphors.

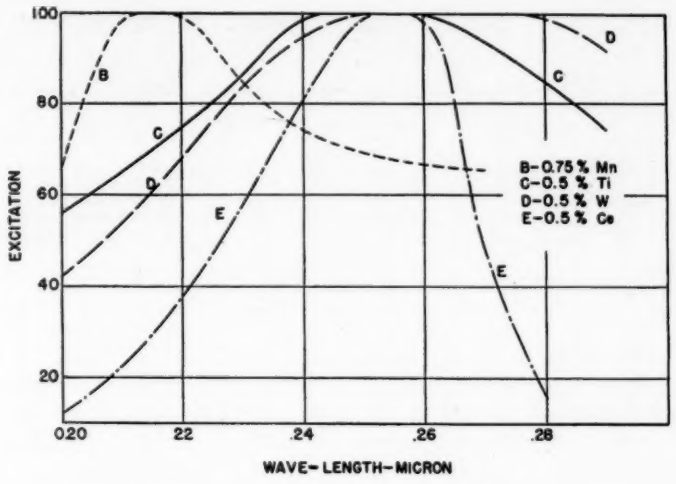

FIG. 7. Excitation spectra of singly activated zinc fluoride phosphors.

taining both titanium and cerium, the cerium emission in the ultraviolet is greatly suppressed and the titanium band in the orange appears at its normal intensity. When the phosphor contains manganese as well as titanium and cerium, the major emission lies in the 5800A manganese band and its intensity is at the same high level associated with sensitization by titanium; in this phosphor both the titanium and the cerium bands are suppressed. A probable explanation is that the titanium is soluble in both phases, ZnF_2 and $ZnF_2:CeF_3$, that its normal emission is associated with the fomer phase, and that it acts as a poison in the latter.

Optical characteristics that are of influence in determining the luminous efficiency are the absorption and excitation spectra. Apparent relative absorption curves are shown in Figs. 5 and 6. It is evident that manganese introduces an absorption band but its position is at such short wave-lengths, 2100A or below, that its intensity at 2537A is extremely weak. On the contrary, the absorption bands introduced by cerium, tungsten and titanium lie at longer wave-lengths. As shown in Fig. 5 for the singly activated phosphors, the intensity of their absorption at 2537A increases in the order named.

The absorption recorded by the curves of Fig. 6 is for the doubly activated phosphors. Comparison with Fig. 5 makes clear that for each combination of activators the absorption is an additive function of the two activators present. Again, the absorption at 2537A increases in the order: Mn, Mn+Ce, Mn+W, Mn+Ti.

Curves of the excitation spectra are given in Fig. 7 for phosphors containing single activators, and in Fig. 8 for the doubly activated. It is noticeable that the peaks in the excitation spectra of the latter all fall in the range 2500–2600A just as for those with single activators other than manganese. For manganese alone, the peak lies at 2150A. The results from both absorption and excitation measurements demonstrate, therefore, that it is the secondary activator which is the effective agent in increasing the luminous efficiency of the manganese emission band under 2537A.

None of these phosphors has shown an emission band which lies within the spectral range of the absorption band. There is consequently no ground for believing that the sensitization is due to the absorption of such an emission band, a case observed by Kröger in the luminescence of cerium sulfate and denominated "self-absorption" by him.[7]

DISCUSSION OF SENSITIZING ACTION

There are certain characteristics of a secondary activator that appear to be essential if it is to sensitize the emission of a primary activator. They are well illustrated by the zinc fluoride phosphors. They can be divided into these three groups:

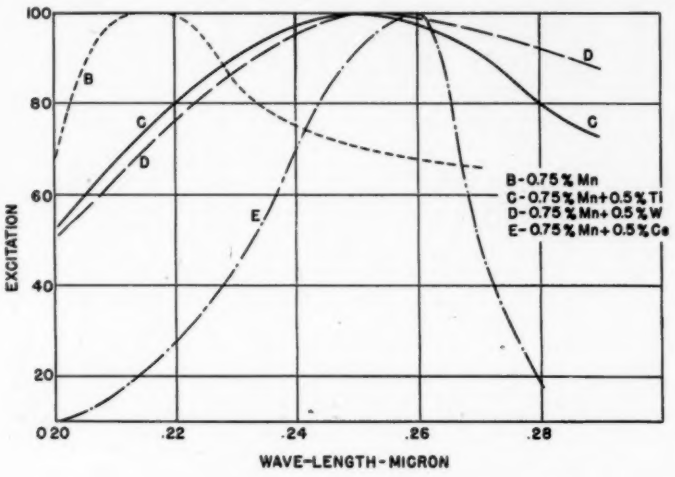

FIG. 8. Excitation spectra of doubly activated zinc fluoride phosphors.

1. The sensitizing element is present in the same phase as the primary activator.

Both titanium and tungsten at low concentration have unique emission spectra. Their uniqueness disappears when their concentration is raised—the titanium emission being suppressed and the tungsten emission passing over into that of a separate phase, $ZnWO_4$. Their unique emission is therefore to be regarded as associated with the zinc fluoride phase which contains the manganese.

The unique emission due to cerium, on the other hand, is at a maximum at a concentration so high that it must be ascribed to an aggregate made up of ZnF_2 and CeF_3. This is in accord with the x-ray patterns. No distinctive emission appears at low concentration, an indication that cerium does not function as activator centers in a zinc fluoride phase. Cerium and manganese are therefore present in separate phases. This accounts for the observation that the cerium emission is not suppressed in the presence of manganese.

2. The sensitizing element introduces an absorption band at the spectral location for which sensitization is desired.

It is, of course, obvious that the absorption must be in the same phase which contains the primary activator. The absorption band observed with cerium in zinc fluoride is of no avail because it characterizes the separate phase, $ZnF_2:CeF_3$.

3. The sensitizing element, when present alone, has an emission band of its own. To be most effective, the spectral location of its emission band should be at shorter wave-length than that of the primary activator. It is suppressed in the presence of the primary activator.

On the basis of these three groups of characteristics, which are illustrated by the observations on the zinc fluoride phosphors as well as by the other recorded cases of sensitization,[3, 8] the conclusion can be drawn that there are three corresponding criteria for a sensitizing agent—(1) it must be present in the same phase as the primary activator, (2) it must introduce an absorption band at the spectral location for which excitation is desired, (3) it must, when present alone, have an emission which is preferably of shorter wave-length than the emission of the primary activator.

We wish to express our gratitude to E. T. Asp of this laboratory for recording the x-ray patterns. They served as guide in carrying out our experiments and as interpreter in understanding them.

[8] F. A. Kröger, *Some Aspects of the Luminescence of Solids* (Elsevier Publishing Company, New York, 1948), Table II, p. 44.

JOURNAL OF THE OPTICAL SOCIETY OF AMERICA VOLUME 38, NUMBER 12 DECEMBER, 1948

Theory of the Corner-Cube Interferometer*

EDSON R. PECK
Department of Physics, Northwestern University, Evanston, Illinois
(Received April 15, 1948)

The corner-cube interferometer is analyzed geometrically and analytically. When the prisms are used near their axis, the instrument is found to behave essentially like an interferometer using triple sets of front-surface mirrors. Equations are obtained describing the fringe patterns when one prism is used far off its axis, and also when both are used near their axis. These fringe patterns are discussed and illustrated.

INTRODUCTION

A MODIFIED interferometer in which each of the two plane mirrors of a Michelson interferometer is replaced by a triple set of mirrors forming a corner right angle has already been described.[1] Such an interferometer, if the mirrors are front-surface reflectors, has two major advantages over the conventional Michelson instrument: it is permanently in adjustment independently of relative angular position of the two mirror sets, and it allows any arbitrary rotation of either mirror set about its corner point without affecting the fringes. It thus is able to measure relative motion between two points regardless of angular motion which may simultaneously occur.

If one of the mirror sets is mounted on a rotating table at some distance from the axis of rotation of the table, the interferometer can measure the chord of the arc through which the corner point of the mirror set moves. In this way, even with a lever arm of only 30 cm, angular motion can theoretically be measured to an accuracy of the order of one-fifth of a second of arc by counting whole fringes. The original application of this interferometer, and of a similar one using double mirrors, is to an infra-red recording spectrometer in which angular motion of the grating must be accurately measured for interpolation purposes.

In practice, the question immediately arises whether the set of front-surface mirrors could be replaced by a corner-cube prism. A corner-cube prism may be considered to be simply a corner cut off from a cubical piece of glass, in which the three mutually perpendicular faces of the cube are the reflecting faces of the prism, and the plane cut surface is the face through which light enters and leaves the prism. This diagonal refracting surface will usually make equal angles with the three reflecting faces in order to give the prism a maximum aperture, although such symmetry is not assumed in this paper. A corner-cube prism has the advantage over a mounting for three plane mirrors of permanence of adjustment within the mirror set, and it is feasible to produce a corner-cube prism to sufficiently close tolerances for interferometric work. However, the refraction occurring at the diagonal surface considerably complicates the theory of the interferometer, and raises the question of the existence of a center point about which the prism could be rotated through moderate angles without affecting the fringes. It seems worth while, accordingly, to present a thorough theoretical description of an interferometer constructed of the corner-cube prisms, and that is the purpose of this paper.

When the central line of sight makes a considerable angle (say 20° or more) with the normal to one of the prism faces, the fringe patterns for low orders of interference are of considerable beauty and interest. These patterns have been observed experimentally, and are found to check qualitatively in great detail with the results of the analysis presented here.

BASIC ANALYSIS

The analysis given here assumes corner-cube prisms in which the three reflecting faces are accurately plane and at exactly 90° to each other, the glass is homogeneous, and the glass-air refracting surface is plane.

* This work was supported in part by Navy Contract NObs 28373 with Northwestern University in connection with development of an infra-red recording spectrograph.
[1] Edson R. Peck, J. Opt. Soc. Am. **38**, 66 (1948).

Definitions

1. Corner point: The point in which the three reflecting faces of the prism intersect.

2. Glass surface: The glass-air refracting surface of the prism.

3. μ: The index of refraction relative to air of the glass of the prism. In numerical examples, the symbol is also used to mean a micron.

4. Optical path lengths will be expressed relative to wave-lengths in air: e.g., if distance l_i is in medium of index μ_i relative to air, then optical path length $\delta = \Sigma_i \mu_i l_i$.

5. Pole: The point of the glass surface at the foot of the normal to it from the corner point.

6. The depth D of the prism: The distance from the corner point to the pole.

7. Incident ray in glass: A ray after entering the glass, but before any of the internal reflections.

8. Emergent ray in glass: A ray in glass after one internal reflection at each of the three reflecting faces of the prism.

9. Incident and emergent rays: Rays in air incident on, and emergent from, the prism, respectively.

10. Glass angle, γ: The angle to the normal of the glass surface made by an incident or an emergent ray in glass.

11. Air angle, α: The angle to the normal of the glass surface made by an incident or an emergent ray (in air).

12. Point of incidence or emergence: A point of the glass surface where it is cut by an incident or an emergent ray.

13. Principal point: The point of the glass surface where for a ray of given direction the points of incidence and emergence coincide.

14. Real prism: The prism of the interferometer which is directly viewed.

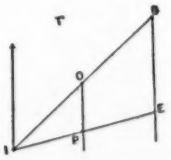

FIG. 1.

I = incident point
O = pole
P = principal point for the ray
E = emergent point
B = a point of construction
Γ = glass surface
(Arrow represents azimuth direction.)

15. Virtual prism: The image formed by reflection at the interferometer dividing plate of the prism seen by reflection.

16. Prism axis: The line passing through the corner point and the pole of a prism.

17. Glass space: Space of indefinite extent having index of refraction μ relative to air, in which rays may be constructed, and in which the reflections at the prism faces occur.

18. Optical center: The point on the prism axis at a depth D/μ below the glass surface.

19. Azimuth direction: The direction of the projection of the incident ray upon the glass surface.

20. Azimuth angle: The angle between the azimuth direction of a ray and a reference direction in the glass surface.

Axioms

The following two well-known properties of right-angle corner mirrors are basic to what follows, and will be taken as axioms.

1. The emergent ray in glass is parallel to the incident ray in glass, but reversed in direction.

2. The image in glass space of a point object in glass space is found by reflecting the object in the corner point: i.e., the image is on the straight line containing the object and the corner, and is located so that the corner is midway between object and image.

Theorems

The first seven of the following theorems follow easily from Snell's law, from the axioms, and from the earlier theorems of the set; so they are given without proof.

1. The emergent ray (in air) is parallel to the incident ray (in air).

2. The image in glass space of the glass surface is a plane parallel to the glass surface at a depth $2D$ below the glass surface.

3. Suppose an incident ray strikes the glass surface in incident point I with an azimuth direction represented by the arrow in Fig. 1, and that after refraction the glass angle is γ. The emergent point E may be found as follows:

Locate point B by reflecting point I in the pole O. From B lay off the distance $2D \tan\gamma$ in direction opposite to the azimuth direction at I,

to locate point E. Then E is the emergent point. See Fig. 1.

4. The emergent point coincides with the incident point when the incident ray in glass passes through the corner point. This locates the principal point for the ray, by definition.

5. The principal point for an incident ray of given direction may be located as follows: From the pole O lay off a line in the opposite direction to the azimuth direction of the incident ray. Locate point P on this line at distance $D\tan\gamma$ from 0. Then P is the required principal point. See Fig. 1.

6. The emergent point corresponding to any incident point of a ray of given direction may be located by reflecting the incident point in the principal point for the given direction. See Fig. 1.

7. The total optical path length of a ray in the prism is $2\mu D\sec\gamma$, as if the ray traveled in the glass straight from A, the image in glass space of the incident point, to E, the emergent point.

8. Let Γ be the glass surface of a corner-cube prism (Fig. 2). Let Π be a reference plane perpendicular to an incident ray which cuts it in A. Let P be the principal point for rays perpendicular to Π. Let I be the incident point, and E the emergent point for the given ray. Pass a plane Σ through P parallel to Π, and let the rays or their extension cut Σ in F and G. Let l be the distance from Π to Σ.

Then the total optical path length of the ray between its crossings of Π is

$$\delta = 2l + 2\mu D\sec\gamma;$$

and hence the optical path length is the same for all rays perpendicular to Π.

Proof: (1) The plane containing the incident and emergent rays contains P. For, by Theorem 6, P lies on the straight line joining I and E, both of which are in the plane.

(2) $\langle IP\rangle = \langle PE\rangle$ by Theorem 6.

(3) $\triangle FIP \cong \triangle GEP$: for they are right triangles whose hypotenuses are equal and whose angles are equal.

(4) $\therefore\ \langle FI\rangle = \langle GE\rangle$.

(5) The part of the optical path in air is $\langle AI\rangle + \langle EB\rangle$, which by (4) is the same as $\langle AF\rangle + \langle GB\rangle$, or $2l$.

(6) The part of the optical path in the glass is $2\mu D\sec\gamma$, by Theorem 7. This completes the proof.

9. In a modified Michelson type of interferometer in which the reflectors are corner-cube prisms, the interference effects may be considered as due to the reflection of an incident ray partly at the real prism and partly at the virtual prism (Definitions 14, 15), provided that no multiple reflection is considered to occur between prisms.

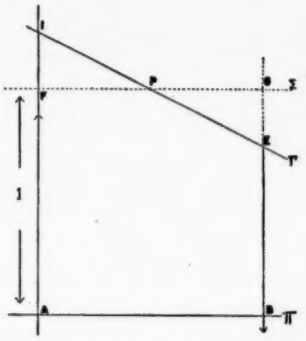

FIG. 2.

This method of analysis is traditional for the Michelson interferometer and does not require proving here. A proof may easily be made by the method used to prove Theorem 7.

10. Let Γ and Γ' be the glass surfaces of the real and the virtual corner-cube prisms in an interferometer (Fig. 3). Let a reference plane perpendicular to the incident ray be Π, cut by the incident ray in A, and cut by the emergent rays from the real and the virtual prisms in B and B', respectively. Let Σ and Σ' be planes parallel to Π, and passing through the principal points, for rays perpendicular to Π, of the real and the virtual prisms, respectively. Let l and l' be the distances of Σ and Σ' from Π; and let $l - l' = s$, the distance between Σ' and Σ.

Then the optical path retardation between the two emergent rays as they cut Π is

$$AB - AB' = \delta - \delta' = 2s + 2\mu D\sec\gamma - 2\mu' D'\sec\gamma',$$

where μ', D', γ' are for the virtual prism.

The proof follows at once from Theorems 8 and 9, the definition of s, and the parallelism (Theorem 1) of the emergent rays to the incident ray.

11. The corner-cube interferometer forms fringes which are in focus at infinity regardless of orientation or position of the corner-cube prisms, and regardless of the values of D and μ of the two prisms.

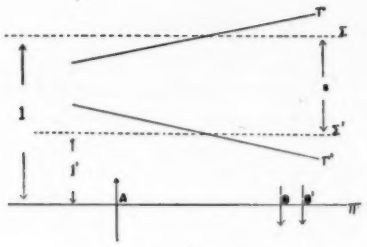

FIG. 3.

Proof: (1) The two emergent rays from a single incident ray are parallel (Theorem 1).

(2) All pairs of emergent rays having a given direction have the same relative optical path retardation with respect to a plane perpendicular to the rays (Theorem 10).

This establishes the theorem. It must be remembered that under certain conditions the fringes become much too fine to observe visually. Such fringes have been observed with a telescope.

12. The optical path length of a ray reflected at a corner-cube prism between its successive crossings of a reference plane II normal to the ray may be expressed as:

$$\delta = 2L + 2\mu D\left(\cos\gamma - \frac{\cos\alpha}{\mu^2}\right),$$

where L is the distance from II to the optical center of the corner-cube prism. (Def. 18). See also definitions 3, 4, 6, 10, and 11.

Proof: Let C, C_0, and O be, respectively, the corner optical center, and pole of the corner-cube prism. For rays normal to II, let the principal point be P. Let Γ be the glass surface of the prism. Let C', C_0', and $0'$ be the corner, optical center, and pole of the same prism rotated so that its surface Γ' is parallel to π, and placed so that C_0' coincides with C_0. Let Γ and Γ' intersect in Q. See Fig. 4.

(1) Compute the optical path δ' for the prism when its surface is parallel to II: then compute the *additional* path $\triangle\delta$ when the prism is rotated about its optical center to make an air angle α with the rays. Then the total path retardation in this position is $\delta = \delta' + \triangle\delta$.

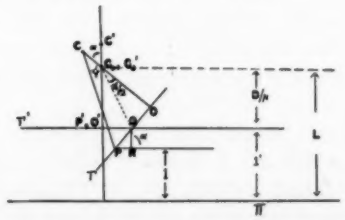

FIG. 4.

(2) $\delta' = 2l' + 2\mu D$ by Theorem 8, since in the primed position $\alpha' = \gamma' = 0$.

(3) $\triangle\delta = 2(l - l') + 2\mu D(\sec\gamma - 1)$ again by Theorem 8.

(4) $l - l' = \langle -QR\rangle$ in Fig. 4.

(5) Now

$$\langle OP\rangle = D\tan\gamma,$$

by Theorem 5

$$\langle OQ\rangle = \frac{D}{\mu}\tan(\alpha/2)$$

$$\langle QP\rangle = \langle OP\rangle - OQ$$

$$\langle QR\rangle = \langle QP\rangle \sin\alpha.$$

(6) Combining (3), (4), and (5) and using Snell's law and trigonometric reduction we obtain:

$$\triangle\delta = 2\mu D\left(\cos\gamma - 1 + \frac{\sin^2\gamma}{1+\cos\alpha}\right).$$

(7) Combining this with (1) and (2), noting that $l' = L - D/\mu$, and reducing, we find that

$$\delta = 2L + 2\mu D\left(\cos\gamma - \frac{\cos\alpha}{\mu^2}\right) \text{Q.E.D.}$$

Note that this expression is rigorous.

13. The total optical path length of a ray reflected at a corner-cube prism, between its successive crossings of a reference plane normal to the ray and at distance L in front of the optical center of the prism, may be expanded as follows in a power series in terms of the angle α in radians:

$$\delta = 2L + 2\mu D\left(1 - \frac{1}{\mu^2}\right) + \frac{D}{4\mu}\left(1 - \frac{1}{\mu^2}\right)\alpha^4 + \frac{D}{24\mu}\left(1 - \frac{1}{\mu^2}\right)\left(\frac{3}{\mu^2} - 1\right)\alpha^6 + \cdots.$$

Proof: Two methods were found for obtaining this expansion. Details will not be given, but the outline of one method is as follows:

(1) Use

$$\cos\gamma = (1 - \sin^2\gamma)^{\frac{1}{2}} = \left(1 - \frac{\sin^2\alpha}{\mu^2}\right)^{\frac{1}{2}}.$$

Expand the radicand and then use the binomial expansion to obtain $\cos\gamma$ expanded in powers of α.

(2) Expand

$$\frac{\cos\alpha}{\mu^2}$$

in powers of α.

(3) Substitute into δ as given in Theorem 12.

Remarks: Note that α does not enter until the 4th power term, and then with a fairly small coefficient. Thus for moderate values of α, δ is essentially independent of α. Table I shows the dependence upon angle of the 4th and 6th power terms for an average prism.

14. Given a corner-cube interferometer in which the distance between optical centers of the real and virtual prisms is S. The relative path retardation for rays making an angle β with S is

$$\delta-\delta'=2S\cos\beta+2\mu D\left(\cos\gamma-\frac{\cos\alpha}{\mu^2}\right)-2\mu' D'\left(\cos\gamma'-\frac{\cos\alpha'}{\mu'^2}\right),$$

where unprimed and primed symbols refer, respectively, to the real and the virtual prism.

Proof: Let Π be a plane normal to the rays. Use Theorems 9 and 12, and the relation $L-L'=S\cos\beta$ (cf. Fig. 5).

Corollary: For front-surface sets of mirrors, this reduces to $\delta-\delta'=2S\cos\beta$ where S now becomes the distance between corner points.

Proof: For front-surface reflectors,

$$\mu=\mu'=1, \quad \gamma=\alpha, \quad \gamma'=\alpha'.$$

15. Let QR be a reference direction of view into a corner-cube interferometer. Let the line of the virtual and real optical centers be S, making an angle d with QR (Fig. 6a). Let NC_0 be the optic axis of the real prism making an angle c with QR, and lying in the same plane as QR and S. Let this plane be the zero azimuth plane, and let the actual direction of view make an angle b with QR and lie at an azimuth angle A, zero azimuth sense being defined so that the direction of view parallel to NC_0 has zero azimuth. (Def. 20.) Let the virtual prism have its axis parallel to QR.

These conventions are shown in the spherical triangles of Fig. 6b, in which vertex A is the direction of reference and the angle at this vertex is the azimuth angle A, vertex V is the direction of view, vertex U is the direction of NC_0, and vertex W is the direction of S.

If now the angle b remains small enough that for the virtual prism only the constant part of the expansion of Theorem 13 need be used, the relative path retardation may be expanded as a power series in b whose terms up to the 3rd degree are:

$$\delta-\delta'=k_1+k_2b\cos A+k_3b^2\cos^2A+k_4b^2+k_6b^3\cos A+k_7b^3\cos^3A+\cdots,$$

where

$$k_1=2D\left[(\mu^2-\sin^2c)^{\frac{1}{2}}-\frac{\cos c}{\mu}\right]-2D'\left(\mu'-\frac{1}{\mu'}\right)+2S\cos d,$$

$$k_2=2D\left[(\mu^2-\sin^2c)^{-\frac{1}{2}}\cos c-\frac{1}{\mu}\right]\sin c+2S\sin d,$$

$$k_3=D(\mu^2-1)(\mu^2-\sin^2c)^{-\frac{3}{2}}\sin^2c,$$

$$k_4=D\left[\frac{1}{\mu}-(\mu^2-\sin^2c)^{-\frac{1}{2}}\cos c\right]\cos c-S\cos d,$$

$$k_6=D\left[\frac{1}{3\mu}-\frac{4}{3}(\mu^2-\sin^2c)^{-\frac{1}{2}}\cos c+(\mu^2-\sin^2c)^{-\frac{3}{2}}\cos^3c\right]\sin c-\frac{1}{3}S\sin d,$$

$$k_7=D(1-\mu^2)(\mu^2-\sin^2c)^{-5/2}\sin^3c\cos c.$$

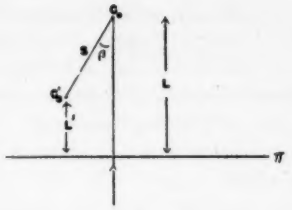

FIG. 5.

Proof: 1. Evaluate the cosines of the angles β, α, γ of Theorem 14 in terms of a power series in the angle b. Use the following relations from spherical trigonometry (Cf. Fig. 6b):

$$\cos\beta=\cos d\cos b+\sin d\sin b\cos A$$
$$\cos\alpha=\cos c\cos b+\sin c\sin b\cos A.$$

In particular we find that to the 3rd degree in b:

$$\cos\beta=\cos d+b\cos A\sin d-\frac{b^2}{2}\cos d-\frac{b^3}{6}\cos A\sin d, \quad \text{(i)}$$

$$\cos\alpha=\cos c+b\cos A\sin c-\frac{b^2}{2}\cos c-\frac{b^3}{6}\cos A\sin c, \quad \text{(ii)}$$

$$\cos\gamma=\frac{1}{\mu}(\mu^2-1+\cos^2\alpha)^{\frac{1}{2}}, \quad \text{(iii)}$$

from Snell's law.

TABLE I. Dependence of retardation upon air angle.*

Angle		4th Power term, microns	6th Power term, microns
Radians	Degrees		
.06	3.44	0.0367	
.08	4.58	0.116	
0.10	5.73	0.282	0.0001
0.12	6.87	0.591	
0.40	22.9	72.3	0.48

* Computed for $D=3$ cm; $\mu=1.55$; $\delta=2L+5.43$ cm $+0.2824$ cm$\alpha^4+0.0117$ cmα^6.

Substituting for $\cos\alpha$ from (ii), we obtain

$$\cos\gamma=\frac{1}{\mu}(\mu^2-\sin^2c)^{\frac{1}{2}}\left[1+\frac{u}{(\mu^2-\sin^2c)}\right]^{\frac{1}{2}},$$

where $u=2b\cos A\sin c\cos c+b^2(\cos^2A\sin^2c-\cos^2c)$
$-(4/3)b^3\cos A\sin c\cos c.$

Binomial expansion in powers of $u/(\mu^2-\sin^2c)$, and rearrangement yields

$$\cos\gamma=\frac{1}{\mu}(\mu^2-\sin^2c)^{\frac{1}{2}}+\left[\frac{1}{\mu}(\mu^2-\sin^2c)^{-\frac{1}{2}}\sin c\cos c\right]b\cos A$$
$$+\left[\frac{1}{2\mu}(\mu^2-\sin^2c)^{-\frac{1}{2}}\sin^2c\right.$$
$$\left.-\frac{1}{2\mu}(\mu^2-\sin^2c)^{-\frac{1}{2}}\sin^2c\cos^2c\right]b^2\cos^2A$$
$$-\left[\frac{1}{2\mu}(\mu^2-\sin^2c)^{-\frac{1}{2}}\cos^2c\right]b^2$$
$$+\left[\frac{1}{2\mu}(\mu^2-\sin^2c)^{-\frac{1}{2}}\sin c\cos^2c\right.$$
$$\left.-\frac{2}{3\mu}(\mu^2-\sin^2c)^{-\frac{1}{2}}\sin c\cos c\right]b^3\cos A$$
$$+\left[\frac{1}{2\mu}(\mu^2-\sin^2c)^{-3/2}\sin^2c\cos^2c\right.$$
$$\left.-\frac{1}{2\mu}(\mu^2-\sin^2c)^{-\frac{1}{2}}\sin^2c\cos c\right]b^3\cos^2A.$$

2. Now

$$\alpha'=b;$$

so that if b is small enough we may use Theorem 13 to replace

$$2\mu'D'[\cos\gamma'-(\cos\alpha')/\mu'^2]$$

by

$$2\mu'D'(1-1/\mu'^2).$$

3. Finally, substitution of these results into Theorem 14 yields the result of the present theorem. Q.E.D.

Remarks: If b remains small, the fringe pattern in the focal plane of an ideal projection lens may be deduced from Theorem 15 by putting $\delta-\delta'=$const. for a fringe, and using $b\cos A=x$, $b^2=x^2+y^2$ etc., but this approximation is not good to the 3rd degree terms, so a further analysis is necessary to derive the fringe curves in the focal plane of a projection lens.

16. Let x and y be rectangular coordinates in the focal surface, assumed plane, of an ideal projection lens of unit focal length used to view the fringes of the corner-cube interferometer. Let the axis of the lens coincide with the reference direction of view, and let the angle of view be defined by polar angle b and azimuth angle A. Take the x axis in the direction and sense of zero azimuth. Let x, y, be small compared to unity; for to apply Theorem 15, we assume $b\leqq\frac{1}{10}$ rad., approximately.

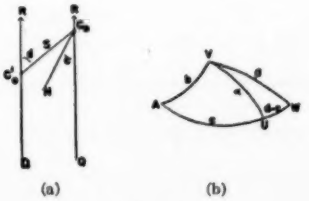

(a) (b)

FIG. 6.

Then the values of x and y are related to b and A by power series in b which are, including the 3rd degree terms:

$$b\cos A=x-\tfrac{1}{3}x(x^2+y^2);\quad b\sin A=y-\tfrac{1}{3}y(x^2+y^2)$$
$$b^2\cos^2A=x^2;\quad b^2\sin^2A=y^2\quad\therefore b^2=x^2+y^2$$
$$b^3\cos A=x(x^2+y^2);\quad b^3\cos^3A=x^3.$$

Proof: 1. By the hypotheses, $\tan b=(x^2+y^2)^{\frac{1}{2}}$

$$\therefore\quad x=\tan b\cos A$$

and

$$y=\tan b\sin A.$$

2. $\therefore\quad b=\tan^{-1}(x/\cos A)=\tan^{-1}(y/\sin A).$

3. Expanding, to 3rd degree term:

$$b=\frac{x}{\cos A}-\frac{x^3}{3\cos^3A}=\frac{y}{\sin A}-\frac{y^3}{3\sin^3A}.$$

4. $\therefore\quad b\cos A=x-\dfrac{x^3}{3\cos^2A}.$

5. But

$$\cos^2A=\frac{x^2}{x^2+y^2};\quad\therefore\ b\cos A=x-\tfrac{1}{3}x(x^2+y^2)$$

and similarly for $b\sin A$.

6. Derive the remaining parts of the theorem by use of these expressions for $b\cos A$ and $b\sin A$.

17. Relative path retardation for the interferometer of Theorem 15 may be expressed to the 3rd degree in the Cartesian coordinates of the focal plane of the ideal projection lens of Theorem 16 as follows:

$$\delta-\delta'=k_1+k_2x+k_3x^2+k_4(x^2+y^2)$$
$$+(k_6-\tfrac{1}{3}k_2)x(x^2+y^2)+k_7x^3\quad(1)$$

where the k's are the coefficients of Theorem 15.

The proof is immediate upon substitutions of the results of Theorem 16 into Theorem 15.

It is convenient to define new coefficients:

$$k_5=k_3+k_4$$
$$k_8=k_6-\tfrac{1}{3}k_2+k_7$$
$$k_9=k_6-\tfrac{1}{3}k_2$$

Then theorem 17 may be written:

$$\delta-\delta'=k_1+k_2x+k_4y^2+k_5x^2+k_8x^3+k_9xy^2,\quad(2)$$

where now k_1, k_2, and k_4 are as before, while

$$k_5=D\left[\frac{1}{\mu}\cos c-(\mu^2-\sin^2 c)^{-\frac{1}{2}}\cos^2 c+(\mu^2-1)(\mu^2-\sin^2 c)^{-\frac{1}{2}}\sin^2 c\right]-S\cos d,$$

$$k_8=D\left[\frac{1}{\mu}-2(\mu^2-\sin^2 c)^{-\frac{1}{2}}\cos c+(\mu^2-\sin^2 c)^{-\frac{1}{2}}\cos^3 c-(\mu^2-1)(\mu^2-\sin^2 c)^{-5/2}\sin^2 c\cos c\right]\sin c-S\sin d,$$

$$k_9=D\left[\frac{1}{\mu}-2(\mu^2-\sin^2 c)^{-\frac{1}{2}}\cos c+(\mu^2-\sin^2 c)^{-\frac{1}{2}}\cos^3 c\right]\sin c-S\sin d.$$

The cubic curves which result when $\delta-\delta'=n\lambda$ are sufficiently good approximations to describe in detail the appearance of the fringes. These curves contain y only to the 2nd degree, so that they are symmetrical about the x axis as also our hypotheses require. They may be described as approximations to conic sections for limited regions about a new origin at x_0 on the x axis as follows:

Let $x'=x-x_0$. Then the equation for the fringes becomes:

$$\delta-\delta'=n\lambda=(k_1+k_2x_0+k_5x_0^2+k_8x_0^3)+(k_2+2k_5x_0+3k_8x_0^2)x'+(k_5+3k_8x_0)x'^2+(k_4+k_9x_0)y^2+k_8x'^3+k_9x'y^2. \quad (3)$$

In sufficiently restricted regions about the new origin, we may neglect the third order terms in the variables, and we have then approximately

$$n\lambda\doteq(k_1+k_2x_0+k_5x_0^2+k_8x_0^3)+(k_2+2k_5x_0+3k_8x_0^2)x'+(k_5+3k_8x_0)x'^2+(k_4+k_9x_0)y^2, \quad (4)$$

x', y small.

Now x_0 will be the center of an approximate elliptic or hyperbolic conic section if the coefficient of x' vanishes:

$$k_2+2k_5x_0+3k_8x_0^2=0$$

so that directions of conic-section centers are given by the solutions:

$$x_0=\frac{-k_5\pm(k_5^2-3k_2k_8)^{\frac{1}{2}}}{3k_8} \quad (5)$$

provided the solution is small enough to be in the field of view at all, and to fit under the limit of Theorem 15. When the coefficient k_8 is small, it may happen that two centers of conic sections are in view simultaneously. The point midway between the solutions (5) may be considered an origin near which the fringes are parabolic, for there the coefficient of x'^2 vanishes.

DETAILED EXAMINATION OF FRINGE PATTERNS

Suppose one of the corner-cubes to be movable by a screw and ways parallel to the reference direction of view, i.e., parallel to the axis of the projection lens. Then $S\cos d$ is the component of S parallel to the screw, while $S\sin d$ is the component of S perpendicular to the screw. Thus if we let $\zeta=S\cos d$, and $\xi=S\sin d$, ζ is a measure of the screw displacement while ξ remains constant during the screw motion. Let us examine the fringe patterns for given choices of ξ as ζ changes continuously from large negative values to large positive values. There will be two general cases of interest: Case I in which glass corner-cube prisms are used, one being cocked at an appreciable angle to the reference direction, the other having its axis parallel to the reference direction, as in Theorem 15; case II in which both prism axes are parallel to the reference direction or front-surface mirrors are used, so that their orientation is irrelevant. The case of front surface reflectors may be obtained immediately by putting $\mu=1$ throughout this paper.

Case I. To obtain a numerical example, take $\mu=1.55$, $D=3$ cm; $C=+20°$. The values of the k's of Theorem 17 are then:

$$k_1=2\zeta+42.6 \text{ microns}$$
$$k_2=2\xi-484.2\mu$$
$$k_3=1424.5\mu$$
$$k_4=-\zeta+665.1\mu$$
$$k_5=-\zeta+2089.6\mu$$
$$k_8=-\xi-3872.0\mu$$
$$k_9=-\xi-3671.7\mu.$$

(a) Choosing $k_2=0$ will cause one of the conic-section centers always to fall at $x_{01}=0$, by Eq. (5). This may be accomplished physically by lateral adjustment of one prism until $\xi=+242.1\mu$.

Then $k_8=-4114.1\mu$, $k_9=-3913.8\mu$, and the position of the other root will be from Eq. (5):

$$x_{02}=-2k_5/3k_8=+1.620\times10^{-4}k_5.$$

TABLE II. Description of fringe patterns with one prism 20° off axis.

k_5	Center 1, at $x=0$ Form of curve	Location	Center 2 Form of curve	Path retardation interval between centers
$<-1425\mu$	Ellipses, major axis horizontal, near circles			
-1425μ	Ellipses, major axis horizontal, ratio of axes 2:1			
-617μ	Ellipses, major axis horizontal, ratio of axes 3.31:1	$-1/10$	Hyperbolae, major axis horizontal ratio of axes 2.68:1	-2.06μ
0	Horizontal lines at origin, rounding off at right. (Cubic terms important.)	0	Horizontal lines at origin, spreading out to left. (Cubic terms important.)	0
$+617\mu$	Hyperbolae, major axis horizontal ratio of axes 1.31:1	$+1/10$	Ellipses, major axis horizontal, ratio of axes 1.94:1	$+2.06\mu$
$+712\mu$	Equilateral hyperbolae			
$+950\mu$	Hyperbolae, major axis vertical, ratio of axes 1:2			
$+1425\mu$	Vertical lines			
$+2849\mu$	Ellipses, major axis vertical, ratio of axes 1:2			
$>2849\mu$	Ellipses, major axis vertical, near circles			

Substitution of these two roots into (4) leads to

$$n\lambda = k_1 + k_5 x'^2 + (k_5 - 1425\mu)y^2 \qquad (6a)$$

for root 1, and for root 2:

$$n\lambda = (k_1 + \tfrac{1}{3}k_5 x_{02}^2) - k_5 x'^2 + (0.3658k_5 - 1425\mu)y^2. \qquad (6b)$$

If we limit x_{02} to the field of view: $|x_{02}| \leqq \frac{1}{10}$. Then $|k_5| \leqq 617\mu$; $\therefore\ 1473 \leqq \zeta \leqq 2707\mu$ is the range in which two centers are seen. Outside of this range, only one center will be visible, that at $x_{01}=0$. When two centers are visible, the path retardation between them is $(k_5/3)x_{02}^2$. Fringes will be elliptical when coefficients of x'^2 and y^2 have like signs, and hyperbolic when they have unlike signs. When two centers are visible, one is hyperbolic and the other elliptical, except in the special case $k_5=0$ for which conic sections are poor approximations, and degenerate into straight lines.

Table II gives the salient characteristics of the pattern for selected values of k_5, which is used rather than ζ since it gives a simpler form to Eqs. (6).

(b) If $k_2 \neq 0$, then the two centers are symmetrically located with respect to the reference direction when k_5 passes through zero; and then they are given by $x_0 = \pm(-k_2/3k_3)^{\frac{1}{2}}$. They are then both real, and are in view if k_2 is small and positive (since k_3 will still be negative): in particular, if

$$0 < k_2 \leqq -0.03k_3.$$

Now we can distinguish one center $x_{0+} > 0$, and the other center $x_{0-} < 0$. The center x_{0+} is the nearer to the reference direction for $k_5 < 0$, while x_{0-} is the nearer for $k_5 > 0$. As $|k_5|$ becomes large, the nearer center approaches the reference direction, and the farther center soon disappears from view.

Now at a center, we may always rewrite Eq. (4) as:

$$n\lambda = (k_1 - k_5 x_0^2 - 2k_3 x_0^3) \pm (k_5^2 - 3k_2 k_3)^{\frac{1}{2}} x'^2 + (k_5 - k_3 + k_3 x_0) y^2, \qquad (7)$$

where the (+) sign of the radical is for x_{0-}, the (−) for x_{0+}. Thus the coefficient of x'^2 always changes sign when we pass from one center to the other. But when both centers are visible together, consideration of the magnitudes of the quantities shows that the coefficient of y^2 remains negative. Thus when both centers are visible together x_{0+} is an elliptical center, while x_{0-} is hyperbolic. When k_5 becomes sufficiently large and positive, x_{0-} becomes a center of ellipses having their major axis vertical; while if k_5 is large and negative, x_{0+} is a center of ellipses having their major axis horizontal. As $|k_5|$ increases, both of these sets of ellipses approach circles.

Cubic Terms

The cubic terms in (3) have the effect of causing the vertical axes of the approximate conic sections to appear curved. To understand this effect it will help to consider the locus of points where the retardation $(\delta - \delta')$ becomes independent of the horizontal coordinate x' or x. Unless the retardation is then also independent of y, these will be points where the fringes have a horizontal slope, and hence will appear to be points on the vertical axis of elliptic or hyper-

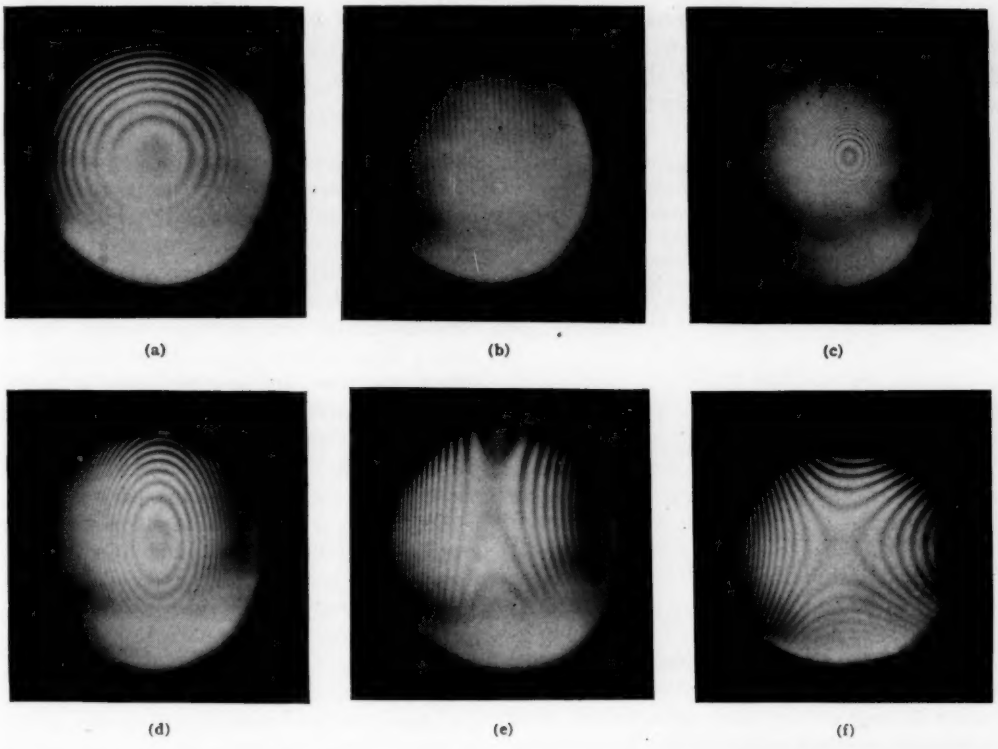

bolic conic sections. From Eq. (2):

$$\frac{\partial(\delta-\delta')}{\partial x}=k_2+2k_5x+3k_8x^2+k_9y^2$$

which when set to zero yields the locus

$$\left(x+\frac{k_5}{3k_8}\right)^2+\frac{k_9}{3k_8}y^2=\frac{k_5^2-3k_2k_8}{9k_8^2}. \qquad (8)$$

The right-hand member of this equation is positive whenever the conic section centers x_0 of Eq. (5) are real. The equation then represents an ellipse when k_8 and k_9 have the same sign, as will usually be the case for the data of our example. The ends of the horizontal axis of this ellipse lie at the positions x_0 of Eq. (5), the conic section centers. The fringes in the neighborhood of the x_0 appear distorted for fairly large values of y^2, as though their vertical axes were bent to follow the locus (8). It is apparent, then, that these "curved axes" for the two conic section centers curve towards each other as y^2 increases when (8) represents an ellipse. The locus (8) has

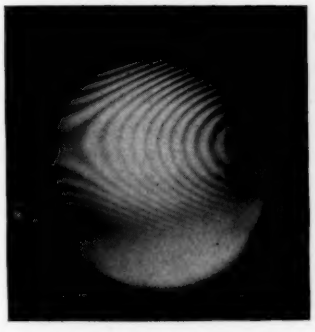

FIG. 7. Photographs of fringes from a corner-cube interferometer. (a) and (b): When properly adjusted. (c)–(g): When one prism is used considerably off axis.

for its ratio of vertical to horizontal axis the value $(3k_8/k_9)^{\frac{1}{2}}$, which for our data will usually approximate $3^{\frac{1}{2}}$.

In the special case $k_2=k_5=0$ when both the x_0 coincide at the origin, (8) degenerates into a point at the origin, and there will be no place in the field of view where the fringes have a horizontal slope outside of the neighborhood of the origin.

Case II. Front-surface reflectors: Throughout this paper, the case of front-surface reflectors may be obtained by simply putting $\mu=\mu'=1$, and $\gamma=\alpha$, $\gamma'=\alpha'$. Then the coefficients of Theorem 17 become:

$$k_1=S\cos d=\zeta$$
$$k_2=2S\sin d=2\xi$$
$$k_3=0$$
$$k_4=-S\cos d=-\zeta$$
$$k_5=-S\cos d=-\zeta$$
$$k_6=-S(\sin d/3)=-\xi/3$$
$$k_7=0$$
$$k_8=-S\sin d=-\xi$$
$$k_9=-S\sin d=-\xi.$$

Important special cases occur when:

$$S\sin d=\xi=0. \qquad (IIa)$$

Then $n\lambda=\zeta-\zeta(x^2+y^2)$ giving circles about the origin, as in the ordinary interferometer.

$$S\cos d=\zeta=0, \quad n\lambda=2\xi x-\xi x^3-\xi xy^2, \quad (IIb)$$

which are approximations to vertical straight, equidistant lines. Here it is a very good approximation to neglect the cubic terms, since their coefficients are small ($\frac{1}{2}$ that of the linear term). Thus in the field of view ($\frac{1}{10}$ radian about the reference direction), the combined magnitude of the cubic terms never exceeds 1 percent of the linear term. The fringes therefore appear straight, parallel, and equidistant.

Fringes from a properly adjusted corner-cube interferometer, in which the axes of both the real and virtual prisms are parallel to the reference direction of view, will, of course, be the same as from front-surface reflectors except for the constant term

$$2D(\mu-1/\mu)-2D'(\mu'-1/\mu')$$

appearing in coefficient k_1. If the prisms are not identical, zero-order fringes may then be circular; and when observed with white light, the effect of dispersion must be taken into account.

Figure 7 shows some typical sodium light fringes photographed directly from a corner-cube interferometer. In Figs. 7a and 7b, both prisms have their axes parallel to the reference direction of view, and so give fringes as for front surface reflectors, cases (*IIa*) and (*IIb*). In Figs. 7c–7g, one prism axis is inclined at an angle of the order of 20°, and in a horizontal plane, from the reference direction, and in such a sense that a direction of view to the right in the photographs is parallel to the tilted prism axis. In these pictures many of the details described under case *I* may be observed.

SUMMARY

We have shown that for monochromatic light, a corner-cube interferometer may be used to perform all the functions of an interferometer using front-surface sets of mirrors, provided the axes of the prisms are properly adjusted, and provided any rotation of the prisms is small and occurs about their optical center. We have obtained general geometrical theorems and analytical formulas applying to the corner-cube interferometer, and have deduced the fringe patterns for special cases.

JOURNAL OF THE OPTICAL SOCIETY OF AMERICA VOLUME 38, NUMBER 12 DECEMBER, 1948

The Effect of Chromatic Adaptation on Achromaticity

HARRY HELSON AND WALTER C. MICHELS
Bryn Mawr College, Bryn Mawr, Pennsylvania

(Received June 2, 1948)

The tristimulus values of a small (foveal) spot which appears achromatic to an eye which is adapted to a uniform chromatic background have been found experimentally. Various colors have been used for the background, and a considerable range of luminances has been employed for both the background and the spot. It is found that the chromaticity coordinates of the achromatic spot can be predicted by interpolation between the coordinates of a "white point," which is independent of the state of adaptation, and those of the background. An empirical interpolation formula, which expresses the effect of adaptation as a function of the tristimulus values of the background and the achromatic spot, is presented.

I. INTRODUCTION

THE problem of defining the achromatic or neutral point of the eye for all states of adaptation has now become central for both theory and practice of colorimetry and for further insight into the nature of the visual response system. Modern colorimetry is based on a standard observer viewing small colored patches against a completely dark surround, hence under a single, restricted adaptation of the eye. Such representations as the I.C.I. trilinear mixture diagram are markedly successful in dealing with color specifications, particularly with reference to color matches, under conditions which do not depart too far from the original viewing conditions of the standard observer. On the other hand, colors are generally observed against various backgrounds, often highly selective, and in various illuminants which may differ considerably from daylight. In view of the great usefulness of the I.C.I. mixture diagram and similar methods of specifying colored stimuli, it seems worth while to attempt to extend the system in order to obtain a better correlation between color specification and perceived colors under all conditions of adaptation.

Previous studies of adaptation, with but few exceptions, have been concerned with the effects of small colored patches well within the macular region. In this study the method of flooding the whole retina with strongly chromatic light, as used by Helson and his co-workers[1,2] and by Judd,[3] has been employed with important modifications. Whereas these writers were concerned with the changes in colors of reflecting stimuli in strongly chromatic illuminants, here we shall be concerned with the effect of general chromatic adaptation upon a foveal stimulus which is physically independent of the background illumination in that it emits its own light and reflects no light. By determining the tri-stimulus values of this stimulus when it was adjusted to achromaticity with various hues and brightnesses of surround, it was possible to trace the movement of the achromatic point as a function of chromatic adaptation.

II. THE COLORIMETER

The colorimeter used to produce the achromatic spot follows a design suggested by Dr. Deane B. Judd. It consists of a metal spherical shell, 25.0 cm. in diameter, coated on the inside with sphere paint. A 1.5-cm. diameter hole serves as the exit pupil for the mixed light. This light is supplied from three lamp housings, separated by 120° longitude and each 110° from a pole at the exit pupil. Each lamp housing contains a 6–8-volt headlight lamp. Light from the lamps is admitted to the sphere through three filters (red, blue, green) and through three "cat's eye" diaphragms which can be adjusted from zero opening to an opening of about four square inches in area.

After aging, a group of lamps were adjusted to

[1] H. Helson, "Fundamental problems in color vision. I. The principle governing changes in hue, saturation, and lightness of non-selective samples in chromatic illumination," J. Exp. Psychol. **23**, 439 (1938).

[2] H. Helson and V. B. Jeffers, "Hue, lightness and saturation of selective samples in chromatic illumination," J. Exper. Psychol. **26**, (1940).

[3] D. B. Judd, "Hue, saturation, and lightness of surface colors with chromatic illumination," J. Opt. Soc. Am. **30**, 2 (1940).

TABLE I. Characteristics of colorimeter sources (standard 40 division opening).

Source color	Tristimulus values (arbitrary units)			Chromaticity coordinates		
	X	Y	Z	x	y	z
Red	1015	410	0	0.713	0.287	0.000
Green	181	472	78	0.249	0.645	0.106
Blue	192	75	1084	0.142	0.056	0.802

color temperature 2848°K. The adjustment was obtained by running spectral distribution curves at several currents for each lamp with a photoelectric spectrophotometer, comparing with a similar curve for two standard lamps, and interpolating to find the correct current for 2848°K operation. Three lamps were found to give this color temperature within ±20° when operated at 1.036 ampere. These three were used in the colorimeter and were operated in series during the subsequent measurements.

The three lamp-diaphragm combinations (without filters) were intercompared by visual photometry, with the diaphrams set at a standard opening (40 scale divisions, almost wide open). An arbitrary unit of luminance was taken as the luminance of the lamp later used with the blue filter. The diaphragms were then calibrated by mounting all three lamps, with their associated diaphragms and filters, on the colorimeter and measuring the light output as a function of diaphragm opening.

The tristimulus values for each lamp filter combination were calculated, using 100 selected ordinates for the red source and 20-A.U. intervals for the blue and green sources. These are given, for the standard diaphragm opening of 40 scale divisions, in Table I along with the chromaticity coordinates of the three sources.

As a check on the colorimeter calibration, two spectral distribution curves of the light emitted from the exit pupil with all three diaphragms partially open were taken. The diaphragm settings for the red, green, and blue sources, respectively, were 40:40:40 and 15:25:40. (The areas of the diaphragm openings vary approximately as the square of the scale readings.) The curves obtained in this way were compared with those calculated from the independent measurements on lamp intensity, filter transmittance, and diaphragm opening. The observed and calculated curves disagreed at no wave-length by more than five percent.

In order that the arbitrary Y values might be converted to luminance at the exit pupil, a series of color matches of the light coming from the colorimeter to a background illuminated by incandescent light were made. At the same time, the background luminance was measured with a Macbeth illuminometer. The conversion factor from our tristimulus units to apparent footcandles (or foot-lamberts) was found to be

$$1\ Y \text{ unit} = 0.00171 \text{ apparent footcandle} \pm 2 \text{ percent.}$$

All luminances given in this paper were calculated from the tristimulus values and this conversion factor.

III. PROCEDURE

The conditions of observation were designed to provide a known, uniform field of stimulation filling the whole eye with strongly chromatic light to insure complete and thorough adaptation at various luminance levels. In the center of the field was an aperture, the exit pupil of the colorimeter, flush with the surround. A semicylindrical booth, four feet in diameter and six feet high, lined with fairly matt, non-selective, highly reflective cardboard (daylight white), was the means by which a uniform surround was provided. Observers sat facing the booth within easy reach of the controls regulating the colorimeter diaphragms. The aperture, which was 1.5 cm in diameter, subtended an angle of 1°35′ at the eye and hence was within the limits of the fovea so far as the stationary eye was concerned. The chromatic field was provided by an incandescent lamp and chromatic, glass-filter combination mounted in a light-tight housing above and behind the head of the observer. The luminance of the surround was varied by inserting perforated cardboard filters between the lamp source and the glass filter. Current on the lamp was held constant, and measurements for chromaticity and luminance of surround were made before the beginning of each observational period by matching the aperture to the surround. The chromaticity coordinates and luminances of the surrounds given in Table III are averages of several matchings by the three observers. Be-

cause of the limitations of the colorimeter, a match between the aperture and the surround was not possible in the case of the red and blue illuminants until a small admixture of incandescent-lamp light (2848°K) was added to the field. This was accomplished by means of a small slit in the lamp housing, directly above the chromatic filter, which could be adjusted to give the minimum amount of incandescent-lamp light necessary for a match.

The chromaticity coordinates and the luminance of the surround for each condition are given in Table III, from which it is seen that five luminance levels ranging from 8.63 to 0.10 app.f.c. were employed with the yellow, four levels ranging from 0.76 to 0.03 app.f.c. with the red, four levels ranging from 0.76 to 0.04 with the green, and two levels, 0.06 and 0.014, with the blue. Since the lower limit of photopic vision is usually given as approximately 0.10 app.f.c. it is seen that some of our field luminances were at the scotopic level but, in spite of this fact, results with these low luminances are consistent with the photopic data. The fact that the whole retina was subjected to chromatic stimulation probably is responsible for effective adaptation at these low luminances. Observers were required to view the surround for five minutes before making any settings. This period of pre-adaptation, plus the use of strongly chromatic surrounds that filled the eyes with uniform stimulation, assured complete chromatic adaptation.

The task set the observers was to make the central spot (the exit pupil of the colorimeter) achromatic or neutral by turning the handles which regulated the amounts of light from the three primaries of the colorimeter. After preliminary practice the following procedure in making the settings was adopted and was found to yield reliable results both from the point of view of individual consistency and inter-observer variation. All settings were made from an initial high, medium, or low luminance of the aperture spot by having the observers adjust the primaries to give scale readings of 45,45,45, or 25,25,25, or 15,15,15. At these positions the aperture color was rarely, if ever, anywhere near achromaticity, and the observers had to produce a satisfactory neutral by readjusting the controls. Three determinations were made of the achromatic point at each of these levels in random order with each surround. Since four different chromaticities at from two to five luminances were employed, the total number of conditions investigated, including the case of achromaticity with completely dark surround, was forty-seven. The total number of determinations of the achromatic point is thus 423 if the three replications by the three observers are taken into account.

Before the final series of observations, observers adjusted the aperture spot to achromaticity under a variety of conditions: dark surround, "white" surround with 2848°K illumination, and some chromatic surrounds. At first observers were faced with the problem as to what constituted a neutral or achromatic spot, since no standard could be furnished for com-

TABLE II. Settings of three observers for achromaticity of a small spot in a strongly chromatic (green) field at relatively high, medium, and low luminance with four field luminances.

Background luminance (App.f.c.)	Background chromaticity coordinates x	y	z	Achromatic spot luminance (App.f.c.)	Achromatic spot chromaticity coordinates x	y	z	observers
0.78	0.243	0.616	0.141	0.99	0.272	0.499	0.229	G
0.75	0.236	0.578	0.186	1.05	0.255	0.479	0.266	H
0.77	0.249	0.645	0.106	1.04	0.227	0.443	0.330	J
0.78	0.243	0.616	0.141	0.35	0.249	0.639	0.112	G
0.75	0.236	0.578	0.186	0.36	0.247	0.471	0.282	H
0.77	0.249	0.645	0.106	0.36	0.211	0.430	0.359	J
0.78	0.243	0.616	0.141	0.12	0.252	0.636	0.112	G
0.75	0.236	0.578	0.186	0.08	0.261	0.638	0.101	H
0.77	0.249	0.645	0.106	0.12	0.252	0.636	0.112	J
0.26	0.243	0.628	0.129	1.17	0.270	0.371	0.359	G
0.27	0.246	0.648	0.106	1.21	0.226	0.283	0.491	H
0.26	0.246	0.649	0.105	1.25	0.230	0.269	0.501	J
0.26	0.243	0.628	0.129	0.47	0.272	0.470	0.258	G
0.27	0.246	0.648	0.106	0.36	0.238	0.428	0.334	H
0.26	0.246	0.649	0.105	0.41	0.217	0.307	0.476	J
0.26	0.243	0.628	0.129	0.12	0.275	0.567	0.158	G
0.27	0.246	0.648	0.106	0.13	0.287	0.611	0.102	H
0.26	0.246	0.649	0.105	0.12	0.252	0.635	0.113	J
0.09	0.244	0.628	0.128	1.17	0.246	0.280	0.474	G
0.10	0.247	0.645	0.108	1.21	0.242	0.260	0.498	H
0.10	0.248	0.647	0.105	1.32	0.254	0.270	0.476	J
0.09	0.244	0.628	0.128	0.60	0.258	0.304	0.438	G
0.10	0.247	0.645	0.108	0.42	0.239	0.276	0.485	H
0.10	0.248	0.647	0.105	0.45	0.242	0.272	0.486	J
0.09	0.244	0.826	0.128	0.25	0.257	0.379	0.364	G
0.10	0.247	0.645	0.108	0.16	0.225	0.306	0.469	H
0.10	0.248	0.647	0.105	0.14	0.239	0.327	0.434	J
0.04	0.250	0.639	0.111	1.30	0.248	0.270	0.482	G
0.04	0.227	0.504	0.269	1.34	0.262	0.270	0.482	H
0.03	0.234	0.594	0.172	1.32	0.276	0.263	0.461	J
0.04	0.250	0.639	0.111	0.46	0.248	0.271	0.481	G
0.04	0.227	0.504	0.269	0.47	0.260	0.274	0.466	H
0.03	0.234	0.594	0.172	0.44	0.250	0.226	0.524	J
0.04	0.250	0.639	0.111	0.15	0.246	0.276	0.477	G
0.04	0.227	0.504	0.269	0.14	0.242	0.237	0.521	H
0.03	0.234	0.594	0.172	0.17	0.246	0.243	0.511	J

TABLE III. Average coordinates of achromatic spots, adaptation-ratio (r), and tri-stimulus sum ratio (R).

Background luminance (app.f.c.)	Background chromaticity coordinates x	y	z	Achromatic spot luminance (app.f.c.)	Achromatic spot chromaticity coordinates x	y	z	r	R
8.63	0.587	0.385	0.027	1.62	0.555	0.409	0.036	1.01	0.18
				1.14	0.594	0.374	0.032	0.96	0.09
2.65				1.68	0.548	0.415	0.037	0.92	0.59
				0.66	0.566	0.401	0.033	1.04	0.24
				0.25	0.579	0.390	0.031	1.00	0.10
0.81				1.79	0.425	0.316	0.259	0.45	2.71
				0.75	0.542	0.393	0.064	1.03	0.87
				0.34	0.569	0.397	0.034	1.01	0.41
0.21				1.68	0.328	0.272	0.400	0.19	10.2
				0.64	0.388	0.288	0.324	0.20	3.90
				0.23	0.526	0.371	0.103	0.82	1.11
0.10				1.42	0.308	0.263	0.429	0.10	20.3
				0.63	0.327	0.254	0.419	0.05	9.3
				0.22	0.364	0.248	0.388	0.10	3.30
0.76	0.698	0.291	0.012	1.12	0.545	0.271	0.184	0.64	1.58
				0.41	0.630	0.297	0.073	0.86	0.52
				0.10	0.681	0.293	0.026	0.98	0.13
0.24				2.11	0.426	0.338	0.256	0.41	7.9
				0.57	0.456	0.251	0.293	0.40	2.63
				0.13	0.680	0.312	0.008	0.98	0.52
0.070				1.48	0.332	0.266	0.402	0.14	22.8
				0.71	0.351	0.262	0.387	0.18	11.2
				0.19	0.512	0.295	0.193	0.58	2.63
0.031				1.32	0.298	0.256	0.446	0.06	49.5
				0.58	0.292	0.221	0.487	0.00	25.2
				0.22	0.381	0.277	0.342	0.26	7.6
0.76	0.241	0.615	0.143	1.03	0.250	0.473	0.277	0.58	1.71
				0.36	0.234	0.496	0.270	0.62	0.56
				0.10	0.259	0.638	0.103	1.10	0.12
0.26				1.20	0.239	0.300	0.461	0.04	9.8
				0.41	0.254	0.384	0.362	0.32	2.64
				0.12	0.272	0.601	0.127	1.00	0.49
0.097				1.23	0.247	0.269	0.484	−0.04	30.0
				0.49	0.235	0.282	0.473	0.00	11.4
				0.18	0.243	0.342	0.415	0.17	3.41
0.038				1.32	0.262	0.269	0.469	−0.01	76.0
				0.45	0.252	0.256	0.492	−0.06	27.3
				0.16	0.266	0.296	0.438	0.08	8.1
0.062	0.166	0.068	0.766	1.08	0.276	0.233	0.491	0.13	5.2
				0.47	0.242	0.186	0.572	0.34	2.83
				0.22	0.218	0.146	0.636	0.56	1.66
0.014				1.34	0.277	0.265	0.458	0.03	24.6
				0.55	0.262	0.242	0.496	0.10	11.2
				0.18	0.273	0.215	0.512	0.16	4.03

parison. This problem is complicated by the white-gray-black question. Whether the spot appears "white,"[4] gray, or "black" depends not only upon its own brightness but even more upon its relation to the surround. For this and other reasons, the luminance of the surround was varied as well as its chromaticity, and observers were asked to adjust to achromaticity at the three levels mentioned previously. Hence the data reported in this study represent achromaticities that are white, near-white, light gray, medium gray, dark gray, very, very dark gray, and, in one or two cases, black, depending upon the brightness ratio of spot to surround. In spite of variation from observer to observer and some lack of consistency within individual settings, the data yielded such clear regularities that averaging of observers seemed justified. Inter-observer variation might have been reduced by correcting each observer for departure from I.C.I. specifications of some standard source. This was not done, and the data represent actual settings in every case. Three observers completed observations for all conditions, one of the authors (H), Miss Louise Gaus, graduate student in physics (G), and Mr. Murray de Jersey, graduate student in psychology (J). Observations made by the other author (M) were in every way confirmatory of the data presented here but are not included because of incompleteness.

The achromatic settings with dark surround agreed well, and the average chromaticity coordinates of the point were found to be

$$x_0 = 0.269 \pm 0.026,$$
$$y_0 = 0.269 \pm 0.040,$$
$$z_0 = 0.462 \pm 0.057.$$

It is of interest that this white point with a dark surround approximates very closely the color of a blackbody radiator at a temperature of 15,000°K, and is considerably bluer than usually accepted white points. It is, however, in the region characteristic of an illuminant in which non-selective reflectances, whether high, medium, or low, should be achromatic, according to Judd (reference 3, p. 9).

IV. RESULTS AND DISCUSSION

A typical set of data, taken when the booth was flooded with green light, is shown in Table II. It will be noticed that the consistency of the

[4] In accordance with modern trends, the terms white and black should be reserved for object colors or colors seen to belong to surfaces and, therefore, having definite localization and a certain hardness and texture. Sometimes the color perceived in the exit pupil of the colorimeter was localized in the plane of the surround and did seem to possess the hard, surfacy texture of object colors, so that it would be proper in these cases to refer to them as white or black. However, the achromatic spots were not always white in the sense of possessing surface properties when they were very, very bright, or black in this sense when they were very, very dark. Hence references to white and black in this study may include cases of extremely bright or dark aperture colors which were not white or black in the above sense. No distinction by means of quotes will be made hereafter between whites and blacks, on the one hand, and extremely bright and dark on the other.

observers in determining the color of the background is considerably better than that obtained in determining the achromatic points. This is not unexpected, since the former determination is the result of a matching process, while the latter depends on the judgments of achromaticity, without reference to a physical standard.

In Table III, the results for four background chromaticities, with two to five luminances for each chromaticity, as obtained by three observers, are summarized. The values of the chromaticity coordinates (x,y,z) given for each background were obtained by averaging the tristimulus values (X,Y,Z) found by the three observers for a given luminance, and then by averaging the chromaticity coordinates for the various luminances. Each observer made two or three brightness and color matches. The luminance of the background was likewise determined by conversion from the average Y value found by all observers. The luminance and chromaticity coordinates for each achromatic spot are similar averages of the values found by three observers. The coordinates of each spot therefore represent nine independent observations. No attempt has been made to estimate the uncertainties of each set of coordinates, but a general review of the data indicates that the values given may vary by about 0.05 from those of any observer.

Certain regularities in the data are immediately apparent. The achromatic point at luminances low compared with that of the background (i.e., dark gray) has chromaticity coordinates approximating those of the background, while at high luminances its coordinates approximate those of the white point with dark surround. The loci of the achromatic points for different background colors are indicated in Fig. 1, which shows the data of Table III on an I.C.I. plot. It is found that, within the tolerance of the observers in judging achromaticity, the various achromatic points fall along a straight line connecting the background point with the achromatic point for a dark surround. This result is in general agreement with the conclusion of Judd (reference 3, Eq. (3a), p. 8) concerning the coordinates of achromatic points as observed against various fields. Such lines may be only first approximations to the achromatic loci, but the present data are insufficient to show whether the departures of the individual points from the lines are significant or accidental. In view of the spread among single observations, the reality of these departures can probably be investigated only by averaging over a larger number of observers.

The movement of the achromatic point along its locus with changing relative luminance is consistent with the idea that the eye is desensitized to any wave-length by the receipt of energy at that and neighboring wave-lengths, not only from the spot being fixated but also from the area surrounding the spot. In the absence of a satisfactory theory of the effects of adaptation, we have tried to find quantitative relations among our data by empirical analysis. A convenient measure of the position of the achromatic point on the straight line locus for a given chromaticity of surround is given by a quantity which we shall call the *adaptation ratio:*

$$r=(x_s-x_0)/(x_b-x_0)=(y_s-y_0)/(y_b-y_0)=(z_s-z_0)/(z_b-z_0), \quad (1)$$

where x, y, and z are chromaticity coordinates. The subscripts s, b, and 0 refer, respectively, to the achromatic spot, the background, and the achromatic spot as found with a dark surround.

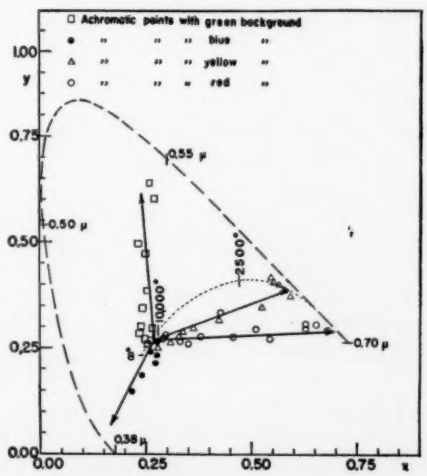

FIG. 1. Achromatic loci: The dashed curve shows the spectral locus, with wave-lengths in microns; the dotted curve is the locus of blackbody radiators, with temperatures in degrees Kelvin; the solid lines join the "white point" with the background points.

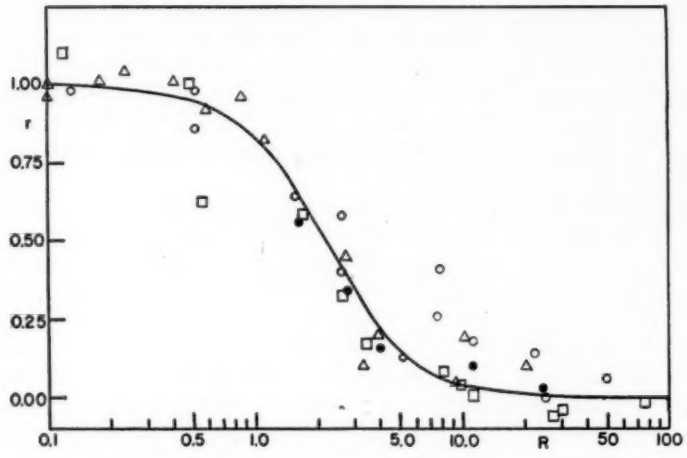

FIG. 2. Adaptation ratio as a function of stimulus sum ratio: The points are keyed to the various backgrounds as in Fig. 1. The solid curve is that of $r=1/(1+0.21R^2)$.

The equality signs are insured by the linearity of the locus and by the condition that $x+y+z=1$. We may expect r to be a function of the stimulation received from the background as well as that received from the spot. Various functions of the specifications of the background and the achromatic spot were tried in an attempt to find a quantity which is functionally related to the adaptation ratio. The only simple quantity which was found to be suitable for all surrounds was the ratio of the sum of the I.C.I. tristimulus values of the spot to a similar sum for the background. We shall therefore define another ratio:

$$R=(X_s+Y_s+Z_s)/(X_b+Y_b+Z_b), \qquad (2)$$

where the capital letters represent the tristimulus values and the subscripts have the same meanings as in Eq. (1).

In order to find whether the presumed functional relationship exists, r and R were calculated for each set of observations made under similar conditions. Each of the three values of r given by Eq. (1) was found independently, unless the denominator of the expression had a value less than 0.10. Such cases were discarded, because the spread of the observations could lead to errors of the order of 100 percent. The values given in the next to the last column of Table III are the averages of either the two or the three values of r calculated for each set of observations. The last column shows the values of the stimulus sum ratio R. In Fig. 2 all values of r are plotted against the corresponding values of R on a semilogarithmic plot. It is interesting that the resulting points for all four hues of surround and at all brightness levels fall very close to the same smooth curve. Attempts to find a function which would represent the data within their uncertainties have led to the relation:

$$r=1/(1+0.21R^2) \qquad (3)$$

as a reasonably good fit. We can see no way, at present, of attaching theoretical significance to Eq. (3), but consider it an empirical relation which allows prediction of an achromatic point of any intensity for a steady state of adaptation of the eye, within the range of our experiments. The function obviously falls off a little too rapidly with large values of R, but only two of the sets of observations depart by more than the average tolerance of an observer from the location on the chromaticity diagram predicted by Eq. (3).

The discrepancy between the values of the adaptation ratio predicted by Eq. (3) and the observed values for large values of R is significant. To test this point, the following sets of check observations were made with one observer. The achromatic settings which had been found suitable for the various chromatic surrounds were pre-set and observed with a dark surround. Included were spots with higher values of R than any given in Table III.[5] The achromatic spots

[5] These data are not given since they were taken only by a single observer.

which had been found for the red and yellow backgrounds showed discernible chroma against the dark surround, even though the ahcromatic stimulus had been determined for values of R as high as 80:1 for the red and 30:1 for the yellow. On the other hand, the achromatic points determined for the blue and green surrounds at values of R as low as 10:1 remained achromatic with a dark surround. As a further check the spot was adjusted to a high intensity of the achromatic setting for a dark surround and was then observed with low intensity of the four chromatic surrounds. In each case the chroma of the spot was sufficiently low so that the observer was willing to accept the spot as achromatic.

Because of the empirical nature of Eq. (3), and because of the surprising fact that the adaptation of the eye appears to be determined by the I.C.I. stimulus sum ratio rather than the luminance ratio, attempts were made to apply to our data the equations which have been proposed by Judd (reference 3, Eq. (3), p. 8) and by Spencer[6] to specify achromaticity. Judd's equation can be modified to fit the conditions of this study by replacing reflectances by luminances. The composite color stimulus tensor of Spencer was defined for conditions essentially identical with those which we have used. Both of these formulations agree qualitatively with our results, but neither predicts the achromatic specifications as closely as does Eq. (3).

One interesting result of this study is the fact that the "white point," i.e., the achromatic point for a small spot of luminance much higher than that of the background, seems to be almost independent of the state of adaptation. If we accept Eq. (3), all values of R greater than 10 should result in a close approximation to this point. In the present data there are 117 individual observations, other than those with the dark surround, which satisfy the condition $R>10$. The white point, as determined by averaging the chromaticity coordinates found in all of these observations, is given by

$$x_0=0.287, \quad y_0=0.254, \quad z_0=0.459.$$

These values agree with the white point found with dark surround within the accuracy of the determinations of this point.

To test whether the state of adaptation is determined by the specification of the light reaching the eye, some observations were made with a low reflecting surround (daylight black). In these observations the intensity of the illuminant was raised to sufficiently high levels that the luminance of the surround duplicated levels used in the main body of experiments, with daylight white surround. In every case the results were in excellent agreement with the data shown in Table III.

One effect which was noticed during the observation of black and dark gray spots indicates that decreased sensitivity of the eye to wavelengths coming from the surround is not the only effect of adaptation. When the exit pupil of the colorimeter was observed at very low brightnesses, an annular ring which showed the complementary hue to that of the illuminant could be observed within the aperture. The addition of small amounts of light of the hue of the surround compensated for this color without appreciably increasing the brightness of the spot. It is probably this effect which allows a reasonably precise determination of the chromaticity coordinates of the very dark spots, which might otherwise have been expected to be indeterminate.

It is a matter of considerable interest that the data obtained in this study with a luminous spot are in agreement with the conclusions which have been drawn from previous studies in which reflecting samples were used. The qualitative generalization which has been drawn from the work of Helson, Helson and Jeffers, and Judd with reflecting samples on non-selective surrounds can be stated: In every viewing situation there is established an adaptation level such that samples with reflectances above this level tend to take the hue of the illuminant, samples with lower reflectances take the after-image complementary to the hue of the illuminant, and samples with reflectances near the adaptation level are either achromatic or weakly saturated. The same principle can be deduced directly from Eq. (3), and from the observations noted in the preceding paragraph. In order that

[6] D. E. Spencer, "Adaptation in color space," J. Opt. Soc. Am. **33**, 10 (1943).

a highly reflecting sample remain achromatic, it is necessary that its spectral reflectance be such that, when multiplied by the spectral distribution of the illuminant, it yield the specifications of the corresponding achromatic point. *Highly reflecting* samples necessarily depart from this condition toward the hue of the illuminant. Similarly, according to Eq. (3), a sample of very low reflectance would be achromatic only if its spectral reflectance, multiplied by the spectral distribution of the illuminant, were to yield the chromaticity coordinates of the surround. The reflectance of selective samples can depart from this requirement in one of two ways, (a) favoring the dominant wave-length of the illuminant and yielding high reflectance, and (b) favoring other wave-lengths, thus causing the color to shift toward the complement of the illuminant. This effect alone cannot explain the behavior of non-selective samples of low reflectance. The appearance of such samples must be due to the after-image complementary effect noted with spots of low brightness. Our results therefore agree with the qualitative principles obtained from observations on reflecting samples.

V. ACKNOWLEDGMENTS

The authors wish to express their indebtedness to Miss Louise Gaus, who did most of the work involved in the calibration of the colorimeter and who acted as an observer, and to Mr. Murray de Jersey, whose help in setting up the apparatus and in observing was of great value. We also wish to thank Mr. Norman Powell for the care and skill which he used in the construction of the colorimeter. This study was assisted by a grant from the income of the Carnegie Corporation Endowment given to Bryn Mawr College for the Coordination of the Sciences.

JOURNAL OF THE OPTICAL SOCIETY OF AMERICA VOLUME 38, NUMBER 12 DECEMBER, 1948

The Design of Triplet Anastigmat Lenses of the Taylor Type

ROBERT E. STEPHENS
Optical Instruments Section, National Bureau of Standards, Washington, D. C.

(Received June 4, 1948)

Equations and methods are developed for computing the lens powers, separations, and lens shapes of preliminary thin lens designs of Taylor-type triplets. The three lens powers and two spaces are determined by specified values of equivalent power, Petzval sum, longitudinal chromatic aberration, lateral chromatic aberration, and spherical aberration. The three lens shapes are determined by desired values of the three Seidel sums relating to coma, astigmatism, and distortion. Procedures for replacement of thin lenses by equivalent thick lenses and for final trigonometric adjustment are outlined. The methods given are not limited to the case of the infinitely distant object, but may be used to determine a system for any specified magnification and having any moderate values of the eight independent variables.

I. INTRODUCTION

THE material so far published on the design of triplet anastigmats[1–8] of the Taylor type leaves much to be desired in several respects. The methods presented for the correction of lateral chromatic aberration have depended upon the treating of dispersion as a continuous

[1] H. D. Taylor, British Patent 22607/93, also U. S. Patents 540122 and 568052.

[2] H. D. Taylor, "Description of the Franklin-Adams astrographic triplet." Monthly notices of the Royal Astronomical Society, May 1904.

[3] K. Schwarzschild, *Untersuchungen zur Geometrischen Optik III* (Weidmannsche Buchhandlung, Berlin, 1905) "Objectiv aus drei getrennten Linsen," p. 40.

[4] Arthur Kerber, "Ein Taylor Objectiv fur astronomische Zweck," Zeits. f. Instrumentenk **35**, 23 (1915).

[5] Arthur Kerber, "Uber die Berechnung der Objectiv von grosserem Gesichtsfelde aus drei getrennten Linsen," Zeits. f. Instrumentenk **36**, 68 (1916).

[6] Arthur Kerber, "Ein Portratobjectiv aus drei getrennten Linsen," Zeits. f. Instrumentenk **36**, 269 (1916).

[7] Henri Chretien, "Cours de Calcul des Combinaisons Optiques," Revue d'optique theoret. et instrument., 359 (1938).

[8] M. Berek, *Grundlagen der praktischen Optik* (W. de Gruyter and Company, Berlin and Leipzig, 1930), "Das einfache Triplet," p. 123.

variable or upon the assumption of fictitious values of dispersion. Neither of these is very satisfactory to a designer who is restricted to a rather limited number of types of glass. Apparently, no treatment of the problem of designing triplet anastigmats for object distances other than infinity has been published. It is the purpose of this paper to present methods in which these limitations do not apply.

II. GENERAL CONSIDERATIONS

In the design of a lens system consisting of three thin elements separated by air spaces, the following constructional features are available to the designer for control of the optical characteristics of the system: three glass types, three lens powers, three lens shapes, two separation distances, and the location of the aperture stop. Treatment of the properties of the glasses (index of refraction and dispersion) as continuous variables is excluded from this work as impracticable. The choice of glasses does, however, have an important effect upon the attainable corrections and must be made as a result of experience, study of published designs,* [9] or a sequence of trials.

The position of the aperture stop is also excluded from treatment as a continuous variable in the algebraic steps of design. The amount of control of aberration that is obtainable by displacement of the stop is small unless the system suffers from considerable aberration. It is assumed in this paper that the triplet is either to be corrected as well as possible itself or that it is to be a component of a corrected system. Another consideration is that the stop cannot be displaced far from the optical center of the triplet if the apertures of the elements are to be utilized to the best advantage.

The eight remaining features may be considered continuously variable over practicable ranges and utilized as such in an analytic solution.

These eight variables are just sufficient for the control of the following eight quantities whose control is a minimum requirement for the design of a fully corrected system of moderate aperture and field: (1) the scale of the system (equivalent focal length), (2) Petzval sum, (3) longitudinal chromatic aberration, (4) lateral chromatic aberration, (5) the Seidel sum, S-I, which is related to spherical aberration, (6) the Seidel sum, S-II, which is related to coma, (7) the Seidel sum, S-III, which is related to astigmatism, (8) the Seidel sum, S-V, which is related to distortion.

The equations governing the first four of these quantities are independent of the lens shapes, and, consequently, the problem of finding solutions is considerably simplified. Further simplification results from the use of the nominal heights of incidence of an auxiliary paraxial ray at the second and third elements as parameters instead of the separation distances.

III. FORMULAS AND NOTATION

The equation governing the scale of an optical system is

$$\sum_{i=1}^{i=k}\left(\frac{h_i}{h_1}\right)\varphi_i=\frac{\alpha_k'-\alpha_1}{h_1}=A. \qquad (1)$$

The dioptric power of the ith element is φ_i; the nominal height of incidence on the ith element of a paraxial ray from the object is h_i; the nominal angles between the axis and this same ray before and after refraction by the system are α_1 and α_k'.

Since, for any particular position of the object, h_1 is proportional to h_{pp}, the height of incidence on the first principal plane of the system, the members of Eq. (1) are proportional to the equivalent power of the system.

The Petzval sum is

$$\sum_{i=1}^{i=k}\frac{\varphi_i}{n_i}=P, \qquad (2)$$

where n_i is the index of refraction of the ith element.

The value of P which will give a suitable image curvature is proportional to the equivalent power of the system and therefore should be chosen in accordance with the chosen value of A in Eq. (1).

* For example, considerable guidance may be obtained from reference 9 in which constructional data and computed characteristics are given for a large number of photographic lenses.

[9] *Handbuch der Wissenschaftlichen and Angewandten Photographie:* Vol. I, *Das Photographische Objectiv* (Verlag Julius Springer, Wien, 1932; lithoprint reproduction—J. W. Edwards, Ann Arbor, Michigan, 1946), and *Erganzungswerk* (Verlag Julius Springer, Wien, 1943; lithoprint reproduction—J. W. Edwards, Ann Arbor Michigan, 1948), Vol. I.

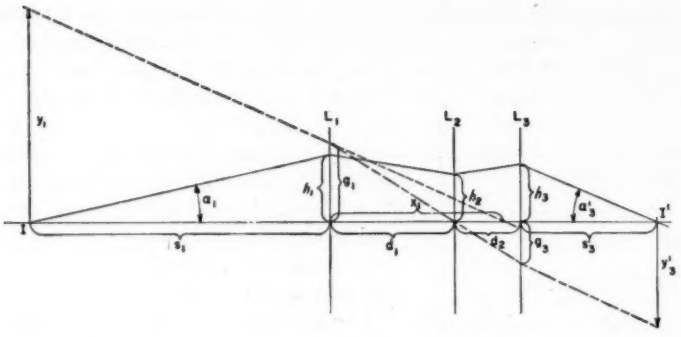

FIG. 1.

The equation giving the longitudinal chromatic aberration of a system of thin lenses is

$$\Delta s_k' = s_k'^2 \left(\frac{h_1}{h_k}\right)^2 \sum_{i=1}^{i=k} \left(\frac{h_i}{h_1}\right)^2 \frac{\varphi_i}{V_i} \tag{3}$$

where s_k' is the final image distance, $\Delta s_k'$ is the longitudinal chromatic aberration, and V_i is the reciprocal relative dispersion of the ith element.

The equation giving the lateral chromatic aberration is

$$\frac{\Delta M}{M} = \frac{-s_1 x_1}{s_1 - x_1} \sum_{i=1}^{i=k} \left(\frac{g_i}{g_1}\right)\left(\frac{h_i}{h_1}\right)\frac{\varphi_i}{V_i} \tag{4}$$

where M is the magnification of the system, ΔM is the chromatic difference of magnification, s_1 is the object distance, x_1 is the distance from the first element to the entrance pupil and g_i is the nominal height of incidence on the i-th element of an auxiliary paraxial ray which intersects the axis at the center of the aperture stop.

Throughout this paper the signs of linear quantities have their usual significance, in accord with the conventions of coordinate geometry, i.e., positive to the right and upward. The signs of the angles α_i, however, follow from the definitions $\alpha_i = h_i/s_i$, and a positive angle represents a turn of less than a right angle from the positive direction of the axis in a *clockwise* direction. These conventions are in agreement with those of Conrady, Schwarzschild, Kerber, and Berek.

IV. FORMULATION OF PROBLEM

A typical system of the type being considered, consisting of three axially aligned thin lenses L_1, L_2, and L_3 with an air space d_1 separating L_2 from L_1, and an air space d_2 separating L_3 from L_2, is illustrated in Fig. 1. The first auxiliary ray emerges from I, the axial point of the object, intersects lenses L_1, L_2, and L_3 at heights h_1, h_2, and h_3 respectively, and again intersects the axis at I', the axial point of the image. This ray makes nominal angles α_1 and α_3' with the axis in object and image spaces, respectively. The second auxiliary ray intersects the axis at the center of L_2 which is assumed to be coincident with the aperture stop. This ray intersects lenses L_1, L_2, and L_3 at heights g_1, zero and g_3, respectively. The entrance pupil is located at a distance x_1 from L_1, where the extension of the portion of the second auxiliary ray in object space intersects the axis.

Before applying the general Eqs. (1), (2), (3), and (4) to the particular problem of the air-spaced triplet, several simplifications will be introduced. Let

$$\frac{h_2}{h_1} = h_2, \quad \frac{h_3}{h_1} = h_3$$

$$\frac{1}{n_1} = m_1, \quad \frac{1}{n_2} = m_2, \quad \frac{1}{n_3} = m_3$$

$$\frac{1}{V_1} = \mu_1, \quad \frac{1}{V_2} = \mu_2, \quad \frac{1}{V_3} = \mu_3. \tag{5}$$

In consequence of Eq. (1), the quantity $s_3'^2(h_1/h_3)^2$ which multiplies the summation in Eq. (3) turns out to be a constant as is shown by the following proof: By Eq. (1)

$$\alpha_3' - \alpha_1 = h_1 A,$$

and by Lagrange's law

$$\frac{\alpha_1}{\alpha_3'} = M.$$

These two equations determine the following:

$$\alpha_1=\frac{h_1AM}{1-M}, \tag{6}$$

and

$$\alpha_3'=\frac{h_1A}{1-M}. \tag{7}$$

Since $\alpha_3'=h_3/s_3'$, by definition,

$$s_3'^2\left(\frac{h_1}{h_3}\right)^2=\left(\frac{1-M}{A}\right)^2$$

Also, by (6) and (7)

$$s_1=\frac{h_1}{\alpha_1}=\frac{1-M}{AM},$$

and (9)

$$s_3'=\frac{h_3}{\alpha_3'}=\frac{h_3(1-M)}{A}.$$

For the analytic design work it will be assumed that the aperture stop is in coincidence with the second element, L_2. This makes $g_2=0$ and results in considerable simplification of the algebra. Of course, during the final adjustment, the stop must be moved into one of the air spaces. The resulting small change in the residual aberrations will then be compensated as described in Section XI. Another consideration resulting from this placement of the stop is that, if the triplet is to be a component of a larger system and its aberrations are to balance those contributed by the rest of the system, the aberrations of the rest of the system must be computed for an estimated position of the stop that will as nearly as possible be in coincidence with the second element of the triplet.

When applied to the air-spaced triplet, with the benefit of the simplifications given above in Eqs. (5) and (8), Eqs. (1), (2), (3), and (4) give

$$\varphi_1+h_2\varphi_2+h_3\varphi_3=A, \tag{10}$$

$$m_1\varphi_1+m_2\varphi_2+m_3\varphi_3=P, \tag{11}$$

$$\left(\frac{1-M}{A}\right)^2[\mu_1\varphi_1+\mu_2h_2^2\varphi_2+\mu_3h_3^2\varphi_3]=\Delta s_3', \tag{12}$$

$$\left(\frac{s_1x_1}{x_1-s_1}\right)\left[\mu_1\varphi_1+\mu_3\frac{g_3}{g_1}h_3\varphi_3\right]=\frac{\Delta M}{M}. \tag{13}$$

The unknown quantities, after the problem is defined and the glasses chosen, are φ_1, φ_2, φ_3, h_2, and h_3. The quantities x_1 and g_3/g_1 are also unknown but are functions of the others and may be replaced as will be done later in the treatment of a special case. These four equations determine four of the unknowns as functions of the fifth, which is to be assumed arbitrarily at this stage and finally determined by the spherical aberration of the system.

V. GENERAL CASE

To find the values of φ_1, φ_2, φ_3, h_2, and h_3, in the general case, when A, P, $\Delta s_3'$ and $\Delta M/M$ all have values different from zero, the procedure is partly algebraic and partly graphical. Equations (10), (11), and (12), being linear in φ_1, φ_2, and φ_3, may easily be solved for these quantities with the following results:

$$\varphi_1=\frac{N_1}{D},\quad \varphi_2=\frac{N_2}{D},\quad \varphi_3=\frac{N_3}{D}, \tag{14}$$

where

$$D=m_2\mu_3h_3^2+m_3\mu_1h_2+m_1\mu_2h_2^2h_3 -m_2\mu_1h_3-m_1\mu_3h_2h_3^2-m_3\mu_2h_2^2, \tag{15}$$

$$N_1=m_2A\mu_3h_3^2+m_3Qh_2+P\mu_2h_2^2h_3 -m_2Qh_3-\mu_3Ph_2h_3^2-m_3A\mu_2h_2^2, \tag{16}$$

$$N_2=P\mu_3h_3^2+m_3A\mu_1+m_1Qh_3 -\mu_1Ph_3-m_1\mu_3Ah_3^2-m_3Q, \tag{17}$$

$$N_3=m_2Q+\mu_1Ph_2+m_1A\mu_2h_2^2 -m_2A\mu_1-m_1Qh_2-P\mu_2h_2^2. \tag{18}$$

In these equations the quantity $[A/(1-M)]^2\Delta s_3'$ has been replaced by Q.

This is as far as the solution by purely algebraic means goes, but before proceeding it is necessary to have d_1, d_2, x_1, and g_3/g_1 expressed as functions of φ_1, φ_2, φ_3, h_2, and h_3. At the first element

$$\alpha_1'=\alpha_1+h_1\varphi_1.$$

At the second element

$$\alpha_2=\alpha_1'$$
$$h_2=h_1-d_1\alpha_1'=h_1-d_1(\alpha_1+h_1\varphi_1)$$
$$\alpha_2'=\alpha_1+h_1\varphi_1+h_2\varphi_2,$$

from which is obtained

$$d_1=\frac{h_1-h_2}{\alpha_1+h_1\varphi_1}=\frac{1-h_2}{\frac{\alpha_1}{h_1}+\varphi_1},$$

and, on substituting for α_1 from (6),

$$d_1=\frac{(1-h_2)(1-M)}{AM+\varphi_1(1-M)}. \tag{19}$$

At the third lens

$$h_3=h_2-d_2\alpha_2'=h_2-d_2(\alpha_1+h_1\varphi_1+h_2\varphi_2).$$

From this and (6) it is found that

$$d_2=\frac{(h_2-h_3)(1-M)}{AM+(\varphi_1+h_2\varphi_2)(1-M)}. \tag{20}$$

From the geometry of the second auxiliary ray, as shown in Fig. 1, it may be seen that

$$g_3/g_1=-d_2/d_1 \tag{21}$$

and, since $x_1'=d_1$,

$$x_1=d_1/(1-d_1\varphi_1). \tag{22}$$

The procedure in solving a practical problem is to assume a value for h_3. If the same glass is chosen for the first and third elements, the best value for h_3 will probably lie between 0.70 and 0.95. Several sets of values of φ_1, φ_2, and φ_3 are then computed, corresponding to several arbitrary values of h_2, by Eqs. (14), (15), (16), (17), and (18). The corresponding values of s_1, d_1, d_2, g_3/g_1, and x_1 are also computed by Eqs. (9), (19), (20), (21), and (22). Each set of these values is then substituted into Eq. (13). By this procedure several values of $\Delta M/M$ are obtained, each corresponding to a different value of h_2. A graph is prepared giving h_2 as a function of $\Delta M/M$ and the value of h_2 corresponding to the desired value of $\Delta M/M$ may be taken from the graph. Then φ_1, φ_2, and φ_3 are computed for this value of h_2.

By this procedure a set of values of φ_1, φ_2, φ_3, h_2, and h_3 is obtained (h_3 chosen arbitrarily) that gives the desired values of equivalent focal length, Petzval sum, and longitudinal and lateral chromatic aberrations. The shapes of the lenses remain to be determined in such a way as to give desired values of the Seidel sums S-II, S-III, and S-V. The procedure for finding these shapes is the subject of Section IX.

VI. OBJECT INFINITELY DISTANT AND LATERAL CHROMATIC ABERRATION PERFECTLY CORRECTED

An important special case occurs if the object is assumed to be infinitely distant, as is the case in the design of ordinary camera lenses of moderate aperture. In this case, the solution for h_2 may be entirely algebraic if it is also assumed that $\Delta M/M=0$.** This assumption is very well justified if the final system is to be corrected for lateral chromatic aberration, since the replacement of thin lenses by equivalent thick ones usually does not introduce much change in the lateral chromatic aberration. Of course, in the final stages of the design work, if it is desired to introduce a small value, not zero, for $\Delta M/M$ so that the final design will be corrected for lateral chromatic aberration at a specified field angle, it will be necessary to revert to the more general method of section V.

In this section the object is assumed to be infinitely distant and the desired lateral chromatic aberration is assumed to be zero. Consequently, $s_1=\infty$, $M=0$, and $\Delta M/M=0$. Also, A becomes the equivalent power of the system.

From Eqs. (19), (20), and (21) it is found that

$$\frac{g_3}{g_1}=\left(\frac{h_3-h_2}{1-h_2}\right)\left[\frac{AM+\varphi_1(1-M)}{AM+(\varphi_1+h_2\varphi_2)(1-M)}\right]. \tag{23}$$

For $M=0$ this becomes

$$\frac{g_3}{g_1}=\left(\frac{h_3-h_2}{1-h_2}\right)\left[\frac{\varphi_1}{\varphi_1+h_2\varphi_2}\right]. \tag{24}$$

On substitution for g_3/g_1, s_1, and $\Delta M/M$, Eq. (13) becomes

$$(1-h_2)\mu_1\varphi_1+(1-h_2)\mu_1h_2\varphi_2 +\mu_3h_3(h_3-h_2)\varphi_3=0. \tag{25}$$

Equations (10), (11), (12), and (25) determine φ_1, φ_2, φ_3, and h_2 (for any arbitrary value of h_3). The elimination of φ_1, φ_2, and φ_3 is performed expeditiously by the application of the determinant

$$\begin{vmatrix} 1 & h_2 & h_3 & A \\ m_1 & m_2 & m_3 & P \\ \mu_1 & \mu_2h_2^2 & \mu_3h_3^2 & Q \\ (1-h_2)\mu_1 & (1-h_2)\mu_1h_2 & \mu_3h_3(h_3-h_2) & 0 \end{vmatrix}=0$$

where now $Q=A^2\Delta s_3'$, since $M=0$. Expanded,

** When the object is infinitely distant $M=0$ and $\Delta M=0$ but $\Delta M/M=(\Delta y'/f\tan\beta_1)$, where f is the front equivalent focal length of the system, β_1 is the field angle in object space, and $\Delta y'$ is the lateral chromatic aberration. Consequently, if correction of lateral chromatic aberration is prescribed, $\Delta M/M=0$.

this becomes

$$h_2^3[m_1\mu_2\mu_3h_3-m_3\mu_1\mu_2+\mu_2Ph_3(\mu_1-\mu_3)]$$
$$+h_2^2[m_3\mu_1(\mu_1+\mu_2)-m_1\mu_3h_3^2(\mu_1+\mu_2)$$
$$-\mu_1Ph_3(\mu_1+\mu_2-\mu_3)+\mu_2\mu_3Ph_3^2$$
$$+m_1Qh_3(\mu_1-\mu_3)]+h_2[\mu_1\mu_3h_3^2(m_1+m_2)$$
$$-m_2\mu_1\mu_3h_3-m_3\mu_1^2+\mu_1Ph_3(\mu_1-\mu_3h_3)$$
$$+Qh_3(m_2\mu_3-m_2\mu_1-m_1\mu_1+m_1\mu_3h_3)]$$
$$+[m_2Qh_3(\mu_1-\mu_3h_3)]=0. \quad (26)$$

The real roots of this cubic equation are the possible values of h_2. By substituting for h_2 and h_3 in Eqs. (14), (15), (16), (17), and (18) the corresponding values of φ_1, φ_2, and φ_3 may be found. The values of d_1 and d_2 may then be found by Eqs. (19) and (20). Usually, only one of these solutions is physically realizable and, if the choice of glasses or of h_3 has been unfavorable, none may be realizable.

If the conditions are such that $Q=0$ further simplification results. Equation (26) reduces to

$$h_2^2[m_1\mu_2\mu_3h_3-m_3\mu_1\mu_2+\mu_2Ph_3(\mu_1-\mu_3)]$$
$$+h_2[m_3\mu_1(\mu_1+\mu_2)-m_1\mu_3h_3^2(\mu_1+\mu_2)$$
$$-\mu_1Ph_3(\mu_1+\mu_2-\mu_3)+\mu_2\mu_3Ph_3^2]$$
$$+[\mu_1\mu_3h_3^2(m_1+m_2)-m_2\mu_1\mu_3h_3$$
$$-m_3\mu_1^2+\mu_1Ph_3(\mu_1-\mu_3h_3)]=0. \quad (27)$$

This, being quadratic in h_2, is much more easily solved than Eq. (29), and much labor may be saved by its use in the early stages of designing a system, even if small chromatic residuals are ultimately necessary. Usually, only the smaller of the two roots results in a physically realizable system.

VII. FIRST AND THIRD ELEMENTS OF THE SAME GLASS AND $h_3=1$

In designing a triplet anastigmat the same glass is often chosen for both the first and third elements. This is a good choice, probably as good as any, if a barium crown is chosen. The solution by the equations given in Section VI becomes indeterminate for the case $h_3=1$, since the equations determining h_2 and D become zero identically.

The solution for this case is obtained by going back to the original Eqs. (10), (11), (12), and (13). In accordance with the assumed conditions, the following substitutions are made

$$m_3=m_1, \quad \mu_3=\mu_1, \quad h_3=1.$$

The equations to be satisfied then become

$$(\varphi_1+\varphi_3)+h_2\varphi_2=A, \quad (28)$$

$$m_1(\varphi_1+\varphi_3)+m_2\varphi_2=P, \quad (29)$$

$$\mu_1(\varphi_1+\varphi_3)+\mu_2h_2^2\varphi_2=\left(\frac{A}{1-M}\right)^2\Delta s_3'=Q, \quad (30)$$

$$\left(\frac{s_1x_1}{x_1-s_1}\right)\mu_1\left(\varphi_1+\frac{g_3}{g_1}\varphi_3\right)=\frac{\Delta M}{M}. \quad (31)$$

The first three of these determine $(\varphi_1+\varphi_3)$, φ_2, and h_2. The result of eliminating $(\varphi_1+\varphi_3)$ and φ_2 is obtained expeditiously by means of the determinant

$$\begin{vmatrix} 1 & h_2 & A \\ m_1 & m_2 & P \\ \mu_1 & \mu_2h_2^2 & Q \end{vmatrix}=0$$

or, expanded,

$$h_2^2\mu_2(m_1A-P)+h_2(\mu_1P-m_1Q)+m_2(Q-\mu_1A)=0,$$

from which is obtained

$$h_2=\frac{(m_1Q-\mu_1P)\pm((m_1Q-\mu_1P)^2-4m_2\mu_2(m_1A-P)(Q-\mu_1A))^{\frac{1}{2}}}{2\mu_2(m_1A-P)}, \quad (32)$$

Of the two possible values of h_2, only the smaller is generally useful.

The quantities $(\varphi_1+\varphi_3)$ and φ_2 may be found by solving any pair of Eqs. (28), (29), and (30), say (28) and (29), with the following results:

$$(\varphi_1+\varphi_3)=\frac{m_2A-h_2P}{m_2-m_1h_2}, \quad (33)$$

and

$$\varphi_2=\frac{P-m_1A}{m_2-m_1h_2}. \quad (34)$$

The quantities φ_1 and φ_3 are found as follows: By Eq. (23), when $h_3=1$,

$$\frac{g_3}{g_1}=\frac{AM+\varphi_1(1-M)}{AM+(\varphi_1+h_2\varphi_2)(1-M)}. \quad (35)$$

Let $(\varphi_1+\varphi_3)=\Phi$, the value of which is given by Eq. (33), then

$$\varphi_3=\Phi-\varphi_1. \tag{36}$$

Substitution for φ_3 and g^3/g in Eq. (31) gives

$$\varphi_1=\frac{Rh_2\varphi_2(1-M)-AM(\Phi-R)}{(1-M)(h_2\varphi_2+\Phi-R)}, \tag{37}$$

where

$$R=\frac{(x_1-s_1)}{\mu_1 s_1 x_1}\frac{\Delta M}{M}.$$

The value of φ_3 is then found by Eq. (36).

The air spaces in this case are

$$d_1=\frac{(1-h_2)(1-M)}{AM+\varphi_1(1-M)} \tag{38}$$

and

$$d_2=\frac{(h_2-1)(1-M)}{AM+(\varphi_1+h_2\varphi_2)(1-M)}. \tag{39}$$

As R and M approach zero, φ_1 approaches zero and d_1 approaches infinity. The solution is therefore discontinuous for $R=M=0$.*** Also, if $R=M=0$, the length of the system becomes large as h_3 approaches 1 and the system becomes useless at values of h_3 considerably less than 1. However, if the magnification M is somewhere near -1, $h_3=1$ may give a solution that is useful in a series of trials and is more easily obtained than the solutions in other cases.

VIII. CONTROL OF THE SEIDEL SUMS

After a set of values of φ_1, φ_2, φ_3, h_2, and h_3 has been found which satisfies the conditions of scale, Petzval sum, longitudinal chromatic aberration, and lateral chromatic aberration, there remains the problem of determining the shapes of the lenses so that the desired values of the Seidel sums are obtained. Only three of the Seidel sums can be controlled at this stage, since there are only three disposable shapes.

The thin lens algebraic expressions for the first, second, third, and fifth Seidel sums†[10,11] are prepared, with the three shape factors as parameters. The values of the object and image distances, necessary for this, are determined by Eqs. (9). Because of the simplifying assumption that the aperture stop is in coincidence with the second lens ($g_2=0$), the second shape factor does not appear in the expressions for the third and fifth Seidel sums. These expressions are quadratics with only two variables, the shape factors of the first and third lenses.

The expressions for the third and fifth Seidel sums are set equal to appropriate constants (usually zero in early trials). These equations are then solved for the values of the first and third shape factors. Usually, a graphical solution is good enough. The shape factors so found are substituted into the expression for the second Seidel sum. The resulting expression is linear, with only one variable, the second shape factor. This expression is set equal to an appropriate constant (also usually zero in early trials). The resulting equation is then solved for the second shape factor.

The shapes thus found satisfy the equations for S-II, S-III, and S-V. They are then substituted into the expression for S-I. If the value of S-I so obtained is unsatisfactory, it is necessary to assume a different value for h_3 and repeat the entire solution. Usually, a satisfactory solution can be found for some value of h_3; if not, the only available expedient is a new start with different glass types.

IX. REPLACEMENT OF THIN LENSES BY EQUIVALENT THICK LENSES

After a satisfactory thin lens solution has been found, the lenses must be given suitable thicknesses to allow construction. Several procedures[6,8] have been invented for this purpose. The writer has preferred to keep the powers and shapes of the thick lenses the same as those of the thin lenses they replace. The spaces are then chosen so that the distances between the adjacent principal planes are the d_1 and d_2 of the thin

*** Kerber and Chrétien have mentioned this discontinuity in references 4 and 7.

† Formulas for the Sidel sums for thin lenses are given in references 3, 4, 5, 7, and 8. Formulas for the Seidel aberrations, which may be used just as well, are given and discussed in English in references 10 and 11. The aberrations are expressed as linear quantities in reference 10 and as angular quantities in reference 11.

[10] A. E. Conrady, *Applied Optics and Optical Design* (Oxford University Press, New York, 1929).

[11] I. C. Gardner, *Application of the Algebraic Aberration Equations to Optical Design*. Sci. Pap. Bur. Stand., No. 550.

lens solution. By this procedure the equivalent power of the system is unchanged.

After the introduction of thicknesses the quantities P, $\Delta s_3'$, $\Delta M/M$, S-I, S-II, S-III, S-V are evaluated by the application of exact paraxial formulas that take account of the thicknesses. These values will usually be somewhat different from the corresponding values for the thin lens system. The differences are approximately the changes to be expected on introduction of thicknesses. (They are exact for the particular case but only approximate for a new solution.) Good correction usually results if the solution is repeated using new values of P, $\Delta s_3'$, $\Delta M/M$, S-I, S-II, S-III, and S-V that differ from the original values by the negatives of the changes expected on introduction of thicknesses.

X. FINAL ADJUSTMENT

After a satisfactory thick lens solution has been obtained, the performance of the system is analyzed trigonometrically to determine its residual aberrations at full aperture and field angle. These residuals guide the designer in the choice of still different values of P, $\Delta s_3'$, $\Delta M/M$, S-II, S-II, S-III, and S-V to be solved for in order to get still better correction of the resulting system.

The analysis of two or more trials with different values of one or more of the Seidel sums will reveal the limitations of aperture, focal length, and field imposed by the glasses selected. It may then be desirable to start over with different glasses.

XI. ACCURACY OF COMPUTATIONS

It may not be superfluous to mention the accuracy desired in the computed values of φ_1, φ_2, φ_3, and h_2 and the precautions necessary to assure it. In the final stages of the computation of a design it may be found necessary to make small changes in h_3 in the neighborhood of $\Delta h_3 = .005$. The solution of the original Eqs. (1), (2), (3), (4) is, in practical applications, never far from indeterminate. As a consequence, in order that the computed changes in φ_1, φ_2, φ_3, and h_2 resulting from a small change in h_3 be sufficiently accurate, it is necessary that the individual terms in Eqs. (15), (16), (17), (18), and (26), if used, each contain five or six significant figures.[12] Two or three significant figures may be lost by subtraction of almost equal terms. Since it is desirable to have φ_1, φ_2, φ_3, and h_2 determined to five significant figures in the final stages of designing, it may be necessary to retain six or more significant figures in each of the terms. The inevitable uncertainty of the m's and μ's does not preclude the necessity for the retention of this large number of figures although they are not significant in the physical sense but are necessary to assure the desired physical significance in the solutions.

The accuracy of the values of φ_1, φ_2, φ_3, and h_2 obtained may be checked by substitution into the original equations. Usually it is found that (1), (2) and (3) are checked satisfactorily, but that (4) is the one that fails to check if the accuracy of the computations has been insufficient.

XII. CONCLUSION

The methods of this paper are long and tedious but systematic and straightforward. They should facilitate the production of good designs without extensive previous experience on the part of the designer.

More complex triplets, for example, those of the Tessar type or Heliar type, may be designed by these methods. The relative powers of the elements of a compound lens are assumed beforehand. In the first part of the solution, by which φ_1, φ_2, φ_3, h_2, and h_3 are determined, equivalent values of m and μ are used. These equivalent values are

$$\bar{m} = (\sum m\varphi / \sum \varphi) \quad \text{and} \quad \bar{\mu} = (\sum \mu\varphi / \sum \varphi).$$

In the expressions for the Seidel sums each element must be considered separately and its contributions computed, using its true index. The shape factor of each additional element may or may not be an additional independent parameter, depending upon whether or not the element is to be cemented to an adjacent element.

---

[12] L. B. Tuckerman, "On the Mathematically Significant Figures in the Solution of Simultaneous Linear Equations," *Annals of Mathematical Statistics*, **XII**, 307 (1941).

JOURNAL OF THE OPTICAL SOCIETY OF AMERICA VOLUME 38, NUMBER 12 DECEMBER, 1948

Photographic Sharpness and Resolving Power

I. The Design and Performance of an Apochromatic Resolving-Power Camera Objective*

FRED H. PERRIN AND H. ORLO HOADLEY
Kodak Research Laboratories, Eastman Kodak Company, Rochester, New York

(Received June 14, 1948)

The excessive residual aberrations of the ordinary achromatic doublet that had been regularly used to photograph resolving-power test objects on film samples in these Laboratories led to the construction of a special air-spaced apochromatic triplet containing fluorite. So excellent is the correction of the new lens that the Airy disk is white and changing the focus setting to fit the spectral sensitivity of the sample is unnecessary, except when the sensitivity peak is at a wave-length longer than 580 mμ. The improvement in measured resolving power over the values obtained with the former lens is slight for materials of high resolution but is marked for materials whose values are below about 100 lines per millimeter. Curves are presented showing the effect on resolving power of stopping down the new objective, and it is shown that this lens, whose aperture is $f/5$, is not adequate for materials exceeding 150 lines per millimeter or so, failing simply because of its comparatively low aperture. These results emphasize the dependence of resolving-power values on the aperture and the corrections of the camera lens. The loss in the resolving power of this lens caused by mal-focusing is also compared with that of an anastigmatic photographic objective.

I. INTRODUCTION

THE efforts to improve the definition of aerial photographs during the recent war pointed up the paucity of unimpeachable information on the phenomena relating to the edges of photographic images. Such phenomena, which for convenience we propose to group under the new term "craspedomorphology**" (from the Greek *kraspedon*, meaning "border" or "margin"), are now being studied, and the results will be published in a series of papers of which this is the first. These papers will appear as the material is collected, rather than after the whole study is completed, so that the results will become available as promptly as may be. Although such a procedure conduces to a less elegant and systematic presentation, we believe that this consideration is outweighed by the earlier availability of the results.

A common method of producing an image on a photographic material for determining the resolving power of the latter is to photograph a suitable test object in a special camera. In the present paper, we shall consider the effect of the aberrations of the camera lens, especially chromatic aberration, upon the measurements thus made. The lenses chiefly discussed are the ordinary cemented telescope doublet formerly in regular use and a special apochromatic air-spaced triplet that has supplanted it. In measuring craspedological phenomena, one always aims to use so nearly perfect a lens that the remaining imperfections do not vitiate the results. For some practical purposes, as for developing equipment to be used in aerial photography, lenses that incorporate the compromises called for in practical photography have to be used to simulate practical conditions, but then the craspedological characteristics of the film are not the sole factors involved. Such studies will not be included in the present series, which concern the properties of the sensitive materials themselves.

II. DESCRIPTION OF THE FORMER (FUESS) LENS

In these Laboratories, resolving power is measured by projecting the image of a test object at a reduction of 75× on the sample and examining the developed image visually through a binocular microscope. The detailed procedure

* Communication No. 1201 from the Kodak Research Laboratories.

** This term is intended to include such phenomena as sharpness, image-widening (often known as "photographic turbidity"), and resolving power. It is comprised in the term "microstructure," but this latter term also includes graininess and granularity, which must be studied by quite different techniques except insofar as granularity causes the edge of an image to be irregular in outline. The word is not intended to include development or gelatin effects near a border arising from the proximity of areas of widely different density, which Wolfe and Barrows (see reference 1) have termed "adjacency effects."

References are listed in a bibliography at the end of the paper.

will not be given here since it has been described elsewhere.[2] The lens that had been in use from at least 1917[3] to December, 1944, was a Fuess achromatic telescope objective of 150.0-mm focal length and $f/5.0$ aperture made of two elements cemented together. Any difference in the position of best focus for materials even as varied in spectral sensitivity as panchromatic and ordinary materials was negligible as judged from practical tests. However, when a sound-recording film, whose sensitivity peak is at 410 mμ instead of the more usual 450 mμ, showed an amazingly low value of resolving power, the seriousness of the secondary chromatic aberration was realized. Moreover, the evil effect of this aberration could not be eliminated entirely by refocusing or by using filters because the difference in focal length over the effective spectral region transmitted by a filter is too great.

The lens was measured on a lens bench for the sodium lines and the usual hydrogen lines, and the color correction was found to be as shown by the solid curve in Fig. 1. It was not possible to measure the spherical aberration visually because the necessarily small openings in the diaphragms did not admit sufficient light, but this was done in the camera by using a set of diaphragms, each containing two holes. By making a pair of exposures through each diaphragm, one exposure within and one beyond the focal point, two images were formed on the film. Simple geometry then sufficed to locate the focal point itself for each diaphragm. The displacement of this point as a function of the separation of the holes in the diaphragms is the spherical aberration, of course. The observations were not precise enough to warrant drawing a curve, but it can be stated that the aberration of the marginal ray was about 0.1 mm, although the two-thirds marginal ray had no aberration that was measurable by this technique.

The importance of the chromatic aberration was assessed by making focus series for various materials combined with various filters. The following types of film were used:

Eastman Sound Recording Film, Type 1357,
Eastman Fine Grain Sound Recording Film, Type 1371,
Eastman Fine Grain Sound Recording Film, Type 5372,
Kodak Micro-File Film, 35-mm,
Kodak Panatomic-X Film, 35-mm.

The filter combinations are listed in the legend of Fig. 1. When the entire range of spectral sensitivity was to be used, a Wratten No. 2 filter was introduced to eliminate the ultraviolet, for which the chromatic aberration of the lens was excessive.

The camera produces a power-of-two exposure series[4] so that resolving power can be plotted as a function of exposure, and the maximum read

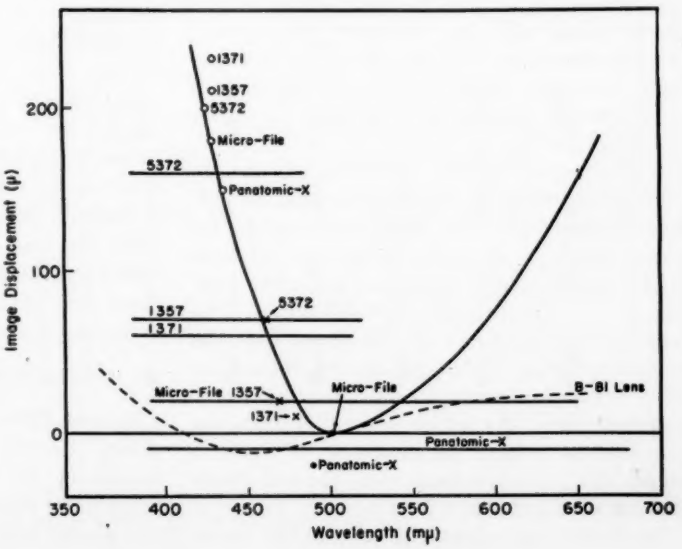

FIG. 1. Color curve of Fuess achromatic doublet as determined on the lens bench. Horizontal lines show image positions for materials indicated, the lengths of the lines representing respective spectral sensitivities. Points show image positions for specified materials used with following filter combinations: Solid circles, Nos. 45 and 4 (green light); crosses, No. 3 (blue-green); open circles, Nos. 36 and 2A (blue and violet). Broken curve shows computed color aberration of B-81 triplet.

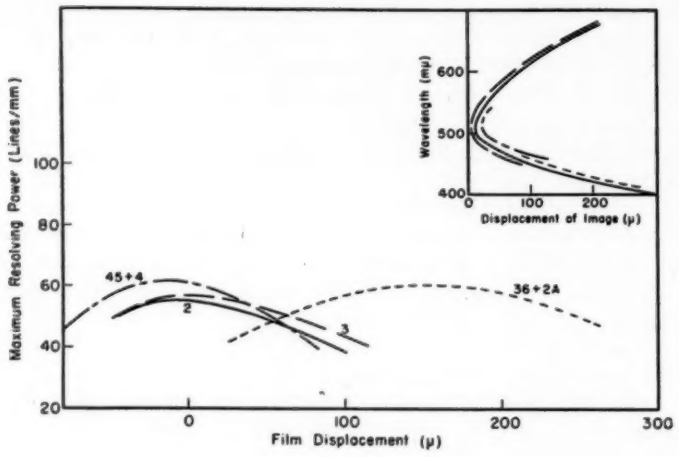

FIG. 2. Variation of maximum resolving power of Kodak Panatomic-X Film with film position, using Fuess doublet and Wratten filters whose numbers are given on the respective curves. Insert shows spectral region covered by each filter in terms of chromatic aberration of the lens.

off the curve. This maximum, when the contrast of the test object is 1000:1 (practically infinity), is generally taken as the characteristic resolving-power value for the material, and it will be the value that is meant everywhere in this paper except where resolving power is given as a function of exposure or density. Figure 2 shows the variation of maximum resolving power as a function of film position for Kodak Panatomic-X used with the four filter combinations. The best values for all the filters and a given film were found to be approximately the same; in the present case, the differences are hardly outside the limits of experimental error. Wedge spectrograms were made to determine the spectral limits represented by each film-filter combination, and these limits for Kodak Panatomic-X are shown in terms of the chromatic aberration of the lens in the insert of Fig. 2.

The accuracy of the measurements for the various combinations can be estimated by plotting the positions of the focal points against the wave-lengths of the peaks of the spectral-sensitivity curves of the respective film-filter combinations and superposing this plot on the chromatic-aberration curve of the lens. This has been done in Fig. 1. The sensitivity peaks of the films when used with the No. 2 filter are so indefinite that the entire spectral ranges are shown, but, despite the crudeness of this criterion, the correspondence with the lens-bench curve is unmistakable.

An interesting method of evaluating lenses has been developed recently by Jones and Wolfe,[4] and Dr. Wolfe and Mr. F. C. Eisen tested this lens by that method. Briefly, the procedure is to form an aerial image of a slit with the lens under test and to make a photomicrograph of this aerial image. An absorbing wedge whose base is normal to the slit is placed against the plate to attenuate the optical image in a lengthwise direction. Thus, the height of the photographic image at any point represents the logarithm of the intensity of the optical image at that distance in a normal direction from the center line of the slit. If the lens were perfect, the contour would be a curve of the theoretical diffraction pattern of the slit on a logarithmic scale. Figure 3 shows the curves of the energy distribution in the optical images (EDI curves) made at different positions along the axis of the Fuess lens with different filters. The lens was focused visually in "white" light; note that apparently the green part of the spectrum is most effective in this procedure and that the best focus settings for the red and the blue regions are farther from the lens than for the green, as would be expected.

III. DESCRIPTION OF THE PRESENT (B-81) LENS

In consultation with Dr. Max Herzberger, the design of a new lens was undertaken. The steps leading to the final form will be described in some little detail because this general type of lens should be suitable for other purposes where

excellent correction over a very small field is required, as in spectrometers.

The first lens to be computed was the ordinary cemented doublet shown in Fig. 4A. Light barium crown and dense flint glasses (LBC-1 and SF-5) were selected because chromatic aberration (between the D- and the G'-lines), spherical aberration, and coma could be corrected simultaneously. The figure shows the resulting axial intersection points for the marginal ray ($f/5.0$), the zonal ray at $f/7.1$, and the paraxial ray plotted against wave-length. The horizontal axis represents the paraxial focal point for the D-line.

The secondary spectrum and chromatic variation of spherical aberration (CVS) were not good, so an attempt was made to improve these. Now, a cemented doublet is always afflicted with CVS for a simple reason: To correct spherical aberration for D-light, the negative element must have a somewhat higher index than the positive so that the cemented surface will be negative in power to compensate for the spherical contributions of the other two surfaces. For achromatism, furthermore, the negative element must have a higher dispersion than the positive, which means that the difference in index becomes still greater for the shorter wave-lengths. In this spectral region, therefore, the power of the cemented surface and hence its contribution to the spherical aberration become greater than at the D-line, and the lens becomes overcorrected.

Figure 4B for a separated doublet made of the same glasses shows that CVS can be reduced by separating the elements; the separation, however, prevents the longitudinal chromatic aberration and the chromatic difference of magnification (CDM) from being corrected simultaneously.

The theory of the secondary spectrum and the conditions required for correcting it are well known.[5] Briefly, the requirement is that the ν-values shall be sufficiently different and that the corresponding partial-dispersion ratios shall be alike. Now, Table I shows that the partial dispersion of SF-5 between G' and h is 0.492, while the value for LBC-1 is 0.429—a difference that explains the large secondary spectrum. On the other hand, a special glass, KzFS-1, originated by Schott but now made in this country, has a partial dispersion of 0.450, which corresponds more nearly with 0.441 for the Bausch and Lomb LBF-1 and 0.432 for LBC-2. The last-mentioned glass differs somewhat more than LBF-1 in its partial dispersion from KzFS-1 but it also differs considerably more in ν-value.

In Table II are listed representative samples of the various types of system that were calculated, including the two already mentioned. For each of them are given the CVS (difference between the spherical aberrations at G' and at D) and the zonal residual of the spherical aberration at D, with some pertinent remarks. (The zonal residual is defined as the spherical aberration at $f/7.1$, minus one-half of the spherical aberration at $f/5.0$.) Each of the lenses has the

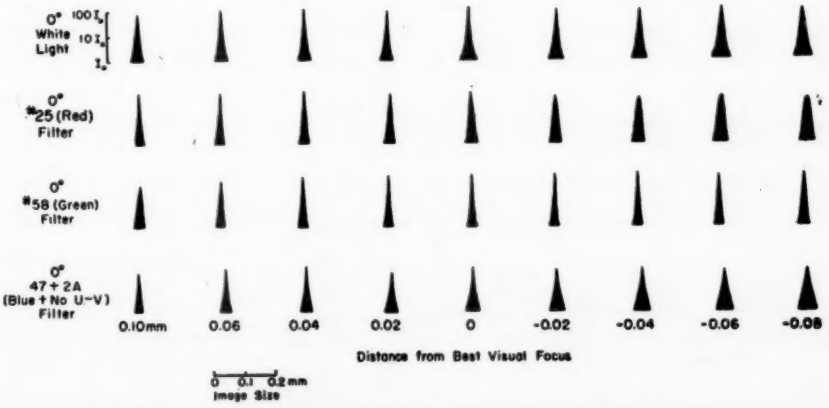

FIG. 3. EDI curves of line source produced by Fuess doublet with filters and at axial positions indicated for field angle of 0°.

TABLE I. Dispersion data for materials used in computing the lenses involved in developing the B-81 objective.

Material	ν	n_D	$n_{G'}$	$\frac{n_A - n_C}{n_C - n_F}$	$\frac{n_{G'} - n_h}{n_C - n_F}$	λ_0
SF-5	32.2	1.67252	1.70038	0.314	0.492	220
KzFS-1	44.0	1.61294	1.63093	0.340	0.450	190
LBF-1	53.4	1.58800	1.60212	0.336	0.441	182
LBC-2	57.4	1.57250	1.58521	0.338	0.432	177
Fluorite*	95.2	1.43387	1.43960	0.349	0.424	168
K-11	61.6	1.50005	1.51035	0.352	0.424	170
LBC-1	59.9	1.54110	1.55257	0.347	0.429	174
SK-16	60.3	1.62031	1.63339	0.349	0.425	171

* Data for fluorite from Landolt-Börnstein, "Physikalisch-Chemische Tabellen," 5th Ed., p. 911. Other data from glass catalogues.

marginal spherical aberration corrected at an intermediate wave-length.

The first trial objective using KzFS-1 was a cemented doublet in which the other glass was LBC-2 (Lens 3, no figure). Because of the very strongly curved cemented surface, the spherical zone and CVS were very bad. The coma could not be corrected.

The negative element was then split and a cemented triplet (Lens 4, Fig. 4C) with a positive element of LBC-2 between two negative elements of KzFS-1 was tried. The zonal aberration was much reduced but the CVS, although better, was still not good enough. Comatic correction was not obtained.

The effect of this pair of glasses on the secondary spectrum proved disappointing, so the next system was calculated with LBF-1 in order to flatten the violet end (Lens 5, no figure). The system was a cemented triplet, having a negative element of KzFS-1 between two positive elements of LBF-1. The zonal residual and CVS were both much worse than before although this time the coma was corrected.

The final attempt to use KzFS-1 consisted of four cemented elements in the order plus-minus-plus-minus, the positive elements again being made of LBF-1 (Lens 6, Fig. 4D). Here the spherical zone was satisfactorily small and comatic correction was achieved. However, although various distributions of the powers among the four elements were tried, it was not found possible to reduce the CVS below the value for the ordinary achromat (Lens 1). Comparison of Fig. 4D with Fig. 4A shows that the secondary spectrum was noticeably flattened, however, particularly in the red, but still it was not as good as was desired.

About this time, Dr. D. C. Stockbarger, of the Massachusetts Institute of Technology, had developed synthetic fluorite for the Office of Scientific Research and Development, and several disks that had been submitted for testing became

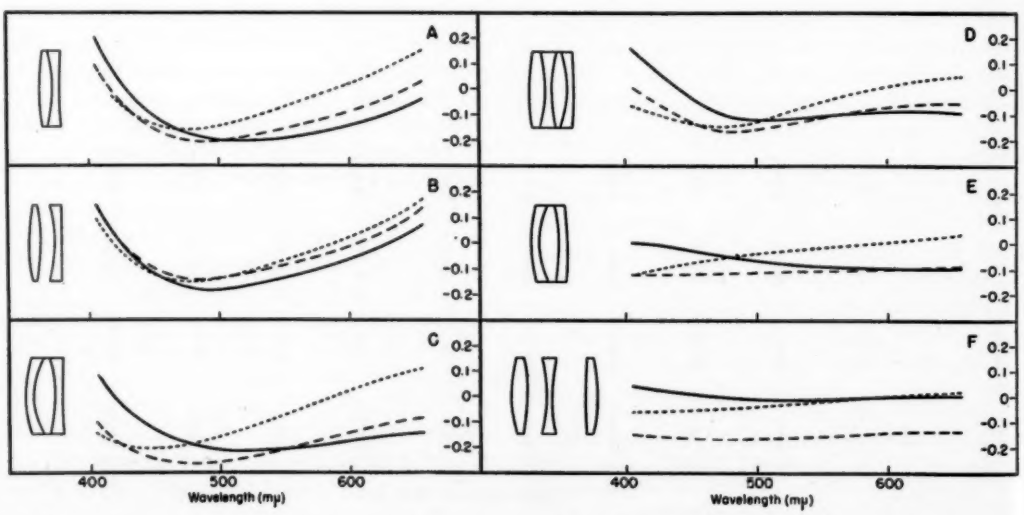

FIG. 4. Cross sections and aberration curves of lenses computed during development of B-81 triplet. Solid lines represent positions of focal points for marginal rays ($f/5.0$); broken lines are for zonal rays at $f/7.1$; dotted lines are for paraxial rays, whose focal points for the D-line are taken as the origin of ordinates for the corresponding lenses.

TABLE II. Summary of lenses that were computed during the development of the B-81 objective.

Lens No.	Fig. No.	Materials		No. of Elements	Type	Sph. Zone	CVS	Remarks
1	4A	SF-5	LBC-1	2	Cem.	−0.026	+0.220	
2	4B	SF-5	LBC-1	2	Sep.	+0.026	+0.094	Bad CDM
3	—	KzFS-1	LBC-2	2	Cem.	−0.252	+0.692	Bad coma
4	4C	KzFS-1	LBC-2	3	Cem.	−0.063	+0.310	Bad coma
5	—	KzFS-1	LBF-1	3	Cem.	−0.131	+0.840	
6	4D	KzFS-1	LBF-1	4	Cem.	−0.033	+0.234	
7	4E	K-11	Fluorite	3	Cem.	−0.056	+0.164	
8	—	K-11	Fluorite	3	Sep.	−0.187	+0.126	
9	4F	LBC-1	Fluorite	3	Sep.	−0.147	+0.075	
10	—	SK-16	Fluorite	3	Sep.	−0.141	+0.067	
11	—	SK-16	Fluorite	3	Sep.	−0.041	+0.021	
5-B-81	5	SK-16	Fluorite	3	Sep.	−0.018	−0.014	Final

available. This material, with its partial dispersion of 0.424, is a good match for the three glasses, LBC-1, K-11, and SK-16, listed in Table I. These glasses also have approximately the same ν-values, which are quite different from that of fluorite, although the glasses differ amongst themselves in index.

The first system containing fluorite to be computed was a cemented triplet with the fluorite positive element between two negative elements of K-11 (Lens 7, Fig. 4E). The system had only a small zonal residual and its CVS was smaller than that of any of the previous cemented lenses.

It was mentioned earlier that CVS can be removed by introducing a considerable separation between the positive and the negative elements but that, if only two elements are used, both longitudinal chromatic aberration and CDM cannot be corrected simultaneously. Accordingly, the type finally adopted had three elements, a positive on either side of a negative and separated from it, so that all three errors could be corrected. Three such triplets were then calculated. They all had fluorite for the outside positive elements but for the middle element they contained in turn K-11 (Lens 8, no figure), LBC-1 (Lens 9, Fig. 4F), and SK-16 (Lens 10, no figure).

The glass of highest index (SK-16) seemed to have the most advantages, particularly for the reduction of the zonal residual, so all subsequent calculations were made with it. By means of small changes in the individual radii, thicknesses, and separations of the system, it was found possible to bring both CVS and the zonal spherical aberration to very small values with this glass. The best lens thus computed was No. 11 in Table II.

The index values for this lens were taken from the Schott catalogue for the SK-16 glass and from Landolt-Börnstein's "Physikalisch-Chemische Tabellen" for crystalline fluorite. The failure of the calculated points to lie on smooth aberration curves and the disappointing behavior of the lens when made and tested indicated errors in the index values, so samples of the actual blanks used were measured. These values, which are slightly different from those in Table I, are shown in Table III. The differences would have been negligible had Lens 11 exhibited the usual amount of secondary spectrum. By recalculating the lens with the new indices, the computed points were found to fall

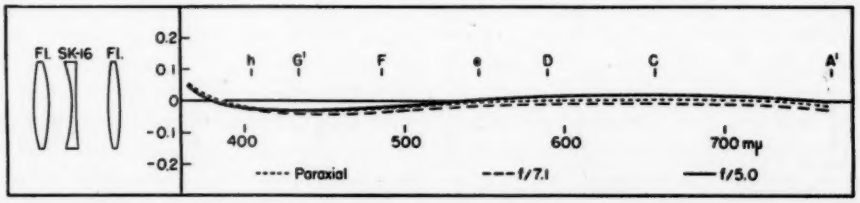

FIG. 5. Aberration curves and cross section of B-81 triplet.

TABLE III. Indices of refraction at 20°C of the two materials composing the B-81 objective, determined at the Kodak Research Laboratories. Temperature coefficients are the changes in the sixth place for a 5°C change in temperature according to Landolt-Börnstein.

		Fluorite		*SK*-16	
Line	λ	n	Δn	n	Δn
A'	768.19 mμ	1.430934		1.613151	
C	656.28	1.432501	−56	1.616745	+20
D	589.25	1.433849	−54	1.619778	+21
e	546.07	1.434974		1.622318	
F	486.13	1.437060	−52	1.626997	+25
g	435.84	1.439512		1.632547	
G'	434.05	1.439618	−51	1.632781	+26
h	404.66	1.441533		1.637151	
m	365.02	1.444906		1.644985	
	1000	1.42895*		1.60841**	
	1400	1.42679*		1.60284**	
$\frac{n_{A'}-n_C}{n_C-n_F}$		0.344		0.351	
$\frac{n_{G'}-n_h}{n_C-n_F}$		0.420		0.426	

* Interpolated from Landolt-Börnstein.
** Computed by Herzberger's formula.

on the smooth aberration curves shown in Fig. 5. The recalculated lens was given the formula number "5-B-81," the "5" indicating the f/-number and the "81" indicating the serial number of the formula. The "B" indicates that the lens is essentially a telescope objective in accordance with Kingslake's[6] classification, although its air spaces are comparatively great and its corrections are superior to those of most lenses in this classification. This lens will be referred to hereafter as the "B-81."

When this lens was made up, its behavior was disappointing. The defects arose chiefly from the difficulty of polishing the soft fluorite, so the surfaces were refigured by hand to make them fit the test plates properly, and the lens was reassembled. A little spherical aberration was then detected, but this was removed by varying the first air space by successive steps of a few hundredths of a millimeter until the expanded star images in white light were identical, both within and beyond the point of best focus. This adjustment proved to be very sensitive and provided a good additional justification for the use of an air-spaced rather than a cemented system. After the final adjustment, the Airy pattern was uncommonly good, the most striking feature being that the central disk was entirely white instead of consisting of concentric colored circles such as are produced by ordinary achromats. No difference in focus could be detected through Wratten *A*, *B*, and *C* filters successively.

The next test was to determine the light distribution experimentally by the Jones-Wolfe technique already described. The resulting EDI plots are shown in Fig. 6, which is comparable with Fig. 3 for the former lens except for the addition of a series made with white light at a

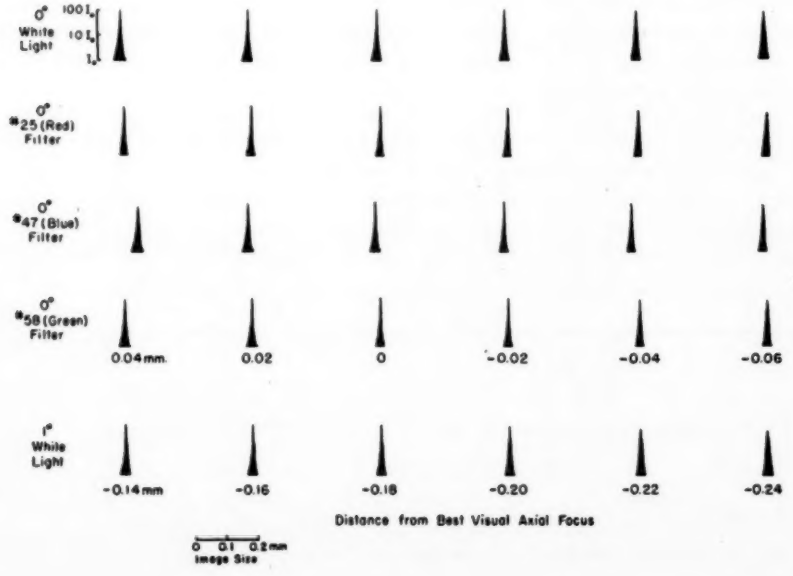

FIG. 6. EDI curves of line source produced by B-81 triplet with filters and at axial positions indicated for a field angle of 0° and, in white light alone, at a field angle of 1°.

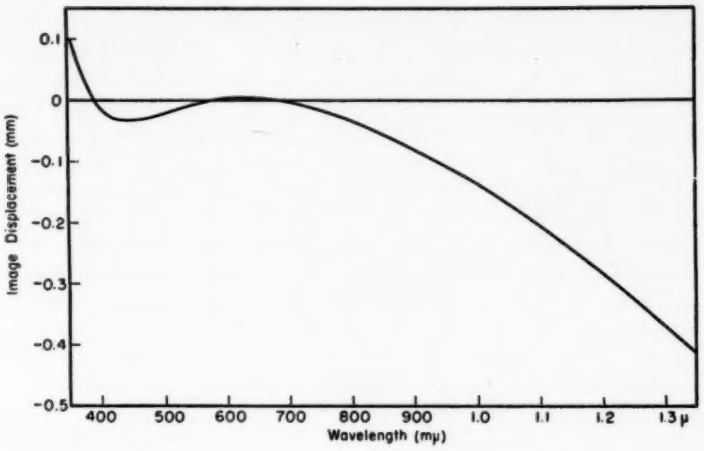

FIG. 7. Chromatic aberration of B-81 triplet for paraxial ray over an extended spectral region.

field angle of 1°. The superior sharpness of the plots compared with those of Fig. 3 is noteworthy.

No convenient means were at hand for determining the aberration curves on the lens bench, but there is no reason for not accepting the calculated curves of Fig. 5. The maximum amount of spherical aberration is about 0.02 mm, compared with almost 0.1 mm for the former lens. The special improvement is in the chromatic aberration, which does not exceed 0.06 mm even for the marginal ray. This improvement is more evident in Fig. 1, where the broken line represents the chromatic aberration for the paraxial ray.

To estimate the course of the color curve outside the visible spectrum, the paraxial ray was calculated for wave-lengths of 1.0 and 1.4μ. The indices of fluorite were interpolated from the published values; the indices of the glass were computed by means of formulas developed by Herzberger.[5] The curve is drawn in Fig. 7, which shows that the lens has the typical apochromatic color curve as defined originally by Abbe, namely, it has two stationary points (a maximum and a minimum) instead of the single one (a minimum) characteristic of achromats. We might expect, however, that a change of focus would be needed for a film-filter combination having a narrow spectral range of effective sensitivity, especially in the red, and Fig. 8 shows that such is the case. (Note that the axis of ordinates is different from that in Fig. 7, having been moved to the position used for panchromatic and color-blind materials in the resolving-power camera.) The scale has been expanded for clearness; for a proper comparison, note the dotted curve for the Fuess lens replotted from Fig. 1. It happens that a single division of the focusing scale represents 20μ, and experience indicates that it is impracticable to make a setting closer than half a division. This is shown by Fig. 9, from which Fig. 8 was made. Indeed, the effect on resolving power of a slight error in focus is so small that the agreement of the experimental with the calculated values is better than might be expected. For both Type 5372 emulsion, whose sensitivity extends unusually far into the ultraviolet, and Micro-File emulsion, which has a typical panchromatic sensitizing, the best focus is somewhere between $+5$ and -15 when no filter is used. This means that the focus setting is sensibly the same for a color-blind material as for a panchromatic, so long as no filter is used. Even with a filter, the focus need not be changed so long as the effective sensitivity is entirely within the short-wavelength region of the visible spectrum. For any combination of film and filter for which the effective spectral sensitivity is predominantly beyond 580 mμ, however, focusing must be done by trial.

The excellence of the correction for chromatism makes this lens a suitable subject for testing a criterion proposed by Harting in 1908 and discussed ten years ago by one of the present

authors.[7] Assuming that glasses follow Hartmann's dispersion formula,

$$n = n_0 + c/(\lambda - \lambda_0),$$

as they do fairly well in the visible spectrum, it can be shown that a thin doublet is achromatic when the elements have the same value of λ_0. The values of ν must be different, of course. The λ_0-values of the materials used for the various trials are shown in the last column of Table I. Without pointing out the correspondence of the λ_0-values for the elements of all the lenses, we may note that the values for Lens 1, made of SF-5 and LBC-1, are 220 and 174, respectively, while the values for the B-81 lens are 171 and 168. Thus, although the lenses under discussion are mostly triplets and are far from thin, Harting's criterion is seen to be an excellent guide to the choice of glass.

Despite the superior performance of the new lens, it possesses a serious disadvantage in its high temperature coefficient of focal length. When the temperature of a camera changes, the indices of the lens elements change, as also do the thickness, separation, and radii of the lens elements and the length of the camera body. In the case of glass, not only the magnitude but even the sign of the temperature coefficient of refractive index depends upon the temperature range; fortuitously, however, the various effects usually neutralize one another so that, except for extreme temperature variations, the effect upon focal length is negligible. For the B-81 lens, on the other hand, the coefficient of index of the glass at the *D*-line, according to the Landolt-Börnstein tables, is about $+0.000021$ while that of the fluorite is -0.000054. The latter figure is so much greater than the former that the effect of temperature changes upon the refractive indices might be expected to predominate over the other effects. Since the fluorite elements have positive powers while their temperature coefficient is negative, and the opposite is true of the glass element, an increase in temperature should increase the focal length of the complete lens, and, indeed, calculations show that the increase in back focus from this source alone should be 70μ for each 5°C rise. A series of experimental determinations ranging from 65°F to 89°F showed that the increase is sensibly linear and amounts to 125μ for each 10°F rise or 110μ for 5°C. The difference between the theoretical and the experimental values is, of course, to be sought in the other effects enumerated above. Since each division of the focusing scale represents 20μ, the approximate magnitude of the correction is one division for every 2°F, which must be taken into account, inasmuch as the room temperature varies from 72°F in winter to 90°F in summer. Insofar as changes in refractive index are concerned, however, the computations show that such a temperature change has no sensible effect on the aberrations.

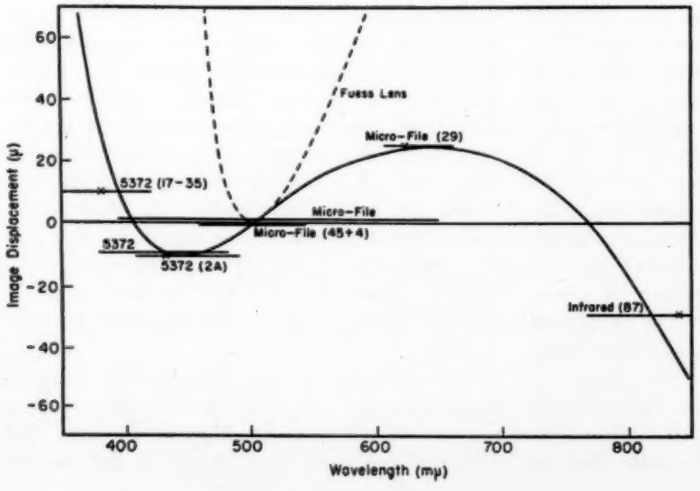

FIG. 8. Calculated color curve of B-81 apochromatic triplet for paraxial ray. Horizontal lines show image positions for specified materials used with indicated filters, lengths of lines representing respective spectral sensitivities. Crosses show peaks of sensitivity. Broken curve is replotted from Fig. 1 for comparison.

It should be remarked that, in spite of the fact that this objective is superficially similar to the familiar triple anastigmat ("Cooke" lens), it has no correction at all for any field aberrations except coma, and the image quality deteriorates rapidly beyond 1° from the axis. This is due largely to two reasons: First, the low index of the fluorite gives the system an exceptionally high Petzval sum, namely, $0.81/f$, compared with about $0.25/f$ for the usual photographic objective. Second, the strong curvature of the second surface necessary for the correction of CVS introduces a large amount of undercorrected astigmatism.

IV. THE CHOICE OF MAGNIFICATION FOR READING

A feature of the technique that in itself is foreign to the immediate subject but which introduces a slight element of uncertainty into comparisons with the former lens relates to the conditions under which the samples are read. Until the past year, the procedure had been invariably to read the images under a magnification of 100×, using a 16-mm (10×) objective and a 10× ocular. For materials of low resolving power, however, which are usually comparatively grainy, the observer's attention is distracted by the graininess at such a high magnification. Moreover, a little reflection will show that the limiting three-line pattern observed when assessing a material whose resolving power is 80, for example, looks twice as large as the pattern observed when the resolving power is 160, which is unfair. Experiments were made on reading the materials of lower resolving power under lower magnifications with gratifying results, and now the routine procedure is to reserve the former combination for materials whose maximum values are over 100 lines per millimeter and to substitute a 32-mm (4×) objective for materials below 120 lines, the resulting over-all magnification becoming 40×. Obviously, this does not maintain a strictly constant relation between observed resolving power and apparent size of pattern, but it is readily performed and does reduce the disparity below that previously obtaining. It goes without saying that the substage iris must be properly set for the objective being used so that about two-thirds of the exit pupil is filled in each case.

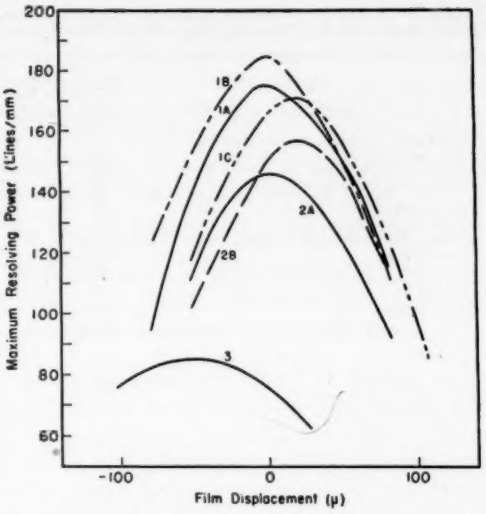

FIG. 9. Variation of maximum resolving power with film position, using B-81 triplet and the following films and filters: 1A, Kodak Micro-File Film, no filter; 1B, same film, Nos. 45 and 4 (green) filters; 1C, same film, No. 29 (red) filter; 2A, Type 5372 film, no filter; 2B, same film, Nos. 17 and 35 (ultraviolet) filter; 3, special infrared film, No. 87 (infrared) filter. Film displacement is measured from position of best focus for Curve 1A.

Experience indicates that there is no definite correlation between the values read at the two magnifications. In the case of materials that gave values of 50-60 lines per millimeter with the former camera lens when read under a power of 100×, reducing the power led to an increase of 10–15 lines per millimeter. Few materials appear to have a resolving power as low as this with the present lens, rarely falling much below 100, and at this value, there appears to be little choice between the two powers. The lower power, however, seems to give an impression of greater certainty.

V. COMPARISON OF RESULTS OBTAINED WITH THE TWO LENSES

Based upon Rayleigh's criterion, the limit of resolution of both lenses for a wave-length of 500 mμ would be about 300 lines per millimeter if the lenses were perfect, since the aperture of both is $f/5$. By setting a microscope behind the camera and examining the aerial image visually under a magnification of 100×, the 275-line

TABLE IV. Values of resolving power of typical materials as obtained with the Fuess doublet and the B-81 triplet.

Material	Maximum Resolving Power Fuess	B-81	Ratio
Kodak Super-XX Panchromatic Roll Film	50	95	1.9
Kodak Panatomic-X Film (35-mm)	65	105	1.6
Kodak Portrait Panchromatic Sheet Film	50	90	1.8
Kodak Tri-X Panchromatic Sheet Film	40	70	1.8
Eastman Duplicating Negative Film, Type 1505	80	105	1.3
Eastman Release Positive Film, Type 1301	60	105	1.7
Eastman High Contrast Positive Film, Type 1363	105	170	1.6
Eastman Fine Grain Duplicating Positive Film, Type 1365	135	170	1.3
Eastman Sound Recording Film, Type 1357	55	100	1.8
Kodak Micro-File Film	170	180	1.1
Kodak Direct Positive Panchromatic Film	75	95	1.3
Kodak 40 Plates	40	70	1.8

image formed by both lenses has been resolved. The lenses differ markedly from each other in their photographic behavior, however, as can be seen from Table IV. Neglecting any effect of the change in reading conditions, which cannot be evaluated readily, recent values for some common materials are listed in comparison with values taken from our files that had been obtained with the Fuess lens. The last column gives the ratio of the new to the old, and it is clear that this ratio is far from being constant. The only generality that can be made is that the materials of low resolving power are more affected by lens aberrations than are the materials of higher resolving power. One reason may be that the leveling influence of diffraction is being exhibited in the latter case, inasmuch as it will be shown presently that materials of high resolving power are not exhibiting values that are as high as they would exhibit if the lens intercepted all the light coming from the test object. In other words, the limitation imposed by diffraction may be becoming more important than that imposed by the aberrations of the inferior lens in the case of such samples. The interaction of lens and emulsion has been considered at length by Selwyn and Tearle,[8] so that we need not go into it here. There is, however, one point brought out by these authors that is of special interest in this connection. By comparing Figs. 3 and 6, it is evident that the diffraction patterns in the former are less sharp, especially at the base, than those in the latter. Now, a material of low gamma and great latitude will record a large part of the pattern in any case, so that the photographic image made with the inferior lens will be broader and more diffuse than that of the superior lens. A material of high gamma, on the other hand, will have too small a latitude to record more than the upper (brighter) part of either pattern, which is narrow in both cases. Since these two types of material have, respectively, relatively low and high resolving powers anyway, the phenomenon just discussed obviously should increase the natural difference between the materials when the aberrations of the lens are considerable. To what extent this mechanism operates, however, cannot be estimated now.

VI. THE VARIATION OF RESOLVING POWER WITH LENS APERTURE

The effect of diffraction by a lens of finite size, of course, is to cause the image of an infinitely sharp boundary between a bright and a dark field to have an illuminance gradient of finite slope in the image. This means that the image of a fine, sharp, linear pattern becomes an approximately sinusoidal pattern of small amplitude. Since the illuminance does not change sharply from a maximum to a minimum, and this minimum is greater than zero, the apparent resolving power of the emulsion being measured is not what it would be if the lens were infinitely large so that the illuminance would vary abruptly from zero to a maximum.

To study the nature and effect of the influence of the lens aperture, a series of stops was made that could be placed against the lens. Four materials were exposed at full aperture and then through all these stops in turn, and the resulting resolving powers were read in the usual way. The maximum values for a test-object contrast of 1000:1 are plotted against linear aperture in Fig. 10.

The striking feature of this figure for materials *A* and *B* is that the curves flatten at about 30 mm, which is the full aperture of the lens. This would indicate that the true resolving powers of these two materials are being read and that the present lens is amply large for them. The curves of materials *C* and *D* are still rising, however, which shows that the aperture of the lens should be greater if its influence is not to be felt.

The range of apertures was extended by exposing these two latter materials in a camera that

uses a microscope objective in the reversed position. The best values thus obtained were about 240 and 400 lines per millimeter, respectively, regardless of whether an objective of $N.A.=0.25$ (16-mm focal length) or one of $N.A.=0.50$ (8-mm focal length) was used. Now, the numerical aperture is defined as the sine of the angle subtended by the semi-diameter of the entrance pupil at the object point, and elementary geometry indicates that, for a simple lens of 150-mm focal length, a linear aperture of 75 mm corresponds to a numerical aperture of 0.25. The flatness of these curves for such an aperture is strongly indicative that the influence of the finite size of the lens has been overcome, and this conclusion is strengthened by the circumstance that the 8-mm objective resulted in no gain in resolving power over that obtained with the 16-mm.

A new camera using a reversed microscope objective is under construction, and when it becomes available, the effect of the lens aperture will be studied further. From a practical standpoint, the significance of Fig. 10 is that the values obtained for the materials of high resolving power with even the B-81 lens are doubtless too low—by reason of the comparatively low aperture, however, and not by reason of aberrations. They represent, however, the maximum that may be expected from a "perfect" lens of $f/5$ aperture, which is a common size in photographic practice.

In passing, it may be remarked that lenses almost invariably show poorer photographic resolution at their largest stops than at intermediate ones. Indeed, the lens described here is the only one the present authors can recall having been described in the recent literature on this subject that does not behave thus.

VII. THE EFFECT OF INACCURATE FOCUSING

A matter of some importance is the tolerance that is allowable in focusing, and, naturally, this depends upon the quality of the lens. In most photographic applications, a field of 10° to 60° or more must be covered, and the compromises forced upon the lens designer in covering such fields mean that the image at the center of the field is inferior to the image formed by the B-81 lens, which needs to cover less than 2°.

To determine the effect of improper focusing, a series of samples was exposed at various settings of the focusing sleeve. The test objects were, respectively, the standard resolving-power test object and a clear line whose geometrical image on the sample was 100μ wide. The images of the line, after development, were scanned with a microdensitometer, and their widths and the sharpness of their edges were determined in a manner to be described below.

It is not part of the present series of investigations to consider the effect of forming resolving-power images with less perfect lenses; the idiosyncrasies of individual lenses make this a study

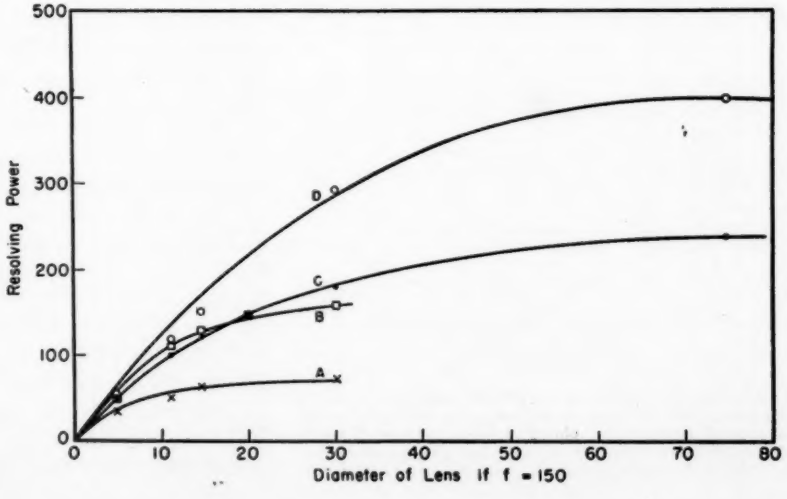

FIG. 10. Variation of maximum resolving power with lens aperture. Values for 75 mm were obtained with reversed microscope objective; the others were obtained with B-81 triplet.

by itself. A 140-mm, $f/4.5$, air-spaced anastigmat happened to be at hand, however, so a similar series of exposures was made with it stopped to $f/5$ for comparison. The Fuess objective was no longer available when these runs were made.

Figure 11A shows the variation in maximum resolving power of an aerographic film as a function of the distance from the best focus for each lens, this distance being given in terms of 1/100 of one percent of the focal length itself. Figure 11B shows the same thing for Kodak Micro-File Film.

The effect of inaccurate focusing can be most readily evaluated numerically from the variation in observed resolving power caused by a given displacement of the lens from its optimum position. For this purpose, let us take one division of the focusing scale, which corresponds to 20μ or 0.013 percent, and let us assume that the anastigmat has the same focal length as the B-81 and is similarly mounted. The results are shown in Table V.

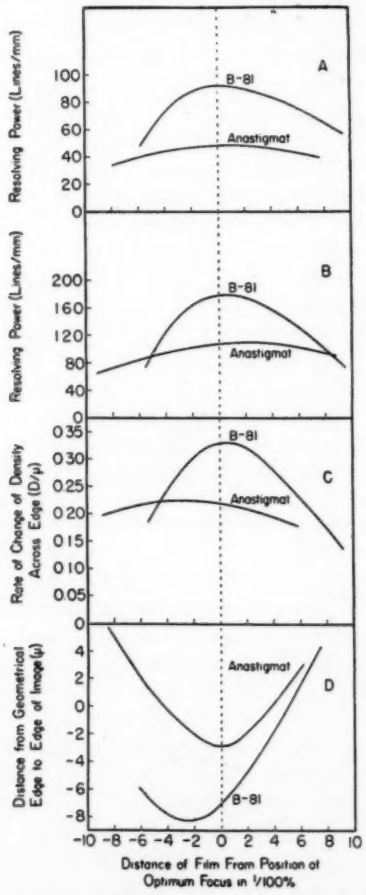

FIG. 11. A, variation of maximum resolving power of an aerographic film with malfocusing for B-81 triplet and for typical anastigmatic photographic objective. B, same for Kodak Micro-File Film. C, variation of edge sharpness, and D, variation of image-width, for Kodak Micro-File Film.

This bears out our *a priori* reasoning that the better lens calls for the more critical focusing. However, no serious error in resolving power arises from an error of upwards of one division in focusing, and even the correction for temperature can be made more closely than that. Moreover, the variation in resolving power is nonlinear, so an error of less than one division does not result in proportionately as great an error as the preceding table would indicate.

The photographic images on the Micro-File film of the clear line mentioned were scanned in the microdensitometer with a slit whose image on the film was 2.5μ wide. The resulting traces showed the variation in density as a function of the distance across the image. At the edges, the traces had the shape of a characteristic H and D curve, which is quite normal. For each focus setting and a constant exposure, the maximum slope was converted into rate of change of density per micron distance normal to the length of the line. Figure 11C shows the sharpness thus determined against the axial displacement of the sample in the camera.

Another feature that can be measured from these traces is the widening of the line as the sample is moved from the position of best focus, but some criterion as to what constitutes the edge of the line must be adopted. This is a research in itself, and for the present we shall take advantage of the circumstance that several observers making visual measurements on photographic images with the filar micrometer have consistently selected the point of the sharpness curve where the toe merges into the straight portion. Adopting this criterion, we have plotted the line width for the Micro-File film in Fig. 11D. This and Fig. 11C are convenient for estimating the damage done to sharpness and line width by inaccurate focusing.

A very significant feature of Fig. 11 is the great inferiority of the anastigmat to the special

resolving-power lens. Doubtless some other camera lenses would behave better, but clearly any resolving-power determinations made with ordinary lenses should be scrutinized closely. Narath[9] has also confirmed this conclusion by comparing the results obtained when using a microscope objective with those obtained when using an ordinary camera lens.

VIII. CONCLUSIONS

1. A telescope objective consisting of two cemented elements and having the ordinary achromatic correction may lead to quite misleading values for the resolving power of photographic materials. A four-element air-spaced photographic anastigmat that was tested was still worse than the telescope objective.

2. An $f/5$ air-spaced triplet consisting of a dispersive crown-glass element between two collective fluorite elements can be made to have almost zero coma and spherical aberration in the center of the field as well as apochromatic color correction over the visible spectrum.

3. This special triplet results in values of photographic resolving power from 10 percent to 90 percent higher than those obtained with an ordinary achromat of the same aperture.

4. No correlation can be made between the values obtained with the two lenses, but the increase for the materials of low resolving power is greater than that for the materials of high resolving power. A possible cause is that the diffuse background arising from the aberrations of the achromat is not recorded on the latter materials by reason of their small latitude, and so it does not clog up the spaces between the lines.

5. Materials whose maximum resolving powers are below 120 lines per millimeter are more easily and consistently read under a magnification of 40× instead of 100×, as had previously been the standard procedure, and a change to the lower power was made for such materials in regular practice. This change may somewhat affect the comparisons adduced above.

4. Materials that read below about 150 lines per millimeter with the special triplet do not read higher when the camera lens has an aperture greater than $f/5$, but materials that read higher apparently would appear to be still better were the aperture greater. The minimum aperture required for materials of different resolving-power characteristics has not been definitely determined, however, nor have the results obtained by optical projection of the test object been compared with the results obtained by contact printing.

TABLE V. Variation in maximum resolving power for one scale division.

Material	Variation in R.P. for one scale division	
	B-81 Lens	Anastigmat
Aerographic Film	4 lines = 4.5%	1 line = 2%
Kodak Micro-File Film	10 lines = 5.3%	2 lines = 1.8%

5. The results summarized in paragraphs 3 and 4 emphasize the dependence of resolving-power values on the aperture and the corrections of the camera lens even when the latter is of high quality.

6. The focus setting of the special triplet is sensibly constant for both color-blind and panchromatic materials as long as the effective wave-length of the exposing light is below 580 mμ. For longer wave-lengths, the focus must be set by trial, the image distance being greater for the red but shorter for the infrared.

7. The temperature coefficient of focal length of the fluorite triplet is annoyingly appreciable, being 110μ for 5°C.

8. An error in focusing of one scale division (20μ) leads to a change in observed resolving power of about 5 percent for the special triplet and to a change of about 2 percent for a certain air-spaced anastigmatic photographic objective.

BIBLIOGRAPHY

[1] R. N. Wolfe and R. S. Barrows, "Adjacency effects in photography, PSA Journal **13**, 554 (1947).
[2] C. E. K. Mees, *The Theory of the Photographic Process* (The Macmillan Company, New York, 1942), pp. 896 ff.
[3] K. Huse, "Photographic resolving power," J. Opt. Soc. Am. **1**, 119 (1917). The focal length is stated there and elsewhere to be 153 mm, but the basis for this statement is unknown since recent measurements give 150 mm.
[4] L. A. Jones and R. N. Wolfe, "A method for the measurement of the energy distribution in optical images," J. Opt. Soc. Am. **35**, 559 (1945).
[5] M. Herzberger, "The dispersion of optical glass," J. Opt. Soc. Am. **32**, 70 (1942).
[6] R. Kingslake, "A classification of photographic lens types," J. Opt. Soc. Am. **36**, 251 (1946).
[7] F. H. Perrin, "A study of Harting's criterion for complete achromatism," J. Opt. Soc. Am. **28**, 86 (1938).
[8] E. W. H. Selwyn and J. L. Tearle, "The performance of aircraft camera lenses," Proc. Phys. Soc. London **58**, 493 (1946).
[9] A Narath, "Eine neue Methode zur Bestimmung des Auflösungsvermögens photographischer Emulsionen," Kinotechnik **17**, 91 and 107 (1935).

JOURNAL OF THE OPTICAL SOCIETY OF AMERICA VOLUME 38, NUMBER 12 DECEMBER, 1948

The Mechanism of Latent Image Formation in a Photographic Emulsion by Mechanical Pressure*

K. B. MATHER
Physics Department, Washington University, St. Louis, Missouri

(Received June 30, 1948)

A latent image may be produced in a photographic emulsion by applying mechanical pressure to the emulsion. The mechanism of this latent image formation has been obscure. An investigation of the effect has been carried out with Ilford Nuclear Research Emulsions which were observed to be especially sensitive to pressure.

The experiments described below were of two kinds: (1) Photographic plates were placed between smooth steel surfaces in an hydraulic press and pressures in the range 70 to 7000-kg cm^{-2} applied. (2) A scriber was drawn across the surfaces of emulsions under varying conditions of pressure, speed, etc. The results of these experiments suggested that the pressure effect might be explained as a temperature effect, the temperature resulting from heat generated by friction.

Such estimates as could be made of the temperature to be expected in individual silver bromide grains at the surface of the emulsion under the conditions of experiment indicated temperatures of the order of 100 to 1000°C. This is in general agreement with such other estimates and measurements of surface temperatures involved in solid friction that have been attempted.

The effect of temperature on a silver bromide grain has been considered in terms of the Gurney and Mott theory of the latent image. While gross uncertainties exist in the values of the activation energies involved in such a calculation, it at least seems plausible that temperatures of the order of magnitude expected could produce a permanent latent image.

INTRODUCTION

THE photographic "pressure effect" was discussed by M. Volmer[1] in 1910. Since then further reports have appeared concerning three aspects of this phenomenon:[2] (1) The effect of mechanical pressure. Here the photographic plate is placed between two flat surfaces and pressure applied perpendicularly to the emulsion. The stress on any element of emulsion is presumably perpendicular to the emulsion surface and hence is anisotropic relative to the individual grains. (2) The effect of pneumatic pressure. Here the plate is placed in a gas chamber in which the gas pressure may be varied. Presumably an element of emulsion is subjected to isotropic bulk stress. (3) The effect of simultaneous application of pressure (either mechanical or pneumatic) and light. No theory of the physical mechanism of any of these has been advanced.

The purpose of this article is to describe some simple experiments which seem to indicate the true nature of the first of these, *viz.* the formation of a photographic latent image by the application of mechanical pressure alone. It should perhaps be emphasized at this stage that in all the work described below no plates were exposed to light or any other electromagnetic radiation. The article is concerned solely with latent images produced by applying pressure to photographic emulsions.

The writer's interest in this problem was stimulated by the use in this laboratory of Ilford Nuclear Research Plates for recording tracks of charged particles. The pressure sensitivity of these plates is remarkable, being greatly in excess of that of regular optical emulsions. The plates require very careful handling to avoid leaving an impression whenever a casual contact is made with the emulsion. The edges of the plates invariably develop heavily where they have been in contact with spacers placed between plates in packing. The extreme pressure sensitivity is, in fact, highly objectionable when the plates are being examined under the microscope for tracks. It constitutes the chief source of background unless the plates are very care-

* This research was stimulated by projects in this Department supported by the Office of Naval Research, Contract N6ori-117, T.O. 1.

[1] M. Volmer, Phot. Umkehrungserscheinungen Treang. Diss. Leipzig (1910). Volmer refers to an earlier paper by Warnercke (1881) not available to the present writer.

[2] F. E. Poindexter, J. Opt. Soc. Am. **21**, 59, (1931); Ny .Tsi-Ze and Tsien-Ling-Chao, Comptes Rendus **194**, 1644 (1932); Sci. et Ind. Phot., Series 2, 4, 1, (1933); Chinese J. Phys. **1**, 66, (1934); IX^e Congres International de Photographie (1936), p. 83. Tsi-Ze and Lu Ta-Yuan, J. Opt. Soc. Am. **26**, 26 (1936); A. J. Reardon, J. Opt. Soc. Am. **29**, 427 (1939); C. Shin-Piaw, J. Opt. Soc. Am. **31**, 186 (1941) and **34**, 285 (1944).

fully handled. There is also a temptation to the novice to regard a long surface streamer of developed grains as a spectacular nuclear track. Such a track can be caused by stroking a single human hair across the emulsion.

Obviously these emulsions provide a unique opportunity for examining the pressure phenomenon. To this end some experiments were made with Ilford Nuclear Research Plates having emulsion types B2 C2 D1 E1, together with various optical emulsions for comparison purposes.

I. EXPERIMENTS WITH MECHANICAL PRESSURE

The equipment used for applying mechanical pressure to the photographic plates is shown in Fig. 1. The photographic plate P is placed emulsion side downward in contact with the flattened face of the ball A which rides on ball B in well W. Both balls are of case-hardened steel and are snug fits to the well which is packed with grease. This mechanical arrangement ensures fairly satisfactory seating of the photographic plate on the ball. (It is absolutely essential to have uniform contact over the face of the ball before appreciable pressure is applied.) The lower face of the plunger D is turned to the same diameter as the face on the ball, and is surface ground and polished. This minimizes stresses in the glass. The whole frame E rests on the bed-plate of a hand-operated hydraulic press, the ram of which is applied to plunger D. A gauge is connected to the press and pressure readings are based on this. With this arrangement and using a 0.25-in. diameter surface on the ball, pressures up to 17,600 kg cm^{-2} could be obtained. The equipment was set up in a photographic darkroom, and all experimental work carried out under a red safelight.

The general procedure was as follows: Ball A was set with its flat surface approximately horizontal, the photographic plate was held lightly against it, and the plunger let down on the back of the plate. At this stage ball A usually squared itself against the emulsion. One could tell by the feel of the plate whether it was seating properly or not. The press was then pumped rapidly to the desired gauge reading. Pressure was usually maintained for one minute and then removed instantaneously by releasing the valve in the pressure chamber.

Plates used were microscope slide size 3″×1″, and a series of exposures was applied to each plate. (The term "exposure" henceforth refers to exposure to pressure.) Plates were developed in Kodak "Dektol" diluted 1:1 for 10 minutes at 20°C and fixed for about one hour. Prolonged processing times were necessary because of the thickness of the emulsions (50μ). The impressions on Ilford N.R. Plates were clearly visible to the naked eye. A typical impression is shown in Fig. 2. The actual degree of blackening depended on the developing conditions presumably in much the same fashion as in the case of exposures to light.

Quantitative studies have been based on comparisons of either optical density ($D=\log_{10}I_0/I$) or the number of developed grains per unit area of plate, determined with an American Optical Company Binocular Microscope using 900× magnification and a calibrated eyepiece graticule. Ideally, grain counts were more reliable because one could select areas suitable for counting and ignore unsuitable areas. (The significance of this will become apparent.) On the other hand, the densitometer reading corresponds to the number of grains per unit area averaged over a considerable area of plate so the discrimination is lost. The advantage of measuring densities lay in the ease and speed of working. Grain counting, to yield reasonably good statistics, proved extremely

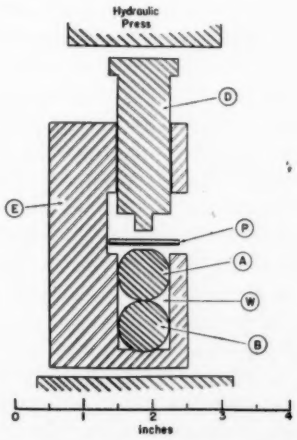

FIG. 1. Cross section of equipment used for applying pressure to photographic plates. Plate P is placed emulsion side downward between ball A and plunger D. Pressure is applied by means of a hand-pumped hydraulic press.

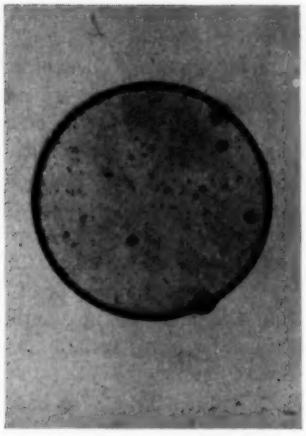

FIG. 2. Typical impression made on an Ilford Nuclear Research Emulsion Type E1 using a pressure of 3520 kg cm^{-2}. The black spots are due to "high spots" on the emulsion (magnification 6×).

laborious. The principle was adopted of first scanning all pressure negatives with the microscope. If the impression was found suitable, densities were measured with the densitometer.

A serious difficulty was encountered in producing uniform surface impressions for which measurements could be significant There were several reasons for this:

(a) At relatively low pressures (approximately 70 kg cm^{-2}) the only impression consisted of small localized areas having dense black cores with grain concentration decreasing radially from the center. The larger of these were visible to the naked eye as black spots. (They can be seen in Fig. 2.) However, the combined area of all the spots would be only a small fraction of the total area. At low pressure the remainder of the pressure area was clear, but as the pressure increased, the whole area began to show developed grains. Conspicuous patchiness centered on the original cores persisted to about 350 kg cm^{-2}. Up to this point grain counts with the above set-up probably had no meaning.

These localized areas of great density were presumably high spots on the emulsion, which therefore bore the load first but were flattened by increased pressure. Some of the Ilford N. R. Plates do, in point of fact, possess distinctly coarse emulsion surfaces, somewhat resembling a fine grade of emery cloth. This source of difficulty imposed on the measurements a lower limit of about 350 kg cm^{-2}, and it is not easy to devise a practicable means of further reducing this. The situation could be met by using very small pressure surfaces, say 0.1 mm diameter, which would have a reasonable chance of avoiding the local high spots on the emulsion. However, these must be accurately flat and pressed normal to the emulsion, which is technically difficult to realize.

(b) Above about 350 kg cm^{-2} the grain concentration was fairly uniform, provided local high spots were avoided, but another source of inhomogeneity appeared unless great care was exercised in the preparation of the pressure surface. It was found that the emulsion reproduced perfect replicas of any surface contour pressed on it. High spots on the surface produced corresponding spots of increased density on the pressure negative. This meant that ball *A* (Fig. 1) had to be surface ground, lapped, and polished.

(c) The edge of each impression showed greater density than the interior, an effect which increased considerably with the increase of pressure.

These several sources of error were avoided as far as possible. Measurements were recorded only above 350 kg cm^{-2} and were confined to the interior of each impression. There was no way of avoiding spurious regions of too high or too low density (resulting from causes (a) and (b)),

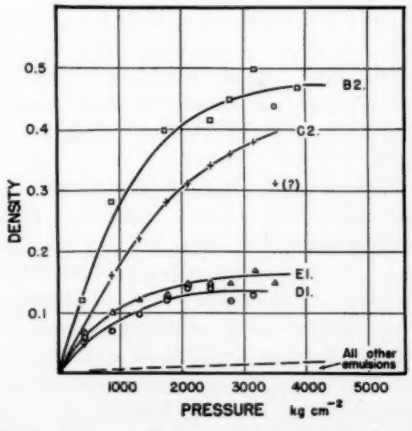

FIG. 3. Photographic density ($\log_{10} I_0/I$) is plotted against pressure applied to the emulsion for Ilford Nuclear Research Emulsions B2, C2, E1, and D1. The densities recorded for all other emulsions lay below the dotted line.

when using the densitometer, as these were small and randomly scattered across the impression. On the other hand, when grain counts were made only selected homogeneous areas were used.

Photographic plates examined were Ilford Nuclear Research Plates B2 C2 E1 D1, Kodak Nuclear Track Plates, Kodak Super XX, Kodak Commercial Safety Film, Kodak 33 Plates, Hammer Panchromatic Plates and Hammer Process Plates (Lantern Slide) for which density was recorded at the following pressures: 440, 880, 1320, 1770, 2110, 2470, 2820, 3180, 3520, 3890 kg cm^{-2}, each being applied for one minute. 4000 was about the limit that could be applied to plates. The glass usually broke above this figure. Kodak Commercial Safety Film was taken as high as 7040 kg cm^{-2}.

Densities for the above plates are recorded in Fig. 3. The figures graphed were obtained from plates which were exposed on the same day and developed simultaneously. All plates showed a small fog background, and density measurements were made on this and subtracted before plotting Fig. 3.

A series of E1 plates was tested using different metallic and non-metallic surfaces in the form of disks placed between the ball surface and the emulsion, e.g., brass, copper, aluminum, glass, paper, and cloth. Some of these were not very smoothly surfaced and the paper and cloth reproduced their fibrous structure, so the negatives were very inhomogeneous. However, the order of magnitude of the density was apparently the same as for the steel surface. Reliable figures were obtained for glass, and these were similar to those for steel.

Several Ilford plates were soaked in distilled water and pressure applied to them wet. Only low pressures could be used or the emulsion was squeezed off the glass. It was possible to verify that some pressure effect existed under such conditions.

The dependence of surface density on the duration of application of pressure was studied for Ilford E1 plates. A pressure of 880 kg cm^{-2} was used and applied for times ranging from 10 to 600 seconds. Densities are recorded in Fig. 4.

In view of the apparent independence of the pressure effect on duration of exposure, a modification of the experiment suggested itself. Intermittent pressure exposures were applied to an E1 plate. A pressure of 1770 kg cm^{-2} was applied for 10 seconds, removed, and immediately reapplied without disturbing the plate in the press. The resulting density was noticeably greater than was obtained by a single application of the same pressure on the same plate. The experiment was repeated on another E1 plate giving a series of exposures having the same pressure applied 1 2 3—10 times, and densities were measured on each exposure (see Fig. 5). The actual values obtained were very variable; in fact, it was found difficult to repeat anything but the general nature of Fig. 5. It seemed fairly certain that an initial increase occurred with several applications of the same pressure but that a saturation value was reached at about 10 applications.

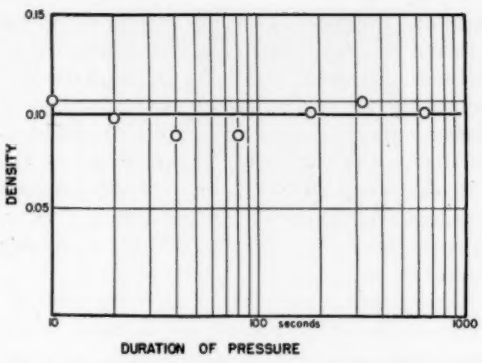

FIG. 4. The photographic density caused by pressure does not depend on the length of time during which pressure is applied to the emulsion. The pressure in this case was 880 kg cm^{-2}.

Up to this time no particular attention had been given to the manner of application of the pressure to the plates. The hydraulic press required hand pumping to the desired pressure. In general, the pressure was reached as smartly as possible without jarring the plate, but meticulous care was certainly not exercised to insure that this operation was performed identically for each exposure. This was examined more carefully. On the same E1 plate two impressions were made, (a) the press was pumped as quickly as possible to 1770 kg cm^{-2}, (b) the pressure was applied very gradually, the attainment of full pressure (1770) being prolonged for some 3

minutes. On development, the density of (a) was 0.16 and that of (b) was 0.12. The qualitative result was repeated many times, although the control of the equipment was much too crude to closely reproduce quantitative results. Incidentally, this result probably explains part of the difficulty experienced in reproducing pressure densities, especially in the preceding "intermittency effect," where the build-up of density seemed to be highly variable.

The following observations are based upon the above series of experiments and detailed microscopic examination of all the pressure negatives involved.

(i) The photographic density produced by mechanical pressure appears to increase with increase of pressure. The functional relation has not been established, but a saturation density of the order of 0.1–0.5 seems to be attained for Ilford Nuclear Research Plates.

(ii) However, densities greatly exceeding the saturation value are observed at high spots on the emulsion or corresponding to high spots on the surface of the press.

(iii) The density produced by any given pressure is variable according to (a) the rate at which the pressure is built up on the plate, (b) whether the pressure is applied continuously or intermittently. Building up the same pressure more rapidly or more frequently produces greater density.

(iv) The density is independent of the duration of the application of pressure. (This and point (iii) suggest that the phenomenon is related to the initial application of pressure rather than the static state of pressure.)

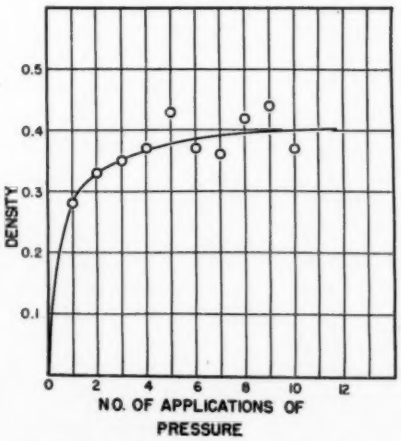

Fig. 5. Density can be increased by applying pressure to the same area of emulsion a number of times in succession, but a saturation density is reached by adout 10 applications.

(v) The density is independent (to a first approximation) of the chemical nature of the surface which applies the pressure, e.g., whether metallic or non-metallic. The pressure effect also exists when the plate is wet.

(vi) Careful microscopic inspection of pressure negatives established the fact beyond all doubt that the density caused by pressure resulted entirely from developed grains on and very close to the surface of the emulsion. Below the surface the normal background fog remains unchanged even at the greatest pressures attained.

(vii) Of the several types of emulsion tested only the Ilford Nuclear Research Plates showed appreciable pressure effect.

It is felt that (vi) established conclusively that the phenomenon cannot be a pure pressure effect. That some other process is involved is suggested by the apparent paradox of (i) and (ii).

One interesting phenomenon was observed which suggested a new approach. Accidentally, the steel ball was not set squarely on the emulsion during the setting up of the press. When the load was applied the ball rotated, the flat surface sliding into full contact. This exposure showed incredibly high density far exceeding that usually shown by this and other pressures. In fact, an intense print-out effect occurred, a black area being conspicuous by the time the plate was removed from the apparatus. The portions of the exposed area which were transparent enough for microscopic examination confirmed the sliding by showing numerous parallel scratch marks. These were tracks and bands of developed grains presumably caused by minute projections on the ball surface as it slid over the emulsion. This seemed to offer a vital clue. The pressure phenomenon appeared to be ultrasensitive to relative motion between the steel surface and the emulsion.

II. EXPERIMENTS INVOLVING SLIDING

One end of a $\frac{1}{8}$-in. brass rod was ground to a hemispherical shape and polished. This was used for scribing across photographic emulsions under various conditions, i.e., emulsions were simultaneously subjected to normal pressure and to sliding.

The method was as follows: A photographic plate was placed on a bench in the darkroom. Using a straight edge, a line was scribed across the emulsion. Since this was done by hand there was no accurate check on the normal force or

speed of motion, but these were of the order of 10 g and 10 cm sec.$^{-1}$, respectively. The result was quite striking. All the Ilford emulsions showed dense black tracks 50–200μ wide. (Fig. 6). These were not very uniform in density and could not be measured, but densities were obviously far in excess of those produced by pure pressure in Part I (e.g., Fig. 2). Other emulsions, e.g., Kodak Commercial, etc., were much less spectacular but usually recorded tracks.

The question arises, of course, just how much of this density may be attributed to pure pressure and how much is introduced by the sliding. Taking the track width as the diameter of the scriber surface in contact with the emulsion, the average pressure was probably of the order of $0.010/\pi 0.005^2 = 130$ kg cm^{-2}, assuming an average track width of 100μ, and a normal force of 10 g. This is much lower than average pressures being used in the static experiments (Part I) where the densities recorded were nevertheless less than 0.5.

An Ilford B2 plate was partly covered with a sheet of thin paper and scribe marks impressed as before, the motion of the scriber being half over paper and half directly on the emulsion but with the same normal force throughout. The resulting tracks were very faint under the paper, although there was a just detectable density, but changed sharply to dense black tracks at the paper's edge. This is clearly shown in Fig. 7. The result was considered to be very convincing proof that the track density was associated almost entirely with the sliding and not with the pure pressure involved which should have been approximately constant over the whole length of track.

A microscopic examination showed tracks from the scriber to vary considerably in density and width. One would expect these to depend on the normal load, and a simple device was set up to give some control over this. The plate was set on the table of a balance and counterpoised. The desired weight was set on the beam. The scriber was drawn across the emulsion by hand, sufficient force being applied to keep the balance floating. This was crude but effective. It was found that track width and density both increased with increase in the normal load. An attempt was made to vary the speed of scribing systematically, using a fixed load, although the actual speeds could only be estimated. They were probably in the range 1–20 cm sec^{-1}. However this result was not definite. The density probably increases with speed, but the set-up used here was rather too crude to ascertain this with certainty.

FIG. 6. Photomicrogram of track produced on Ilford E1 Plate by a brass scriber (magnification 200×, normal force about 10 g). Note the inhomogeneous character of the track.

Several plates were scribed while wet. These were placed in petri dishes containing liquid which just covered them and scribed *in situ*. Distilled water, tap water, and developer were used. Tracks were produced under all three liquids although the densities were much reduced. Tracks were also somewhat wider and rather more uniform, as would be expected with the emulsion in a viscous state.

The following points emerged from the experiments on sliding:

1. The pressure effect on photographic emulsions is greatly enhanced if sliding accompanies pressure. For the same normal pressure there is a kinematic pressure effect which causes far greater densities than the static effect.
2. The greater the normal pressure during sliding the greater the density produced. There is some indication that the density increases with the speed of sliding, but the dependence does not seem to be very sensitive.
3. A latent image can be formed by sliding when the emulsion is wet, but the effect is considerably reduced.

III. DISCUSSION

A number of possible explanations of the photographic pressure effect come to mind. How-

ever, the evidence in Parts I and II rejects most of these.

For instance, the traditional viewpoint has been that the grains are in some way activated by being compressed. This is categorically ruled out by the static pressure experiments showing developed grains on the surface only and not through the full depth of the emulsion where the same pressure must have existed.

Another thought is that a contact potential might develop between the AgBr and the surface pressed against it. That the effect is enhanced by sliding, encourages the idea. It is rejected by the fact that the density is apparently independent of the surface in contact with the emulsion, e.g., metallic or non-metallic, and also by the fact that the pressure effect is observed beneath the surface of an electrolyte.

Chemical action is likewise ruled out by the independence of the nature of the surface. (Of course there may be a small chemical effect superposed. One would expect AgBr crystals in intimate contact with, say, a copper surface to be activated by copper.)

The surface grains of AgBr may be disrupted by combined pressure and sliding, and small grains have a greater chance of development. It is difficult to see how this could occur in the static pressure experiments, but it may be a contributing factor when sliding occurs.

However, the evidence does suggest one very plausible physical picture which seems to correlate the salient features of the phenomenon. It is now considered that the so-called mechanical pressure effect is in reality a temperature phenomenon resulting from the following mechanism:—friction attending sliding of a surface over an emulsion, with resulting development of heat and a high temperature in individual grains sufficient to cause development.

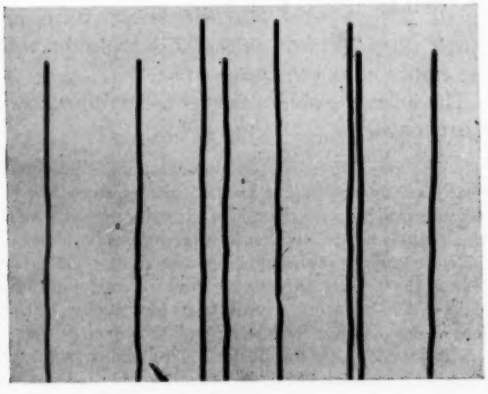

FIG. 7. This Ilford B2 Plate was partly covered with thin paper and a scriber drawn across. The track is evident only where the scriber has been in direct contact with the emulsion. A faint trace may be seen on the negative where the plate was covered with paper (magnification 6×).

This is regarded as the explanation of the sliding experiments in Part II and probably also of Part I. However, the mechanism of the static experiments may be somewhat different and will be discussed later.

Consider the effect of an increase in temperature on a photographic emulsion. It is a well-known fact of observation that this effect is considerable. All emulsions exhibit a certain fog which increases fairly rapidly with increase in ambient temperature. (Hence the precaution of storing plates in refrigerators, etc.) Moreover it has been noticed in this laboratory that Ilford N.R. emulsions are especially responsive to temperature conditions.

According to the Gurney and Mott[3] theory of the latent image there are two essential processes proceeding in a AgBr crystal, (a) the production of free electrons by some agency and (b) appreciable silver ion conductivity through the crystal lattice.

Accepting the picture presented by Gurney and Mott of the nature of the latent image, it appears that rise in temperature may produce a latent image by some such mechanism as the following: Electrons thermally liberated from interstitial bromine ions in the AgBr lattice diffuse through the lattice forming an electron gas in the grain. The number of free electrons so produced can be expected to be highly temperature sensitive, their concentration being proportional to $xe^{-A/kT}$, where A is the electron affinity of an interstitial bromine ion and x is the fractional occurrence of interstitial ions. (x is itself exponentially dependent on temperature.)**

[3] R. W. Gurney and N. F. Mott, Proc. Roy. Soc. **A164**, 151 (1938).

** In addition, some trapped electrons will be thermally liberated from lattice vacancies normally filled by bromine ions. The number of such freed electrons will also increase rapidly with temperature, and their effects will in general be indistinguishable from those freed from bromine interstitial ions.

Some of these electrons are trapped at silver specks in the crystal. At the same time other electrons will evaporate from the potential well associated with the silver speck and return to the conduction band of the AgBr (see Fig. 8). If E is the activation energy for this process the number of electrons evaporating per unit volume of silver is proportional to $e^{-E/kT}$. The formation of the latent image by temperature increase may be taken as depending upon the predominance of the first process over the second, in fact the condition for growth of a silver speck depends on the ratio r of the exponentials

$$r = x \exp[(E-A)/kT].$$

k is the Boltzmann constant and T the absolute temperature. Values of E and A are not available. The values of r in Table I are for three temperatures 20, 250, and 426°C (the last being the melting point), assuming $E-A=0.1$ and 0.2 ev, respectively, and assuming values of x from Mott and Gurney.[4] At $E-A=0.2$ ev, r increases with temperature but is not nearly so sensitive to temperature as at $E-A=0.1$ ev. Gurney and Mott estimated E to be ≈ 0.4 ev, suggesting that $A \approx 0.2-0.3$ ev. This kind of analysis is rather limited in view of the uncertainty in the activation energies. However the requisite values of $E-A \approx 0.1-0.2$ ev are at least quite plausible.

The ionic conductivity of silver halides is also very temperature sensitive, in all probability assisting the latent image formation (although ionic conductivity at room temperature is almost certainly adequate) e.g., the specific conductivity of AgBr increases by a factor of 10^5 ohm^{-1} cm^{-1} in the temperature range from room temperature to 200 C.[5]

The sliding experiments can be considered theoretically so as to give estimates of the expected temperature at and near the surface of an emulsion.

To do this we must idealize conditions in the emulsion as the scriber is drawn across it.

Assume a one-dimensional heat flow, i.e., a semi-infinite solid having heat supplied uniformly to it at one face. In reality, heat is applied non-uniformly over a finite area of a finite slab, and there will be heat diffusion in all directions. However this is a reasonable approximation for a point A (Fig. 9) near the surface of the emulsion and somewhere near the middle of the track. Also the thermal properties of glass resemble those of emulsion, making the assumption of semi-infiniteness tolerable even though the emulsion itself is only 50μ thick, especially as we are to be concerned with temperatures at or near the surface.

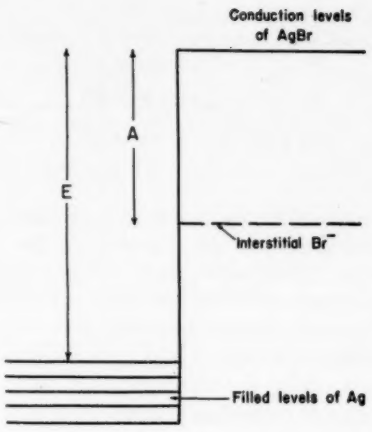

FIG. 8. Energy level diagram for the production of free electrons from interstitial Br$^-$ and evaporation of electrons trapped by a Ag speck.

Assume that the emulsion is homogeneous in composition instead of being a matrix of AgBr and gelatin, and assume average values for its various thermal properties.

Assume that equal fractions of the frictional heat generated go into the scriber and the emulsion.

Ignore heat loss by radiation from the emulsion surface. This is reasonable if we are concerned only with times comparable with the time required for the scribing surface to pass a point. There can be no heat radiation from the surface while the scriber is actually covering that part of the surface.

Consider an element of unit area and of thickness dy lying on the surface and having a temperature drop across it dT. The energy entering the element per second $=\alpha\mu mgv/JA$ cal sec.$^{-1}$ cm^{-2}, and the energy leaving the element

[4] N. F. Mott and R. W. Gurney, *Electronic Processes in Ionic Crystals* (Oxford University Press, London, 1940), p. 48.

[5] W. Lehfeldt, Zeits. f. Physik **85**, 717, (1933).

TABLE I.

$E-A$	Temperature 20°C $x=8.3\times10^{-4}$	250°C 1.8×10^{-3}	426°C 2×10^{-2}
0.1 ev	$r=0.044\times10^{-2}$	1.9×10^{-2}	960×10^{-2}
0.2 ev	$r=2.3\times10^{-2}$	15×10^{-2}	55×10^{-2}

per second $=KdT/dy$, where mg is the normal force in dynes, v is the velocity of the scriber across the surface in cm sec.$^{-1}$, and μ is the coefficient of friction between the scriber and the emulsion. (This was measured by placing a block of the same material as the scriber on a photographic plate and tilting the plate until the block just slid. Then $\mu=\tan\phi$ where ϕ is the angle of sliding. μ was found to be in the region of 0.5 for brass on Ilford emulsions.) A is the contact area of the scriber in cm^2, α is the fraction of heat generated appearing in the emulsion, J is the mechanical equivalent of heat $=4.2\times10^7$ erg cal.$^{-1}$, and K is the thermal conductivity of emulsion in cal. cm^{-1} deg.$^{-1}$ sec.$^{-1}$. The gain in energy per second $=\alpha\mu mgv/JA-KdT/dy$ which must appear as an increase in temperature.

The equation of heat is

$$\alpha\mu mgv/JA-KdT/dy=C\rho dydT/dt,$$

where C is the specific heat of emulsion in cal. g^{-1} deg.$^{-1}$, ρ is the density of emulsion in g cm^{-3}. If we consider a surface element Δy thick enough so that the heat will not have diffused deeper than this in the time Δt considered, we can neglect KdT/dt and write:

$$\alpha\mu mgv/JA=C\rho\Delta y\Delta T/\Delta t,$$
$$\therefore\quad \Delta T=\alpha\mu mgv\Delta t/JAC\rho\Delta y.$$

In the general temperature diffusion equation,

$$\partial T/\partial t=D\nabla^2T,$$

where D, the coefficient of diffusion $(=K/\rho C)$, may be associated with a diffusion length Δy and time of diffusion Δt by $\Delta y\approx(D\Delta t)^{\frac{1}{2}}$,

$$\therefore\ \Delta T\approx\frac{4\alpha\mu mg}{\pi J}(v/Kc\rho d^3)^{\frac{1}{2}},$$

where d is the scriber width, Δt is the time for the scriber to pass a point on the emulsion, and Δy is the diffusion distance of heat during this time.

Substitute:

$$\alpha=0.5\ \text{(assumed)},$$
$$\mu=0.5,$$
$$mg=20\times980,$$
$$J=4.2\times10^7,$$
$$d=10^{-2},$$
$$\rho=1.3,$$
$$C=0.5,$$
$$K=10^{-3},$$
$$v=10,$$

whence $\Delta T\approx20°$. The values assumed are very uncertain and the method of analysis questionable, but this at least gives an order of magnitude approximating the surface temperature under the conditions as represented. The order of magnitude is in general agreement with estimated temperatures between two sliding surfaces under corresponding conditions of speed, load, etc. In fact the proposed explanation of the pressure effect depends upon essentially the same mechanism as does solid friction *viz.*, the generation of very high temperatures in minute localized high spots, resulting in intermittent welding and breaking on a microscopic scale.

However the above picture requires considerable modification to approach the practical conditions believed to exist. The value of d assumed is certainly overestimated. The over-all width of track was about 10^{-2} cm, but the track was not uniform over this width. It is evident from the appearance of the track under a microscope that the scriber rides on its high spots which may well be only $\frac{1}{10}$ or less of the total track width. Since $\Delta T\alpha\, d^{-\frac{1}{2}}$, this means a much higher temperature rise at local high spots, e.g., $\approx600°$. This is con-

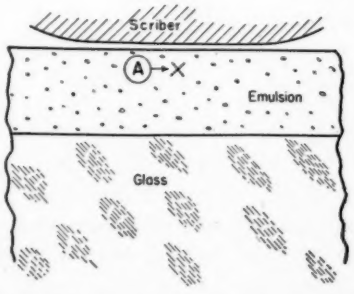

FIG. 9. Section of brass scriber and photographic plate as used in Part II (approximately to scale, the emulsion thickness being 50μ).

firmed by further evidence. Since the diffusion distance $\Delta y \approx (D\Delta t)^{\frac{1}{2}}$, where $D \approx 10^{-3}$ and taking as before $\Delta t \approx 10^{-3}$, $\Delta y \approx 10^{-3}$ cm. Hence we might expect development through some 10μ of emulsion from the surface, but it has been noted that the development is confined to a shallow layer of emulsion not greater than several μ thick, indicating that Δt must actually be less than 10^{-3} sec. Putting $\Delta t \approx 10^{-4}$ sec. corresponding to $d \approx 10^{-3}$ cm $\Delta y \approx 3\mu$ which is in better agreement with experiments.

Temperatures of 600°C and higher have been recorded by Bowden and Ridler[6] for metal surfaces when using the adjacent surfaces as one junction of a thermocouple, again yielding confirmation of a general nature of the picture presented above. Moreover for any given rate of application of heat to the emulsion its surface will reach a higher temperature than would a metallic surface because of the low coefficient of temperature diffusion of the emulsion.

Within the emulsion the temperature can be expected to decrease exponentially according to the relation

$$T = \Delta T \exp(-y^2/D\Delta t),$$

where T is the temperature at depth y below the surface. By way of illustration, Fig. 10 displays $T(y)$ taking $\Delta T = 400$°C (the melting point of AgBr is about 400°C so we are not interested in temperatures higher than this), and $D\Delta t = 10^{-7}$ corresponding to $\Delta t = 10^{-4}$ sec.

A corollary to the temperature theory is that local temperatures might be sufficiently high at contacting points of contiguous surfaces to produce momentary light emission which could contribute to the latent image. In fact this has been observed in connection with work on metal friction.[7] The effect would not fundamentally change the explanation in terms of temperature. However, it might be expected that if this mechanism were present the pressure patterns should be rather more diffuse than they are observed to be.

The temperature theory provides a general explanation of the photographic pressure effect

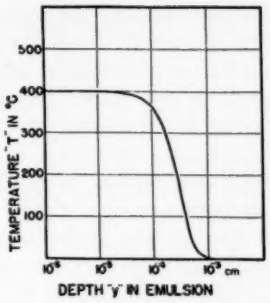

FIG. 10. Showing the dependence of temperature T at depth y below the surface of an emulsion according to $T = \Delta T \exp(-y^2/D\Delta t)$ taking $\Delta T = 400$°C and $D\Delta t = 10^{-7}$.

but leaves a number of details of the mechanism rather obscure. For instance, it is more successful in explaining the sliding experiments than the static pressure experiments. There is good reason to believe that the static effect (Part I) is also a temperature effect. This is strongly suggested by the facts that variation of the rate of application of the pressure varied the final density, and that the effect was independent of duration of pressure but depended only on the initial application of the pressure.

However the difficulty in this is to account for the source of thermal energy. Actually densities observed here were much lower than in the sliding experiments and, in fact, were either not detected at all or were on the limit of detection for all emulsions except Ilford N. R. Plates, the latter yielding densities as high as 0.5.

Microscopically, both the highly polished metal surface of the press and the emulsion surface are rough. The simplest conjecture concerning the mechanism is that the high spots of the metal either compress or shear into the emulsion (the magnitudes involved possibly being 10^{-4} or 10^{-5} cm) the emulsion undergoing a general flattening against the metal at the same time, the heat generated by these processes being responsible for the latent image. The greater the pressure the more intimate the contact between the contours and the greater the density (e.g., Fig. 3). (The extra density noticed at the edges of an impression was probably due to the emulsion flowing slightly under pressure.) The more rapidly the pressure is applied the more closely adiabatic conditions are realized, the higher the

[6] F. P. Bowden and K. E. W. Ridler, Proc. Roy. Soc. **A154**, 640 (1936).

[7] F. P. Bowden and M. A. Stone, Experientia **2**, 186 (1946).

temperature generated, and the greater the ultimate density (see Part I). If the pressure is not being increased a static condition exists, and no further increase in the latent image could be expected (see Fig. 4). Similarly, the intermittent application of pressure should produce densities increasing with the number of applications of pressure. A saturation value of the density should be reached when all the grains which can be activated by the temperature corresponding to a pressure of this magnitude have been rendered developable (see Fig. 5). A reduced pressure effect under a liquid is to be expected from the lubricating property of the liquid and its heat dissipation. Beyond this point of showing the qualitative plausibility of the temperature theory any analysis is purely speculative.

An interesting feature of the whole investigation is the unique classification of Ilford Nuclear Research Emulsions which have shown a vastly greater sensitivity to pressure than have all other types of emulsions examined. To a large extent this is superficial.*** However, it is quite reasonable in terms of what is known of the nature of this class of emulsions that their grains should actually be more temperature sensitive.

It will be recalled that the intrinsic stability of a AgBr grain is a variable factor which can be controlled by the ripening process during manufacture of the emulsion, and seems to depend on the number and size of sensitizing specks of silver sulfide formed on the surface of the grain. The grains of the Ilford emulsions are very unstable, deliberately prepared to require a minimum ionization per grain to render them developable by charged particles. For instance, the emulsions age rapidly and are very responsive to ambient temperature, humidity, etc. Presumably the grains are abnormally unstable with respect to all physical processes which yield free electrons, e.g., electromagnetic radiation, charged particles, temperature, chemical action, etc. Consequently an enhanced sensitivity to temperature and hence pressure is understandable.

*** Eastman Kodak Nuclear Track Emulsions NTA, NTB, and NTC have essentially similar grain size and weight of AgBr per unit volume of emulsion to Ilford Nuclear Research Emulsions and hence might be expected to have similar characteristics. However, the Kodak Nuclear Plates tested failed to show any pressure effect together with all the regular Kodak films and plates listed above. It now appears that all Kodak emulsions have an inactive surface coating of gelatin about 1μ thick over their surfaces (private communication from Eastman Kodak Company). More recently Kodak Nuclear Track Emulsions without the over-coating have been manufactured, and it has been verified that these exhibit a strong pressure effect.

CONCLUSION

It is hoped that this discussion of the photographic pressure effect may serve to draw attention to the phenomenon and to the new emulsions which appear to exhibit it strongly. The explanation as a temperature effect is advanced tentatively. There are several aspects left untouched, and the new emulsions seem to offer an excellent opportunity for profitable work in this field.

(i) For the sake of completeness the pure pressure effect should be re-examined using a wider range of pressures especially, if possible, in the region 0–350 kg cm^{-2}, and also using a wider range of emulsion types.

(ii) Experiments using pneumatic pressure. The initial application of pressure may produce a compression and heating of AgBr grains, and hence form a latent image. Experiments approximating isothermal or adiabatic conditions suggest themselves.

(iii) Simultaneous exposures to pressure (mechanical or pneumatic) and monochromatic light sources of various wave-lengths. This phenomenon should be re-examined systematically using Ilford N. R. Emulsions at various wave-lengths throughout the spectrum. Pressures of the order of 10^4 kg cm^{-2} might be expected to shift the absorption spectrum of AgBr a detectable amount and hence influence the sensitivity of an emulsion to any particular light source. An interpretation of the anomalous behavior of emulsions described in this connection may be possible on some such basis.

ACKNOWLEDGMENTS

It is a pleasure to refer to the interest and friendly assistance of Dr. H. Primakoff in numerous general discussions of the nature of the pressure effect.

The writer acknowledges his Studentship from the Science and Industry Endowment Fund, Commonwealth of Australia.

JOURNAL OF THE OPTICAL SOCIETY OF AMERICA VOLUME 38, NUMBER 12 DECEMBER, 1948

Applications of the Photographic Pressure Effect

K. B. MATHER
Department of Physics, Washington University, St. Louis, Missouri
(Received June 30, 1948)

Because of their sensitivity to mechanical pressure, photographic emulsions will reproduce accurately surface contours pressed against them. This offers a new method for preparing high contrast transparent replicas for microscopy. Some photomicrograms of replicas which have been prepared in this way are reproduced here. The technique may find useful application in the microscopy of metallurgical and other opaque surfaces.

THE pressure sensitivity of Ilford Nuclear Research Plates has been discussed in the preceding article, and their ability to reproduce faithfully surface contours was mentioned. High spots on the surface pressed against the emulsion are reproduced with greater density, indentations on the surface with lesser density. The nature of a three-dimensional surface can therefore be revealed on a plane photographic plate, the third dimension being indicated by the density of development at any point on the impression. Interesting reproductions of irregular surfaces may be prepared in this way.

At the present time the pressure effect is something of a scientific curiosity. However a number of possible applications suggest themselves, several of which are indicated in the captions of Figs. 1 to 6.

The photomicrograms reproduced in the figures were obtained as follows: The press used was that described in the previous article. The specimen surface was pressed against the photographic emulsion usually at about 1000 kg cm^{-2}. There is a rough optimum of pressure for any surface, but this is not at all critical. Pressures were usually applied for about one minute, but this is a matter of convenience only. The photographic plate which was subjected to pressure was then developed in the conventional manner. The plate was not exposed to light at any time. The resulting negative reproduced the surface contour pressed against it. This negative, or replica, must be examined with a microscope of appropriate magnification. The pictures reproduced here were made with a photomicrograph from negatives prepared by pressure as described.

FIG. 1. Impression of a steel surface machined with a surface grinder. Dark lines correspond to elevations on the steel surface. The blackness at any point is an indication of the contour of the surface (magnification 176×).

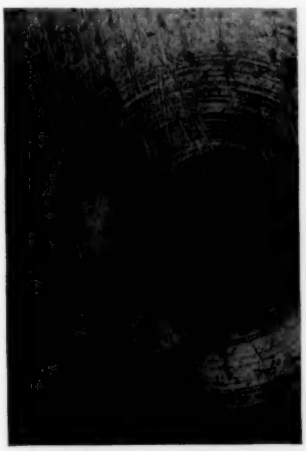

FIG. 2. Portion of an end-turned steel cylinder which has been scratched across with coarse abrasive (magnification 20×). The pressure used in forming these replicas was about 1000 kg cm^{-2}.

FIG. 3. Reproduction of a fabric pressed on the emulsion surface with the hydraulic press as for the other specimens. Note the details in the interlacing threads (magnification 30×).

This is essentially a simple technique for preparing high contrast transparent replicas of a specimen surface. It offers the advantage for microscopy of opaque surfaces, that direct bright field illumination may be used. Furthermore these emulsions have very fine grain size, making the resolution obtained in such a replica very high. (The AgBr grains are initially $\approx 0.2\mu$ and the developed grains $\approx 0.5\mu$.)

One difficulty encountered in preparing replicas by this method was due to the emulsion itself, which was not flat. The specimen surface

FIG. 4. Structure of lens tissue paper reproduced in the manner of Fig. 3 (magnification 30×). Ilford Nuclear Research Emulsions Type E1 were used for this set of figures.

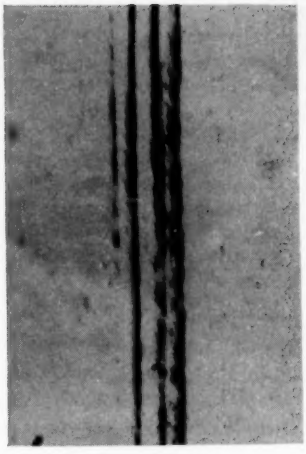

FIG. 5. The quadruple track is due to a 5-mil tungsten wire drawn lightly across the emulsion surface. Individual tracks correspond to ridges formed on the wire by the die during wire-drawing. The picture illustrates the extreme sensitivity of the emulsions to frictional contacts (magnification 360×).

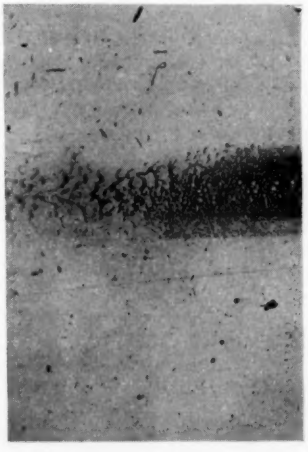

FIG. 6. This picture is an interesting magnification of a track formed by drawing a brass rod across an emulsion. Part of the plate had been immersed in water, and the brass rod was drawn across from the wet to the dry section. The picture shows the transition stage from slightly damp to completely dry emulsion. The mottled pattern on the left indicates sporadic breakdown of boundary lubrication. The blacker parts correspond to greater friction where there was no lubrication. The track becomes continuous on the right where the emulsion was dry. The technique may have some useful aspects for the study of lubrication (magnification 100×).

rode on the high spots of the emulsion and gave a spurious impression of the contour unless the pressure used was large enough to insure intimate contact.

ACKNOWLEDGMENT

The writer acknowledges his Studentship from the Science and Industry Endowment Fund, Commonwealth of Australia.

Errata: New Contributions to the Optics of Intensely Light-Scattering Materials. Part I

[J. Opt. Soc. Am. **38**, 448 (1948)]

PAUL KUBELKA

1. On page 453, right column: in the Gurevic formula the power index "2" should be shifted inside the bracket; the formula should read:

$$T=\frac{(1-R_\infty^2)\exp(-bSX)}{1-R_\infty^2\exp(-2bSX)}.$$

2. On page 456, Table III, in the denominator of the last member of formula (38), the letter "Y" should be replaced by the cipher "1." The member should read:

$$R\approx\cdots\approx 1-\frac{1-R_g}{(1-R_g)SX+1}.$$

3. In the same table, in the last member of formula (43), a minus sign was dropped. The formula should read:

$$R\approx\cdots\approx R_g+[(a-R_g)^2-b^2]SX.$$

4. On page 457, left column, in the second Gurevic differential equation, the letter "E" should be replaced by "K:"

$$dT=-T(S+K-SR_0)dX.$$

Fabrication of Boric Acid Glass for Luminescence Studies*

M. KASHA
Department of Chemistry, University of California, Berkeley, California

(Received July 22, 1948)

An extrusion process is described, permitting the fabrication of boric acid glass into strips having dimensions on the order of 10 cm×1 cm×0.3 mm. The applications of such material in optical studies of complex organic molecules are outlined.

I. LOW MELTING INORGANIC GLASSES AS A TOOL FOR OPTICAL RESEARCH ON COMPLEX ORGANIC MOLECULES

A SIGNIFICANT fraction of the literature on the luminescence of complex molecules involves the use of low melting, inorganic glasses, a variety of which have been proposed for this purpose.[1–4] A complex molecule in solid solution in such a glass exhibits the phenomenon of phosphorescence, and most of the previous researches on these systems have involved a study of the gross physical optical properties.

When the spectroscopic interpretation of this phosphorescence as a triplet-singlet emission was made,[5,6] it became clear that a study of this luminescence and the phenomena associated with it could yield much useful information regarding the triplet state of a complex molecule (having a singlet ground state). The direct study of the properties of the triplet state is possible as a consequence of the phosphorescence saturation phenomenon,[7,8] arising from the long mean-lifetime (on the order of seconds, in some cases) of the phosphorescent state, whereby a large fraction of the molecules can be held in this metastable state by illumination with an intense beam of light. Thus, the *color* of the triplet state (triplet-triplet absorption; when ground state is singlet), the *vibration frequencies* of the molecule in this state,[9] and the *paramagnetism* of this state, could be measured directly.

For quantitative spectroscopic studies it was necessary to develop means by which the glasses could be fabricated into ribbons, thin sheets, or blocks of any desired dimensions, instead of the crudely shaped fragments which sufficed for the earlier physical optical studies. The object of this report is to describe a process which was developed for the purpose of preparing thin strips of glassy "phosphor" material, having dimensions of approximately 10 cm×1 cm×0.3 mm. Fabricated strips of this size were required for the determination of (1) the absorption spectrum of a dye in boric acid glass, (2) the phosphorescence saturation curve, and subsequently, (3) the paramagnetic susceptibility of the dye in its phosphorescent state. The latter results are being reported concurrently in another place.[10]

II. PHYSICAL CHARACTERISTICS OF "BORIC ACID GLASS"

Of the several substances suggested as glasses for complex molecule studies, "boric acid glass" presents a number of advantages: (a) the glass is not deliquescent and has good physical properties; (b) the fusion point of boric acid (H_3BO_3) crystals is below the boiling point and decomposition temperature of many complex molecules; (c) the solvent power of the glass for the latter is moderately good.

* This work was conducted under a contract between the Office of Naval Research and the University of California.

[1] E. Tiede, Ber. d. chem. Ges. **53**, 2214 (1920); E. Tiede and P. Wulff, *ibid.* **55**, 588 (1922).
[2] R. Tomaschek, Ann. d. Physik **67**, 612 (1922).
[3] M. Travniček, Ann. d. Physik **17**, 654 (1933).
[4] H. Chomse, Zeits. f. anorg. allgem. Chemie **233**, 140, 145 (1937).
[5] G. N. Lewis and M. Kasha, J. Am. Chem. Soc. **66**, 2100 (1944); *ibid.* **67**, 994 (1945).
[6] M. Kasha, Chem. Rev. **41**, 401 (1947).
[7] W. L. Lewschin and L. A. Vinokurov, Physik. Zeits. Sowjetunion **10**, 10 (1936).
[8] G. N. Lewis, D. Lipkin, and T. T. Magel, J. Am. Chem. Soc. **63**, 3005 (1941).
[9] This topic for study was suggested by Professor E. B. Wilson, Jr. after the Symposium on Color and Electronic Structure of Complex Molecules, Northwestern University, December 1946 (Cf. reference 6).
[10] G. N. Lewis, M. Calvin, and M. Kasha, manuscript in preparation. Semi-quantitative results were given in the note: G. N. Lewis and M. Calvin, J. Am. Chem. Soc. **67**, 1232 (1945). A preliminary report of the present quantitative work was given in reference 6, Section V.

The chief disadvantage of such a glass is that its composition is variable, and is dependent upon the conditions of preparation.[1] However, by standardizing the procedure it was possible to reproduce the density to within 0.3 percent or better, which was sufficient for the present purpose. The glass is made by melting boric acid crystals under the conditions described in the next section and supercooling the melt. It consists of partially dehydrated *ortho*-boric acid, probably a mixture of H_3BO_3 and B_2O_3.

When first prepared the glass is a virtually colorless, highly transparent, hard and brittle material. Upon standing in moist air a day or longer, or touching with the hand, it acquires an opaque white coating due to hydration. This may be prevented by storing in a very dry atmosphere, by lacquering of the surface, or storing in or coating with mineral oil. The last procedure has been found quite satisfactory for most purposes. Upon prolonged standing crystallization sets in, destroying transparency, until finally the material becomes almost opaque. The rate at which transparency is lost depends on the thermal treatment during the supercooling stages, the most perfect glasses from this point of view resulting from rapid and direct cooling of the molten mass.

The refractive index of the glass described below was not determined. The *luminescence* of the glass itself is a very feeble, blue-violet phosphorescence, persisting for several seconds. In almost all cases this was negligible in comparison with the luminescences of the dissolved complex molecules. A more important disadvantage is the *light absorption* of the boric acid glass. This begins at about 3800A, becomes strong at 3500A, and is intense at 3000A. This puts a severe limitation on the type of complex molecule which may be studied in this glass, naturally excluding all except those which absorb strongly between about 3500 and the infra-red. Only the dyes and other relatively complex organic molecules fall into this category.

III. EXTRUSION PROCESS FOR FABRICATION OF THIN STRIPS OF BORIC ACID GLASS

Reagent grade boric acid crystals (to which the dye or other substance may be added in powdered form) are fused by heating approximately 15 minutes at 240°C in 6×1-inch (actual internal dimensions $5\frac{3}{4}\times\frac{3}{4}$-inch) Pyrex test tubes. The degree of dehydration, and consequently the density and refractive index, depend upon the temperature, heating time, size of tube, degree of filling of the tube, and crystal form of the H_3BO_3 used. The tubes should be filled up to the level reached by the heating bath (see below), with slight tamping. (Note: there is some danger of an explosion occurring if the tubes are filled above the level of the heating bath, since the first step in the fusion process is the formation of a solid plug and slight expansion, preventing escape of vapors. This does not occur when the crystal level is below the bath level.) During the fusion process there is considerable bubbling of the mass (which contributes to its homogeneity) caused by the evolution of water vapor; a significant amount of sublimation also occurs (complicating the solute concentration problem; see below). Two tubes of material are required for one filling of the press described below.

The critical point concerning the fusion process is the removal of the melt from the bath just *before* the last pellet of solid crystal has vanished. Prolonging the heating for only a few minutes results in more complete dehydration and formation of an excessively viscous or even a tough, fibrous mass which cannot be fabricated readily thereafter.

A determination was made of the weight loss upon fusion of boric acid crystals (H_3BO_3, C. P. Baker's) under the conditions described above. The fraction of the weight of the initial crystal remaining after fusion and solidifying was 0.660, the results of several trials being reproducible to about 0.3 percent. An absolute density determination by a volumetric displacement method yielded 1.830 g/cm³ at 20°C, average of several trials, reproducible to about 0.2 percent.

As a bath for heating the tubes containing boric acid, oil was found undesirable because of the excessive fuming and decomposition at 240°C of all the available commercial oils. A very satisfactory bath, providing that precautions demanded for its safe use were observed,[11] was a

[11] Precautions: (a) the hot molten salt should not be brought into contact with the skin, as painful burns result, (b) organic matter should not be brought into contact with the hot bath, since it is an active oxidant, (c) the

FIG. 1. Monel-metal tank containing a molten salt mixture as a 240° bath for fusing boric acid crystals. The test tubes of crystal are held down in the bath by a weighted hook as shown.

eutectic salt bath consisting of an equimolar mixture of sodium nitrite and potassium nitrate.[12] This was fused in a monel metal tank 6-inches high and 5 inches in diameter, heated by a Meker-type gas burner. The tank, its stand, and cover are shown in the photograph of Fig. 1. The tubes containing the crystalline boric acid were held down by means of a small hook set into a brass block as a weight; one of these is shown resting on the tank cover. The temperature was maintained by means of a small gas flame and was followed by a 360-degree glass thermometer dipping into the molten salt bath.

An extrusion press machined from solid brass which was found suitable in this work is illustrated in Fig. 2. The piston (top of drawing) is a solid brass rod fitted with a ferruled bakelite handle. This fits into the cylinder drilled in the block, shown next in the figure. The actual measurements of the piston and cylinder diameters are 1.245 and 1.256 inches, respectively; the large clearance of 0.011 inch is permissible because of the self-sealing action of the highly viscous melt. The third element depicted in Fig. 2 is the removable bottom which is flanged between the cylinder block and the base; it contains a sliding tongue which permits adjustment of the extrusion slit width. A working drawing of the cylinder block is given in Fig. 3. The press is clamped (Fig. 4) after preliminary warming (see below), to a heavy table (1) (weighted with a large concrete block and covered with transite) by means of a heavy-duty C-clamp (2). The piston (3) is compressed by means of a 1-m lever (4) of heavy wrought iron, acting in an inverted-U yoke (5). The extruded glass strip (6) is allowed to slide onto a lightly oiled tin plate (7), is clipped free with shears, and is allowed to harden.

While melting the boric acid crystals, the press is simultaneously heated to 140° by direct immersion in a hot oil bath (White Oil No. 1). (If the melt is poured into the cold press, the piston freezes and the fine slit becomes clogged, necessitating rewarming for separation of the parts.) Similarly, as soon as the melt is removed from the heating bath, it is poured into a casserole which has been pre-warmed to 140°C, and the melt is allowed to cool several minutes by standing at room temperature.

The art of the process comes in pouring the viscous mass at the moment when it may be extruded into firm but pliable, well-formed ribbons. If it is too liquid, it will merely run through the slit in a fine stream; whereas if too viscous, it will not be extruded at all. After a number of trials, the steps become synchronized, and if one takes the care to time the various intervals involved, success in processing perfect ribbons may be achieved in as much as 30 percent of the runs.

The ribbons thus formed should be protected from moisture by coating with a film of (or storing in) mineral oil immediately after hardening and cooling. They are usually slightly warped at this point, but may be rendered flat quite readily since the boric acid glass is thermoplastic. The desired length of strip is placed on a horizontal piece of tin plate (fitted with a vertical rod handle), lowered in this position into a mineral oil bath held at 140°. At the instant that the strip softens and becomes flattened under its own weight, the horizontal tin plate is quickly withdrawn and allowed to cool. An

working range should not be exceeded under any conditions (about 400°C), since violent decomposition may occur, (d) in melting the bath, heating should start near the top of the container, proceeding downward, since geysers of liquid salt may be ejected otherwise.

[12] "Drawtemp 275," E. F. Houghton and Co. (Philadelphia, Detroit, Chicago, San Francisco); "Heat Treating Salt No. 2," Du Pont.

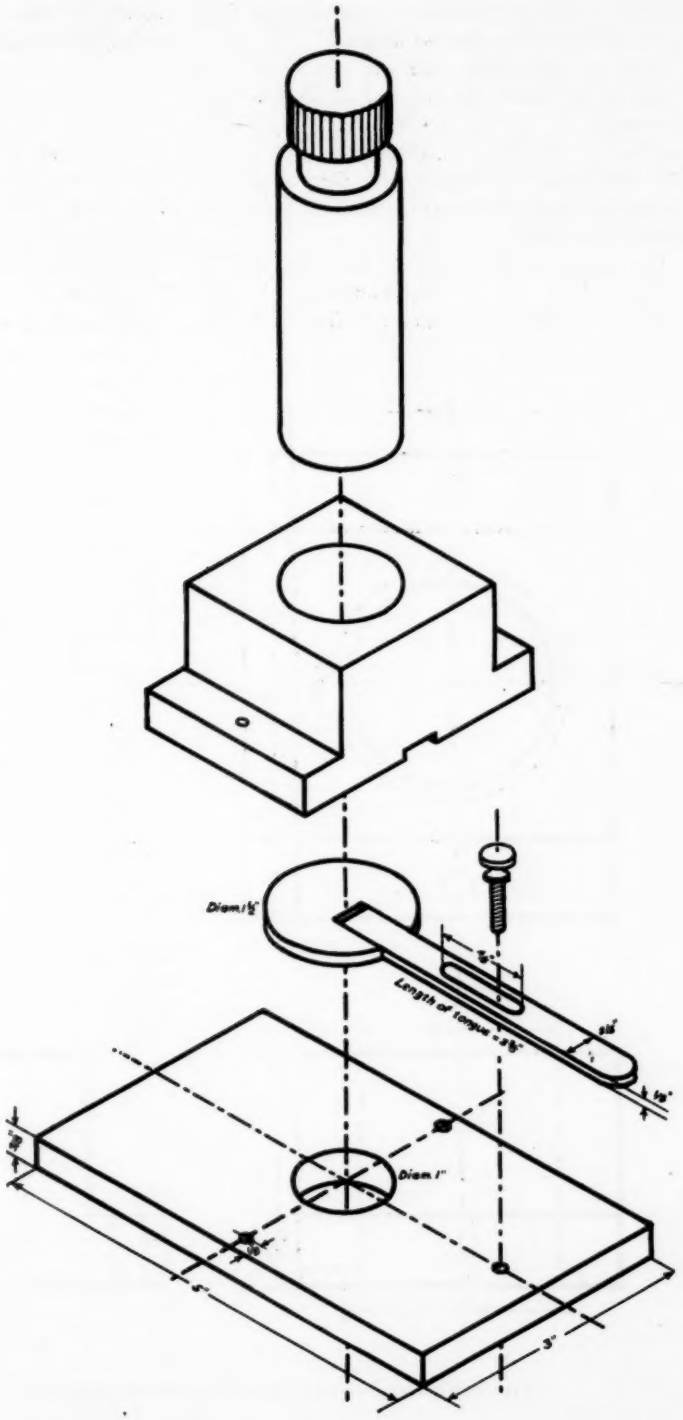

FIG. 2. Dissembled extrusion press for fabrication of boric acid glass. Made of machined brass. The cylinder block, for which a working drawing is given in Fig. 3, is held to the base by knurled nuts. The actual measurements of the piston and cylinder are 1.245 and 1.256 inches, respectively.

electrically heated hot-wire cutter may be used for trimming to the desired length.

This process yields uniform strips of any length up to about 40 cm, and of cross-section dimensions in the range 1 cm×0.3 mm, depending on the size and adjustment of the slit. The thickness is probably best determined by calculation from the length, width, weight, and density of a strip.

The *concentration of solute* in the glass may be determined by one of two methods. The *dry* method, suitable for a non-volatile solute, involves calculation of the concentration, in moles/liter of glass by

$$C = 1000(wd/WfM),$$

where w = weight of solute in grams, d = density of the glass in g/cm³ (= 1.830 in our experiments), W = weight of boric acid crystals, f = weight fraction of initial boric acid remaining after fusion (= 0.660 in our experiments), and M is the molecular weight of the solute. In the *wet* method, the glass is dissolved in a suitable sol-

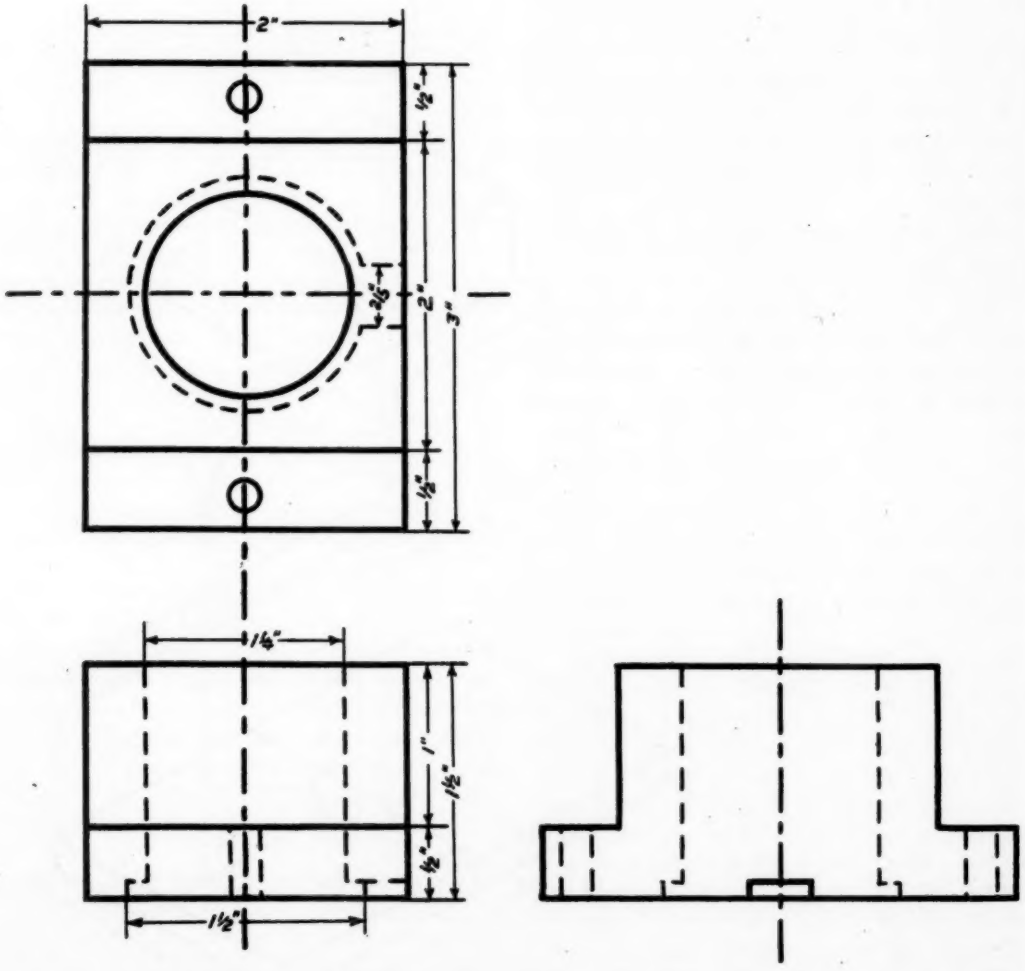

FIG. 3. Working drawing of the cylinder block for the extrusion press of Fig. 2.

vent, and the analysis for the solute of the glass is made spectrophotometrically. For comparison, an absorption spectrum of the substance in the same system (solvent plus boric acid at the prevailing concentration) must be used. Water or 95 percent ethyl alcohol may be used to dissolve a weighed portion of the boric acid glass and the *p*H adjusted afterwards as required by the chemistry of the solute molecule.

If *blocks* of boric acid glass are desired, of dimensions in the range <1 cm $\times 3$ cm^2, they may be cast by pouring the glass melt directly into a lightly oiled mold consisting of a sheet of thin tin plate as a bottom, onto which is held by weights a sheet metal vertical rim of the desired shape and size. Rapid cooling must be avoided to prevent internal fracture of the glass.

Other materials which have been proposed[1–4] for glasses of the sort described here include aluminum sulfate, sugars (such as dextrose and glucose), boro-glycerides, mixtures of sodium borate and sodium metaphosphate, mixtures of silicates and phosphates, etc. Each of these has particular disadvantages, but also substantial advantages which may complement those described for boric acid glass in this report.

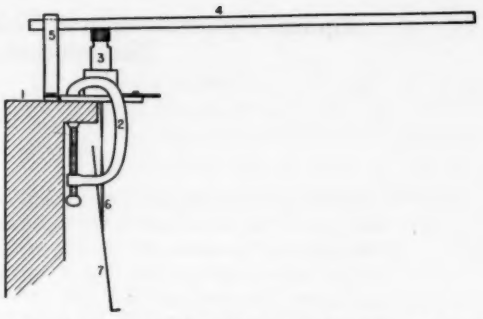

FIG. 4. Manipulation of the extrusion press. The parts are (1) heavy, weighted table, (2) heavy-duty C-clamp, (3) piston of extrusion press, (4) 1 meter lever of heavy wrought iron, (5) inverted U-yoke, (6) extruded glass strip, and (7) oiled tin plate for receiving and hardening of glass strip.

ACKNOWLEDGMENT

The author acknowledges with thanks the drafting work of Mr. W. Zelinsky and the machine shop work of Mr. P. Pfaendtner. Most of the tricks of manipulation of the boric acid glass, except for the extrusion process itself, were shown to me by the late Prof. G. N. Lewis. The encouragement and advice of Prof. M. Calvin during the early stages of the work was very valuable.

Optical Determination of Thin Films on Reflecting Bases in Transparent Environments

A. B. WINTERBOTTOM
*University of Manchester, England**

(Received August 4, 1948)

The classical theory of metal and film optics is recapitulated and its implications in connection with various optical methods of studying films and surfaces are indicated. The experimental technique of determination of thin films *in situ* from the change produced in the reflection of a polarized wave is then outlined. Optical techniques are not advocated to supplant other methods of studying surfaces such as weight increment, gas absorption, electron diffraction, x-ray diffraction, and electrochemical analysis, but rather to supplement these in selected cases. In particular, the optical techniques are of value in making continuous studies of films *in situ* in transparent environments when conditions render the application of other methods difficult. Examples of applications are given.

FILM OPTICS

THE classical theory of film optics developed at the end of last century, notably by Drude,[1] and very clearly expounded by Fry,[2] considers the propagation of plane waves at the boundary of two optically different media separated by a uniform film of a third medium. Consideration can be restricted to those cases of practical interest in which the first medium (immersion medium) is transparent and isotropic, and the other two (base and film) may be, in general, absorbing and anisotropic. In the present paper, it is desirable to restrict consideration still further to the simpler cases where base and film are isotropic. Drude has provided a detailed analysis of reflection at surfaces of absorbing uniaxial and biaxial crystals with various orientations.[3] These results can be used to develop general expressions by Fry's method of equivalent beams (See Fig. 1.) for cases of reflection at anisotropic bases covered with anisotropic films. Mallemann and Suhner have made both analytical and experimental studies of transparent anisotropic films on transparent anisotropic bases.[4]

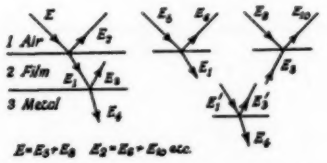

FIG. 1. Reflection at a film-covered surface—Fry's equivalent beams.

The results of an analysis of the isotropic case under consideration are conveniently expressed in the form of complex Fresnel coefficients for the reflection of plane waves with electric vectors vibrating, respectively, parallel and normal to the plane of incidence:

$$R^{\nu}=(r_{12}{}^{\nu}+r_{23}{}^{\nu}\cdot e^{-2i\delta})/(1+r_{12}{}^{\nu}\cdot r_{23}{}^{\nu}\cdot e^{-2i\delta}) \quad (1)$$

with $\nu=p$ or n for parallel and normal electric vectors,

$$r_{\alpha\beta}{}^{p}=(n_{\alpha}\cos\varphi_{\beta}-n_{\beta}\cos\varphi_{\alpha})/(n_{\alpha}\cos\varphi_{\beta}+n_{\beta}\cos\varphi_{\alpha}),$$
$$r_{\alpha\beta}{}^{n}=(n_{\alpha}\cos\varphi_{\alpha}-n_{\beta}\cos\varphi_{\beta})/(n_{\alpha}\cos\varphi_{\alpha}+n_{\beta}\cos\varphi_{\beta}),$$

$\alpha=1$ or 2, $\beta=2$ or 3, and $\delta=2\pi\cdot n_2\cdot\cos\varphi_2\cdot d/\Lambda_0$.

Here d and Λ_0 are film thickness and wave-length (in vacuum), respectively, in the same units. The n's are the complex refractive indices of the media indicated by the suffixes of the form $n=N(1+iK)$ where the N's are the refractive indices and the K's absorption coefficients, i.e., the NK's are absorption indices. The φ's are the angles of propagation in the media indicated by the suffixes related to each other by expressions of the form $n_1\sin\varphi_1=n_2\cdot\sin\varphi_2$. These are also complex for absorbing media.

It is easily verified that the expression (1) gives

* Now Norwegian Institute of Technology, Trondheim, Norway.

[1] Paul Drude, Wied. Ann. **36**, 532, 865 (1889); **39**, 481 (1890).

[2] Thornton C. Fry, J. Opt. Soc. Am. **15**, 137 (1927); **16**, 1 (1928); **22**, 307 (1932).

[3] Paul Drude, Wied. Ann. **32**, 616 (1887).

[4] R. de Mallemann and F. Suhner, Rev. d'Opt. **23**, 20 (1944).

the correct limiting values for $d \to 0$ and $d \to \infty$, *viz.* $r_{13}{}^{p}$ in the former case and in the latter, for absorbing films, $r_{12}{}^{p}$. Expressions for multiple films are also easily developed similar to (1) by starting from the outside and writing successive expressions for $R_{23}{}^{p}$, $R_{34}{}^{p}$, etc., until the base medium is reached.

The linear approximate expression for thin films of Drude can be obtained by expansion of the exponential terms in a power series, discarding terms of higher power than the first. Alternatively, the binomial approximation gives Leberknight and Lustman's approximation,[5] which is physically equivalent to the assumption of a single reflection in the film and which is therefore increasingly accurate the greater the absorption in the film. The absolute changes in amplitude and phase given by the Fresnel coefficients for parallel and normal electric vectors are not easily investigated experimentally, but relative changes are conveniently studied by determining the changes in the parameters of a general elliptical vibration produced by the reflection. These relative changes are given by the ratio of the Fresnel coefficients, the relative amplitude reduction being the ratio of the moduli $|R^{p}|/|R^{n}|$, and the relative phase retardation the difference of the arguments, Δ.

It is seen on inspection of (1) that the expressions for the Fresnel coefficients are, in fact, linear transformations of the periodic vector term $e^{-2i\delta}$. Plots of the Fresnel coefficients for growing films are therefore conformal representations of the plots of the periodic term itself. Over the range where the Leberknight and Lustman approximation is valid, the plot of the ratio of the Fresnel coefficients is also a conformal representation of the periodic term.

Examples of plots of the Fresnel coefficients and of their ratio are given in Figs. 2–5 for the four cases:

An absorbing film on an absorbing base.
A transparent film on an absorbing base.
An absorbing film on a transparent base.
A transparent film on a transparent base.

In all cases incidence at $\pi/3$ and a wave-length of 5461A are assumed and the figures on the curves refer to the light path length in the film in wave-lengths.

The constants used in computing Fig. 2 correspond to iron base with an iron oxide film, for Fig. 3 the constants correspond to aluminium base with an aluminium oxide film, for Fig. 4 the constants correspond to crown glass base with an aluminium film, while for Fig. 5 the constants correspond to crown glass base with a transparent film of lower refractive index.

It is seen that in the case of transparent films the plots are closed figures and the character of the reflection goes through periodic changes which repeat indefinitely for a growing film. In the cases of absorbing films, the periodic changes gradually become less as the film grows until the terminal point corresponding to massive film substance is reached. Figures 2 and 3 also include the plots of $|R^{p}|/|R^{n}|$, the relative amplitude change, and Δ, the difference of the arguments of R^{p} and R^{n}, i.e., the relative phase

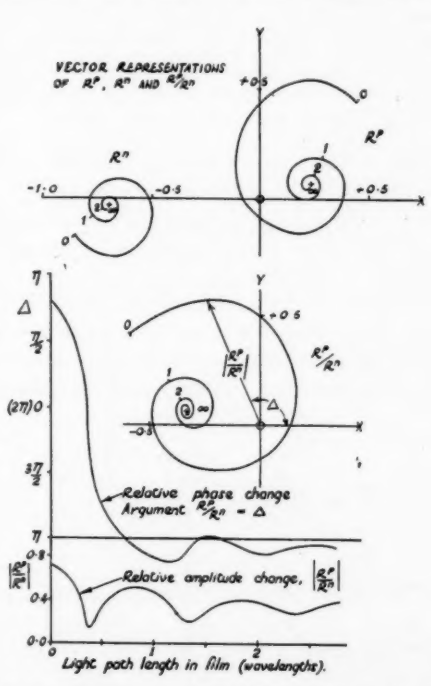

FIG. 2. Reflection at an absorbing base with an absorbing film. Fresnel coefficients for parallel and normal electric vectors and ratio of coefficients plotted in the complex plane, together with plots of relative amplitude change and relative phase change, as functions of path length in film. (Figures on curves are path length in film in wave-lengths.)

[5] C. E. Leberknight and B. Lustman, J. Opt. Soc. Am. 29, 59 (1939).

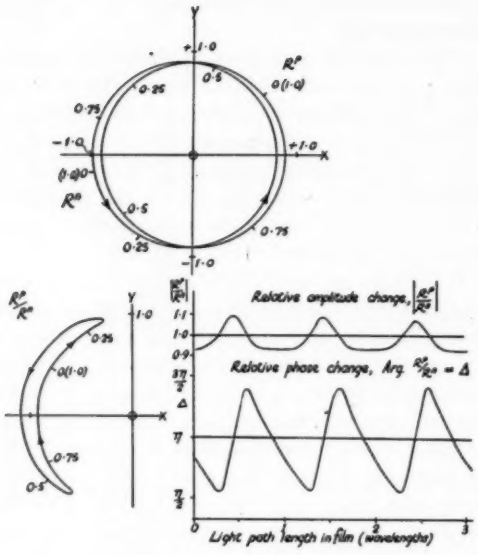
Relative amplitude change, $\left|\frac{R^p}{R^n}\right|$
Relative phase change, Arg $\frac{R^p}{R^n} = \Delta$
Light path length in film (wavelengths)

FIG. 3. Reflection at an absorbing base with a transparent film. Fresnel coefficients for parallel and normal electric vectors and ratio of coefficients plotted in the complex plane, together with plots of relative amplitude change and relative phase change, as functions of path length in film. (Figures on curves are path length in film in wave-lengths.)

change, as functions of light path length in film, i.e., film thickness. These plots bring out the periodic character of the changes and, in the case of an absorbing film, the gradual approach to reflection at massive film substance.

Examples of the variation with angle of incidence of the relative amplitude reduction and relative phase retardation for film-free absorbing and transparent bases are given in Figs. 6 and 7, while examples of the variations with angle of incidence of the changes in these two magnitudes produced by thin films are given in Fig. 8. It is apparent that the changes for a given thin film are largest for fairly large angles of incidence, the actual position of the maximum depending on the optical constants of the film.

REFLECTIVITY AND INTERFERENCE PHENOMENA

Reflectivity for unpolarized radiation is obtained by taking the mean of the reflectivities for parallel and normal electric vectors, which in their turn are simply the squares of the moduli of the corresponding Fresnel coefficients. The reflectivity film thickness curves of Fig. 9 have been computed in this way from the data of Figs. 2 and 3. It will be noted that the first-order minima are at appreciably smaller film paths than a half-wave. For normal incidence, the expressions for the Fresnel coefficients become identical apart from a difference of sign (i.e., a phase difference of π) and are considerably simplified, *viz.*:

$$R^p = (r_{12}^p + r_{23}^p \cdot e^{-2i\delta})/(1 + r_{12}^p \cdot r_{23}^p \cdot e^{-2i\delta}) = -R^n,$$
$$r_{12}^p = (n_2 - n_1)/(n_2 + n_1) = -r_{12}^n,$$
$$r_{23}^p = (n_3 - n_2)/(n_3 + n_2) = -r_{23}^n,$$

and

$$\delta = -2\pi n_2 d/\Lambda_0. \qquad (2)$$

It can be shown that the film thicknesses for the various reflection minima are given to a close degree of approximation by the expression

$$dm \sim \frac{\Lambda_0}{2N_2}\left\{\frac{\text{Arg } r_{12} - \text{Arg } r_{23}}{2\pi} + \frac{2m+1}{2}\right\}$$

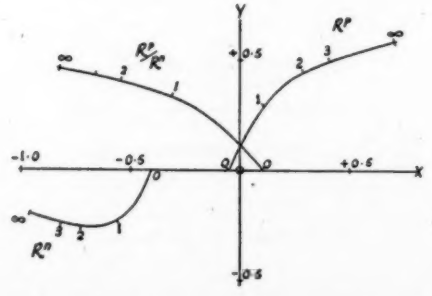

FIG. 4. Reflection at a transparent base with an absorbing film. Fresnel coefficients for parallel and normal electric vectors and ratio of coefficients. (Figures on curves are path length in film in hundredths of wave-length.)

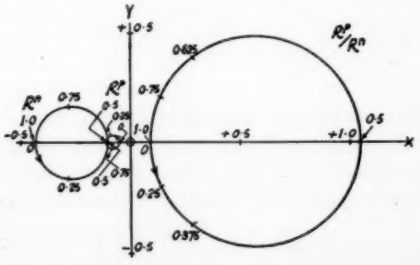

FIG. 5. Reflection at a transparent base with a transparent film. Fresnel coefficients for parallel and normal electric vectors and ratio of coefficients. (Figures on curves are path length in film in wave-lengths.)

for

$$m = 1, 2, 3, \text{ etc.} \qquad (3)$$

The difference of the arguments of the Fresnel coefficients for the outer and inner film interfaces here appears as a correction to the expression for minima in reflection from an isolated thin transparent film. Since r_{23}' is always complex for an absorbing base, this correction term can only be zero in the rare case when the film substance is also absorbing with optical constants such that the phase change at the outer surface of the film is identical to that at the film base interface. Computations are made most simply and with sufficient accuracy by graphical methods.

Thicknesses computed on this basis may differ considerably from those estimated on the erroneous assumption, often made, that the difference of the phase jumps at the inner and outer surfaces of the film is zero. In the case of oxide films on copper determined electrochemically by Campbell and Thomas, discrepancies between electrochemical and optical thicknesses are largely removed when the above expression is used for the optical thickness calculations.[6]

IMPLICATIONS OF THEORY IN CONNECTION WITH OPTICAL TECHNIQUES FOR STUDYING SURFACES

The foregoing theory is fundamental for the various optical methods of studying surfaces and films. In the case of the interference techniques depending on path differences for rays reflected at different surface features, it is evident that differences in optical character of the reflecting features can also give rise to difference in phase, which must then affect the geometrical interpretation. This also applies to incident light phase contrast microscopy. The difficulties encountered with high aperture objectives in incident polarized light microscopy, to which Short refers,[7] are also explained by the fundamental theory. Dayton[8] has used a cross-shaped condenser diaphragm to restrict illumination, when using a plane polarization, to those beams with plane of incidence parallel or normal to the polarization azimuth. In this way it is possible to investigate anisotropy of the object without obscuring the phenomena by polarizations of varying azimuth and ellipticity, due to reflection of plane polarizations of varying azimuth referred to the planes of incidence. The present author has suggested a double reflection of a circular polarization as a possible line of development of high aperture incident polarized light microscopy.[9]

When precision methods of incident polarized

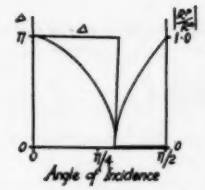

FIG. 7. Variation of relative amplitude reduction and relative phase retardation with angle of incidence for a transparent reflector.

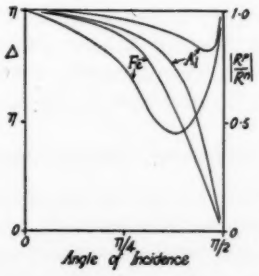

FIG. 6. Variation of relative amplitude reduction and relative phase retardation with angle of incidence for an absorbing reflector.

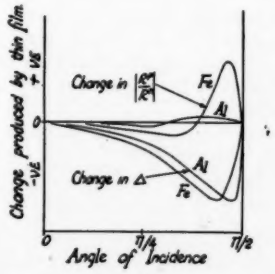

FIG. 8. *Changes* in relative amplitude reduction and relative phase retardation produced by thin films of constant thickness at various angles of incidence on two metals.

[6] W. E. Campbell and U. B. Thomas, Electrochem. Soc. 76, 314 (1939).

[7] M. N. Short, *Microscopic Determination of the Ore Minerals* (U. S. Geological Survey Bulletin 914, Washington, 1940), p. 66.

[8] R. W. Dayton, Trans. Am. Inst. Min. Met. Eng. 119, 17 (1935).

[9] Arthur B. Winterbottom, unpublished work.

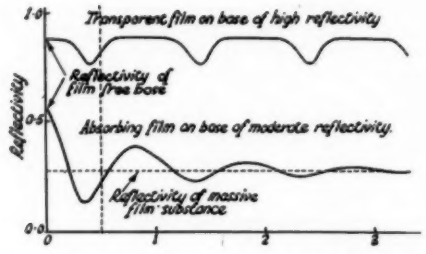

FIG. 9. Reflectivity variation with film thickness.

light and phase contrast microscopy are developed, it should be feasible to make studies of film formation on a microscale similar to those now made with present technique on a macroscale. The recent application of a polarized light method to the determination of grain size and orientation in aluminium is an interesting indication of possibilities of this kind.[10]

EXPERIMENTAL ARRANGEMENTS FOR POLARIMETRIC STUDIES

General Plan

From the foregoing theoretical discussion, it will be apparent that the following are the requirements for a profitable application of the polarimetric technique:

1. Macroscopically uniform, preferably single crystal experimental reflecting surfaces.
2. Transparent environment.
3. Means of producing an initial film-free surface and of producing uniform films, preferably up to thicknesses of the order of about $\frac{1}{10}$ wave-length.
4. Means of studying the Fresnel coefficients of the surface, that is, the change produced by reflection at a suitable angle of incidence in the parameters of a monochromatic polarized wave.

The first two conditions need no further discussion. In regard to the third, it should be noted that surfaces of all kinds prepared by mechanical polishing methods are unavoidably covered with a thin flowed layer of deformed material and an adsorbed moisture film with initially chemically formed films (oxides), in the case of metals. Cleaving methods in the case of suitable crystals avoid the production of flowed layers, but not the adsorbed or the chemically formed films. Where applicable, electrolytic polishing methods yield reflecting surfaces without deformed layers[11] but, by the very nature of the process, adsorbed and chemical films cannot be excluded. Surfaces produced by condensation in high vacuum on cleaned supports would appear to be free from chemical and adsorbed films immediately after formation, but other features such as crystal size and orientation may not be so advantageous. Surfaces polished by any method may be cleaned by treatment with gases at high temperature followed by evacuation.

The fourth requirements will now be considered in more detail. It is apparent from the theory that the ratio of the Fresnel coefficients can be determined by finding either the parameters of an elliptical vibration obtained by reflecting a plane one in $\pi/4$ azimuth, i.e., with equal p and n components, or by finding the parameters of the elliptical vibration which gives a plane one on reflection. The latter procedure is particularly convenient, as it is possible to compensate any phase difference with a $\frac{1}{4}$ wave plate fixed in $\pm\pi/4$ azimuth when the polarizer azimuth is varied from $-\pi/4$ to $+\pi/4$ azimuth. This can be seen from the Poincaré representation, Fig. 10. The relative phase retardation, Δ, and the relative amplitude reduction, $|R^p|/|R^n| = \tan\psi$, are then given by the following relations:

$$\left.\begin{aligned} \tan\Delta &= \sin\delta K/\tan 2P \\ \cos 2L &= \cos\delta K\cdot\cos 2P \\ \tan\psi &= \tan L/\tan A_N = \cot L/\tan A_S \end{aligned}\right\} \quad (4)$$

and

$$\tan^2\psi = \cot A_N\cdot\cot A_S,$$

where δK is the relative retardation of the $\frac{1}{4}$ wave plate, P the polarizer azimuth, $\tan L$ the ratio of the components of the incident vibration, and A_N and A_S the analyzer azimuths corresponding to incident elliptic vibrations of opposite sense.

Polarization Spectrometer

Practical instruments operating on these principles, which have been variously termed crystal elliptometers or polarization spectrometers, have already been described.[12,13] Their main features may be summarized:

[10] A. Hone and E. C. Pearson, Metal Progress **53**, 363 (1948).

[11] Lowery, Wilkinson, and Smare, Phil. Mag. **22**, 769 (1936).

[12] Arthur B. Winterbottom, J. Sci. Inst. **14**, 203 (1937).

[13] Richard M. Emberson, J. Opt. Soc. Am. **26**, 444 (1936).

1. A powerful monochromatic source, usually mercury arc with filters.
2. A spectrometer with collimator and telescope arms swinging in a vertical or horizontal plane with provision for reading angles on a large fixed circle.
3. Polarizer and $\frac{1}{4}$-wave compensator mounted in circles on collimator arm.
4. Analyser mounted in circle with alternative half-shade systems on telescope arm.
5. Lenses to produce real images of the collimator diaphragm or half-shades on the cross wires and a Ramsden eyepiece to observe cross wires and images.
6. Independent tables, cells, and chambers for experimental surfaces provided with gas- or liquid-tight windows in the latter two cases.

An instrument on the lines of this specification is shown diagrammatically in Fig. 11.

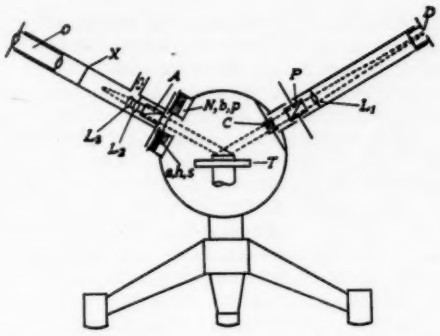

FIG. 11. Polarization spectrometer (diagrammatic).

Computations from Instrument Readings

It is convenient to use the relations (4) to calculate a skeleton table of $2P$ and Δ values and then to make a table of differences of $2P$ and Δ, which are usually small, and vary only slowly with P. Relative phase retardations are thus quickly obtained by doubling polarizer readings and making small corrections from the table. For stable surfaces, doubled polarizer azimuths are obtained directly by difference of polarizer readings with wave plate in $+\pi/4$ and $-\pi/4$ azimuths (i.e., with similar elliptic vibrations of opposite sense). The 2ψ values, $\psi = \tan^{-1}|R^p|/|R^n|$ are also obtained by making small corrections to differences of the appropriate analyzer settings in the case of a stable surface. For rapidly changing surfaces, individual compensation settings must be used for computation with the formulas or interpolation in tables based on these. With practice, settings can be made in about ten seconds. The polarizer setting is usually the one changing most rapidly and the timing of this is then the more significant. With green mercury, radiation settings can be made with a precision of *ca.* 5 min. of arc or when sets of settings are taken the doubled azimuths are obtained with a precision better than one minute. These represent a sensitivity of about 0.5–0.1A in the case of iron oxide films on iron. When sets of settings can be made, systematic errors due to circle zeros and unbalance of half-shades are eliminated. Errors due to multiple reflection in the instrument are not eliminated and are difficult to compute but, while their effects on determinations of optical constants are appreciable, there is only a second-order effect on the determination of thin films. It would, however, be desirable to eliminate multiple reflection by suitable coating of the optical components, i.e., wave plate, windows of apparatus, cover glasses of half-shades and possibly inner end faces of polarizer and analyzer.

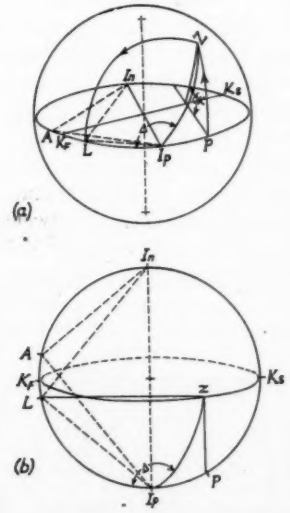

FIG. 10. Poincaré representation of polarization spectrometer compensation process: a—Perspective; b—plan.

Design of Experiments and Evaluation of Results

In actual studies of film formation, the logical application of the foregoing theory in the design of the experiments and in the evaluation of observations is the following scheme:

1. Determination of relative phase change and relative amplitude change for a film-free surface in order to determine the optical constants of the base.

2. Determination of the same magnitudes for surfaces with various degrees of film formation resulting from the progressive reaction under investigation and plotting of $\tan\psi e^{i\Delta} = R^p/R^n$ in the complex plane. In many cases when the range of film thicknesses is not great, direct plotting of the experimentally determined ψ, i.e., $\tan^{-1}|R^p|/|R^n|$ against Δ is often more convenient. Such plots are almost linear in accordance with the Drude approximation.

3. Fitting plotted data with a theoretical curve computed with optical constants of base determined in 1 and hence determination of the optical constants of the film and very probably its nature.

4. Determination of film thicknesses corresponding to observations of 2 by means of the thickness parameter scale of the fitted plot 3 and hence relation of film thickness to reaction time or other parameter.

Such a scheme in favorable cases should therefore enable the nature of the film substance and the kinetics of its formation to be established. While the making of experimental observations is simply and quickly done, the evaluation of these and their full interpretation demands considerable tedious computation. The technique is consequently not advocated to supplant other methods of study where these are adequate, but rather to supplement them in cases of special difficulty or where results obtained in other ways are not conclusive. For example, in the case of films on immersed surfaces, many methods of investigation involve withdrawal from the liquid environment, which may involve modification of the film. It is also sometimes of interest to study films on metallic electrodes subject to electrolytic polarization. There are also cases where X-ray or electron diffraction methods, particularly the latter, are unable to discriminate between alternative film substances.[14] In such cases the polarimetric method may provide additional information of optical character, enabling a decision to be made.

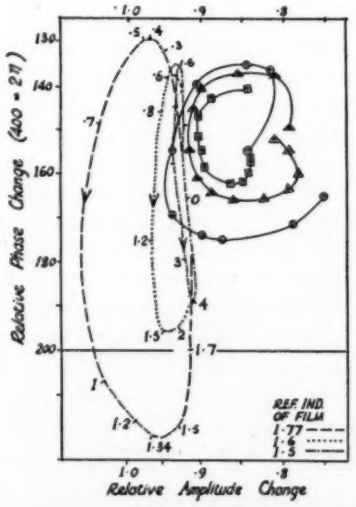

FIG. 12. Films on aluminium in concentrated nitric acid —Tronstad and Høverstad's observations (see reference 22) plotted together with theoretical curves for various film constants. Points on the plots of observations are at successive 20-minute intervals after immersion. The figures on the theoretical curves are film thicknesses in thousands of Angstrom units.

BRIEF HISTORY OF DEVELOPMENTS IN APPLICATIONS OF THE POLARIMETRIC TECHNIQUE

It is interesting to trace briefly the chief stages in the development and application of the polarimetric technique. In 1927 Freundlich, Patscheke, and Zocher applied it to demonstrate *qualitatively* that optical changes observed in iron carbonyl mirrors on making them passive by exposure to air are consistent with the formation of an oxide film.[15]

Tronstad, working at Berlin and Stockholm, applied the same technique to *quantitative* studies of the formation of passive films on iron and steel immersed in various electrolytes when polarized anodically using approximate expressions of the Drude type for the analysis.[16] Later, Tronstad and Feachem, working at Cambridge, studied fatty acid monolayers on mercury using the same technique and method of analysis.[17]

In America, Ives and Johnsrud[18] determined thicknesses of films of alkali metal on glass by interpolation of observations between theoretical curves relating the observable optical magnitudes with angle of incidence, computed for various thicknesses of film using Fry's *rigorous analysis*.[2] Leberknight and Lustman, working at the

[14] E. A. Gulbransen and J. W. Hickman, Metals Tech. A.I.M.E. (Oct. 1946, T. P. 2068).

[15] Freundlich, Petscheke, and Zocher, Zeits. f. physik. Chemie **128**, 321 (1927); **130**, 289 (1927).

[16] Leif Tronstad, Det Kgl. Norske Vid. Sels. Skrifter, No. 1 (1931); Zeits. f. physik. Chemie **A142**, 241 (1929); Trans. Faraday Soc. **31**, 1151 (1935).

[17] L. Tronstad and C. G. P. Feachem, Proc. Roy. Soc. **145A**, 127 (1934).

[18] H. E. Ives and A. L. Johnsrud, J. Opt. Soc. Am. **15**, 374 (1927).

Carnegie Institute, studied oxide film formation on iron and nickel, analyzing their observations by fitting simultaneously the plots of the Δ and $|R^p|/|R^n|$ observations as functions of square root of oxidation time with theoretical Δ and $|R^p|/|R^n|$ film thickness curves computed with assumed film constants.[5] In this work the approximation derived on the assumption of a single reflection in the film was used. Lustman and Mehl employed the same method later in a study of the oxidation of copper.[19]

The present author, working at Trondheim, applied the polarimetric technique to studies of oxide film formation on copper, iron, and steels at elevated temperatures, at first utilizing the Drude approximate analysis.[20] Prior to interruption of this work by the recent war, the principles of the method of applying the rigorous analysis, here described, had been elaborated. Application to the observations on filmed iron had also been started. In the course of this work, it was appreciated that the rigorous theory of interference phenomena in absorbing films on absorbing bases had not been sufficiently expounded. This was therefore done.[21] Resumption of the work has been delayed, however, by difficulties involved by the removal of the instrument, but it is hoped soon to be able to apply the improved method to further selected cases and to adapt the analysis to the general case of absorbing anisotropic films on an anisotropic absorbing base.

In the meantime, as an indication of the possibilities of the method, examples of two applications at present in process of analysis are given. These are the film on aluminium in concentrated nitric acid and the film formed on iron in air at moderately elevated temperatures. In both cases the surfaces were polycrystalline.

Aluminium Surfaces in Concentrated Nitric Acid

The observations discussed here were originally made by Tronstad and Høverstad[22] on polycrystalline aluminium of technical grade (99.8 percent Al) using single instrument settings, i.e., not the more precise technique of complete sets. Values of relative phase retardation and relative amplitude reduction taken from the smoothed curves of observations have been plotted in ordinary cartesian coordinates, together with theoretical curves for transparent isotropic films with various refractive indices, Fig. 12. It is evident that while the experimental plots are all probably parts of closed curves, differing somewhat in size for the individual experiments though of the same general shape, they are more nearly circular than the elongated ones of the theoretical curves. Furthermore, the experimental curves are located in a lower range of $|R^p|/|R^n|$ values.

These features suggest that the film on the aluminium is transparent but not isotropic, i.e., exhibits structural double refraction as a result of a regular fiber or pore structure, and that the proportion of voids is considerable. This is highly probable since Huber has shown that oxide films stripped from aluminium previously anodized do exhibit structural double refraction.[23] Since the range of Δ values in the experimental curves is of the same order as that for the theoretical curve for a film refractive index of 1.5, the thickness parameters of this curve are probably of the same order as those for the experimental curve. On this assumption, the film thicknesses at the end of the experiments were probably of the order of several

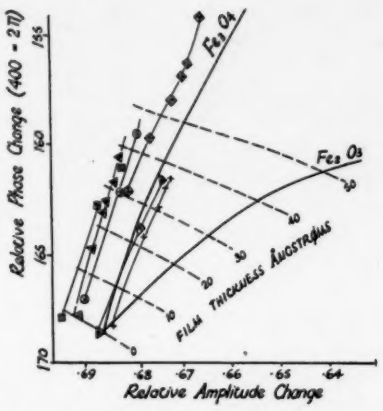

FIG. 13. Films on iron in air. The plotted points are from hitherto unpublished observations of the author, and the two curves are theoretical ones computed for film constants corresponding to αFe_2O_3 and Fe_3O_4.

[19] B. Lustman and R. F. Mehl, Trans. Am. Inst. Min. Met. Eng. **143**, 246 (1941).
[20] Arthur B. Winterbottom, Nature **140**, 364 (1937) and unpublished work.
[21] Arthur B. Winterbottom, Electrochem. Soc. **76**, 327 (1939); Trans. Faraday Soc. **42**, 495 (1946).
[22] L. Tronstad and T. Høverstad, Trans. Faraday Soc. **30**, 349 (1934).
[23] Huber, Helv. Chim. Acta **28**, 1416 (1945).

thousand Angstrom units, which is consistent with Tronstad and Høverstad's observation of interference colors in air after removal from the nitric acid followed by washing and drying. The displacement of the experimental curves with respect to the theoretical ones would seem to imply a difference in the optical constants of the base in the experiments and those used in computing the theoretical curves. Since the experimental surfaces were of mechanically polished aluminium of technical purity, the base as a whole probably has constants corresponding to somewhat lower $|R^p|/|R^n|$ values, further reduced in the vicinity of the surface as a result of the deformation introduced by mechanical polishing. If this view is correct, the experimental curves represent gradual conversion of the deformed surface material into a porous structurally anisotropic film, i.e., a complete interpretation would probably require two-film analysis. However, it is evidently desirable to repeat the experiments with electrolytically polished single crystal surfaces, using the improved technique of taking sets of readings. It would probably also be advantageous to make observations at several angles of incidence.

Oxidation of Iron Surfaces in Air at Moderately Elevated Temperatures

Some of the author's observations made at Trondheim, which have not yet been completely evaluated, are plotted in Fig. 13, together with theoretical curves for film constants corresponding to hematite and magnetite. Optical constants for γ-hematite are not known, but it may be possible to make an estimate of them from structure density and other known properties. All the observations relate to reoxidation in dry air of polished polycrystalline iron surfaces after reduction and annealing in pure hydrogen. It will be noted that the trend of the observations differs considerably from that of the curve for the αFe_2O_3 film and is very close to that of the theoretical curve for Fe_3O_4 Further, it is apparent that the choice of film constants does not greatly influence the film thicknesses assigned to the data.

In one experiment with carbonyl iron of large grain size it was observed that after oxidation had progressed for some time the film thicknesses on adjacent grains became more and more different. When the relative phase change was plotted against time of reaction, the curve therefore branched into two with different growth rates. This is, of course, in agreement with the well-known phenomenon of heat tinting and the observations of Mehl and McCandless.[24] Clearly this emphasizes the desirability of single-crystal experimental surfaces in future work. At the same time a further advantage of the polarimetric technique is revealed, *viz.*, the ability to study reactions occurring on selected small areas.

[24] R. F. Mehl and E. L. McCandless, Trans. Am. Inst. Min. Met. Eng. **125**, 531 (1937).

JOURNAL OF THE OPTICAL SOCIETY OF AMERICA VOLUME 38, NUMBER 12 DECEMBER, 1948

A Photometer for Measurement of Sky Brightness Near the Sun

JOHN W. EVANS*
Harvard University, Cambridge, Massachusetts
(Received June 14, 1948)

Measurement of the brightness of the sky near the sun is difficult because instrumental scattered light originating in the solar disk is usually many times brighter than light from the sky. An optical system for eliminating this scattered light and providing means for a visual photometric comparison between the sky and the sun has been constructed and tested. The principles of the instrument are explained in sufficient detail to permit the design of similar instruments for a wide range of applications.

IN connection with research on the solar corona, the High Altitude Observatory of Harvard University and the University of Colorado (hereafter abbreviated to HAO) has been using a simple visual photometer for determining the brightness of the sky immediately surrounding the sun. Its performance has been very satisfactory. Since such a photometer has many interesting applications, including the meteorological, a short description of it is given below.

The principal difficulty in measuring sky brightness very near the sun is the elimination of the sun's light itself from the measuring instrument. Somewhere, either in the instrument or in the eye of an observer, an image of the sky must be formed, undiluted by stray light from the sun. Since, in a really clear atmosphere the sun is of the order of 10^6 times as bright as the neighboring sky, the problem of scattered light is acute. The scatter by diffraction from the edge of an aperture diaphragm fully illuminated by direct sunlight is, by itself, many times brighter than the image of the clear sky near the sun. Added to this is the scattering from dust and film on lenses and the multiple reflections between lens surfaces.

Several possible devices for the elimination of scattered sunlight would doubtless be satisfactory. The HAO photometer consists essentially of a rudimentary Lyot coronagraph[1] of 3 mm aperture equipped with an external occulting disk which shades the entrance aperture, and a photometric comparison surface illuminated by direct sunlight through an adjustable optical wedge. Its satisfactory operation depends both on careful adjustment and cleanness of the optical parts.

The optical system is shown schematically in Fig. 1.

The external occulting disk, O_1, completely shades the 3 mm aperture, a_1, so that no point on the sun can be seen from any point in the aperture. (Distance O_1 to a_1 is 100 cm.) If an observer looks through a_1, however, he sees the edge of O_1 brilliantly illuminated by diffraction. The main function of the remainder of the optical system is to eliminate this diffracted light. Behind a_1 is a simple telescope consisting of the objective, l_1, ($f=25$ cm) and eye piece, l_2, ($f=10$ cm). The telescope is folded by reflection from an uncoated black glass mirror, m, into a compact unit with the eye piece in a comfortable position. (Direct vision solar instruments are definitely neck wringing at lunch time in the summer.) A second occulting disk, O_2, is set in the focal plane of l_1. It is large enough to intercept the somewhat out of focus image of the brilliant edge of O_1, and the narrow ring of the sky around the sun which suffers from vignetting due to the fact that the sky and O_1 cannot be simultaneously in focus. The second occulting disk stops the bulk of the diffracted light, but not all. In passing the edge of the aperture a_1, the light diffracted originally at O_1 is diffracted a second time. As seen from a point in the field near O_2, the edge of the aperture appears very bright, and it constitutes a source which scatters light over the whole field quite comparable in intensity with the image of a clear sky near the sun. To suppress this source of scatter, a second aperture diaphragm, a_2, is mounted concentric with the exit pupil where a_1 is imaged by lens l_2. The opening in a_2 is slightly

* Of the High Altitude Observatory of Harvard University and the University of Colorado.
[1] Bernard Lyot, M.N.R.A.S. 99, 580 (1939).

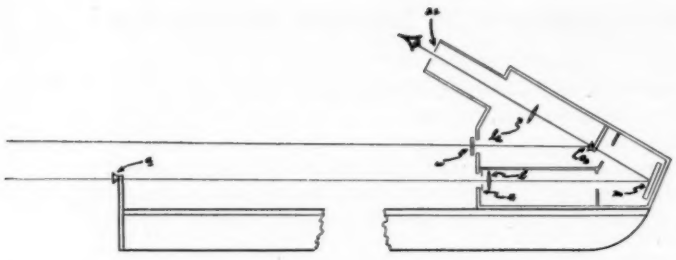

FIG. 1. Schematic diagram of sky photometer. (Not drawn to scale.)

smaller than the image of the bright edge of a_1, and effectively prevents the diffracted light from that edge from entering the observer's eye.

For photometric purposes, the back surface of O_2 is painted a diffuse white. Direct sunlight illuminates it after passing through the optical wedge, w. When the observer looks into the eyepiece he sees O_2 surrounded by an image of the sky. Measurement consists in adjusting the wedge until the two appear equal in brightness. From the known density of the wedge, then, the sky brightness in terms of the average brightness of the sun is readily calculated. It is

$$B = B_0 \frac{\varphi^2 r_2 \cos\beta}{t_1 r_m} t_w$$

where

B = brightness of sky
B_0 = brightness of sun
φ = angular radius of sun (.0047 radian)
β = angle of incidence of sun light on O_2
t_1 = transmission of l_1
t_w = transmission of wedge at balance
r_2 = diffuse reflecting power of white surface on O_2
r_m = reflecting power of mirror, m.

The instrumental constants of the HAO photometer give:

$$B = 494 \times 10^{-6} B_0 t_w.$$

This instrument is restricted to measurements of sky less than 500 millionths as bright as the sun. Since skys of this brightness are completely useless for coronal observation, the range is adequate. But for other studies, the range can be extended as far as seems desirable, preferably by increasing the illumination of O_2 with a simple lens system. The alternative of putting an absorbing screen in the sky beam should be used with caution as it is necessary that the absorber be completely specular to avoid damaging scattered light. A second reflection from a black glass mirror might be the safest device.

When the HAO photometer was first tested, it was found, surprisingly, that at levels of less than 100 millionths the sky near the solar limb was still very blue. Comparisons with the white surface of the occulting disk were troublesome and their interpretation was doubtful. The difficulty was overcome by mounting a green filter (Wratten No. 58) over the exit aperture, a_2—a satisfactory remedy in this instance since the corona is observed chiefly in the light of a green emission line at λ5303.

Mention has been made of the vignetting of an area of the sky adjacent to the limb of the sun. This vignetting is a necessary evil in any instrument with a non-zero entrance aperture and an external occulting disk at a finite distance. Instruments of this type are unsuitable for measuring sky brightness right up to the solar limb. The HAO instrument was made with the second occulting disk large enough to cover up the vignetted area, which was, in this case, a circle of 1.6 solar diameters. The minimum sizes of the occulting disks which assure freedom from vignetting in the visible image are given by the following relations:

$$\psi = 2\varphi + \alpha,$$
$$\theta = \psi + \alpha,$$

where

ψ = angular diameter of O_1 seen from a_1
α = angular diameter of a_1 seen from O_1
2φ = angular diameter of the sun (0.0094)
θ = angular diameter of area of sky covered by O_2, or angular diameter of O_2 seen from l_1.

If we let O_1, O_2 and a_1 represent diameters; d, the distance between O_1 and a_1; and f_1 the focal length of l_1, we find for the minimum linear

diameters of the occulting disks:

$$O_1 = 2\varphi d + a_1$$

$$O_2 = 2f_1\left(\varphi + \frac{a_1}{d}\right).$$

As the diameter of O_1 and O_2 are made slightly larger than these minima, the instrumental adjustment naturally becomes less critical.

A rather rough experimental study indicates that when the instrument is properly adjusted and clean, the HAO photometer still has detectable scattered light superposed on the image of the sky. It amounts to about 1 millionth of the brightness of the sun, and appears to originate in the rather serious surface imperfections in the objective lens, l_1. The scattered light could presumably be reduced to a fraction of its present level by use of an undamaged lens, or better, a specially polished lens similar to the lens of a coronagraph.

The accuracy of the photometer in its present form is not high, but is quite adequate for its intended use. The accidental mean error of repeated settings is about ± 5 percent for most observers. Personal differences between observers usually appear smaller than the accidental errors of an individual observer.

The systematic errors of the sky photometer depend largely upon the method and accuracy of calibration. If the density curve of the wedge is measured independently and combined with r_2, r_m, and t_1 to calculate B, then obviously the accuracy of the result depends upon the precision with which these constants are known. Furthermore, unless the wedge is quite specular, its density curve is dependent on the particular manner in which it is used. In view of the numerous possibilities of error in the determination of the constants, a direct calibration on an artificial sky of controllable brightness is to be recommended if systematic errors are to be reduced to a minimum.

Because of the excellent performance of its visual photometer, the HAO now has a photoelectric instrument under construction. It will use the same type of optical system for the elimination of scattered light and is designed to be mounted equatorially, either on a mounting of its own or on a telescope. It will keep a continuous record of sky brightness on a Micromax recorder.

Fourth Annual Analytical Symposium and Exposition of New Analytical Tools in Pittsburgh

The Fourth Annual Analytical Symposium sponsored by the Analytical Division of the Pittsburgh Section of the American Chemical Society will be held at the Hotel William Penn on January 20 and 21, 1949. Some seventeen addresses have already been scheduled, and discussion periods will follow these. Those interested in obtaining separate copies of the complete program and abstracts, which will be printed early in January in Chemical and Engineering News, should write to Dwight L. Deardorff, Mellon Institute, Pittsburgh 13, Pennsylvania.

JOURNAL OF THE OPTICAL SOCIETY OF AMERICA VOLUME 38, NUMBER 12 DECEMBER, 1948

An Infra-Red Chopped-Radiation Analyzer*

GILBERT KIVENSON, RALPH T. STEINBACK, AND MYRTLE RIDER
Mellon Institute, Pittsburgh, Pennsylvania

(Received May 20, 1948)

A design is presented for a double-beam infra-red analyzer that utilizes the chopped-light principle. The advantages of this instrument are low rate of drift at high sensitivities, freedom from the effects of ambient temperatures, and general ruggedness, all of which make the system adaptable to plant analytical and control problems. The receiving system consists of a thermistor bolometer and tuned amplifier. Performance data are given for the butadiene recycle impurity system of a GR-S synthetic rubber plant stream.

INTRODUCTION

WITH the lapse of military demands on the synthetic rubber industry, more thought has been given by the GR-S plants to precision quality control and the utilization of recently developed instrumentation. Significant among the types of instruments considered was the double-beam infra-red analyzer.[1-3] Sensitive, rugged, and adaptable to recording and control, it seemed a likely device for analyzing several important streams in synthetic rubber production. Investigation of commercial instruments available at the time, however, revealed that extensive changes (both optical and electronic) would have to be made in each type before it would be suitable for this problem. After discussing the matter with Philips Laboratories, Irvington, New York, it was decided to build an experimental model that would contain apparently desirable features, make tests with various synthetic mixtures, and evaluate the components of the design in terms of constructing a final laboratory instrument. In the meantime, arrangements were concluded with Philips for the design and construction of a plant-type instrument, to be used on the actual streams. It is the purpose of this paper to describe the design finally used for the experimental bench model, because this instrument is sufficiently different from the Philips plant model to be of general interest.

* This development is part of the program sponsored by the Office of Rubber Reserve, Reconstruction Finance Corporation, and has been approved by that office for publication.

[1] H. Schmick, U. S. Patent No. 1,758,088.

[2] N. Wright and L. W. Hercher, J. Opt. Soc. Am. **36**, 198 (1946).

[3] W. G. Fastie and A. H. Pfund, J. Opt. Soc. Am. **37**, 762 (1947).

A. PRELIMINARY CONSIDERATIONS

One of the streams, the analysis of which is desired, is that carrying recycle butadiene from the polymerization units. This material is blended with high purity butadiene and re-entered into the process. A typical analysis of recycle butadiene[4] is as follows:

	Percentage
Butadiene	75.0
Isobutene	6.0
Isobutane	0.3
Butene-1	9.8
Butene-2 (low boiling)	8.2
Butene-2 (high boiling)	0.2
Normal butane	0.5

A sample of this stream (which is liquid) could be periodically vaporized and passed through an infra-red analyzer or the liquid could be sent directly to an instrument equipped with thin absorption cells capable of withstanding pressures of 50 to 60 pounds per square inch.

Owing to the range in which the desired analysis occurs, the over-all sensitivity of any infra-red analyzer would need to be rather high. This fact is evident from the slope of calibration curves of this type of instrument.[4] The shape of the signal output *versus* concentration curve decreases rapidly as concentrations greater than about ten percent are reached. The proper choice of filter materials tends to decrease the change in slope (greater selectivity), but does so at the expense of sensitivity. Figure 1 illustrates typical curves obtained with two cell arrangements. In curve 1, the butadiene is determined directly while in curve 2 the butenes and saturates are

[4] National Bureau of Standards Report No. 46-06-09, June 14, 1946.

determined, the butadiene being obtained by difference.

Instrument drift and non-reproducibility caused by ambient temperature changes, amplifier characteristics, electrical pick up, etc., must be reduced to a minimum if these lower sensitivity measurements are to be made. The over-all accuracy desired by the rubber plants in the 75 percent butadiene range is ± 0.2 percent.

B. GENERAL DESCRIPTION OF APPARATUS

The analyzer has been constructed on an optical-bench principle to allow maximum flexibility in the moving and replacement of components. Sources, absorption cells, detectors, and mirrors can be moved horizontally or vertically on stainless steel rods and can be clamped at any desired position. Figure 2 is a perspective view of the apparatus. The source consists of a Chromel ribbon wound into a spiral cone, one inch long and three-eighths of an inch wide at the base. The cone is fastened into a steel tube, which in turn is silver-soldered inside a larger brass tube. The annular space serves as a cooling water jacket. Cooling water at the rate of 150 cc per minute is supplied from a constant head tank. The leads, which are connected to opposite ends of the cone, leave at the rear of the source housing. A Chromel-Alumel thermocouple, placed inside the apex of the cone, permits estimation of over-all source temperature. The turns of the Chromel ribbon cone are electrically and thermally insulated from the inner brass tube by means of a layer of Alundum cement. At a potential of 14 volts a.c., the power requirement is 75 watts, the temperature at the apex of the cone being 730 degrees Kelvin. A one-kilowatt Sorensen voltage regulator, operating through a Variac, makes possible a wide range of source temperatures. This arrangement, originally designed to give approximate blackbody conditions[5,6] and to provide flexibility in testing, proved to be more stable and less noisy than the Globar and Nernst glowers tried later. Of materials used in the cone, Chromel had much greater stability than either Nichrome or tungsten.

The radiation leaving the source (Fig. 2) is divided by two front surface concave mirrors and focused back on two chopper blades. The beams then traverse the absorption cells and are refocused onto a single Thermistor bolometer. The chopping system is so arranged as to give alternate pulses of 33 milliseconds' duration at the rate of 15 per second in each beam. The bolometer is thus alternately illuminated by one beam and then the other.

Micrometer-driven light trimmers are placed in each beam to enable balancing of the optical paths.

The cells shown in Fig. 2 are made of one-eighth-inch brass plate. The window material is silver chloride cemented to the brass with Glyptal. A Cellophane washer inserted between the silver chloride and the cell body prevents corrosion of the brass. The windows are painted, prior to cementing, with a dilute solution of gilsonite in benzene to reduce solarization.

Figure 3 is a view of the completed optical bench showing the source, choppers blades, gas manifold system, and thermistor bolometer. The

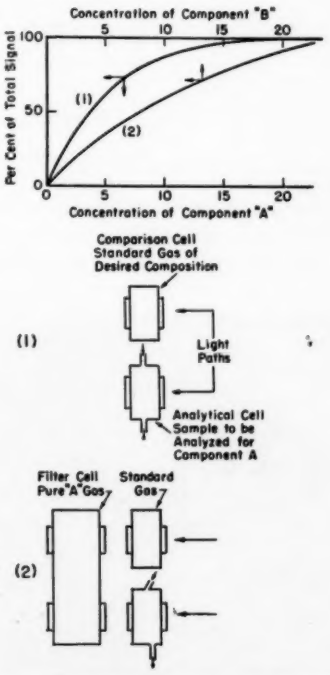

FIG. 1. Typical cell arrangements and the corresponding calibration curves.

[5] C. E. Mendenhall, Astrophys. J. **33**, 91 (1911).
[6] A. G. Worthing, Phys. Rev. **25**, 846 (1925).

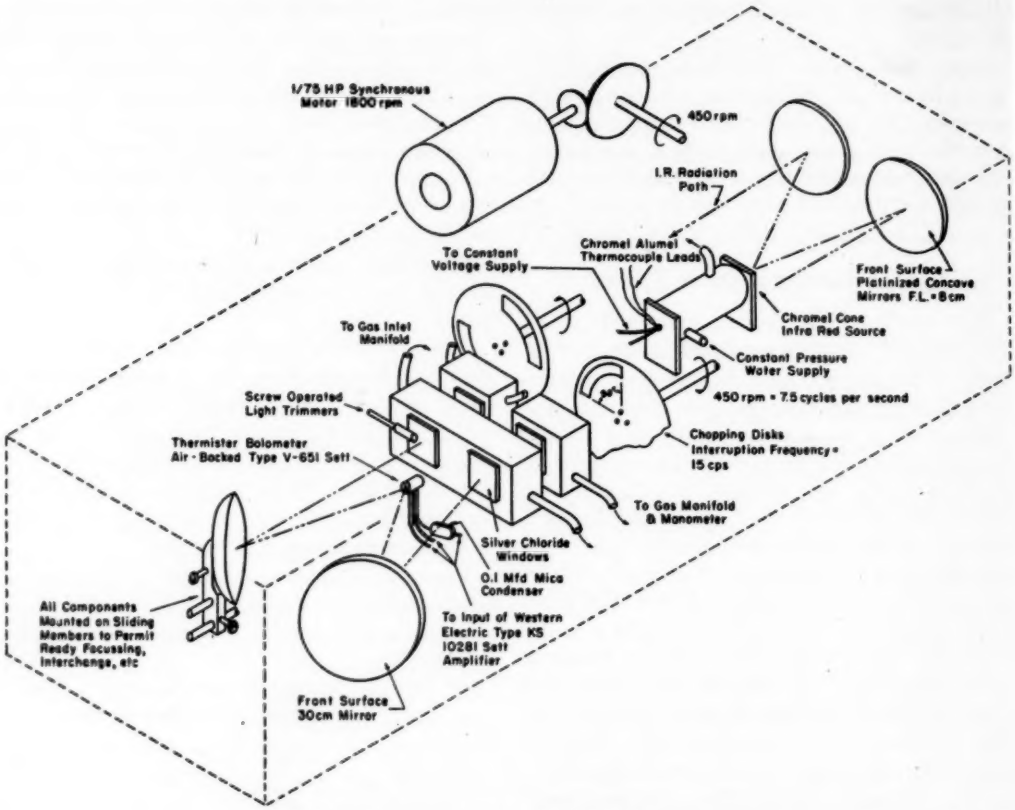
1/75 HP Synchronous Motor 1800 rpm
450 rpm
I.R. Radiation Path
To Constant Voltage Supply
Chromel Alumel Thermocouple Leads
Front Surface Platinized Concave Mirrors F.L. = 8 cm
Chromel Cone Infra Red Source
To Gas Inlet Manifold
Constant Pressure Water Supply
Screw Operated Light Trimmers
450 rpm = 7.5 cycles per second
Thermister Bolometer Air-Backed Type V-651 Sett
Chopping Disks Interruption Frequency = 15 cps
To Gas Manifold & Manometer
Silver Chloride Windows
0.1 Mfd Mica Condenser
All Components Mounted on Sliding Members to Permit Ready Focussing, Interchange, etc
To Input of Western Electric Type KS 10281 Sett Amplifier
Front Surface 30cm Mirror

FIG. 2. Optical system of infra-red double-beam analyzer.

plane mirror arrangement presented in Fig. 3 was used in the earlier work but was replaced by concave mirrors for greater light efficiency.

FIG. 3. Over-all view of analyzer with top removed.

C. THERMISTOR BOLOMETER AND AMPLIFIER

The bolometer is an air-backed type V-651 Thermistor made by Western Electric.[7] It has a time constant of 65 milliseconds that matches the interruption frequency. Its active area is 5 mm by 0.5 mm and it is 10 microns thick. The amplifier used is a Western Electric type KS-10281, tuned to 15 cycles. The band width was determined by the use of an audiosignal generator. The curve obtained is presented in Fig. 4. The width at amplifier band width at 50 percent response is ± 3.5 cycles.

The Thermistor bolometer was found, in agreement with the observations of other users,[8]

[7] W. H. Brattain and J. A. Becker, "Thermistor bolometers," presented at the Winter Meeting of the Optical Society of America, March 7–9, 1946, Cleveland, Ohio.

[8] L. W. Gildart, "An investigation of the comparative merits of the Thermistor-a.c. amplifier system and the thermocouple-galvanometer system," Final report sub-

to be microphonic and to be subject to electrical and magnetic fields. In order to keep change-over noise in the chopping system to a minimum, single aperture interrupter disks were first used. The 15-cycle vibration set up by these disks and their shafts produced a microphonic signal of the tuned frequency, thus reducing the signal to noise ratio. By changing the gear system and using disks with two apertures, the microphonic signal was limited to frequencies of 7.5 and 30.0 cycles, thus considerably decreasing the noise. The connection from the Thermistor to the amplifier was placed in a rigid metal conduit and the latter carefully grounded. Magnetic pick-up was reduced by physical isolation but later eliminated almost completely by proper shielding.

The equivalent circuit of the bolometer as used in this instrument is illustrated in Fig. 5. If *A* and *B* represent the two beams illuminating the bolometer, it can be seen that no change in output signal would theoretically be observed when both are equal. The change-over time, however, between the two sets of blades provides an interval in which both beams are either shut off or passing through the cells at once. This produces an undesired signal at each pulse. The "background noise" originating in this manner depends on the design of the optical system and chopper blades. The changeover signal is of 30-cycle frequency and at an amplifier voltage gain of approximately 93 (determined by a 15-cycle standard signal) amounts to about 3.5 millivolts. The signal obtained at this gain by completely blocking one beam is 408 millivolts, this corresponding, of course, to a decrease of 50 percent in the total energy reaching the bolometer per cycle. From the sensitivity rating figures of the bolometer this would mean a decrease of 92.5 microwatts in radiant energy per cycle and represents the total signal available for analytical purposes in the instrument at a source temperature of 730 degrees Kelvin. Under these conditions the minimum detectable concentration change is one that will decrease the intensity of one beam by 0.9 percent. Since the noise level is almost independent of source temperature, it was possible to raise the latter until an experimentally determined sensitivity was reached such that a concentration change of 0.2 percent of butadiene in the 75 percent range was detectable. This temperature was approximately 960 degrees Kelvin. Figure 6 is a temperature sensitivity curve made with butadiene synthetics. The method will now be described.

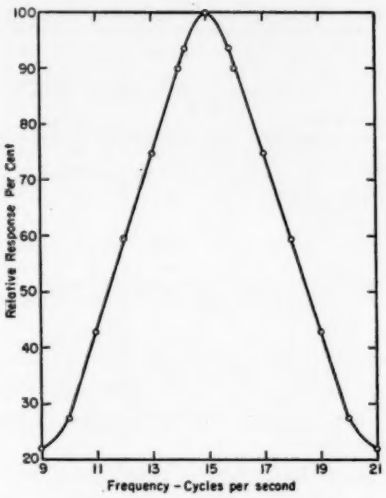

FIG. 4. Band pass characteristic curve of the tuned amplifier.

D. INSTRUMENT PERFORMANCE

The total drift was three percent of full scale in 12 hours when the sensitivity was set so that 100 percent butene-1 in both beams gave a zero reading and 100 percent butadiene in one beam and 100 butene-1 in the second gave full-scale deflection (220 small divisions). Figure 7A is a chart record showing the drift under these conditions.

The over-all energy sensitivity during this run was 47.8 microvolts/microwatt. Figure 7B

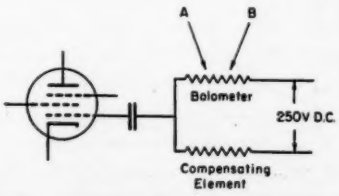

FIG. 5. Equivalent bolometer circuit.

mitted by E. F. Barker, Technical Representative, N.D.R.C. Contract OEMsr-1132, University of Michigan, Ann Arbor, Michigan—PB 27342.

TABLE I. Comparison of silver chloride and quartz cell windows.* Source temperature 960°K.

Impurity in binary	Percent Impurity in binary	Deflections (equivalent percentage butadiene concentration change) Silver chloride windows	Quartz windows
Isobutene	24.6	5.7	0.9
Isobutane	24.6	1.4	3.0
Butene–1	24.6	1.3	0.4
Butene–2 (low boiling)	24.6	4.5	0.2
Butene–2 (high boiling)	24.6	8.9	0.2
Normal Butane	24.6	1.1	2.4

* Cell arrangement: butadiene (99.8 percent, 720 mm-Hg) across both beams in filter cell, recycle butadiene (75.4 percent, 720 mm-Hg) in one beam and blended binary (75.4 percent, 720 mm-Hg) in the other.

shows the drift and noise at a sensitivity of four times the previous value. Although the noise has increased, the drift is still of the same magnitude.

Owing to the failure of Beer's Law in this type of arrangement, calibrations were made empirically over relatively narrow ranges and a linear relationship was assumed. As it is planned to use the final instrument at sensitivities of one percent butadiene concentration change to give full-scale deflection, a linear output *versus* concentration curve can be considered sufficiently accurate. In the 75 percent butadiene range, for instance, two samples differing in butadiene concentration by two percent were compared in the two beams. Using pure butadiene in the filter cell, the deflection divided by two gives an average sensitivity in terms of deflection per percentage of concentration change. These values are the ordinates in the temperature-sensitivity curve in Fig. 6.

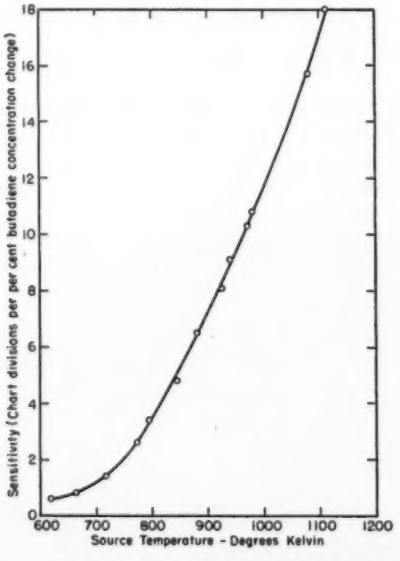

FIG. 6. Showing the relationship between average source temperature and the sensitivity (silver chloride windows).

To study the effect of interfering substances on the over-all accuracy of analyses, actual samples of the plant recycle stream were obtained over a period of time, mixed, and analyzed chemically for butadiene. Synthetic mixtures containing one impurity each were blended to the exact butadiene content of the plant sample. The instrument was nulled with the plant material in the analyzing and comparison cells and with butadiene in the large filter cell. The analyzing cell was then evacuated and the synthetic introduced. The deflection thus obtained, divided by the pre-determined sensitivity, gave values that enabled estimation of the interference effect of the particular impurity used in that synthetic. This would amount to the total possible error of the analysis if the impurities in the plant stream were to vary so that any one predominated and the other became vanishingly small. Since, in plant application of this type of instrument, calibrations will be made with materials containing all the impurities (in their representative amounts), the figures obtained in the comparison work would represent extreme conditions and thus serve as a criterion for laboratory testing. Runs were made using silver chloride, calcite, quartz, and Pyrex cell windows. Of these, the quartz was found to give the lowest average deflection for the impurities. Table I records representative results obtained for silver chloride and quartz.

It is to be noted that the two highest deflections (for quartz windows) are obtained with isobutane and normal butane, materials that are present in comparatively small amounts in the plant stream. These tests establish the over-all feasibility of the analysis. Long-term plant tests will be required, however, to determine the accuracy of the method.

In addition, work has also been done on styrene-butadiene mixtures in the 70 percent butadiene range, using thin high pressure cells de-

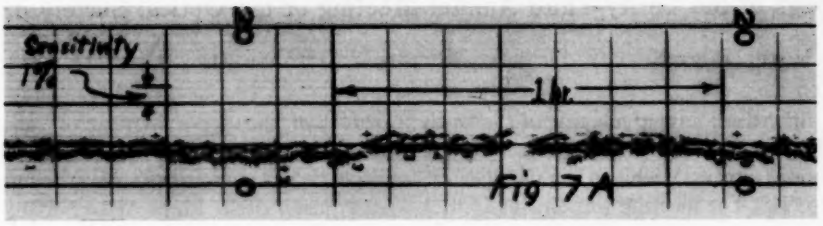

A.

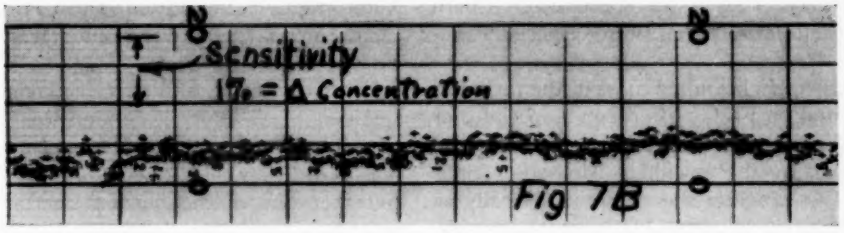

B.

FIG. 7. Typical recorder charts of sensitivity drift studies.

veloped for this purpose. The results of these experiments will be published.

E. RECOMMENDATIONS

A much greater signal-to-noise ratio is obtainable in this instrument by means of a synchronized rectifier of the commutator or generator type. Such an arrangement in the output can be phased to eliminate much of the change-over signal, thereby making the thermal noise of the bolometer instead of the changeover signal the absolute limit of detection. This improvement is being incorporated in the commercial instruments.**

The amplifier used in this work did not have as narrow a pass band as was originally expected. Therefore the signal-to-noise ratio could also be somewhat improved by sharpening the tuning.

For plant use it seems desirable to incorporate a convenient means for introducing a standard sample in the analyzing chamber to permit zero adjustments to be made if necessary.

F. CONCLUSIONS

A sensitive infra-red laboratory gas analyzer has been designed utilizing chopped radiation and a high speed bolometer. Its low rate of drift and excellent stability make it suitable for much plant analytical survey work. The electrical characteristics of the instrument would permit adaptation to recording and control, and it should find application in a variety of industrial fields. The ultimate practical sensitivity exceeds by a factor of 4 that obtained in the author's laboratory with steady radiation instruments.

G. ACKNOWLEDGMENTS

The authors wish to express appreciation to Albert Roth for his cooperation, to Dr. O. G. Koppius, Philips Laboratories, Inc., for advisory aid, and to Dr. E. E. Stahly and Dr. O. W. Burke, Jr., for their many helpful suggestions and constant encouragement.

** Philips Laboratories, Inc., Irvington, New York (private communication).

Proceedings of the Thirty-Third Annual Meeting of the Optical Society of America

HOTEL FORT SHELBY, DETROIT, MICHIGAN, OCTOBER 21, 22, AND 23, 1948

THE thirty-third annual meeting of the Optical Society of America was held in the Fort Shelby Hotel, Detroit, Michigan, on October 21, 22, and 23, 1948. The meeting was unusually well attended, the registration being approximately 550. The number of papers, 76, broke all previous records. Papers on spectroscopy, both emission and absorption, were especially numerous.

Invited papers keynoted most of the technical sessions, and on Friday afternoon a special program of invited papers was presented in a general session held at the Rackham Memorial Auditorium. This program was announced locally as being open to the public and attracted many nonmembers. The estimated attendance was 800. One high point of this general session was a beautifully executed demonstration of a new method of graphic reproduction, "xerography," developed jointly by the Battelle Memorial Institute and the Haloid Company.

An exhibit of optical instruments was held in conjunction with the meeting. Ten companies participated, resulting in a very representative showing of spectroscopic equipment, together with instruments in the color and x-ray fields.

A unique feature of the meeting was the plant-visit program, offered to members on October 20, the day before the meeting started. Members had their choice of visiting twenty-two laboratories and plants in the Detroit area. The work shown in these laboratories covered a wide range of interests. Nearly 100 visitors participated in this pre-meeting program.

The annual dinner attendance was 365. The principal address was by Dr. C. F. Kettering of the Research Laboratories Division of General Motors, who spoke on the importance of optics in the future conservation of our resources of stored energy. The dinner program was also the occasion of the presentation of the Adolph Lomb Medal for 1948 to David S. Grey of the Polaroid Corporation.

A few special features of the meeting appealed particularly to the members. Arrangements were made to keep the members in each session informed of the paper in progress at the simultaneous session. Lists of registrants were mimeographed and made available to members at the registration desk. Maps of the area around the hotel were distributed, and chartered buses conveyed the group to and from the Rackham Auditorium. By invitation, Dean Harrison and Dean Sawyer spoke over radio station WJR at 10:30 A.M. on Saturday.

The enthusiastic and effective cooperation of members of the Detroit Section was largely responsible for the unusual success of the meeting. It is hoped that this is a sign of things to come, and that one of the benefits accruing to the national society from its newly organized local sections will be a continually improving tone and vigor of its technical meetings. At the invitation of Professor Ballard, representatives of the local sections met together on Thursday evening to discuss questions of mutual interest.

BUSINESS SESSION

A business session was held on Friday afternoon, President Kingslake presiding. The reports of the Secretary, Treasurer, and Editor of Publications for the fiscal year 1947 were presented and accepted. The President announced that the next meeting of the Society would be held at the Hotel Pennsylvania, New York, New York, on March 10, 11, and 12, 1949, and that the annual meeting would be held at the Hotel Statler, Buffalo, New York, on October 27, 28, and 29, 1949.

CONTRIBUTED PAPERS

The abstracts of the contributed papers are appended.

MEETING OF THE BOARD OF DIRECTORS

A meeting of the Board of Directors was held on Wednesday, October 20. The minutes of this meeting appear on page 1107 of this issue.

G. M. RASSWEILER, *Vice-Chairman*
Program Committee

Program of Sessions

Titles and Abstracts of Papers

1. Invited paper, entitled "A Classification of Color Order Systems," BY CARL E. FOSS, *Princeton, New Jersey.*

2. Comparison of Color Systems with Respect to Uniform Visual Spacing. ROBERT W. BURNHAM, *Eastman Kodak Company.*

The present study is a comparison of ten systems of color specification, for a restricted chromatic area around the neutral at a single luminance level, with respect to their relative adherence to uniform visual spacing. A sample of 20 visually equi-spaced (Munsell renotation) chromaticities at the same luminance were used. Chromatic coordinates for these colors were expressed in each of the ten systems and plotted in their respective chromaticity diagrams. Then all data were reduced to the same scale, after which radial saturation distances and hue angles were compared to those in the Munsell renotation criterion. Rank orders of departure from the criterion were determined for hue and saturation separately, and a mean rank obtained by combining the two ranks for each system. Results are limited by the approximate nature of the empirically determined visual criterion, by the limited chromatic area involved in the study, by the applicability of the present results only to large color differences, by the fact that straight-line radial saturation distances and hue angles must be treated separately, and by all of the unknowns involved in measuring color distances which do not fall along radii or which do not lie in a single plane; the non-Euclidean nature of visual space is recognized.

BIBLIOGRAPHY: S. M. Newhall, D. Nickerson, and D. B. Judd, "Final report of the O.S.A. subcommittee on the spacing of Munsell colors," J. Opt. Soc. Am. **33**, 385 (1943).
D. Nickerson, "Interrelation of color systems," Tech. Assn. Pap. 472 (1947).

3. Visual Sensitivities to Combined Chromaticity and Luminance Difference. W. R. J. BROWN AND D. L. MACADAM, *Kodak Research Laboratories.*

In order to determine the noticeability of color differences in the complete, three-dimensional, I.C.I. frame of reference, about fifteen thousand color matchings have been made by two observers. Silberstein[1] has shown that data from three-color matchings may be used to compute the noticeability of any color change (e.g., any combination of dominant wave-length, purity, and luminance variations) from a central color. For this purpose color matchings were made at thirty points in the chromaticity diagram. Each chromaticity was investigated at a single level of luminance. The levels for the several chromaticities were between one-half and ten foot-lamberts.

The matchings were made on a three-color, additive-mixture colorimeter. The visual field subtended an angle of two degrees at the eye. The surrounding field was not illuminated. The primaries were produced by placing Wratten filters 48, 58, and 25 in three separate beams from tungsten lamps.

The results are represented by small ellipsoids surrounding each color center. The length of the radius vector in any direction is the standard deviation of color matching in that direction. The ellipsoids vary in size and orientation throughout the color domain, each figure being defined by the coefficients of the normal equation of an ellipsoid. These coefficients were calculated for each of the thirty color centers, using Silberstein's corrected formulas.[2]

[1] L. Silberstein, Phil. Mag. **37**, 126 (1946).
[2] L. Silberstein, Phil. Mag. **39**, 82 (1948); J. Opt. Soc. Am. **38**, 71 (1948).

4. A Comparison of Direct Colorimetry of Titanium Pigments with Their Indirect Colorimetry Based on Spectrophotometry and a Standard Observer. DEANE B. JUDD, *National Bureau of Standards.*

It has recently been reported by Jacobsen[1] that the I.C.I. standard observer[2] weighs too lightly the spectral region below 430 mμ to accord with visual perception by average observers. This report agrees with two previous results, one an indirect indication from chromaticity-sensibility data,[3] the other a direct indication from the foveal thresholds determined by Wald.[4] Since Jacobsen's results are open to other interpretations[5] than that given by him, a further study of the colorimetry of titanium pigments has been made. Four of the seven observers used checked Jacobsen's report; three checked closely the standard observer. A modified standard observer based upon the spectral luminosity determinations of Gibson and Tyndall[6] and Wald[4] has been derived and is shown to account closely for the settings of the group of 4 observers that disagreed with the standard observer. It is concluded that a re-examination of the luminosity function below 460 mμ would be worth while, and that there is some prospect that a true characterization of the average observer for a two-degree field would be adequate as a basis for technical standardization even though technical color matches customarily refer to visual fields subtending considerably more than two degrees.

[1] A. E. Jacobsen, "Non-adaptibility of the I.C.I. system to some near-whites which show absorption in the far-blue region of the spectrum," J. Opt. Soc. Am. **38**, 442 (1948).
[2] Proceedings of the 8th Session, Commission Internationale de l'Eclairage, Cambridge, England, pp. 19–29 (1931).
[3] D. B. Judd, "A Maxwell triangle yielding uniform chromaticity scales," J. Research Nat. Bur. Stand. **14**, 50 (1935); J. Opt. Soc. Am. **25**, 31 (1935).
[4] G. Wald, "Human vision and the spectrum," Science **101**, 653 (1945).
[5] A. C. Hardy, "The applicability of Judd's color tolerance formula in the case of titanium pigments," J. Opt. Soc. Am. **38**, 650 (1948).
[6] K. S. Gibson and E. P. T. Tyndall, "Visibility of radiant energy," Sci. Pap. Bur. Stand. **19**, 74 (1923).

5. Optical Measurements of Light Scattering Liquids. J. L. SAUNDERSON AND E. W. PETERSON, *Spectroscopy Laboratory, The Dow Chemical Company.*

A method based upon the two constant theory[1] is described for measuring the reflectance of liquids con-

taining suspended pigments. The method involves reflectance measurements for two thicknesses of the sample, one of which is a thickness for which the sample is essentially opaque.[2] Surface corrections and certain geometrical corrections applicable to the G.E. recording spectrophotometer, as well as the appropriate Kubelka and Munk formulas, are discussed. Applications include calculation of the changes in pigment concentrations required in matching a standard.

[1] P. Kubelka and F. Munk, Zeits. f. tech. Physik **12**, 593 (1931).
[2] J. L. Saunderson, J. Opt. Soc. Am. **32**, 727 (1942).

6. The Diffusion of Light by Ground Glass, with Special Reference to Color Changes. W. E. KNOWLES MIDDLETON AND F. D. SMITH,* *National Research Council of Canada.*

By special methods of grinding it has been found possible to make reproducible ground-glass surfaces. A series of six surfaces of increasing roughness was produced in crown glass, and a similar series in flint. These were illuminated at normal incidence by 2850° light in a photoelectric goniophotometer and intensity was measured at various angles. The apparent color-temperature of the light diffused at each angle was also measured photoelectrically, with visual checks at some angles. Photomicrographs were taken of some of the surfaces, and finally the recording spectrophotometer was used to measure the diffuse reflectance, diffuse transmittance, and transmittance over a half-angle of about 8°, of several glasses. Some sandblasted samples were also studied. The transmitted light is most reddish near 0°, while at angles of more than 60° most of the glasses raise the apparent color-temperature of the light. With the most finely ground glasses the color-temperature at 0° reaches 2300°K. Some theoretical studies lead to the belief that most of the color changes are due to scattering, while diffraction plays a minor part.

* Now at the University of Rochester.

7. Accuracy, Precision, and Stability of New Photoelectric Color-Difference Meter. RICHARD S. HUNTER, *Henry A. Gardner Laboratory, Inc.*

At the March, 1948, meeting of the Optical Society, a photoelectric tristimulus color and color-difference meter was described. This new instrument measures 45°, 0° values of surface color directly on three scales: R_d (reflectance), a (redness when plus, 0 when gray, greenness when minus), b (yellowness when plus, 0 when gray, blueness when minus). Equations relate these three scales to the I.C.I. standard scales for color. To determine the accuracy of this new instrument, results from it were compared with values of color by the spectrophotometer and computation. To determine precision, results from one instrument were compared with those for the same colored panels on two similar instruments, and with results from the same instrument on three other occasions. For these comparisons, the N.B.S. unit of color difference representing the maximum difference tolerable in rather critical commercial color matching was used. The specimens were ten porcelain-enameled panels representing the standardized colors for kitchen and bathroom accessories. The disparities were as follows:

	(N.B.S. units)
Observed *vs.* computed color	3.9
Between 3 instruments (white std.)	2.5
Between 4 sets data (white std.)	0.8
Between 3 instruments (colored stds)	0.6
Between 4 sets data (colored stds)	0.2

8. Report on Paris Meeting of the International Commission on Illumination, July, 1948. DEANE B. JUDD, *National Bureau of Standards.*

9. Invited paper, entitled "Recent Work on the Theory of Polyatomic Molecules," BY E. BRIGHT WILSON, JR., *Harvard University.*

10. The Flame Spectrum of Acetylene from 1 to 5 Microns. CURTIS J. HUMPHREYS AND EARLE K. PLYLER, *National Bureau of Standards.*

The spectrum of an acetylene-oxygen flame obtained with a welding torch has been observed and measured using a Perkin-Elmer spectrometer, with a LiF prism. Bands were observed at 1.2, 1.3, 1.52, 1.85, 2.0, 2.3, 2.48, and 2.8μ, which agree in position and general appearance with bands originating in the methane flame, except for newly observed bands at 1.5 and 2.3μ. The 1.5-μ-band probably represents the $\nu_1+\nu_3$ combination in the C_2H_2 molecule, and the 2.3-μ-band is probably the R-branch of the $2\nu_1$ band of CO, the P-branch being overlapped by the R-branch of the 2.7-μ-H_2O band. The band at 2.8μ shows fine structure on the long wave-length side consisting of 29 lines between 2.8 and 3.6μ, when a flame of reduced oxygen content is used. With a hot flame obtained with the maximum amount of oxygen, this number is reduced to 12, some of which show good agreement with calculated values for the $2\rightarrow1$ band of OH. On the long wave-length side of the intense CO_2 emission band at 4.48μ, 27 rotational lines have been observed, some of which agree closely with the rotational absorption lines of the CO fundamental. This structure was also observed in the methane-oxygen flame.

BIBLIOGRAPHY: (1) Earle K. Plyler, "Infrared radiation from a Bunsen flame," J. Research Nat. Bur. Stand. **40**, 113 (1948), RP 1860.
(2) Earle K. Plyler and Curtis J. Humphreys, "Infrared emission spectra of flames," J. Research Nat. Bur. Stand. **40**, 449 (1948), RP 1890.

11. Infra-Red Absorption of Atmospheric Gases.* M. V. MIGEOTTE AND R. M. CHAPMAN, *Mendenhall Laboratory of Physics, Ohio State University.*

The solar spectrum has been examined under high dispersion, from 2μ to 13μ, using a recording prism-grating spectrometer of the Pfund type designed and built in this laboratory. The spectra have been compared with those of gases obtained in the laboratory under controlled conditions. The resolution of the solar spectra was sufficient to establish definitely the identity of several of the constituents of the earth's atmosphere, in particular N_2O and CH_4. A careful search has been made in the

region of the intense NH_3 fundamental band near 10μ. No evidence, whatever, was obtained of absorption by NH_3.

* This work performed under U. S. Army Research Contract N-33-038-ac-14485.

12. The Infra-Red Absorption Spectra of Some Benzene Derivatives. EARLE K. PLYLER, *National Bureau of Standards.*

The infra-red absorption spectra of fourteen benzene derivatives in the liquid state have been measured to 38μ. The main emphasis has been placed on the region from 15 to 38μ. By the use of a thallium bromide-iodide prism the region from 22 to 38μ was measured with cells up to 2 mm in thickness. Bands were observed in mesitylene at 30.0 and 36.4μ, in toluene at 28.7μ. Also bands were observed in chlorobenzene at 24.1 and 33.7μ, in bromobenzene at 22.2 and 31.9μ, and in iodobenzene at 22.2μ. In *o*-bromoanisole the bands appeared at 22.9, 30.5, and 35.8μ, and in *p*-bromoanisole at 30.8 and 37.9μ. The absorption spectra of six other benzene derivatives containing methyl and ethyl groups have been observed. Data will be presented on the absorption spectra in the region from 2 to 15μ for some of these compounds.

13. The Infra-Red Spectra of Normal Propane, 1-Deuteropropane, and 2-Deuteropropane. H. L. MCMURRY, V. THORNTON, AND F. E. CONDON, *Phillips Petroleum Company.*

The infra-red spectra of very pure normal propane, 2-deuteropropane and 1-deuteropropane have been obtained using a Perkin Elmer model 12B spectrometer. The spectrum of normal propane exhibits the same features reported by Wu and Barker, with the important exceptions that the sharp bands found at 720 cm^{-1} and 1179 cm^{-1} in their work are absent in the present spectrum. These bands must be foreign to propane. The data show unambiguously that the propane frequencies at 748 cm^{-1} and 1052 cm^{-1} arise from motions of the CH_2 group. These bands are strongly modified in 2-deuteropropane and much less so in 1-deuteropropane. The work of Sheppard and Sutherland, and of Jones and Sutherland, has already established the 748-cm^{-1} propane band as caused by a rocking of this group about an axis in the C_3 plane and normal to the molecular symmetry axis.[1] The shape of the 1052-cm^{-1} propane band and its behavior in the deuteropropanes show it to be due to the wagging of the CH_2 about an axis normal to the C_3 plane. While the other propane frequencies cannot be assigned so unambiguously, possible improvements over previous assignments will be discussed. Assignments for the bands in the deuterated propanes will also be discussed.

[1] N. Sheppard and G. B. B. M. Sutherland, Nature **159**, 739 (1947); V. Jones and G. B. B. M. Sutherland, Nature **160**, 567 (1947).

14. Infra-Red Spectra of Alcohols. C. W. YOUNG, *Dow Chemical Company.*

The infra-red absorption spectra of a number of alcohols are analyzed using a double beam sodium chloride spectrometer with particular attention to frequencies associated with bending motions of the hydroxyl group. The corresponding deuteroxyl compounds of some of the alcohols are also investigated in order to distinguish the hydroxyl frequencies from those due to other modes of vibration. The effect of dilution on the associated bands is considered, and characteristic differences are pointed out among primary, secondary, and tertiary alcohols.

15. Practical Aspects of the Preparation and Application of an Infra-Red Bibliography. J. D. STROUPE, A. G. KNOX, AND J. F. WOODMAN, *Rohm and Haas Company.*

For the efficient application and development of infra-red spectroscopy the extensive original literature must be made readily available by means of a bibliographic system. It is particularly necessary to devise a satisfactory means for recording, filing, and making effective use of infra-red absorption spectra. The Key-sort system of Tingey and Hampton[1] seems best designed to fill this need. It is the purpose of the present paper to describe the practical aspects of planning, preparing, and applying a two-card infra-red bibliography of similar type. Beginning with the planning of the body and coded contents of both "abstract" and "compound" cards, the outline of the project will discuss the important matters of personnel and time required for the preparation of the bibliography and for its maintenance, growth, and application. The results of experience in the use of an empirical formula index, the representation of literature spectra on "compound" cards, and the performance of a suitably coded and punched spectral frequency field in correlation and identification work will be discussed.

[1] H. C. Tingey and R. R. Hampton, J. Opt. Soc. Am. **37**, 984 (1947).

16. The Bezold-Brücke Phenomenon and the Hering Theory of Vision. DEANE B. JUDD, *National Bureau of Standards.*

If two spots of light of identical spectral character, such as to yield chromatic color perceptions but of different luminance, be compared, the observer will, in general, report that the hues of the color perceptions are different. The brighter of two such yellowish red spots appears more yellowish; that of two such yellowish green spots, also more yellowish; and, similarly, bluish red and bluish green tend toward blue with higher luminance. This effect is called from its discoverers the Bezold-Brücke[1] phenomenon. Hering[2] pointed out long ago that his theory of vision with its antagonistic response pairs red-green and yellow-blue is suited to qualitative explanations of this phenomenon. The explanation proposed here is that the blue-yellow response pair is more stable at high luminance than the red-green. By using the I.C.I. standard observer expressed in a Hering coordinate system,[3,4] it is possible to make this explanation quantitative. Purdy's[5] data on spectral hue as a function of retinal illuminance have been closely duplicated by assuming simply that the red-green

responses are reduced by 40 percent compared to the yellow-blue responses for the brighter of two fields (1000 and 100 photons, respectively).

[1] W. von Bezold, "Ueber das Gesetz der Farbenmischung und die physiologischen Grundfarben," Pogg. Ann. **150**, 221 (1873); E. Brücke, "Ueber einige Empfindungen im Gebiete des Sehnerven," Sitz. Akad. Wiss. Wien (3) **77**, 39 (1878).
[2] E. Hering, "Zur Erklärung der Farbenblindheit," Lotos, N.F., 1, 9 (1880).
[3] E. Q. Adams, "X–Z planes in the 1931 I.C.I. system of colorimetry," J. Opt. Soc. Am. **32**, 168 (1942).
[4] D. B. Judd, "Response curves for types of vision according to the Müller theory," J. Opt. Soc. Am. **35**, 805 (1945).
[5] D. McL. Purdy, "Spectral hue as a function of intensity," Am. J. Psychol. **43**, 541 (1931).

17. Variation in Sensitivity among Cones in the Human Fovea, and the Hecht Theory of Visual Acuity. BRIAN O'BRIEN AND E. DICKERMAN O'BRIEN, *Institute of Optics, University of Rochester.*

Increase of visual acuity with brightness has been explained by Hecht by assuming variation of more than 1000-fold in threshold sensitivity among foveal cones. A double star test object was presented for monocular observation in the center of a black disk subtending 15 minutes of arc, and surrounded by a large white adapting field. The stars were separated by 8 minutes of arc and could be resolved easily at all levels of illumination used. Illumination of the surrounding field was steady, but the stars were presented as a single flash of 25 microseconds duration to reduce image drift during flash to less than the diameter of a single cone. By careful refraction of observers, and by artificial pupil, approximately $\frac{3}{4}$ of flux in star image was concentrated in the area of 3 foveal cones. At the surrounding brightness from 0.01 to 100 foot-lamberts, the star illumination necessary for visibility of both stars was never more than twice the illumination at which neither was visible. It is concluded that the small variation among foveal cones here observed is inconsistent with the Hecht theory.

18. A Test of Ocular Tremor and the Scanning Theory of Visual Acuity.* BRIAN O'BRIEN AND E. DICKERMAN O'BRIEN, *Institute of Optics, University of Rochester.*

The possibility that variation of visual acuity with brightness is associated with a scanning motion of the image due to ocular tremor has been discussed in some detail by L. A. Jones and associates. Tremor in voluntary muscle tissue such as the extrinsic ocular muscles is to be expected, but whether this is communicated to motion of the eye in its orbit does not appear to have been demonstrated. A single star test object was presented for monocular observation in the center of a black disk subtending 15 minutes of arc and surrounded by a large white adapting field illuminated steadily. The star was illuminated by a short burst of 10-microsecond flashes. The frequency of flash repetition within a burst was varied from 18 to 240 per second, and the duration of a burst from 1/5 to 1/100 second. In no case were multiple star images visible, indicating that no ocular tremor movement as great as 2 minutes of arc occurred during a burst of flashes. Double star acuity, under single flash ballistic stimulation, was found to be consistently lower than under equivalent steady illumination. These results appear to eliminate involuntary tremor as a factor, but support the belief that voluntary scanning improves acuity.

* A part of this work has been carried out under Contract W33-038-ac-18317 with the Air Materiel Command, Wright Field, Dayton, Ohio.

19. A Standard Luminosity Filter. RAY P. TEELE AND KASSON S. GIBSON, *National Bureau of Standards.*

In 1938 a glass-liquid luminosity filter was described that was satisfactorily reproducible from specification[1] and that would give results of considerable accuracy even for such highly selective distributions as those of the standard railroad signal glasses. The filter was designed for use with a non-selective receiver in a physical photometer. However, the filter transmitted a small amount of radiant energy between 850 and 1200 mμ, totaling from 1 to 2 percent of the total energy transmitted. This necessitated application of an annoying and slightly uncertain correction factor for the most accurate measurements. Recently the American Optical Company has developed a greenish glass which has made possible the elimination of this infra-red energy without destroying the agreement with the standard luminosity factors in the visible. The composition of the new filter is tentatively as follows: 1. *Solution:* $CuSO_4 \cdot 5H_2O$, 17.50 grams; $CoSO_4(NH_4)_2SO_4 \cdot 6H_2O$, 1.80 grams; $K_2Cr_2O_7$, 150 milligrams; H_2SO_4 (sp. g. 1.835), 10 ml; H_2O, distilled, to make one liter of solution. Used in a 5-cm thickness. 2. *Glasses:* Corning No. 3780 or equivalent, transmittance at 486 mμ equal to 0.40 ± 0.01; American Optical Company "heat screen," transmittance at 700 mμ equal to $0.43 \pm .01$. The spectral transmittance of the filter and its components will be illustrated.

[1] Kasson S. Gibson, Ray P. Teele, and Harry J. Keegan, "An improved luminosity filter," J. Opt. Soc. Am. **29**, 144 (1939); see also J. Opt. Soc. Am. **28**, 178 (1938).

20. The Brightness and Altitude of the Luminosity of the Night Sky. E. O. HULBURT, *Naval Research Laboratory.*

Measurements are described of the night sky brightness B observed with visual photometers in Brazil, Bikini, Maryland, and New York State. For clear air, no moon and no aurorae B on the average decreased from about 225 millimicrolamberts at 15° above the horizon to 130 millimicrolamberts at the zenith, in latitudes from −17° to 45°. Some values of B for the Milky Way, the zodiacal light, the Magellanic clouds, and moonlight are given. Effects of starlight are discussed. From the observed curves of brightness against zenith angle, with corrections for atmospheric attenuation and scattering from the calculations of S. L. Piotrowski (Astrophys. J. **106**, 466, 1947), it came out that the altitude of the night sky luminosity was between 300 and 600 km However, the

agreement between theory and observation was not entirely satisfactory, and therefore too great confidence cannot be placed in the value derived for the altitude. It is suggested that further measurements be made at as high altitudes as possible in order to reduce the corrections resulting from attenuation by the lower portions of the atmosphere.

21. Daytime Zenith Sky Brightness at 18,000 to 38,000 Foot Altitudes. D. M. PACKER AND C. LOCK, *Naval Research Laboratory.*

Measurements were made from an Air Force B-29 operated for the Navy out of Inyokern, California. Most of the data were collected during 13 flights, in clear weather, over desert areas of southern California and Arizona. The sky photometer was equipped with a polarizing prism and utilized a 1P22 photo-multiplier tube fitted with a filter correcting the tube response to that of the photopic eye. Observations of the brightness and polarization of the zenith sky were made for solar altitudes from 35° to 75° at 18,000, 27,500, 34,000 and 38,000 feet (pressure altitude) levels. Zenith sky brightness values obtained for the four altitudes were compared with theoretical values based upon the treatment of the problem by Tousey and Hulburt.[1] Agreement between theoretical and observed values was good, considering the experimental conditions, for solar altitudes between 35° and 50°. For solar altitudes greater than 50°, the zenith sky brightness increased, as the sun approached the zenith, at a rate much greater than predicted. Measured polarization factors of zenith skylight were higher than expected for all solar altitudes encountered. No significant change with altitude from 18,000 to 38,000 feet was observed in the polarization.

[1] R. Tousey and E. O. Hulburt, J. Opt. Soc. Am. **37**, 78 (1948).

22. The Relations between Visual Sensitivity and Viewing Distance.* H. RICHARD BLACKWELL, *University of Michigan.*

An extensive but inconsistent literature is available relating various visual abilities and viewing distance. Variables not adequately controlled include: (1) observer refractions; (2) angular size of the stimulus surround; (3) stimulus definition, particularly at distances of only a few feet; and (4) validity of the measured response. To re-examine the effect, various visual capacities were studied at viewing distances of 1.5, 3.0, 7.0, 13.0, and 20.0 feet. Point source detection, extended object detection, and two-point resolution were each investigated at 50 foot-lamberts brightness, utilizing foveal vision. The data in each case showed no significant variation in sensitivity as a function of viewing distance. In contrast, both foveal point source detection and foveal two-point resolution at zero brightness showed a significant loss in sensitivity at the closest distance. This effect is believed to result from stimulus-blurring ocular oscillations which increase as convergence tension increases. Point source detection and two-point resolution were each studied at zero brightness 7° parafoveally. Two observers showed greater sensitivity at the shorter distances, two showed greater sensitivity at the longer distances. These results are believed to result from peripheral refractive errors, such as those reported by Ferree, Rand, and Hardy.

* This work was carried out under the terms of Contract N-5-ori-116, Task Order 5, between the Medical Sciences Division of the Office of Naval Research and the University of Michigan.

BIBLIOGRAPHY: C. F. Ferree, G. Rand, and C. Hardy Arch. Ophth. **5**, 717 (1931).

23. A Study of Methods of Visual Threshold Determination.* H. RICHARD BLACKWELL, *University of Michigan.*

Threshold determinations have become standard procedure for studying mechanism of physiological optics. It was the purpose of this study to compare the degree to which various measurement methods provide threshold values which are independent of variation in procedure, instructions, or observer attitude. Fifteen variations on three basic methods were tested, utilizing a physically identical brightness discrimination situation. The three basic methods involved: (1) Manipulation of the stimulus by the subject to threshold. (2) Adjustment of the stimulus by the experimenter to certain fixed values, at each of which the subject judged whether he had discriminated the presence of the stimulus and responded with "yes" or "no." (3) Adjustment of the stimulus as in (2) above, but with the subject required to make a discrimination of some attribute of the stimulus, such as its spatial position or location in time, the correctness of the discrimination being verifiable by the experimenter.

The results demonstrated that only method (3) above possessed satisfactory validity. A supplementary experiment revealed that the errors involved in method (2), a very common threshold procedure, varied as a function of the value of one physical stimulus variable. Such distortion in the threshold values leads to erroneous inferences concerning the underlying visual mechanisms.

* This work was carried out under the terms of Contract N-5-ori-116, Task Order 5, between the Medical Sciences Division of the Office of Naval Research and the University of Michigan.

24. An Automatic Presentation, Recording, and Analysis Device for Vision Experimentation.* H. RICHARD BLACKWELL AND BENJAMIN S. PRITCHARD, *University of Michigan.*

A device which permits the determination of visual thresholds without an experimenter is described, consisting of tape-reader, punch recorder, timers, and relay panel. The tape-reader works through the relay panel to light orientation lights, sound buzzers which warn the observers of the presence and magnitude of the stimulus, open shutters to present stimuli, and vary the stimulus brightness by operating a rotary filter wheel. Provision is made to warn the observers if they fail to respond and to erase data if any irregularity has occurred.

The observers are required to discriminate some attribute of the stimulus, such as its spatial position or

location in time, indicating their response by depressing one of four plunger contacts. At the conclusion of fifty presentations, the device is shut off. The device records stimuli brightnesses, true responses, and responses of each of four observers for the fifty presentations by holes punched into a permanent 8″×12″ card. Through the relay panel, the responses of each of the observers are analyzed, correct responses being segregated for each stimulus brightness, and the results indicated on electric counters.

* This work was carried out under the terms of Contract N-5-ori-116, Task Order 5, between the Medical Sciences Division of the Office of Naval Research and the University of Michigan.

25. Invited paper, entitled "The Presentation of Absorption Spectra Data," BY WALLACE R. BRODE, *National Bureau of Standards.*

26. The Ultraviolet Absorption Spectra and the Structures of the Isomeric Amidones. L. A. STRAIT, W. D. KUMLER, P. P. T. SAH, E. L. ALPEN, AND F. N. H. CHANG, *University of California.*

The ultraviolet absorption spectra of the isomeric amidones (morphine substitutes) and their nitriles have been measured in ethyl alcohol, hexane, and acidic and basic water solutions. The spectra are characterized not only by the expected phenyl absorptions near 260 mμ but also by an apparently anomalous absorption band near 300 mμ and an unexpected appearance of a strong band below 260 mμ in the spectrum of amidone and its nitrile in basic and hexane solutions, in contrast with isoamidone and its nitrile. The differences (interchange of a methyl group between adjacent carbon atoms) in the "accepted" structures of amidone and isoamidone and their nitriles are incompatible with these spectrum differences. We propose that amidone has only *one* rather than the "accepted" two phenyl groups on the number four carbon atom to explain the spectrum characteristics. The spectrum of isoamidone is compatible with the "accepted" two phenyl groups on the same carbon atom. These differences in structure also account for the otherwise inexplicable discrepancies in their chemical behaviors. Amidone nitrile has a corresponding change in structure. We attribute the strong band below 260 mμ to the enol and enamine structures, thus possible only in amidone and its nitrile. The band at 290–300 mμ, present in the amidones and absent in amidone carbinol and the nitriles, is associated with an α-phenyl carbonyl structure.

BIBLIOGRAPHY: E. Schultz, G. Robb, and J. Sprague, J. Am. Chem. Soc. **69**, 2454 (1947).
N. Easton, J. Gardner, and J. Stevens, J. Am. Chem. Soc. **69**, 976 (1947).
Mme. Bruzeau, Ann. Chem. **1**, 257 (1943).

27. Infra-Red Absorption Analyses Used in Control of a Pilot Plant Triptane Process. D. L. FRY, *Research Laboratories Division, General Motors Corporation.*

The methods described herein are of general interest because they illustrate the effectiveness of infra-red in the analysis of hydrocarbons and the control of experimental and pilot plant processes. A number of particular problems are discussed. These problems vary in complexity from analyzing for two components in a mixture of two, to analyzing for three components in a mixture of twelve or six in a mixture of six. In some cases the analyses are possible only for certain ranges of concentration; in other cases the concentrations of the components can vary from 0 to 100 percent. The analyses were determined with an accuracy of plus or minus one percent, providing the range of concentration of the various components stayed within the limits for which the method was calibrated. In some cases it was necessary to set up calibration curves with inadequate standard samples. It is most interesting that even under these adverse conditions it was possible to attain reasonable accuracy and to make a contribution to the problem of controlling the pilot plant. In control problems it is frequently not important to know the absolute composition; it is sufficient to know relative values of concentration from day to day.

28. Construction and Performance of a Double Beam Infra-Red Spectrometer. JOHN U. WHITE AND MAX D. LISTON, *The Perkin-Elmer Corporation.*

A new double beam infra-red spectrometer recording directly in percent transmission *vs.* wave-length has been built on the principles described by Wright.[1] Its detection and control systems are described in the preceding paper. The spectrometer and recorder are a single unit (40″ long, 22″ high, 18″ wide) with external amplifier and power supplies. The instrument makes direct reading transmission records on 32″×11″ charts, employs a 60° Littrow mounted rock salt prism with 60-×75-mm faces, and has 5″ of length available for sample cells in each beam. Wave-lengths and slit widths are read directly on Veeder counters. Special features are accuracy, convenience, and wide range of operating conditions. Available wave-length drive speed varies from about two minutes to 300 hours for the rock salt region, speed of response from 4 seconds to over a minute for full scale, with the possibility of a further increase to five minutes if needed, resolution from close to the theoretical limit of the prism to about a tenth as much, paper drive speed giving uniform scales from 1 to 50 inches per micron by integral factors. By changing cams, spectra can be recorded on constant wave number or other scales. Prisms of LiF, KBr, and other materials can be accommodated.

[1] N. Wright and L. W. Hersher, J. Opt. Soc. Am. **37**, 211 (1947).

29. The Detection and Control System for a Double Beam Infra-Red Spectrometer. MAX D. LISTON AND JOHN U. WHITE, *The Perkin-Elmer Corporation.*

The detection, amplification, and control system for a double beam, percent transmission *versus* wave-length, infra-red spectrometer will be discussed. Its general construction and performance will be described in the following paper. A fast pin-type vacuum thermocouple has been developed which permits light modulation at 13 cycles

per second, with only 30 percent loss in response. A simple 13-cycle amplifier servo system, expressly developed for double beam infra-red spectrographs, will be described. This system employs a special high gain input transformer and preamplifier which is located at the base of the thermocouple to eliminate the pick-up troubles experienced in previous instruments. An automatic wave-length drive decreases the scanning speed when detail spectra are present. An electrically cammed slit control that permits easy variation of slit programming will be disclosed. Various over-all response characteristics and their noise *versus* "spectrum following ability" will be described.

30. An Infra-Red "Lens"* ROBERT A. OETJEN, *The Ohio State University.*

An arrangement of mirrors is described whereby a diverging beam of radiation may be changed to a converging beam. Since there is no absorbing glass in the path of the radiation, it may be used for radiation of all wave-lengths, including the infra-red. Both the object and image are on the axis of the system; hence, extra-axial aberrations are kept to a minimum. The components of the system include two concave mirrors and a double-sided flat with a hole in the center.

* The work described in this paper was carried out, in part, under Contract W33-038-ac-15407 between the Air Materiel Command, Wright-Patterson Air Force Base, and the Ohio State University Research Foundation.

31. An Infra-Red Instrument for Industrial Product Control. N. C. JAMISON, T. R. KOHLER, AND O. G. KOPPIUS, *Philips Laboratories, Inc.*

An infra-red differential comparator with no dispersion has been built for routine product control in industrial plants. Good stability is obtained without thermostatic control by means of a flicker system using a single source of radiation, a single radiation detector, and a.c. amplification. A thermistor bolometer is used as the heat sensitive element; the samples of known purity and unknown purity are compared six times per second and the difference in absorption is recorded. The design, construction, and operating characteristics of the instrument will be considered in some detail.

32. Invited paper, entitled "Optics in the Pharmaceutical Industry," BY J. M. VANDENBELT, *Parke, Davis, and Company.*

33. Phase Microscopy with Critical Illumination. HAROLD OSTERBERG, *American Optical Company, Scientific Instrument Division.*

The amplitude and phase distribution in the image plane of a phase microscope employing Kohler illumination is in general radically different from the amplitude and phase distribution obtained when the same microscope is illuminated by critical illumination. It will be shown theoretically that, although the amplitude and phase distributions are highly dissimilar, the total energy distributions in the image plane are alike with Kohler and critical illumination provided that the area of the source of light extends over a great number of wave-lengths and provided either that the amplitude and phase transmission of the object slide does not vary appreciably with the inclination of the incident light or that the cone of incident light is very narrow. In practical phase microscopy, the contrast in the image will not be markedly different with the use of Kohler or critical illumination. This conclusion has been verified experimentally.

34. Rotating Two Dimensionally Patterned Gratings. MARCEL J. E. GOLAY.*

The substitution of these gratings for the entrance and exit slits of a far infra-red spectrograph permits the utilization of a considerably greater fraction of the radiation from available infra-red sources. The realizable gain in s/n ratio is one-quarter the ratio of the greatest allowable length of a conventional slit over its width, less the transmission losses through the gratings.

* In collaboration with the Eppley Laboratories, Newport, Rhode Island.

35. The Absolute Sensitivity of Existing Heat Detectors. R. CLARK JONES, *Research Laboratory, Polaroid Corporation.*

This paper presents the results of a study of the absolute sensitivity of 50 detectors representing 20 different types of thermocouples, thermopiles, and bolometers. The absolute sensitivity and a factor of merit for each of these detectors have been calculated and will be presented in graphical form. The detectors reported include nearly all of the commonly used heat detectors. A systematic exposition of the conceptual background of the study will be given. Included in the exposition will be classification of the types of noise which serve to limit detector sensitivity, a classification of the types of time constants involved in radiation detectors, a classification of the detectors themselves on the basis of the way that the minimum detectable power depends on the time constant, a specification of a reference condition of measurement, and the reasons behind the definition of the factor of merit used in the presentation.

36. Low Temperature Radiation Pyrometry. J. C. MOUZON AND C. A. DYER, *The Brown Instrument Company, Division of Minneapolis-Honeywell Regulator Company, Philadelphia, Pennsylvania.*

Some general problems associated with low temperature radiation pyrometry, such as radiation detectors, surface emissivity, lens materials, reference temperatures, and humidity effects, will be discussed. A low temperature radiation pyrometer suitable for temperature measurements in the range of 100°F to 400°F will be described.

37. Invited paper, entitled "Recent Trends in Applied Emission Spectroscopy," BY MARY E. WARGA, *University of Pittsburgh.*

38. Recent Infra-Red Work at Cambridge. G. B. B. M. SUTHERLAND, *Pembroke College, Cambridge, England.*

Advances in the technique of infra-red detection will be discussed, particularly the development of lead telluride cells, which are sensitive to 5.5μ and far superior to thermocouples or bolometers in sensitivity and speed of response. Some applications of infra-red methods of analysis to the structure of large molecules will be discussed, with special emphasis on proteins and on diamond. Some recent work on polarized infra-red radiation and on atmospheric absorption will also be outlined.

39. A Spectrochemical Method for the Determination of Uranium.* L. T. STEADMAN, *University of Rochester School of Medicine and Dentistry.*

Microgram amounts of U are analytically determined by means of the d.c. carbon arc and a B. & L. medium quartz spectrograph. If necessary, the U is separated from extraneous materials by a modification of the ether extraction method of Furman and co-workers. The sample is placed in the negative electrode, the light from which is focused on the prism. The sample is burned in the crater of a purified graphite rod or, for higher sensitivity, is arced on the flat end of a carbon electrode. Relative intensities are determined by a sector method employing a rotating half-cylinder in front of the slit, with a slit width of 10 microns. A 50-fold increase in sensitivity is obtained by adding about 10 mg RbCl as an enhancing agent to the electrode along with the sample. Lines measured are the unresolved U lines 2882.6, 2882.7, and 2882.9A, and the line 2650.8A of the internal standard Pt. The calibration curves extend from 0.02 to 20 micrograms of U in the arc. The standard error of a single determination is about ±15 percent.

* This paper is based on work performed under contract with the U. S. Atomic Energy Commission at The University of Rochester Atomic Energy Project, Rochester, New York.

40. A Preliminary Investigation of the Spectra of Uranium Isotopes. J. RAND MCNALLY, JR., *Carbide and Carbon Chemicals Corporation, Oak Ridge, Tenn.*

The isotope displacement effect[1] is discussed with relation to other spectro-isotopic effects. The results of a preliminary investigation of this effect in uranium isotopes are presented. Spectrum shifts as large as a wave number between the U^{235} and U^{238} spectra are not uncommon, the shifts usually being toward the violet for the lighter isotope. These wave-length differences have been correlated to the spectroscopic energy systems of U *I* and U *II* and are found to be of two types: (1) a simple isotopic displacement arising from configuration-nucleus interaction, and (2) a complex isotopic displacement arising from perturbations between close-lying levels. The magnitude of the shift in U *I* is generally of the order of 0.3 cm^{-1}, but ranges from -0.7 cm^{-1} to 1.5 cm^{-1} in U *II*. Configurations involving the s^2 electron group show the largest isotope shifts indicating an additive type of interaction for the *s* electrons and the nucleus.

[1] See S. Tolansky, *Hyperfine Structure in Line Spectra and Nuclear Spin* (Methuen and Company. Ltd., London, 1946).

41. Spectrographic Analysis of Vitallium Alloys. Y. T. SIHVONEN, D. L. FRY, R. E. NUSBAUM,* AND R. R. BAUMGARTNER,** *Research Laboratories Division, General Motors Corporation.*

A spectrochemical method of analysis to be used for control purposes in casting Vitallium is described in this paper. The need for such a method was so urgent that only a small amount of development time was possible; control analyses were being made within three days of the time the problem was submitted. Improvements were made in the method in the course of the work. Reproducibility and accuracy data are given in the paper. This problem illustrates that a great deal of analytical work can be done with a spectrograph even though accurate comparison standards are not available.

* Now at North American Aviation, Inglewood, California.
** Now at Redford High School, Detroit, Michigan.

42. The Spectrochemical Determination of Hafnium-Zirconium Ratios. CYRUS FELDMAN, *Oak Ridge National Laboratory.*

A spectrochemical technique is presented for determining hafnium-zirconium ratios in the range $(Hf \times 100)/Zr = 0.073 - 9.23$ by weight, with and without the aid of hafnium-free zirconium preparations. The sample is brought into solution in 10 percent H_2SO_4, and sparked by the porous cup technique. The intensity ratio Hf *II* 2641.406/Zr *II* 2761.911 is measured, and the Hf/Zr ratio read from a standard curve.

43. A Rapid Mobile Analyzer for Minute Amounts of Lead in Air. HENRY AUGHEY, *Chemical Department, Experimental Station, E. I. du Pont de Nemours & Company, Wilmington, Delaware.*

Atmospheric contamination by lead presents acute problems in analysis and control to the chemical industry. A mobile instrument of extreme sensitivity has been developed which furnishes a rapid indication and an approximate assay of localized relatively high concentrations of lead, combined or elemental. Samples are drawn through a condensed spark discharge adjusted to minimize air lines and to excite the lead spectrum which is photographed with a small quartz instrument. Visual examination of a series of exposures provides data on lead concentration as a function of time and location. A sensitivity of better than one part in 20 million can be maintained in routine operation. Instantaneous response has been realized by substitution of the photoelectric Geiger counter for the photographic plate, as described in detail in the following paper.

44. Detection of Lead in Air with the Aid of a Geiger-Müller Counter. O. G. KOPPIUS, *Philips Laboratories, Inc.*

A detector of lead in air will be described. It utilizes a spark source for the excitation of the lead spectrum, a small quartz spectrometer for the dispersion, and a quartz Geiger-Müller counter for the detector of the radiation. The lower limit of detection is of the order of 20 micro-

grams of lead per cubic foot of air. The instrument is mobile and ideally suited to locate areas of high lead concentration in air.

45. Stainless Steel Analysis with the Direct Reading Spectrometer. JACOB H. JURMAIN AND JOHN STERNER, *Baird Associates, Inc.*

With minor modification, the Direct Reading Spectrometer has been applied to the rapid analysis of chromium, nickel, manganese, and silicon in stainless steels. Working curve sets are described, and their application to practical problems in industry is discussed. Repeatability results are presented, showing that characteristic reproducibility of the instrument falls well within the limits required for industrial control.

BIBLIOGRAPHY: Carpenter, DuBois, and Sterner, "Direct reading spectrometer for ferrous analysis," J. Opt. Soc. Am. **37**, 707 (1947).

46. Invited paper, entitled "Seeing Light and Color," BY RALPH M. EVANS, *Eastman Kodak Company.*

47. Invited paper, entitled "Solar Infra-red Spectroscopy," BY LEO GOLDBERG, *University of Michigan.*

48. Invited paper, entitled "Xerography. A New Principle of Graphic Reproduction," BY R. M. SCHAFFERT AND COLLEAGUES, *Battelle Memorial Institute,* AND J. C. WILSON, *The Haloid Company.*

49. Invited paper, entitled "Optics and Semi-Conductors," BY FREDERICK SEITZ, JR., *Carnegie Institute of Technology.*

50. Measurements of the Physical Properties of Infra-Red Optical Materials.* LEWIS S. COMBES AND STANLEY S. BALLARD, *Baird Associates, Inc. and Tufts College.*

Technical data on the various physical properties of optical materials of interest in infra-red instrumentation have been collected, and new data obtained where they could not be found in the literature. Measurements have been made of Knoop hardness, Young's modulus, flexural apparent elastic limit, modulus of rupture, modulus of rigidity, torsional apparent elastic limit, specific gravity, thermal conductivity, and coefficient of thermal expansion for some or all of the following materials: AgCl, KRS-5, KRS-6, NaCl, KCl, KBr, LiF (air and vacuum grown), CaF_2, $CaCO_3$, $NaNO_3$, crystal quartz, and fused quartz. In some cases unexpected results were obtained. For example, the flexural apparent elastic limit of vacuum-grown LiF is more than three times that for the air-grown crystals and the modulus of rupture is more than double, while the Young's modulus is approximately the same for both the vacuum-grown and air-grown crystals. Also, all the elastic properties measured for KRS-5 and KRS-6 were of about the same magnitude with the exception that the torsional apparent elastic limit of KRS-5 was about 2½ times that of KRS-6.

* This work has been supported by Contract W-44-009-eng-473 between the Engineer Research & Development Laboratories, Fort Belvoir, Virginia, and Baird Associates, Inc., Cambridge, Massachusetts.

51. The Infra-Red Properties of Polar Crystals. ELIAS BURSTEIN, *Crystal Section, Naval Research Laboratory.*

The transmission and reflections of MgO[1] indicate that there is appreciable coupling between the normal modes of vibration of the lattice. The extensive coupling is associated with the large overlapping of the ions (homopolar bonding) in MgO and in particular with the large change in polarizibility of the ions with interatomic distance.[2] This suggests that the change in polarizibility of the ions with interatomic distance during vibration is one of the important factors determining the magnitude of those anharmonic terms in the potential function which in existing theoretical discussions[3] are introduced phenomenologically to explain the optical transitions between the vibrations. On this basis it is possible to reach qualitative conclusions concerning the relative magnitude of the intensity and width of absorption bands, the number of secondary bands, and the effect of temperature in comparing the properties of different crystals. Data on the change in polarizibility of the ions with interatomic distance is obtained from photoelastic properties, static dielectric constant, and the change in molar polarizibility in going from the independent ions in the gas to the solid state. It is possible to obtain additional data from a study of Raman spectra, since the intensity of scattering depends among other things upon the change in polarizibility of the ions during vibration.

[1] E. Burstein, J. Oberly, and E. K. Plyler, "The infra-red properties of MgO," to be published shortly.
[2] E. Burstein and P. Smith, "The photoelastic constants of cubic crystals," Phys. Rev. **74**, 229 (1948).
[3] M. Blackman, "On the absorption of polar crystals in the infra-red," Phil. Trans. Roy. Soc. **A236**, 103 (1936).
R. Bowling Barnes, R. Brattain, and F. Seitz, "On the structure and interpretation of the infra-red absorption spectra of crystals," Phys. Rev. **48**, 582 (1935).

52. On the Inelastic Deformation and Crystal Orientation of Thallium Halides. ALEXANDER SMAKULA AND MYRON W. KLEIN, *Engineer Research and Development Laboratories, The Engineer Center and Fort Belvoir, Fort Belvoir, Virginia.*

Thallium halide crystals are finding extensive use as prisms and plates in infra-red research. For successful mechanical working such as shaping, grinding, and polishing it is desirable to know the crystal orientation which can be determined very simply by inelastic deformation patterns. Under the pressure of a cone the cubic thallium halides show two kinds of very sharply limited pattern, the "superficial" and the "transmitted." The first appears around the press point and has wings whose length and symmetry depend on the lattice orientation. The second develops on the opposite side of the press point and has a square or a rhombic shape. The patterns are explained by localized distortion of the single crystal in the neighborhood of the press point into small parts which slip in planes of the dodecahedron faces in the direction of cube faces. The superficial patterns can be applied for determination of lattice orientation within a few degrees. Temporary strains are distributed symmetrically around the press patterns. Under conical pressure sodium chloride crystals

show splitting in diagonal directions of the cube face. Silver chloride crystals give only diffuse patterns.

53. Refractive Index of Optical Glass at Low Temperature. FRED A. MOLBY, *West Virginia University*, AND A. FRANCIS TURNER, *Bausch & Lomb Optical Company.*

At the Cleveland meeting of the Optical Society of America, results of measurements on some of Schott's glasses and some of Bausch & Lomb's glasses were reported.[1] The Eastman Kodak Company has made specimens from four of its glasses for an extension of the study of the effect of temperature on index of refraction of glasses. The work on these specimens has been done in the same way that was reported at Cleveland. The general conclusions stated at that time have been found to hold for the Eastman Kodak Company's glasses. Several slides showing comparative results will be shown.

[1] Fred A. Molby, J. Opt. Soc. Am. **36**, 350 (A) (1946).

54. Schmidt System Tolerances. ROBERT A. WOODSON, *Consultant Optical Engineer.* (15 min.)

The design and manufacturing tolerances which are specified for Schmidt systems can be found by adapting methods used for systems of spherical surfaces.[1] However, the simple Schmidt catadioptric system warrants a specific design and tolerance analysis of its own. Its aberrations are unique. The aspheric corrector plate curve is usually weak enough to justify first-order approximations in its analysis. This simplifies the problem. However, the high relative apertures frequently encountered in Schmidt systems introduce complications. The optimum design for a specific application depends upon a combination of optical performance requirements and the method of manufacture. Examples of such design and tolerance specifications will be given. Conclusions apply also to the meniscus type catadioptric systems of Maksutov.[2]

[1] Paul C. Foote and Robert A. Woodson, J. Opt. Soc. Am. **38**, 590 (1948).
[2] D. D. Maksutov, J. Opt. Soc. Am. **34**, 270 (1944).

55. Curved Field Lens and Camera. ROBERT E. HOPKINS, JOHN C. EVANS, WILLIAM COVELL, AND DONALD FEDER, *Institute of Optics, University of Rochester.*

A 6-inch focal length f:1 lens and camera have been constructed. Unusually excellent image correction in the lens has been attained by allowing the Petzval surface to be inward curving to a radius of 4.9 inches. The film is pressed into the focal surface with compressed air introduced between the final element and the film. The camera uses a standard roll of 5½-inch film. The film is transported automatically, the camera being built to take approximately one picture per second. After the film has run through the camera, it shows no appreciable stretching; it can be processed in standard equipment and printed in a flat plane printer. Details of the lens performance and camera mechanism will be discussed.

56. A New Spectrophotometer Employing a Glass Féry Prism. WM. C. MILLER, *National Technical Laboratories.*

The Féry prism, first described in 1910, has been used in relatively few applications, all of these apparently being spectrographs. The present paper describes the application of a borosilicate Crown glass Féry as the dispersive element in a monochromator covering the spectral range from 320 mμ to 1000 mμ. Performance characteristics of the prism are given. A new Beckman spectrophotometer employing the Féry prism is described along with its performance characteristics. A novel wave-length control mechanism and a new slit device are described.

BIBLIOGRAPHY: Charles Féry, J. de Phys. **9**, 762 (1910). Astrophys. J. **34**, 79–87 (1911).

57. Invited paper, entitled "Spectrographic Light Sources," BY R. A. WOLFE, *University of Michigan.*

58. Criteria for High Precision Analyses with d.c. Arc Excitation. VELMER A. FASSEL, *Institute for Atomic Research, Iowa State College.*

The d.c. arc between graphite electrodes possesses definite advantages in convenience, general application, and sensitivity as an excitation source for the spectrographic analysis of inorganic materials. However, the poor reproducibility usually associated with this discharge greatly limits its usefulness for quantitative analyses. In a method recently reported[1] for the determination of major amounts of gadolinium and yttrium in complex rare earth oxide mixtures, it was observed that the standard deviation was only 2 to 2.5 percent. The precision was thus comparable to that obtained from more carefully controlled excitation sources. The results from a quantitative study of (a) vaporization rates, (b) intensity diagrams of the internal standard line pairs along the longitudinal axis of the arc discharge, and (c) the effect of large changes in external excitation conditions on the intensity ratios show that this high precision can be attributed to nearly ideal internal standard compensation of excitation variables. The data to be presented indicate that the difficulties of d.c. arc excitation can largely be overcome by satisfying the essential criteria of the internal standard principle.

[1] Velmer A. Fassel and Harley A. Wilhelm, J. Opt. Soc. Am. **38**, 518 (1948); **38**, 666 (1948).

59. An Air Interrupter Type Spectrographic Light Source. J. H. ENNS AND R. A. WOLFE, *University of Michigan.*

The principle feature of this source is an air interrupter, some of whose operating characteristics have been described in two earlier papers.[1,2] This paper presents a general technical description of the source to illustrate its unusual flexibility. A procedure followed in selection of source parameters is outlined. Several examples are given to show the most suitable source conditions for some widely different type samples.

[1] J. H. Enns and R. A. Wolfe, Special Technical Publication No. 76, Symposium on Spectrographic Light Sources (1946). Published by A.S.T.M. (1948).
[2] J. H. Enns and R. A. Wolfe, Paper O. S. A. Meeting, Feb. 21, 1947.

60. A Combination Spark-Arc Source Unit for Spectrochemistry. M. F. HASLER AND J. W. KEMP, *Applied Research Laboratories, Glendale, California.*

The a.c. arc unit has enjoyed a certain popularity because of the simplicity of its circuit and its sensitivity as a spectrum source. However, it has suffered from the small gap spacing required and its very low electrical efficiency. Both of these defects can be easily eliminated by using a spark-ignited arc. The authors describe such an arc utilizing a 900-peak volt transformer to supply three or six amperes in the arc circuit and ignited with high voltage power from a standard spark circuit. Power in the ignitor is reduced by means of resistance in the oscillating circuit of the spark. The spark circuit is a conventional rotary gap arrangement except that a single control gap is utilized by means of a brush system on the rotary gap. This plus a large diameter rotor, large tungsten electrodes, and ultraviolet irradiation provides good precision at high intensity. The unit is particularly suited for routine metal analysis either with a spectrograph or a quantometer.

61. Instrumentation for Direct-Reading Spectrochemistry. M. F. HASLER, J. W. KEMP, AND D. R. PROCTOR, *Applied Research Laboratories, Glendale, California.*

The various systems of direct-reading spectrochemical analysis reported to date are analyzed in comparison with a new system proposed by the authors. The problems connected with the spectrometer and the recording system are analyzed in detail and the relative merits of the various proposed solutions are considered. A direct-reading adapter suitable for grating spectrographs and utilizing the newly developed system is described.

[1] M. F. Hasler and H. W. Dietert, J. Opt. Soc. Am. **34**, 751 (1944).
[2] G. H. Dieke, Progress Report W-193 W.P.B.
[3] G. H. Dieke and H. M. Crosswhite, J. Opt. Soc. Am. **35**, 471 (1945).
[4] G. A. Nahstoll and F. R. Bryan, J. Opt. Soc. Am. **35**, 646 (1945).
[5] Saunderson, Coldecourt, and Peterson, J. Opt. Soc. Am. **35**, 681 (1945).
[6] K. G. Kessler and R. A. Wolfe, J. Opt. Soc. Am. **37**, 133 (1947).
[7] R. Hanan and R. A. Wolfe, J. Opt. Soc. Am. **38**, 377 (1948).
[8] F. R. Bryan and G. A. Nahstoll, J. Opt. Soc. Am. **38**, 510 (1948).
[9] M. F. Hasler, R. W. Lindhurst, and J. W. Kemp, J. Opt. Soc. Am. (in publication).

62. Invited paper, entitled "A Method of Measuring and Specifying the Quality of Optical Images," BY OTTO H. SCHADE, *Radio Corporation of America.*

63. Out-of-Focus Diffraction Patterns. L. IVAN EPSTEIN, *Bausch & Lomb Opt. Company.*

The diffraction pattern which represents the image of a luminous point when observed out of focus has been calculated by A. E. Conrady,[1] A. Buxton,[1] and G. Lansraux.[2] Conrady and Buxton used numerical integration. Such a process yields a sequence of values of the complex amplitude at a particular point in the diffraction pattern for a particular lack of focus, and for any given integration, the distance W of the point under consideration from the center of the pattern, and the lack of focus p, are functions of the upper limit of integration. If p is plotted against W, the path obtained is a parabola, $p=aW^2$. The author has found a method whereby any desired path of integration can be followed instead of a parabola. In particular, if the point of observation is near the edge of the purely geometrical diffusion disk and remains at a constant distance from it as p changes, then, for large values of p, the form of the diffraction fringes is approximately independent of p and their intensity is inversely proportional to p^2.

[1] A. E. Conrady, Monthly Notices Roy. Astronom. Soc. **79**, 575 (1919), and A. Buxton, *ibid.* **81**, 547 (1921).
[2] G. Lansraux, Revue d'Optique **26**, 24 (1947).

64. Reflected Light and Ghosts in Optical Systems. A. E. MURRAY, *Bausch & Lomb Optical Company.*

Each surface in an optical system reflects a small fraction of the incident flux, which thus is lost to the image; these surfaces singly and in combination form ghost images of the light source. The number of first-order ghosts is equal to the number of surfaces, and the number of second-order ghosts equals the number of pairs of surfaces. In the general case of s interreflections, $s>1$, combinatorial theory indicates that the number of ghosts is equal to the number of pairs plus twice the number of triplets plus three times the number of quadruplets plus . . ., and so forth. The relations are applied to a system of triplet condensers and projection lenses, coated and uncoated in every combination. Even though the ghost flux is minimum in the condenser-unfilmed, objective-filmed combination, it offers no advantages over the all-filmed case, because of the lower transmission.

65. A Method for Evaluating the Intensity of Focused Stray Light from Concave Diffraction Gratings. F. S. JOHNSON AND R. TOUSEY, *U. S. Naval Research Laboratory, Washington, D. C.*

For certain applications, the usefulness of a diffraction grating is limited by the amount of stray light which it focuses into the spectrum. The stray light is heterogeneous in wave-length; therefore, its importance varies with the intensity distribution of the light falling on the grating and with the wave-length response characteristics of the receiver or spectrographic film. It also varies widely from grating to grating. For the NRL solar ultraviolet rocket spectroscopy program, gratings are compared using Eastman 103-0 ultraviolet sensitized film with a shielded carbon arc crater as source. The blackening of the film caused by the focused stray light falling in the spectrum at a wave-length just below the air cut-off near 1850A is compared with the blackening caused by the carbon arc spectrum just above the air cut-off, and a ratio of useful to stray light obtained. This is done for incidence on each side of the grating normal. A comparison of the useful light intensities from various gratings is also obtained, using an arbitrarily selected grating as a standard. This then permits the evaluation of each grating in terms of useful light intensity and ratio of useful to stray light for incidence on either side. A series of 24 gratings tested in this way showed useful to stray light ratios from as high as 40 to well below unity, and useful light intensities near 2000A from 200 percent to about one percent of the arbitrary standard. Some were echelettes where one side was especially weak, and some showed good intensity on

each side. In general, the absolute intensity of the stray light did not differ greatly between sides. This method is very useful in the selection of gratings for photographing the ultraviolet spectrum of the sun from rockets. The method also is suitable for comparing different films for response to useful and to stray light.

66. Preconstruction of Triplet. M. HERZBERGER, *Kodak Research Laboratories.*

Nomograms are presented from which, for an arbitrarily chosen set of ν-values, a survey may be made of the possible range of the data of a triplet, corrected for longitudinal and lateral color.

67. The Plano-Interferometer. DAVID RICHARDSON, *Bausch & Lomb Optical Company.*

Two simple interferometers have been developed for use as flatness testers. These instruments possess many advantages over optical flat test glasses, both in ease of manipulation and in the type of test that can be made with them. A number of interesting applications of plano-interferometers to both laboratory and manufacturing problems will be described.

68. Interference Fringes near a Critical Angle Boundary. P. J. Leurgans, A. F. Turner, AND O. A. ULLRICH, *Bausch & Lomb Optical Company.*

Total reflection at a surface is disturbed by the close proximity of a second surface. This is commonly demonstrated by placing a slightly convex surface against the hypotenuse face of a totally reflecting prism and viewing the system through one of the prism faces. For angles smaller than the critical, Newton's rings appear. The rings do not cross the critical angle position but, on approaching it, distort to fringes running asymptotic to it. For a very small separation of the surfaces no sharp dividing edge can appear. Beyond the critical angle there are no fringes, but only a gradual increase in intensity as the angle or separation increase. Although this behavior is fully established by classical physical optics, the fact that incorrect statements may still be found in the literature concerning interference beyond the critical boundary region prompts this review of the subject. Photographs and curves will show the dependence of reflectivity and interference on angle and on second surface proximity.

69. Thin Sheet Plastic Fresnel Lenses of High Aperture. O. E. MILLER, J. H. MCLEOD, AND W. T. SHERWOOD, *Eastman Kodak Company.*

Fresnel type lenses of high precision and excellent surface quality have been made in thin sheet plastic materials. The prismatic elements are very fine—about 0.003" to 0.005"—and are not visible to the average unaided eye. A high degree of correction for spherical aberration has been achieved. Molded from high precision molds, lenses have been made in diameters of two to fifteen inches and focal lengths of 2½ to 22½ inches. Relative apertures in excess of f:1.0 have been made. These lenses have found many applications as light collecting elements where weight and space are limited. Such applications include uses for large condensers, large field lenses in finders, camera viewing screens, and translucent screens for projection.

70. Invited paper, entitled "Progress and Prospects in the Spectrochemical Analysis of Non-Metallic Materials," BY ROBERT W. SMITH, *AC Spark Plug Division, General Motors Corporation.*

71. Spectrographic Analysis of Alumina in Silica Brick. P. R. IRISH, *Bethlehem Steel Company.*

A method for determining alumina in the range of 0.25 percent–1.50 percent in silica brick is described. The procedure for analyzing this non-conducting material while not new has not been prominently employed. With this method the sample in powdered form is fused in a small electric furnace (1100°C) with alkali salts, sodium carbonate, and borax along with an internal standard element, columbium oxide. While the fusion material containing the brick sample in solution is molten, a carbon electrode is dipped into the molten pool. The fusion material adheres to the carbon, thus forming an electrode that is tipped with the solidified fusion material which contains the brick sample and internal standard element in solid solution. Electrodes thus formed are rugged enough for use with a spark source. In a test of the accuracy for 92 samples only three samples showed deviations greater than 0.03 percent Al_2O_3 from the average umpire analysis of four chemical laboratories. The method is well adapted to routine control and gives the usual spectrographic speed, the elapsed time of a single determination being 20 to 25 minutes.

72. The Spectrographic Determination of Fluorine in Organic Substances. CHARLES W. RANKIN, *New York State Police Scientific Laboratory.*

During the recent war sodium fluoroacetate or "1080" was developed, and proved highly effective against an unlimited variety of rodent species. A serious objection to its use is its high toxicity for all mammalian species, dogs having succumbed to doses as low as 0.1 mg per kilo as compared with a lethal dose of 2 mg per kilo for sodium fluoride. When "1080" became commercially available it was natural that this laboratory should receive cases of suspected "1080" poisoning. We became interested, therefore, in determining fluorine in trace quantities by spectrographic methods. Two methods were attempted: (1) the detection of the 5291A band of CaF_2[1] and (2) the detection of fluorine in the high current density spark.[2] Using either method, as little as 100 micrograms of "1080" have been detected.

[1] Papish, Hoag, and Snee, Ind. Eng. Chem. Anal. Ed. **2**, 263 (1930).
[2] Pfeilsticker, Zeits. Metallk. **33**, 267–272 (1941).

73. Optical and Electrical Alterations to a Michigan Microphotometer. H. H. GROSSMAN, E. W. PETERSON, J. L. SAUNDERSON, AND V. J. CALDECOURT, *Spectroscopy Laboratory, The Dow Chemical Company.*

A microphotometer of the type described by Vincent and Sawyer[1] has been altered optically and electrically to

eliminate certain objectionable features. Scattered light, dependence of the focus of the plate projection lens upon the aperture of the plate illumination system, photo-cell fatigue, relatively short life of the projection lamp, and the need for a constant voltage power supply have been eliminated. Plate calibration curves obtained with the altered instrument on wide bands and narrow lines are essentially identical.

[1] H. B. Vincent and R. A. Sawyer, J. Opt. Soc. Am. **31**, 639 (1941).

74. Three-Line Method of Obtaining Characteristic Curves for Heterochromous Photometry. MILTON GREEN, *Signal Corps Engineering Laboratories.*

By employing three spectral lines of iron, two in one wave-length range, and a third in the second wave-length range, it is possible to construct the two characteristic curves for heterochromous photometry. The method for performing this will be described and its advantages and disadvantages will be discussed.

75. Ultraviolet Absorption Spectra of Biological Compounds at Low Temperatures. R. L. SINSHEIMER, J. F. SCOTT, AND J. R. LOOFBOUROW, *Massachusetts Institute of Technology.*

It is often possible to increase the detail observable in the absorption spectra of complex molecules by refrigeration of the absorbing substance. The investigations to be reported seek to take advantage of this principle to improve the spectroscopic characterization of biological compounds. Special methods have been devised for this work. Spectra of purines, pyrimidines, and derivatives, and of amino acids and derivatives, taken at liquid nitrogen and liquid hydrogen temperatures will be presented. Empirical generalizations, drawn from the results thus far obtained, will be discussed.

BIBLIOGRAPHY: J. F. Scott, R. L. Sinsheimer, and J. R. Loofbourow, Science **107**, 302 (1948).

76. Photoelectric Determination of Interference Maxima. GEORGE R. HARRISON AND JAMES C. ANDERSON, *Massachusetts Institute of Technology.*

A photoelectric scanning device has been developed which locates maxima of interference fringes, spectrum lines, or scale marks while they are at rest or in motion. As applied to the Winmac device,[1] the scanner consists of a 10-in. glass disk rotated at 450 r.p.m., on which has been photographed a slit of varying width in the form of a spiral obtained by plotting in polar coordinates the parabolic relationship between order of interference and diameter of Fabry-Perot fringes. By projecting an enlarged image of the interference pattern from the Fabry-Perot etalon on a horizontal slot intersecting this parabolic spiral, it is possible to scan the pattern out from the center at a rate varying in each direction with the local dispersion. Two photo-multiplier tubes connected through an electronic switching circuit to a common amplifier and maximum picker circuit of the type previously described[2] alternately indicate passage of a density or intensity maximum. Each tube fires its own strobolamp as a maximum is crossed, giving a direct reading of ϵ (the fractional order of interference shown by the fringe pattern) on a rotating dial connected to the scanning disk. Maxima of several rings can be automatically combined to give a single average ϵ value. The probable error of a set of "picker" determinations obtained in a fraction of a second was found, on patterns of moderate sharpness, to be about five times less than with ordinary eye setting, giving wave-length precision to about one part in thirty million in the cases used. The scanning method is being applied in modified form to the control of a partially completed ruling engine for twelve-inch gratings placed at our disposal by the University of Chicago.

[1] G. R. Harrison, J. Opt. Soc. Am. **36**, 644 (1946).
[2] G. R. Harrison and J. P. Molnar, J. Opt. Soc. Am. **30**, 343 (1940).

Author Index of Papers

Alpen, E. L.—see Strait, L. A.
Anderson, James C.—see Harrison, George R.
Aughey, Henry—No. 43
Ballard, Stanley S.—see Combes, Lewis S.
Baumgartner, R. R.—see Sihvonen, Y. T.
Blackwell, H. Richard—Nos. 22 and 23
—— and Benjamin S. Pritchard—No. 24
Brode, Wallace R.—No. 25
Brown, W. R. J. and D. L. MacAdam—No. 3
Burnham, Robert W.—No. 2
Burstein, Elias—No. 51
Caldecourt, V. J.—see Grossman, H. H.
Chang, F. N. H.—see Strait, L. A.
Chapman, R. M.—see Migeotte, M. V.
Combes, Lewis S. and Stanley S. Ballard—No. 50
Condon, F. E.—see McMurry, H. L.
Covell, William—see Hopkins, Robert E.
Dyer, C. A.—see Mouzon, J. C.
Enns, J. H. and R. A. Wolfe—No. 59
Epstein, L. Ivan—No. 63
Evans, John C.—see Hopkins, Robert E.
Evans, Ralph M.—No. 46
Fassel, Velmer A.—No. 58
Feder, Donald—see Hopkins, Robert E.
Feldman, Cyrus—No. 42
Foss, Carl E.—No. 1
Fry, D. L.—No. 27
——see Sihvonen, Y. T.
Gibson, Kasson S.—see Teele, Ray P.
Golay, Marcel J. E.—No. 34

Goldberg, Leo—No. 47
Green, Milton—No. 74
Grossman, H. H., E. W. Peterson, J. L. Saunderson, and V. J. Caldecourt—No. 73
Harrison, George R. and James C. Anderson—No. 76
Hasler, M. F., J. W. Kemp, and D. R. Proctor—No. 61
—— **and J. W. Kemp**—No. 60
Herzberger, M.—No. 66
Hopkins, Robert E., John C. Evans, and Donald Feder—No. 55
Hulburt, E. O.—No. 20
Humphreys, Curtis J. and Earle K. Plyler—No. 10
Hunter, Richard S.—No. 7
Irish, P. R.—No. 71
Jamison, N. C., T. R. Kohler, and O. G. Koppius—No. 31
Johnson, F. S. and R. Tousey—No. 65
Jones, R. Clark—No. 35
Judd, Deane B.—Nos. 4, 8, and 16
Jurmain, Jacob H. and John Sterner—No. 45
Kemp, J. W.—see Hasler, M. F.
Klein, Myron W.—see Smakula, Alexander
Knox, A. G.—see Stroupe, J. D.
Kohler, T. R.—see Jamison, N. C.
Koppius, O. G.—No. 44
—— **see Jamison, N. C.**
Kumler, W. D.—see Strait, L. A.
Leurgans, P. J., A. F. Turner, and O. A. Ullrich—No. 68
Liston, Max D. and John U. White—No. 29
——**see White, John U.**
Lock, C.—see Packer, D. M.
Loofbourow, J. R.—see Sinsheimer, R. L.
MacAdam, D. L.—see Brown, W. R. J.
McLeod, J. H.—see Miller, O. E.
McMurry, H. L., V. Thornton, and F. E. Condon—No. 13
McNally, J. Rand, Jr.—No. 40
Middleton, W. E. Knowles and F. D. Smith—No. 6
Migeotte, M. V. and R. M. Chapman—No. 11
Miller, O. E., J. H. McLeod, and W. T. Sherwood—No. 69
Miller, William C.—No. 56
Molby, Fred A. and A. Francis Turner—No. 53
Mouzon, J. C. and C. A. Dyer—No. 36
Murray, A. E.—No. 64
Nusbaum, R. E.—see Sihvonen, Y. T.
O'Brien, Brian, and E. Dickerman O'Brien—Nos. 17 and 18
O'Brien, E. Dickerman—see O'Brien, Brian
Oetjen, Robert A.—No. 30
Osterberg, Harold—No. 33
Packer, D. M. and C. Lock—No. 21
Peterson, E. W.—see Saunderson, D. L.
——**see Grossman, H. H.**
Plyler, Earle K.—No. 12
——**see Humphreys, Curtis J.**
Pritchard, Benjamin S.—see Blackwell, H. Richard
Procter, D. R.—see Hasler, M. F.
Rankin, Charles W.—No. 72
Richardson, David—No. 67
Sah, P. P. T.—see Strait, L. A.
Saunderson, J. L. and E. W. Peterson—No. 5
——**see Grossman, H. H.**
Schade, Otto H.—No. 62
Schaffert, R. M., Colleagues, and J. C. Wilson—No. 48
Scott, J. F.—see Sinsheimer, R. L.
Seitz, Frederick, Jr.—No. 49
Sherwood, W. T.—see Miller, O. E.
Sihvonen, Y. T., D. L. Fry, R. E. Nusbaum, and R. R. Baumgartner—No. 41
Sinsheimer, R. L., J. F. Scott, and J. R. Loofbourow—No. 75
Smakula, Alexander and Myron W. Klein—No. 52
Smith, F. D.—see Middleton, W. E. Knowles
Smith, Robert W.—No. 70
Steadman, L. T.—No. 39
Sterner, John—see Jurmain, Jacob H.
Strait, L. A., W. D. Kumler, P. P. T. Sah, E. L. Alpen, and F. N. H. Chang—No. 26
Stroupe, J. D., A. G. Knox, and J. F. Woodman—No. 15
Sutherland, G. B. B. M.—No. 38
Teele, Ray P. and Kasson S. Gibson—No. 19
Thornton, V.—see McMurry, H. L.
Tousey, R.—see Johnson, F. S.
Turner, A. F.—see Leurgans, P. J.
——**see Molby, Fred A.**
Ullrich, O. A.—see Leurgans, P. J.
Vandenbelt, J. M.—No. 32
Warga, Mary E.—No. 37
White, John U. and Max D. Liston—No. 28
——**see Liston, Max D.**
Wilson, E. Bright, Jr.—No. 9
Wilson, J. C.—see Schaffert, R. M.
Wolfe, R. A.—No. 57
——**see Enns, J. H.**
Woodman, J. F.—see Stroupe, J. D.
Woodson, Robert A.—No. 54
Young, C. W.—No. 14

Minutes of the Thirty-Second Meeting of the Board of Directors of the Optical Society of America, Incorporated

HOTEL FORT SHELBY, DETROIT, MICHIGAN, OCTOBER 20, 1948

IN addition to the transaction of routine business, the following items of general interest to members of the Society were considered.

Announcements by Secretary

Results of letter ballots:

1. Approval of appointment of Committee on Uniform Color Scales:

D. B. Judd, *Chairman*

I. A. Balinkin	W. C. Granville
B. R. Bellamy	D. L. MacAdam
F. L. Dimmick	S. M. Newhall
C. E. Foss	D. Nickerson
I. H. Godlove	J. L. Saunderson

2. Approval of appointment of Committee on Honorary Membership:

H. E. Ives, *Chairman*

A. H. Pfund	L. A. Jones

3. Approval of appointment of Committee on Transfer to Regular Membership:

R. C. Gibbs, *Chairman*

Wallace R. Brode	Seibert Q. Duntley

4. Approval of resolution to award the Adolph Lomb Medal for 1948 to:

David S. Grey

5. Approval of resolution to hold annual meeting of Society at the Hotel Statler, Buffalo, New York, on October 27, 28, and 29, 1949.

6. Approval of appointment of Program Committee for Winter Meeting, Hotel Pennsylvania, New York, New York, on March 10, 11, and 12, 1949:

Julian H. Webb, *Chairman*
G. R. Fonda, *Vice Chairman*

David L. MacAdam	Daniel Smith
Philip Nolan	George S. Monk

7. Approval of nomination of Brian O'Brien to succeed Deane B. Judd as O.S.A. representative on the Division of Physical Sciences of the National Research Council for a term of three years to expire on July 1, 1951.

8. Approval of appointment of Ralph M. Evans to membership on the O.S.A. Colorimetry Committee.

Announcements by President

1. Appointment of Roger S. Estey as official representative of the O.S.A. at the dedication of the Michelson Laboratory, U. S. Naval Ordnance Test Station, Inyokern, California, on May 8, 1948.

2. Appointment of W. E. Forsythe as official representative of the O.S.A. at the Inauguration Ceremonies for T. Keith Glennan as President of the Case Institute of Technology in Cleveland, on May 20 and 21, 1948.

3. Appointment of William F. Meggers as official representative of the O.S.A. at the Centennial Celebrations of the A.A.A.S. in Washington, D. C., September 13–17 inclusive, 1948.

Actions by the Board of Directors

1. Appointment of George R. Harrison as Editor of Publications for a term to expire on December 31, 1952.

2. Appointment of O.S.A. representatives on the Inter-Society Color Council for a term to expire in October, 1950:

*Deane B. Judd, *Chairman*

E. Q. Adams	*Arthur C. Hardy
Blanche R. Bellamy	Richard S. Hunter
Carl E. Foss	*David L. MacAdam
G. A. Fry	Dorothy Nickerson

J. L. Saunderson

3. Nomination of A. H. Pfund to succeed himself as O.S.A. representative on the Governing Board of the American Institute of Physics for a term to expire in February, 1952.

4. Appointment of U. S. National Committee of the International Committee on Optics:

Stanley S. Ballard, *Chairman*

I. C. Gardner	Deane B. Judd
Max Herzberger	Rudolf Kingslake
H. E. Ives	George Wald
Francis Arthur Jenkins	Mary Warga

Dues

Because of constantly rising costs of publication, it was voted to increase the annual dues of associate members to $7.00, the annual dues of regular members to $10.00, and the annual dues of corporation members to $75.00, effective January 1, 1950. Pending study by a duly appointed committee, applications for life membership will not be accepted.

Membership

The Secretary reported informally a net gain in membership of eighty-eight members between January 1, 1948, and October 1, 1948. On recommendation of the Committee on Transfer, forty-one associate members were approved for transfer to regular membership. The names of those transferred will appear in the annual report of the Secretary for 1948.

ARTHUR C. HARDY, *Secretary*

* Voting delegates.

Author Index to Volume 38

References with (A) are abstracts of papers presented at meetings of the Optical Society of America; (T) designates title only; (L) designates Letters to the Editor.

Aklin, G. H. Effect of high index glasses on the field characteristics of photographic objectives—841
Alpen, E. L. (see Strait, L. A.)—666(A)
Ambrose, E. J. (see Elliott, A.)—212
Anderson, James C. (see Harrison, George R.)—1105(A)
Arenberg, David L. Observations of anticoronae on Mt. Washington—481(L)
Astheimer, R. W. (see Hawkes, J. B.)—617, 804
Aughey, Henry. Rapid mobile analyzer for minute amounts of lead in air—1100(A)

Badger, Richard M. (see Giguere, Paul A.)—987(L)
Baez, A. V. (see Kirkpatrick, Paul)—766
Ball, Joseph J. (see Plyler, Earle K.)—988(L)
Ballard, Stanley S. (see Combes, Lewis S.)—1101(A)
Barach, J. L. (see Mersereau, E. P.)—568(A)
Bartlett, N. R. (see Sweet, A. L.)—329
Barr, N. F. (see Reymann, George L.)—660(A)
Bartley, S. Howard. Book review—328
Bass, Arnold M. Short wave-length cut-off filters for the ultraviolet—977
Baumgartner, R. R. (see Sihvonen, Y. T.)—1100(A)
Beggs, J. S. (see Nusbaum, R. E.)—740(L)
Benford, James R. Book review—560
—— **and John E. Bock.** Normal probability curve as an approximation to the distribution curve of the high intensity searchlight—527
——, **Gwen P. Lloyd, and Sally Schwarz.** Coefficients of reflection of magnesium oxide and magnesium carbonate —445
——, **Sally Schwarz, and Owen P. Lloyd.** Coefficients of reflection in the ultraviolet of magnesium carbonate and oxide—964
Bennett, A. H., D. L. Woernley, and A. J. Kavanagh. Ultraviolet phase microscopy—739(L)
Bigeleisen, Jacob (see Vier, Dwayne T.)—811
Billings, B. H. and E. H. Land. Comparative survey of some possible systems of polarized headlights—819
Biltz, M. and J. H. Webb. Photographic reciprocity-law failure for radiations of different wave-length—561
Blackwell, H. Richard. Relations between visual sensitivity and viewing distance—1097(A)
——Study of methods of visual threshold determination —1097(A)
—— **and Benjamin S. Pritchard.** Automatic presentation, recording, analysis device for vision experimentation—1097(A)
Bloem, Harold H. Investigation of the visibility of physical defects in optical instruments—669(A)
Blout, Elkan R. and Dwight P. Merrill. Infra-red spectra of linearly oriented high polymers—663(A)
Bock, John E. (see Benford, Frank)—527
Bodó, Z. On the inadequacy of the measurement of emission characteristics of fluorescent substances without spectral resolution—815(L)
Boeder, Paul (see Ogle, Kenneth N.)—723
Bouman, M. A. and H. A. van der Velden. Two-quanta hypothesis as a general explanation for the behavior of threshold values and visual acuity for the several receptors of the human eye—570
—— **and H. A. van der Velden.** Quanta explanation of vision and the brightness impression for various times of observation and visual angles—231
Brennan, Josephine G. and Sidney M. Newhall. I. C. I. specifications of difference limens for Munsell hue, value, and chroma—696
Brewer, W. L. and F. R. Holly, Jr. Syntheses of spectral-distribution curves—858
Brode, Wallace R. Presentation of absorption spectra data —1098(A)
Brown, W. R. J. and D. L. MacAdam. Visual sensitivities to combine chromaticity and luminance difference—1093(A)
Brozek, Josef (see Simonson, Ernst)—384, 830
Bryan, Ford R. and George A. Nahstoll. Industrial application of Geiger-Müller counters to the analysis of phosphorus in steels—510
Buchdahl, H. A. Algebraic theory of the primary aberrations of the symmetrical optical optical system—14
Bueche, F. Optical properties of Ni, Co, Fe, Mn, and Cd—806
Burnham, Robert W. Comparison of color systems with respect to uniform visual spacing—1093(A)
Burstein, Elias. Infra-red properties of polar crystals—1101(A)

Caldecourt, V. J. (see Grossman, H. H.)—1104(A)
Chang, F. N. H. (see Strait, L. A.)—1098(A)
Chapanis, Alphonse. Comparative study of five tests of color vision—626
Chapman, R. M. (see Migeotte, M. V.)—1094(A)
Clapper, Franklin R. (see Hopkins, Robert E.)—661(A)
Clark, M. D. (see Evans, J. C.)—664(A)
Coleman, Howard S. and Samuel W. Harding. Loss in resolving power caused by primary astigmatism, coma, and spherical aberration in telescopic systems—217
—— **and W. S. Verplanck.** Comparison of computed and experimental detection ranges of objects viewed with telescopic systems from aboard ship—250
Combes, Lewis S. and Stanley S. Ballard. Measurements of the physical properties of infra-red optical materials —1101(A)
Condit, H. R. (see Jones, Loyd A.)—123
Condon, F. E. (see McMurry, H. L.)—1095(A)
Covell, William (see Hopkins, Robert E.)—1102(A)
Crook, A. W. Reflection and transmission of light by any system of parallel isotropic films—954
Crossmon, Germain C. "Optical staining" of tissue—417(A)

Dench, Edward C. (see Hardy, Arthur C.)—308
Dennison, D. M. (see Hadley, L. N.)—483, 546

DeVore, J. R. Calibration of a photo-multiplier photometer—692
Dexter, F. C. and E. I. Stearns. Example of metamerism: Extreme example of color change with varying illuminant—816(L)
Dieke, G. H. Spectroscopic temperature measurements—661(T)
—— (see Rank, D. H.)—966
—— **and D. H. Rank.** Determination of the depolarization factors of highly polarized Raman lines—281
Douglas, C. A. Atmospheric transmissometer: Its calibration and applications—667(A)
Dreyfus, Marc G. Paraxial differential transfer coefficients of a lens system—703
Duntley, Seibert Q. Reduction of apparent contrast by the atmosphere—179
—— Spectrophotometric studies of living human skin—660(A)
—— Visibility of distant objects—237
Dyer, C. A. (see Mouzon, J. C.)—1099(A)

Eastmond, E. John and Bernice E. Williams. Wide range analysis for zinc using spectrographic line widths—666(A), 800
Edwards, Edward A. Spectrophotometry of living human skin as a research tool in medicine—660(A)
Eisen, Fred C. (see Wolfe, Robert N.)—667(A), 706
Elliott, A., E. J. Ambrose, and R. Temple. Polarization of infra-red radiation—212
Enns, J. H. and R. A. Wolfe. Air interrupter type spectrographic light source—1102(A)
Epstein, L. Ivan. Out-of-focus diffraction patterns—1103(A)
Evans, John W. Photometer for measurement of sky brightness near the sun—1102(A),1083
Evans, J. C. and M. D. Clark. Molding optical elements of thallium bromide iodide (KRS5)—664(A)
Evans, Lyle W. (see Shulman, James H.)—817(L)
Evans, Ralph M. Seeing light and color—1101(T)

Fano, U. On the theory of imperfect diffraction gratings—921
Fassel, Velmer A. Criteria for high precision analyses with d.c. arc excitation—1102(A)
—— **and Harley A. Wilhelm.** Quantitative spectrographic analysis of the rare earth elements. I. Determination of samarium in neodymium. II. Determination of europium in samarium—666(A), 518
Feder, Donald. Curved field lens and camera—1102(A)
Feldman, Cyrus. Spectrochemical determination of hafnium-zirconium ratios—1100(A)
Fonda, Gorton R. and Frank J. Studer. Double activation of zinc fluoride phosphors—665(A)
—— **and Frank J. Studer** Optical properties of zinc fluoride phosphors—1007
Foote, Paul C. and Robert A. Woodson. Lens design and tolerance analysis methods and results—590
Forrest, John W., Norbert V. Kreidle, and Tyler G. Pett. Color variations in glasses containing iron—554
Foss, Carl E. Classification of color order systems—1093(T)
Foster, L. V. and E. M. Thiel. Achromatic ultraviolet microscope objective—689
Freeman, Ellis. Illuminant-stable color vision test. I—532
—— **and M. A. Zaccaria.** Illuminant-stable color vision test. II. Experimental-statistical evaluation—971
Friedel, R. A. (see McKinney, D. S.)—222
Fry, D. L. Infra-red absorption analyses used in control of a pilot plant triptane process—1098(A)
—— (see Sihvonen, Y. T.)—1100(A)
Fuson, Nelson. Infra-red sensitivity of superconducting bolometers—845

Gardner, Irvine C. and Francis E. Washer. Lenses of extremely wide angle for airplane mapping—421
Geffner, Joseph. Evaluation of the elementary causes of deviations in spectrochemical analysis—665(A)
Gibson, Kasson S. Questionnaire on illumination—67(L)
—— (see Teele, Ray P.)—1096(A)
Giguère, Paul A. and Richard M. Badger. Elimination of water vapor in infra-red spectrometers—987(L)S
Ginther, Robert J. (see Shulman, James H.)—817(L)
Golay, Marcel J. E. Rotating two dimensionally patterned gratings—1099(A)
Goldberg, Benjamin. Electroformed precision prisms—409
Goldberg, Leo. Solar infra-red spectroscopy—1101(T)
Green, Milton. Three-line method of obtaining characteristic curves for heterochromous photometry—1105(A)
Grey, David S. Aspheric surfaces in optical systems for television projection—667(A)
——Athermalization of optical systems—542
Grossman, H. H., E. W. Peterson, J. L. Saunderson, and V. J. Caldecourt. Optical and electrical alterations to a Michigan microphotometer—1104(A)
Gunter, Roy C., Jr. Electro- and magneto-optical shutters for aerial cameras—419(L)

Hadley, L. N. and D. M. Dennison. Erratum: Reflection and transmission interference filters. Part I. Theory—546
—— **and D. M. Dennison.** Reflection and transmission interference filters. Part II. Experimental, comparison with theory, results—483
Haendler, H. M. Nomographs for spectral band width of the Beckman DU spectrophotometer—417(L)
Hamburger, Ferdinand, Jr. and Ellwood J. King. Recording photometer and its use in studies of cathode-ray screen displays—875
Hammad, A. Scattered and rescattered sunlight—611
Hanau, Richard and Ralph A. Wolfe. Investigation of the use of Geiger-Müller photoelectron counters in the spectrographic analysis of phosphorus in steel—377
Hanes, R. M. and S. B. Williams. Visibility on cathode-ray tube screens: The effects of light adaptation—363
Hansen, G. Multiprism spectrographs with glass optics by Carl Zeiss, Jena—759
Harding, Samuel W. (see Coleman, Howard S.)—217
Hardy, Arthur C. Applicability of Judd's color tolerance formula in the case of titanium pigments—650(L)
—— Book review—874
—— Early history of recording spectrophotometry—675(T)

—— **and Edward C. Dench.** Electionic method for solving simultaneius equations—308
—— **and F. L. Wurzburg, Jr.** Color correction in color printing—300
—— **and F. L. Wurzburg, Jr.** Photoelectric method for preparing printing plates—295
—— **and F. Mansfield Young.** In defense of Beer's law—854
Harper, D. C. and J. H. McLeod. Method of calculating the allowable number of Newton rings for telescope optics—669(A)
—— **and W. T. Sherwood.** Method of calculating the permissible size of appearance defects for visual instruments —669(A)
Harris, Louis, Rosemary T. McGinnies, and Benjamin M. Siegel. Preparation and optical properties of gold blacks —582
Harrison, George R. and James C. Anderson. Photoelectric determination of interference maxima—1105(A)
Hartmann, Werner and Betty E. Prescott. Quantitative spectrochemical determination of barium, strontium, and calcium—539
Hasler, M. F. and J. W. Kemp. Combination spark-arc source unit for spectrochemistry—1102(A)
——, **J. W. Kemp, and D. R. Procter.** Instrumentation for direct-reading spectrochemistry—1103(A)
——, **R. W. Lindhurst, and J. W. Kemp.** Quantometer, a direct reading instrument for spectrochemical analysis —789
Hawkes, J. B. and R. W. Astheimer. Improved Jamin interferometer—617
—— **and R. W. Astheimer.** Temperature coefficient of the refractive index of water—804
Hecht, Selig (see Lamar, Edward S.)—741
Helson, Harry and Walter C. Michels. Effect of chromatic adaptation on achromaticity—1025
Hemmendinger, Henry. Orientation of insoluble dyes in cellulose—659(A)
Hendley, Charles. (see Lamar, Edward S.)—741
Henry, R. L. Transmission of powder films in the infra-red —775
Herman, Robert C., Charles F. Meyer, and Helen S. Hopfield. Theory of electron retrapping in phosphors—999
—— **and Shirleigh Silverman.** Cinema-spectrograph for photographing rapid spectral sequences—209
Herzberger, Max. Image error theory for finite aperture and field. I. Image of a point; geometry of the wave surface—736
—— Performance of an optical system as the sum of the contributions of its construction elements—324
—— Preconstruction of triplet—1104(A)
Higgins, George C. (see Jones, Loyd A.)—398
—— **and L. Stultz.** Visual acuity as measured with various orientations of a parallel-line test object—756
Hoadley, H. Orlo (see Perrin, Fred H.)—1040
Holly, F. R. (see Brewer, W. L.)—858
Hopfield, Helen S. (see Herman, Robert C.)—999
Hopkins, Robert E. and Franklin R. Clapper. Gratings made by photographing interference fringes 661—(A)
——, **John C. Evans, William Covell, and Donald Feder.** Curved field lens and camera—1102(A)
Hulburt, E. O. Brightness and altitude of the luminosity of the night sky—1096(A)
—— (see Tousey, R.)—886
Humphreys, Curtis J. Spectral response of a cadmium sulfide crystal—664(A)
—— **and Earle K. Plyler.** Flame spectrum of acetylene from 1 to 5 microns—1094(A)
Hunter, Richard S. Accuracy, precision, and stability of new photoelectric color-difference meter—1094(A)
—— Photoelectric color-difference meter—661(A)
Huxford, W. S. and John R. Platt. Survey of near infra-red communication systems—253
Hyde, W. L. Polarization techniques in the infra-red— 663(A)

Ingalls, A. L. and K. Pestrecov. Centering of optical systems—343
Irish, P. R. Spectrographic analysis of alumina in silica brick—1104(A)
Ives, Herbert E. Behavior of an interferometer in a gravitational field. II. Application to a planetary orbit—413
—— Measurement of the velocity of light by signals sent in one direction—879

Jacobsen, A. E. Non-adaptability of the I.C.I. system to some near-whites which show absorption in the far blue region of the spectrum—442
Jamison, N. C., T. R. Kohler, and O. G. Koppius. Infrared instrument for industrial product control—1099(A)
Jerrard, H. G. Optical compensators for measurement of elliptical polarization—35
Johnson, E. Parker. (see Riggs, Lorrin A.)—662(A)
Johnson, F. S. and R. Tousey. Method for evaluating the intensity of focused stray light from concave diffraction gratings—1103(A)
Jones, Loyd A. and H. R. Condit. Sunlight and skylight as determinants of photographic exposure. I. Luminous density as determined by solar altitude and atmospheric conditions—123
—— **and George C. Higgins.** Photographic granularity and graininess. IV. Visual acuity thresholds; dynamic *versus* static assumptions—398
—— **and C. N. Nelson.** Control of photographic printing: Improvement in terminology and further analysis—897
Jones, R. Clark. Absolute sensitivity of existing heat detectors—1099(A)
—— New calculus for the treatment of optical systems. VII. Properties of the N-matrices—671
Judd, Deane B. Comparison of direct colorimetry of titanium pigments with their indirect colorimetry bases on spectrophotometry and a standard observer—1093(A)
—— Report on Paris Meeting of the International Commission on Illumination, July, 1948—1094(T)
—— Bezold-Brücke phenomenon and the Hering theory of vision—1095(A)
Jupnik, Helen, Harold Osterberg, and G. E. Pride. Phase microscopy with vertical illumination—338
Jurmain, Jacob H. and John Sterner. Stainless steel analysis with the direct reading spectrometer—1101(A)
—— Transmission filters for the ultraviolet—929

Kasha, Michael. Fabrication of boric acid glass for luminescence studies—1068
Katz, Amrom H. Aerial photographic equipment and applications to reconnaissance—604
Kavanagh, A. J. (see Bennett, A. H.)—739(L)
Keegan, Harry J. Standards of reflectance—658(A)
Kemp, J. W. (see Hasler, M. F.)—1103(A), 789
Kennard, R. B. Schlieren method of shock wave analysis—662(T)
Kenyon, Westcott C. (see Osborn, Robert H.)—660(A)
King, Ellwood J. (see Hamburger, Ferdinand, Jr.)—875
Kirkpatrick, Paul and A. V. Baez. Formation of optical images by x-rays—766
Kivenson, Gilbert, Ralph T. Steinback, and Myrtle Rider. Infra-red chopped-radiation analyzer—1086
Klasens, H. A. (see Wise, M. E.)—226
——, **W. Ramsden, and Chow Quantie.** Relation between efficiency and exciting intensity for zinc-sulfide phosphors—60, Erratum—649(L)
Klein, Myron W. (see Smakula, Alexander)—1101(A)
Knoll, H. A. (see Koomen, M.)—719
Knox, A. G. (see Stroupe, J. D.)—1095(A)
Kohler, T. R. (see Jamison, N. C.)—1099(A)
Koomen, M. R. Tousey, and H. A. Knoll. Infra-red pupillometer—719
Koppius, O. G. Detection of lead in air with the aid of a Geiger-Müller counter—1100(A)
—— (see Jamison, N. C.)—1099(A)
Kreidl, Norbert J. (see Forrest, John W.)—554
Kubelka, Paul. New contributions to the optics of intensely light-scattering materials. Part I—448, Erratum—1067
Kumler, W. K. (see Strait, L. A.)—1098(A)
Kvalheim, Aslak. Erratum: Spectrochemical determination of the major constituents of minerals and rocks—479

Ladenburg, R. Wind tunnel optics—especially interferometry—662(T)
Lamar, Edward S., Selig Hecht, Charles D. Hendley, and Simon Shlaer. Size, shape, and contrast in detection of targets by daylight vision. II. Frequency of seeing and the quantum theory of cone vision—741
Land, Edwin H. Reply to Lloyd E. Varden's "Comments regarding 'a new one-step photographic process'"—70(L)
—— (see Billings, B. H.)—819
Larson, D. A. (see Studer, Frank J.)—665(A), 480(L)
Laufer, Maurice K. Book review—989
Law, R. R. and I. G. Maloff. Projection screens for home television receivers—497
Le Grande, Yves. Standard response functions for protanopic and deuteranopic vision—815(L)
Leurgans, P. J., A. F. Turner, and O. A. Ullrich. Interference fringes near a critical angle boundary—1104(A)
Lindhurst, R. W. (see Hasler, M. F.)—789
Liston, Max D. (see White, John U.)—1098(A)
—— **and John U. White.** Detection and control system for a double beam infra-red spectrometer—1098(A)
Lloyd, Gwen P. (see Benford, Frank)—445, 964
Lock, C. (see Packer, D. M.)—1097(A)
Loofbourow, J. R. (see Sinsheimer, R. L.)—1105(A)
Lukiesh, Matthew. Recommended footcandle levels for prolonged critical seeing—712

MacAdam, David L. Colorimetric behaviors of dye mixture—659(A)
—— (see Brown, W. R. J.)—1093(A)
Macht, David I. and Marcus Ostro. Pharmacological properties of blood sera and drugs treated with various x-rays—663(A)
—— treated with various x-rays—663(A)
Mahan, A. I. and E. E. Price. Focal plane diffraction doubling in the Amici roof prism—667(A)
Maloff, I. G. (see Law, R. R.)—497
Martin, A. E. Stray radiation in Littrow-type spectrometers which employ collimating mirrors—70(L)
Mather, K. B. Applications of the photographic pressure effect—1066
—— Mechanism of latent image formation in a photographic emulsion by mechanical pressure—1054
McCartney, J. S. (see Rank, D. H.)—279, 287
McGinnies, Rosemary T. (see Harris, Louis)—582
McLeod, J. H. (see Harper, D. C.)—669(A)
—— (see Miller, O. E.)—1104(A)
McKinney, D. S. and R. A. Friedel. Calibration method for infra-red prism spectrometers—222
McMurry, H. L., V. Thornton, and F. E. Condon. Infra-red of normal propane, 1-deuteropropane, and 2-deuteropropane—1095(A)
McNally, J. Rand, Jr. Preliminary investigation of the spectra of uranium isotopes—1100(A)
Meggers, William F. Light wave of artificial mercury as the ultimate standard of length—7
—— Wave-lengths emitted by mercury 198—665(A)
Merrill, Dwight P. (see Blout, Elkan R.)—663(A)
Merrill, John B. and James H. Schulman. $CaSiO_3$: (Pb + Mn) phosphor—471
Meyer, Charles F. (see Herman, Robert C.)—999
Mersereau, E. P. and V. L. Barach. Application of spectrophotometry in the textile industry: Testing dyestuff shipments—658(A)
Michels, Walter C. (see Helson, Harry)—1025
Middleton, W. E. Knowles. Measurement of strongly reflecting transmission samples with the commercial recording spectrophotometer—74(L)
—— Photometry and colorimetry of railroad fuses—660(A)
—— **and F. D. Smith.** Diffusion of light by ground glass, with special reference to color changes—1094(A)
Migeotte, M. V. and R. M. Chapman. Infra-red absorption of atmospheric gases—1094(A)
Miller, O. E., J. H. McLeod, and W. T. Sherwood. Thin sheet plastic Fresnel lenses of high aperture—1104(A)
Miller, Wm. C. New spectrophotometer employing a glass Féry prism—1102(A)
Molby, Fred A. Refractive index of optical glass at low temperature—1102(A)
Moon, Parry. Table of Planckian radiation—291
—— **and Domina Eberle Spencer.** Color of unstained wood—405; Visual performance and the surround—650(L)

Mouzon, J. C. and C. A. Dyer. Low temperature radiation pyrometry—1099(A)
Muchmore, Robert B. Optimum band width for two-layer antireflection films—20
Mueller, Hans. Foundation of optics—661(A)
Murray, Allen E. Reflected light and ghosts in optical systems—1103(A)

Nahstoll, George A. (see Bryan, Ford R.)—510
Nelson, C. N. (see Jones, Loyd A.)—897
Newhall, Sidney M. (see Brennan, Josephine G.)—696
Nickerson, Dorothy. Illuminant in textile color matching—458
Nicoll, F. H. Note on ultraviolet absorption of zinc oxide phosphors—417(L)
—— Temperature dependence of the emission bands of zinc oxide phosphors—817(L)
Nusbaum, R. E. (see Sihvonen, Y. T.)—1100(A)
—— **and J. S. Beggs.** Test on the process of photographing the trajectory of a rapidly moving distant light source—740(L)

O'Brian, Brien and E. Dickerman O'Brien. Test of ocular tremor and the scanning theory of visual acuity—1096(A); Variation in sensitivity among cones in the human fovea, and the Hecht theory of visual acuity—1096(A)
O'Brien, E. Dickerman (see O'Brien, Brian)—1096(A)
Oetjen, Robert A. Infra-red "lens"—1099(A)
Ogle, Kenneth N. and Paul Boeder. Distortion of stereoscopic spatial localization—723
Organ, T. J. and S. L. Parsons. Method of spectrographic analysis of impurities in materials for oxide coating of thermionic cathodes—191
Osborn, Robert H. and Westcott C. Kenyon. Spectrophotometric study of the color of rosin—660(A)
Osterberg, Harold. Multipupil in phase microscopy—668(A), 685
—— Phase microscopy with critical illumination—1099(A)
—— (see Jupnik, Helen)—338
—— **and J. Ernest Wilkins, Jr.** Resolving power of a coated objective—668(A)
Ostro, Marcus (see Macht, David I.)—663(A)
Oughton, C. D. (see R. M. Schaffert)—991

Packer, D. M. and C. Lock. Daytime zenith sky brightness at 18,000- to 38,000-feet altitudes—1097(A)
Parsons, S. L. (see Organ, T. J.)—191
Peck, Edson R. New principle in interferometer design—66(L)
—— Theory of the corner-cube interferometer—1015
Penner, S. S. and S. Weinbaum. Some considerations of the effect of radiation on the performance of liquid fuel rockets—599, Erratum—840(L)
Perrin, Fred, H. Whose absorption law?—72(L)
—— **and H. Orlo Hoadley.** Photographic sharpness and resolving power. I. The design and performance of an apochromatic resolving-power camera objective—1040
Pestrecov, K. Computation of distortion of an "out-of-focus" image—669(A)
—— (see Ingalls, A. L.)—343
Peterson. E. W. (see Grossman, H. H.)—1104(A)
—— (see Saunderson, J. L.)—1093(A)
Pett, Tyler G. (see Forrest, John W.)—554
Platt, John R. (see Huxford, W. S.)—253
—— (see Snyder, Hartland S.)—269
Plyler, Earle K. Infra-red absorption spectra of some benzene derivatives—1095(A)
—— Spectrometry with a thallium bromide iodide prism—664(A)
—— (see Tilton, Leroy W.)—663(A)
—— **and Joseph J. Ball.** Infra-red absorption of deposited blacks—988(L)
Plymale, W. S., Jr. Electronic apparatus for determining phosphorescent decay—664(A)
Prescott, Betty E. (see Hartmann, Werner)—539
Price, E. E. (see Mahan, A. I.)—667(A)
Pride, G. E. (see Jupnik, Helen)—338
Pritchard, Benjamin S. (see Blackwell, H. Richard)—1097(A)
Procter, D. R. (see Hasler, M. F.)—1103(A)

Quantie, Chow (see Klasens, H. A.)—60, 649

Ramsden, W. (see Klasens, H. A.)—60, 649
Rank, D. H. Empirical relationships between the partial dispersions of the ordinary types of optical glasses—885
—— (see Douglas, A. E.)—281
—— **and A. E. Douglas.** Light scattering in optical glass—966
—— **and J. S. McCartney.** Some spectral characteristics of mercury arcs for use in study of the Raman effect—279
——, **J. S. McCartney, and G. J. Szasz.** Intensity and polarization of Brillouin spectra—287
Rankin, Charles W. Spectrographic determination of fluorine in organic substances—1104(A)
Reiss, Max. Notes on the $\cos^4$ law of illumination—980
Revmann, George L., Kenneth H. Smith, and N. F. Barr. Spectrophotometric method for determination of lead—660(A)
Richards, Oscar W. Image contrast control with phase microscopy—668(A)
Richardson, David. Plano-interferometer—1104(A)
—— **and Robert B. Tackaberry.** Micro-interferometer study of diffraction gratings—662(A)
Richardson, E. E. Some techniques and accessories to facilitate the application of a G. E. recording spectrophotometer—657(A)
Richartz, M. Improvement of Savart's polariscope—623
Rider, Myrtle (see Kivenson, Gilbert)—1086
Riggs, Lorrin A. and E. Parker Johnson. Electrical response of the human retain to lights of various wavelengths—662(A)
Rose, Albert. Sensitivity performance of the human eye on an absolute scale—196
Rozsa, J. T. Practical applications of a seplica grating spectrograph installation—666(A)

Sah, P. P. T. (see Strait, L. A.)—1098(A)
Sambursky, S. and G. Wolfsohn. Measurement of fluorescence spectra—739(L)

Saunderson, J. L. and E. W. Peterson. Optical measurements of light scattering liquids—1093(A)
—— (see Grossman, H. H.)—1104(A)
Schade, Otto. Method of measuring and specifying the quality of optical images—1103(T)
Schaffert, R. M. and colleagues, and J. C. Wilson. Xerography—a new principle of photography and graphic reproduction—991, 1101(T)
Schulman, James H. (see Merrill, John B.)—471
Schultz, Melvin L. (see Vier, Dwayne T.)—811
Schulz, L. G. Preparation of aspherical refracting optical surfaces by an evaporation technique—432
Schwarz, Sally (see Benford, Frank)—445, 964
Scott, J. E. (see Sinsheimer, R. L.)—1105(A)
Seitz, Frederick, Jr. Optics and semi-conductors—1101(T)
Sherwood, W. T. (see Harper, D. C.)—669(A)
—— (see Miller, O. E.)—1104(A)
Shlaer, Simon (see Lamar, Edward S.)—741
Shulman, James H., Robert J. Ginther, and Lyle W. Evans. Infra-red stimulability of $CaSiO_3$:Pb and $CaSiO_3$:(Pb+Mn)—817(L)
Siegel, Benjamin M. (see Harris, Louis)—582
Sihvonen, Y. T., D. L. Fry, R. E. Nusbaum, and R. R. Baumgartner. Spectrographic analysis of vitallium alloys—1100(A)
Silberstein, Ludwik. Errata: On two accessories of three-dimensional colorimetry—71(L)
Silverman, Shirleigh. Emissivity of globar—989(L)
—— Rapid scanning infra-red spectrometer for emission spectra—664(A)
—— (see Herman, Robert C.)—209
Simon, Frederick T. Applications of spectrophotometry in a textile plant—659(A)
Simonson, Ernst and Josef Brozek. Effect of spectral quality of light on visual performance and fatigue—830
—— **and Josef Brozek.** Effects of illumination level on visual performance and fatigue—384
Sinclair, D. A. Condensed arc source unit for spectrochemical analysis—547
Sinsheimer, R. L., J. E. Scott, and J. R. Loofbourow. Ultraviolet absorption spectra of biological compounds at low temperatures—1105(A)
Sloan, Louise L. and Lorraine Wollach. Case of unilateral deuteranopia—502
Smakula, Alexander and Nyron W. Klein. On the inelastic deformation and crystal orientation of thallium halides—1101(A)
Smith, F. D. (see Middleton, W. E. Knowles)—1094(A)
Smith, Kenneth H. (see Reymann, George L.)—660(A)
Smith, Robert W. Progress and prospects in the spectrochemical analysis of non-metallic materials—1104(T)
Snyder, Hartland S. and John R. Platt. Principles of optical communication systems. General properties of non-image forming projectors and receivers—269
Spencer, Domina Eberle (see Moon, Parry)—405, 650(L)
Starkiewicz, J. Lead selenide photo-conductive cells—481(L)
Steadman, L. T. Spectrochemical method for the determination of uranium—1100(A)
Steinback, Ralph T. (see Kivenson, Gilbert)—1086
Sterns, E. I. (see Dexter, F. C.)—816(L)
Stempel, Walderman M. Differential adjustment method of refining optical systems—935
Stephens, Robert E. Design of triplet anastigmat lenses of the Taylor type—1032
—— Reduction of sphero-chromatic aberration in catadioptric systems—666(A), 733
—— (see Tilton, Leroy W.)—663(A)
Sterner, John (see Jurmain, Jacob H.)—1101(A)
Strait, L. A., W. K. Kumler, P. P. T. Sah, E. L. Alpen, and F. N. H. Chang. Ultraviolet absorption spectra and the structures of the isomeric amidones—1098(A)
Stroupe, J. D., A. G. Knox, and J. F. Woodman. Practical aspects of the preparation and application of an infra-red bibliography—1095(A)
Studer, Frank J. Method for automatically plotting spectral energy distrubution of luminescent materials—467
—— (see Fonda, Gorton R.)—665(A), 1007
—— **and D. A. Larson.** Emission spectra of zinc cadmium sulfides—665(A), 480(L)
Stultz, K. (see Higgins, G. C.)—756
Sutherland, G. B. B. M. Recent infra-red work at Cambridge—1100(A)
Sweet, A. L. and N. R. Bartlett. Visibility on cathode-ray tube screens: Signals on a P7 screen seen at different intervals after excitation—329
Szasz, G. J. (see Rank. D. H.)—287
Szekeres, George. New determination of the Young-Hemholtz primaries—350

Tackaberry, Robert B. (see Richardson, David)—662(A)
Teele, Ray P. and Kasson S. Gibson. Standard luminosity filter—1096(A)
Temple, R. (see Elliott, A.)—212
Thiel E. M. (see Foster. L. V.)—689
Thorton, V. (see McMurry, H. L.)—1095(A)
Tilton, Leroy W., Earle K. Plyler, and Robert E. Stephens. Refractive indices of two thallium bromide-iodide crystals for visible and infra-red radiant energy—663(A)
Tousey, R. (see Johnson, F. S.)—1103(A)
—— (see Koomen, M.)—719
—— **and E. O. Hulburt.** Visibility of stars in the daylight sky—886
Turner, A. F. and O. A. Ullrich. Continuously variable interference filters—662(A)
—— (see Leurgans, P. J.)—1104(A)

Ullrich, O. A. (see Turner, A. F.)—662(A)
—— (see Leurgans, P. J.)—1104(A)

van der Velden, H. A. (see Bouman, M. A.)—231, 570
Varden, Lloyd E. Comments regarding "a new one-step photographic process" by Edwin H. Land—69(L)
Verplanck, W. S. (see Coleman, H. S.)—250
Vier, Dwayne T., Melvin L. Schultz, and Jacob Bigeleisen. Flourescence of uranium trioxide hydrates—811

Warga, Mary E. Recent trends in applied emission spectroscopy—1099(T)
Washer, Francis E. (see Gardner, Irvine C.)—421
Webb, J. H. Absolute sensitivity measurements on single-grain-layer photographic plates for different wavelengths—312
—— Effect of light absorption on the shape of the photographic H and D curve—27
—— (see Biltz, M.)—561
Weinbaum, S. (see Penner, S. S.)—599, 840(L)
Weyl, F. J. Task of wind tunnel interferometry—662(T)
White, John U. (see Liston, Max D.)—1098(A)
—— **and Max D. Liston.** Construction and performance of a double beam infra-red spectrometer—1098(A)
Widmyer, J. H. Method for calculating the dominant wave-length of a dichroic amber glass for any thickness —658(A)
Wilhelm, Harley A. (see Fassel, Velmer A.)—518 666(A)
Wilkins, J. Ernest, Jr. (see Osterberg, Harold)—668(A)
Williams, Bernice E. (see Eastmond, E. John)—666(A), 800
Williams, S. B. (see Hanes, R. M.)—363
Wilson, E. Bright, Jr. Recent work on the theory of polyatomic molecules—1094(T)
Wilson, J. C. (see Schaffert, R. M.)—991, 1101(T)
Winterbottom, Arthur B. Optical determination of thin films on reflecting bases in transparent environments—1097
Wise, M. E. and H. A. Klasens. Fluorescence efficiency and hole migration in zinc sulfides—226
Woernley, D. L. (see Bennett, A. H.)—739(L)
Wolfe, R. A. Spectrographic light sources—1102(T)
—— (see Enns, J. H.)—1102(A)
—— (see Hanau, Richard)—377
Wolfe, Robert N. and Fred C. Eisen. Irradiance distribution in a Lloyd mirror interference pattern—667(A) 706
Wolfsohn, G. (see Sambursky S.)—739(L)
Wollach, Lorraine (see Sloan, Louise L.)—502
Woodman, J. F. (see Stroupe, J. D.)—1095(A)
Woodson, Robert A. Optical characteristics of hyperbolic araboloidal mirrors—667(A)
—— Schmidt system tolerances—1102(A)
—— (see Foote, Paul C.)—590
Wright, Norman. Absorption spectra with polarized infra-red radiation—663(A)
—— Transmitting polarizer for infra-red radiation—69(L)
Wurzburg, F. L., Jr. (see Hardy, Arthur C.)—295, 300

Young, C. W. Infra-red spectra of alcohols—1095(A)
Young, F. Mansfield (see Hardy, Arthur C.)—854
Young, N. W. Infra-red spectra of alcohols—1095(A)

Zaccaria, M. A. (see Freeman, Ellis)—971
Zernike, F. Diffraction theory of lens errors—661(A)

JOURNAL OF THE OPTICAL SOCIETY OF AMERICA VOLUME 38, NUMBER 12 DECEMBER, 1948

Analytic Subject Index to Volume 38

References with (A) are to abstracts of papers presented at meetings of the Optical Society of America, (L) designates Letters to the Editor.

Absorption, including absorption spectra
Absorption and excitation of luminescent zinc silicate, Frank J. Studer and D. A. Larson—665(A)
Construction and performance of a double beam infra-red spectrometer, John U. White and Max D. Liston —1098(A)
Effect of light-absorption on the shape of the photographic H. and D. Curve, J. H. Webb—27
In defense of Beer's law, Arthur C. Hardy and F. Mansfield Young—854
Infra-red absorption analyses used in control of a pilot plant triptane process, D. L. Fry—1098(A)
Infra-red absorption of atmospheric gases, M. V. Migeotte and R. M. Chapman—1094(A)
Infra-red absorption of deposited blacks, Earle K. Plyler and Joseph J. Ball—988(L)
Infra-red absorption spectra of some benzene derivatives, Earle K. Plyler—1095(A)
Infra-red spectra of linearly oriented high polymers, Elkan R. Blout and Dwight P. Merrill—663(A)
Nomographs for spectral band width of the Beckman DU spectrophotometer, H. M. Haendler—417(L)
Non-adaptability of the ICI system to some near-whites which show absorption in the far blue region of the spectrum, A. E. Jacobsen—442
Note on ultraviolet absorption of zinc oxide phosphors, F. H. Nicoll—417(L)
Preparation and optical properties of gold blacks, Louis Harris, Rosemary T. McGinnies, and Benjamin M. Siegel—582
Transmission filters for the ultraviolet, Michael Kasha —929
Ultraviolet absorption spectra and the structures of the isomeric amidones, L. A. Strait, W. K. Kumler, P. P. T. Sah, E. L. Alpen, and F. N. H. Chang—1098(A)
Whose absorption law?, Fred H. Perrin—72(L)
Announcements
Alphabetical directory of members—76
Centennial celebration of A.A.A.S.—408
Geographical directory of members—111
Installation of the Ohio Valley Section of the Optical Society of America—735
International Commission of Optics—337
Ives Medalist for 1947—1

July 1948 Meeting of the International Commission of Optics—965
Physics Abstracts—323, 829
Report on colorimetry and artificial daylight—803
Symposium on electron and light microscopy—470
Symposium on luminescence—810
Symposium on modern instrumental methods of analysis —65
Symposium on molecular structure and spectroscopy—65

Biological applications

"Optical staining" of tissue, Germain C. Crossmon—417(L)
Pharmacological properties of blood sera and drugs treated with various x-rays, David I. Macht and Marcus Ostro—663(A)
Ultraviolet absorption spectra of biological compounds at low temperatures, R. L. Sinsheimer, J. E. Scott, and J. R. Loofbourow—1105(A)
Wide range analysis for zinc using spectrographic line widths, E. John Eastmond and Bernice E. Williams —666(A), 800

Book reviews

An introduction to color, by Ralph M. Evans, Arthur C. Hardy—874
Reading and visual fatigue, by Leonard Carmichael and Walter F. Dearborn, S. Howard Bartley—328
Symposium on searchlights, Maurice K. Laufer—989
The microscope—its theory and applications, by J. H. Wredden, James R. Benford—560

Color and colorimetry

Accuracy, precision and stability of new photoelectric color-difference meter, Richard S. Hunter—1094(A)
Applicability of Judd's color tolerance formula in the case of titanium pigments, Arthur C. Hardy—650(L)
Application of spectrophotometry in the textile industry: testing dyestuff shipments, E. P. Mersereau and J. L. Barach—658(A)
Application of spectrophotometry in a textile plant, Frederick-T. Simon—659(A)
Case of unilateral deuteranopia, Louise L. Sloan and and Lorraine Wollach—502
Cinema-spectrograph for photographing rapid spectral sequences, Robert C. Herman and Shirleigh Silverman —209
Coefficients of reflection of magnesium oxide and magnesium carbonate, Frank Benford, Gwen P. Lloyd, and Sally Schwarz—445
Color correction in color printing, Arthur C. Hardy and F. L. Wurzburg, Jr.—300
Color of unstained wood, Parry Moon and Domina Eberle Spencer—405
Color variations in glasses containing iron, John W. Forrest, Norbert J. Kreidl, and Tyler G. Pett—554
Colorimetric behaviors of dye mixture, David L. MacAdam—659(A)
Comparative study of five tests of color vision, Alphonse Chapanis—626
Comparison of color systems with respect to uniform visual spacing, Robert W. Burnham—1093(A)
Comparison of direct colorimetry of titanium pigments with their indirect colorimetry based on spectrophotometry and a standard observer, Deane B. Judd—1093 (A)
Effect of chromatic adaptation of achromaticity, Harry Helson and Walter C. Michels—1025
Electronic method for solving simultaneous equations, Arthur C. Hardy and Edward C. Dench—308
Example of metamerism: extreme example of color change with varying illuminant, F. C. Dexter and E. I. Stearns—816(L)
I.C.I. specification of difference limens for Munsell hue, value, and chroma, Josephine G. Brennan and Sidney M. Newhall—696
Illuminant in textile color matching, Dorothy Nickerson —458
Illuminant-stable color vision test, I, Ellis Freeman—532
Illuminant-stable color vision test, II. Ellis Freeman and M. A. Zaccaria—971
Method for calculating the dominant wave-length of a dichroic amber glass for any thickness, J. H. Widmyer—658(A)
New determination of the Young-Helmholtz primaries, George Szekeres—350
Non-adaptability of the I.C.I. system to some near-whites which show absorption in the far blue region of the spectrum, A. E. Jacobsen—442
On two accessories of three-dimensional colorimetry (errata), Ludwik Silberstein—71
"Optical staining" of tissue, Germain C. Crossmon—417(L)
Orientation of insoluble dyes in cellulose, Henry Hemmendinger—659(A)
Photoelectric color-difference meter, Richard S. Hunter —661(A)
Photoelectric method for preparing printing plates, Arthur C. Hardy and F. L. Wurzburg, Jr.—295
Photometry and Colorimetry of railroad fuses, W. E. Knowles Middleton—660(A)
Some techniques and accessories to facilitate the application of a G.E. recording spectrophotometer, E. E. Richardson—657(A)
Spectrophotometric studies of living human skin, Seibert Q. Duntley—660(A)
Spectrophotometric study of the color of rosin, Robert H. Osborn and Westcott C. Kenyon—660(A)
Spectrophotometry of living human skin as a research tool in medicine, Edward A. Edwards—660(A)
Standards of reflectance, Harry J. Keegan—658(A)
Syntheses of spectral-distribution curves, W. L. Brewer and F. R. Holly, Jr.—858
Visual sensitivities to combined chromaticity and luminance difference, W. R. J. Brown and D. L. MacAdam—1093(A)

Dispersion

Method for automatically plotting spectral energy distribution of luminescent materials, Frank J. Studer —467

Electro-optics
Calibration of a photo-multiplier photometer, J. R. DeVore—692.
Electrical response of the human retina to lights of various wave-lengths, Lorrin A. Riggs and E. Parker Johnson—662(A)
Electro- and magneto-optical shutters for aerial cameras, Roy C. Gunter, Jr.—419(L)
Electronic apparatus for determining phosphorescent decay, W. S. Plymale, Jr.—664(A)
Electronic method for solving simultaneous equations, Arthur C. Hardy and Edward C. Dench—308
Method for automatically plotting spectral energy distribution of luminescent materials, Frank J. Studer —467

Eye
Calibration of a photo-multiplier photometer, J. R. DeVore—692
Case of unilateral deuteranopia, Louise L. Sloan and Lorraine Wollach—502
Distortion of stereoscopic spatial localization, Kenneth N. Ogle and Paul Boeder—723
Effect of chromatic adaptation of achromaticity, Harry Helson and Walter C. Michels—1025
Effect of spectral quality of light on visual performance and fatigue, Ernst Simonson and Josef Brozek—830
Effects of illumination level on visual performance and fatigue, Ernst Simonson and Josef Brozek—384
Electrical response of the human retina to lights of various wave-lengths, Lorrin A. Riggs and E. Parker Johnson—662(A)
Illuminant-stable color vision test, I, Ellis Freeman —532
Illuminant-stable color vision test, II. Ellis Freeman and M. A. Zaccaria—971
Infra-red pupillometer, M. Koomen, R. Tousey, and H. A. Knoll—719
New determination of the Young-Helmholtz primaries, George Szekeres—350
Photographic granularity and graininess. IV. Visual acuity thresholds; dynamic *versus* static assumptions, Loyd A. Jones and George C. Higgins—398
Quanta explanation of vision and the brightness impression for various times of observation and visual angles, M. A. Bouman and H. A. van der Velden —231
Recommended footcandle levels for prolonged critical seeing, Matthew Luckiesh—712
Reduction of apparent contrast by the atmosphere, Seibert Q. Duntley—179
Sensitivity performance of the human eye on an absolute scale, Albert Rose—196
Two-Quanta hypothesis as a general explanation for the behavior of threshold values and visual acuity for the several receptors of the human eye, M. A. Bouman and H. A. van der Velden—570
Visibility on cathode-ray tube screens: signals on a P7 screen seen at different intervals after excitation, A. L. Sweet and N. R. Bartlett—329
Visibility of distant objects, Seibert Q. Duntley—237

Filters
Continuously variable interference filters, A. F. Turner and O. A. Ullrich—662(A)
Reflection and transmission interference filters. Part II. L. N. Hadley and D. M. Dennison—483
Errata to Part I—546
Short wave-length cut-off filters for the ultraviolet, Arnold M. Bass—977
Standard luminosity filter, Ray P. Teele and Kasson S. Gibson—1096(A)
Transmission filters for the ultraviolet, Michael Kasha —929

Flourescence and phosphorescence
$CaSiO_3$:(Pb+Mn) phosphor, John B. Merrill and James H. Schulman—471
Emission spectra of zinc cadmium sulfides, Frank J. Studer and D. A. Larson—480(L)
Fluorescence efficiency and hole migration in zinc sulfides, M. E. Wise and H. A. Klasens—226
Fluorescence of uranium trioxide hydrates, Dwayne T Vier, Melvin L. Schultz, and Jacob Bigeleisen—811
Infra-red stimulability of $CaSiO_3$:Pb and $CaSiO_3$:(Pb+Mn), James H. Shulman, Robert J. Ginther, and Lyle W. Evans—817(L)
Measurement of fluorescence spectra, S. Sambursky and G. Wolfsohn—739(L)
On the inadequacy of the measurement of emission characteristics of fluorescent substances without spectral resolution, Z. Bodó—815(L)
Relation between efficiency and exciting intensity for zinc-sulfide phosphors, H. A. Klasens, W. Ramsden, and Chow Quantie—60; Erratum—649
Short wave-length cut-off filters for the ultraviolet, Arnold M. Bass—977
Temperature dependence of the emission bands of zinc oxide phosphors, F. H. Nicoll—817(L)
Theory of electron retrapping in phosphors, Robert C. Herman, Charles F. Meyer, and Helen S. Hopfield —999
Visibility on cathode-ray tube screens: signals on a P7 screen seen at different intervals after excitation, A. L. Sweet and N. R. Bartlett—329

Glass, properties of
Athermalization of optical systems, David S. Grey—542
Color variations in glasses containing iron, John W. Forrest, Norbert J. Kreidl, and Tyler G. Pett—554
Diffusion of light by ground glass, with special reference to color changes, W. E. Knowles Middleton and F. D. Smith—1094(A)
Effect of high index glasses on the field characteristics of photographic objectives, G. R. Aklin—666(A), 841
Electroformed precision prisms, Benjamin Goldberg—409
Empirical relationships between the partial dispersions of the ordinary types of optical glasses, D. H. Rank —885
Fabrication of boric acid glass for luminescence studies, M. Kasha—1068
Light scattering in optical glass, D. H. Rank and A. E. Douglas—966

Preparation of aspherical refracting optical surfaces by an evaporation technique, L. G. Schulz—432

Illumination

Effect of spectral quality of light on visual performance and fatigue, Ernst Simonson and Josef Brozek—830

Effects of illumination level on visual performance and fatigue, Ernst Simonson and Josef Brozek—384

Example of metamerism: extreme example of color change with varying illuminant, F. C. Dexter and E. I. Stearns—816(L)

Illuminant in textile color matching, Dorothy Nickerson —485

Illuminant-stable color vision test, I, Ellis Freeman—532

New contributions to the optics of intensely light-scattering materials. Part I, Paul Kubelka—448; Erratum—1085

Normal probability curve as an approximation to the distribution curve of the high intensity searchlight, Frank Benford and John E. Bock—527

Notes on the $\cos^4$ law of illumination, Max Reiss—980

Phase microscopy with critical illumination, Harold Osterberg—1099(A)

Phase microscopy with vertical illumination, Helen Jupnik, Harold Osterberg, and G. E. Pride—338

Questionnaire on illumination, Kasson S. Gibson—67(L)

Recommended footcandle levels for prolonged critical seeing, Matthew Luckiesh—712

Standards of reflectance, Harry J. Keegan—658(A)

Sunlight and skylight as determinants of photographic exposure. I. Luminous density as determined by solar altitude and atmospheric conditions, Loyd A. Jones and H. R. Condit—123

Infra-red

Absorption spectra with polarized infra-red radiation, Norman Wright—663(A)

Calibration method for infra-red prism spectrometers, D. S. McKinney and R. A. Friedel—222

$CaSiO_3$: (Pb+Mn) phospor, John B. Merrill and James H. Schulman—471

Construction and performance of a double beam infra-red spectrometer, John U. White and Max D. Liston—1098(A)

Detection and control system for a double beam infra-red spectrometer, Max D. Liston and John U. White—1098(A)

Elimination of water vapor in infra-red spectrometers, Paul A. Giguère and Richard M. Badger—987(L)

Emissivity of globar, Shirleigh Silverman—989(A)

Infra-red absorption analyses used in control of a pilot plant triptane process, D. L. Fry—1098(A)

Infra-red absorption of atmospheric gases, M. V. Migeotte and R. M. Chapman—1094(A)

Infra-red absorption of deposited blacks, Earle K. Plyler and Joseph J. Ball—988(L)

Infra-red absorption spectra of some benzene derivatives, Earle K. Plyler—1095(A)

Infra-red chopped-radiation analyzer, G. Kivenson, R. T. Steinback, and Myrtle Rider—1086

Infra-red instrument for industrial product control, N. C. Jamison, T. R. Kohler, and O. G. Koppius—1099(A)

Infra-red "lens," Robert A. Oetjen—1099(A)

Infra-red properties of polar crystals, Elias Burstein —1101(A)

Infra-red pupillometer, M. Koomen, R. Tousey, and H. A. Knoll—719

Infra-red sensitivity of superconducting bolometers, Nelson Fuson—845

Infra-red spectra of alcohols, N. W. Young—1095(A)

Infra-red spectra of linearly oriented high polymers, Elkan R. Blout and Dwight P. Merrill—663(A)

Infra-red spectra of normal propane, 1-deuteropropane, and 2-deuteropropane, H. L. McMurry, V. Thornton, and F. E. Condon—1095(A)

Infra-red stimulability of $CaSiO_3$:Pb and $CaSiO_3$: (Pb+Mn), James H. Schulman, Robert J. Ginther, and Lyle W. Evans—817(L)

Measurements of the physical properties of infra-red optical materials, Lewis S. Combes and Stanley S. Ballard—1101(A)

On the inelastic deformation and crystal orientation of thallium halides, Alexander Smakula and Myron W. Klein—1101(A)

Polarization of infra-red radiation, A. Elliott, E. J. Ambrose, and R. Temple—212

Polarization techniques in the infra-red, W. L. Hyde —663(A)

Practical aspects of the preparation and application of an infra-red bibliography, J. D. Stroupe, A. G. Knox, and J. F. Woodmen—1095(A)

Preparation and optical properties of gold blacks, Louis Harris, Rosemary T. McGinnies, and Benjamin M. Siegel—582

Rapid scanning infra-red spectrometer for emission spectra, Shirleigh Silverman—664(A)

Recent infra-red work at Cambridge, G. B. B. M. Sutherland—1100(A)

Refractive indices of two thallium bromide-iodide crystals for visible and infra-red radiant energy, Leroy W. Tilton, Earle K. Plyler, and Robert E. Stephens—663(A)

Stray radiation in Littrow-type spectrometers which employ collimating mirrors, A. E. Martin—70(L)

Survey of near infra-red communication systems, W. S. Huxford and John R. Platt—253

Theory of electron retrapping in phosphors, Robert C. Herman, Charles F. Meyer, and Helen S. Hopfield —999

Transmission of powder films in the infra-red, R. L. Henry—775

Transmitting polarizer for infra-red radiation, N. Wright—69(L)

Intensity measurements

Absolute sensitivity measurements on single-grain layer photographic plates for different wave-lengths, J. H. Webb—312

Atmospheric transmissometer: its calibration and applications, C. A. Douglas—667(A)

Intensity measurements (continued)
Determination of the depolarization factors of highly polarized Raman lines, A. E. Douglas and D. H. Rank—281
Effects of illumination level on visual performance and fatigue, Ernst Simonson and Josef Brozek—384
Electronic apparatus for determining phosphorescent decay, W. S. Plymale, Jr.—664(A)
Emissivity of globar, Shirleigh Silverman—989(L)
Intensity and polarization of Brillouin spectra, D. H. Rank, J. S. McCartney, and G. J. Szasz—287
Light scattering in optical glass, D. H. Rank and A. E. Douglas—966
Normal probability curve as an approximation to the distribution curve of the high intensity searchlight, Frank Benford and John E. Bock—527
On the theory of imperfect diffraction gratings, U. Fano —921
Photometer for measurement of sky brightness near the sun, John W. Evans—1083
Photometry and colorimetry of railroad fuses, W. E. Knowles Middleton—660(A)
Relation between efficiency and exciting intensity for zinc-sulfide phosphors, H. A. Klasens, W. Ramsden, and Chow Quantie—60; Erratum—649
Some spectral characteristics of mercury arcs for use in study of the Raman effect, D. H. Rank and J. S. McCartney—279
Spectral response of a cadmium sulfide crystal, Curtis J. Humphreys—664(A)
Sunlight and skylight as determinants of photographic exposure. I. Luminous density as determined by solar altitude and atmospheric conditions, Loyd A. Jones and H. R. Condit—123

Interference
Irradiance distribution in a Lloyd mirror interference pattern, Robert N. Wolfe and Fred C. Eisen—667(A), 706
Reflection and transmission interference filters. Part II. Experimental, comparison with theory, results, L. N. Hadley and D. M. Dennison—483
Errata to Part I—546.

Lenses and mirrors
Achromatic ultraviolet microscope objective, L. V. Foster and E. M. Thiel—689
Aspheric surfaces in optical systems for television projection, David S. Grey—667(A)
Athermalization of optical systems, David S. Grey—542
Centering of optical systems, A. L. Ingalls and K. Pestrecov—343
Cinema-spectrograph for photographing rapid spectral sequences, Robert C. Herman and Shirleigh Silverman—209
Computation of distortion of an "out-of-focus" image, K. Pestrecov—669(A)
Curved field lens and camera, Robert E. Hopkins, John C. Evans, and Donald Feder—1102(A)
Design of triplet anastigmat lenses of the Taylor type, Robert E. Stephens—1032
Differential adjustment method of refining optical systems, Waldemar M. Stempel—935
Diffraction theory of lens errors, F. Zernike—661(A)
Effect of high index glasses on the field characteristics of photographic objectives, G. R. Aklin—841
Lens design and tolerance analysis methods and results, Paul C. Foote and Robert A. Woodson—590
Lenses of extremely wide angle for airplane mapping, Irvine C. Gardner and Francis E. Washer—421
Loss in resolving power caused by primary astigmatism, coma, and spherical aberration in telescopic systems, Howard S. Coleman and Samuel W. Harding—217
Method of calculating the allowable number of Newton rings for telescope optics, D. C. Harper and J. H. McLeod—669(A)
Multipupil in phase microscopy, Harold Osterberg—668(A), 685
Notes on the $\cos^4$ law of illumination, Max Reiss—980
Optical characteristics of hyperbolic paraboloidal mirrors, Robert A. Woodson—667(A)
Paraxial differential transfer coefficients of a lens system, Marc G. Dreyfus—703
Photographic sharpness and resolving power. I. The design and performance of an apochromatic resolving-power camera objective, Fred H. Perrin and H. Orlo Hoadley—1040
Preparation of aspherical refracting optical surfaces by an evaporation technique, L. G. Schulz—432
Reduction of sphero-chromatic aberration in catadioptric systems, Robert E. Stephens—666(A), 733
Schmidt system tolerances. Robert A. Woodson—1102 (A)
Thin sheet plastic Fresnel lenses of high aperture, O. E. Miller, J. H. McLeod, and W. T. Sherwood—1104 (A)

Letters to the Editor
Applicability of Judd's color tolerance formula in the case of titanium pigments, Arthur C. Hardy—650
Comments regarding "a new one-step photographic process" by Edwin H. Land, Lloyd E. Varden—69
Electro- and magneto-optical shutters for aerial cameras, Roy C. Gunter, Jr—419
Elimination of water vapor in infra-red spectrometers, Paul A. Giguère and Richard M. Badger—987
Emission spectra of zinc cadmium sulfides, Frank J. Studer and D. A. Larson—480
Emissivity of globar, Shirleigh Silverman—989
Example of metamerism: extreme example of color change with varying illuminant, F. C. Dexter and E. I. Stearns—816
Infra-red absorption of deposited blacks, Earle K. Plyler and Joseph J. Ball—988
Infra-red stimulability of $CaSiO_3$:Pb and $CaSiO_3$:(Pb+Mn), James H. Schulman, Robert J. Ginther, and Lyle W. Evans—817
Lead selenide photo-conductive cells, J. Starkiewicz—481
Measurement of fluorescence spectra, S. Sambursky and G. Wolfsohn—739

Measurement of strongly reflecting transmission samples with the commercial recording spectrophotometer, W. E. Knowles Middleton—74
New principle in interferometer design, Edson R. Peck —66
Nomographs for spectral band width of the Beckman DU spectrophotometer, H. M. Haendler—417
Note on ultraviolet absorption of zinc oxide phosphors, F. H. Nicoll—417
Observations of anticoronae on Mt. Washington, David L. Arenberg—481
On the inadequacy of the measurement of emission characteristics of fluorescent substances without spectral resolution, Z. Bodó—815
"Optical staining" of tissue, Germain C. Crossmon—417
Questionnaire on illumination, Kasson S. Gibson—67
Reply to Lloyd E. Varden's "comments regarding 'a new one-step photographic process,'" Edwin H. Land —70
Standard response functions for protanopic and deuteranopic vision, Yves Le Grand—815
Stray radiation in Littrow-type spectrometers which employ collimating mirrors, A. E. Martin—70
Temperature dependence of the emission bands of zinc oxide phosphors, F. H. Nicoll—817
Test on the process of photographing the trajectory of a rapidly moving distant light source, R. E. Nusbaum and J. S. Beggs—740
Transmitting polarizer for infra-red radiation, N. Wright—69
Ultraviolet phase microscopy, A. H. Bennett, D. L. Woernley, and A. J. Kavanagh—739
Visual performance and the surround, Parry Moon and Domina Eberle Spencer—650
Whose absorption law?, Fred H. Perrin—72

Light sources, properties and measurement

Absolute sensitivity measurements on single-grain layer photographic plates for different wave-lengths, J. H. Webb—312
Absorption and excitation of luminescent zinc silicate, Frank J. Studer and D. A. Larson—665(A)
Condensed arc source unit for spectrochemical analysis, D. A. Sinclair—547
Double activation of zinc fluoride phosphors, Gorton R. Fonda and Frank J. Studer—665(A), 1007
Light wave of artificial mercury as the ultimate standard of length, William F. Meggers—7
Some spectral characteristics of mercury arcs for use in study of the Raman effect, D. H. Rank and J. S. McCartney—279
Spectral response of a cadmium sulfide crystal, Curtis J. Humphreys—664(A)
Sunlight and skylight as determinants of photographic exposure. I. Luminous density as determined by solar altitude and atmospheric conditions, Loyd A. Jones and H. R. Condit—123
Visibility of stars in the daylight sky, R. Tousey and E. O. Hulburt—886
Wave-lengths emitted by mercury 198, William F. Meggers.—665(A)

Meetings

Minutes of the thirty-first meeting of the Board of Directors of the Optical Society of America, Incorporated—651
Minutes of the thirty-second meeting of the board of Directors of the Optical Society of America, Incorporated—1107
Proceedings of the thirty-third annual meeting of the Optical Society of America—1092
Proceedings of the winter meeting of the Optical Society of America—657

Microscopy

Achromatic ultraviolet microscope objective, L. V. Foster and E. M. Thiel—689
Image contrast control with phase microscopy, Oscar W. Richards—668(A)
Multipupil in phase microscopy, Harold Osterberg—685
Phase microscopy with critical illumination, Harold Osterberg—1099(A)
Phase microscopy with vertical illumination, Helen Jupnik, Harold Osterberg, and G. E. Pride—338
Ultraviolet phase microscopy, A. H. Bennett, D. L. Woernley, and A. J. Kavanagh—739(L)

Optical instruments

Behavior of an interferometer in a gravitational field. II. Application to a planetary orbit, Herbert E. Ives —413
Calibration of a photo-multiplier photometer, J. R. DeVore—692
Centering of optical systems, A. L. Ingalls and K. Pestrecov—343
Comparison of computed and experimental detection ranges of objects viewed with telescopic systems from aboard ship, H. S. Coleman and W. S. Verplanck—250
Construction and performance of a double beam infrared spectrometer, John U. White and Max D. Liston 1098(A)
Formation of optical images by x-rays, Paul Kirkpatrick and A. V. Baez—766
Improved Jamin interferometer, J. B. Hawkes and R. W. Astheimer—617
Improvement of Savert's polariscope, M. Richartz—623
Industrial application of Geiger-Müller counters to the analysis of phosphorus in steels, Ford R. Bryan and George A. Nahstoll—510
Infra-red chopped-radiation analyzer, G. Kivenson, R. T. Steinback, and Myrtle Rider—1086
Infra-red sensitivity of superconducting bolometers, Nelson Fuson—845
Investigation of the use of Geiger-Müller photoelectron counters in the spectrographic analysis of phosphorus in steel, Richard Hanau and Ralph A. Wolfe—377
Investigation of the visibility of physical defects in optical instruments, Harold H. Bloen—669(A)
Lens design and tolerance analysis methods and results, Paul C. Foote and Robert A. Woodson—590
Multiprism spectrographs with glass optics by Carl Zeiss, Jena, G. Hansen—759
Multipupil in phase microscopy, Harold Osterberg—685

Optical instruments (continued)
New principle in interferometer design, Edson R. Peck —66(L)
New spectrophotometer employing a glass Féry prism, Wm. C. Miller—1102(A)
Optical compensators for measurement of elliptical polarization, H. G. Jerrard—35
Optical and electrical alterations to a Michigan microphotometer, H. H. Grossman, E. W. Peterson, J. L. Saunderson, and C. J. Caldecourt—1104(A)
Photoelectric color-difference meter, Richard S. Hunter —661(A)
Photoelectric determination of interference maxima, George R. Harrison and James C. Anderson—1105(A)
Photometer for measurement of sky brightness near the sun, John W. Evans—1083
Plano-interferometer, David Richardson—1104(A)
Practical applications of a replica grating spectrograph installation, J. T. Rozsa—666(A)
Principles of optical communication systems-general properties of non-image forming projectors and recievers, Hartland S. Snyder and John R. Platt—269
Projection screens for home television receivers, R. R. Law and I. G. Maloff—497
Quantometer, a direct reading instrument for spectrochemical analysis, M. F. Hasler, R. W. Lindhurst, and J. W. Kemp—789
Rapid scanning infra-red spectrometer for emission spectra, Shirleigh Silverman—664(A)
Recording photometer and its use in studies of cathode-ray screen displays, Ferdinand Hamburger, Jr. and Ellwood J. King—875
Refractive indices of two thallium bromide-iodide crystals for visible and infra-red radiant energy, Leroy W. Tilton, Earle K. Plyler, and Robert E. Stephens —663(A)
Survey of near infra-red communication systems, W. S. Huxford and John R. Platt—253
Transmitting polarizer for infra-red radiation, N. Wright —69(L)

Optical materials
$CaSiO_3$:(Pb+Mn) phosphor, John B. Merrill and James H. Schulman—471
Measurements of the physical properties of infra-red optical materials, Lewis S. Combes and Stanley S. Ballard—1101(A)
Molding optical elements of thallium bromide iodide (KRS5), J. C. Evans and M. D. Clark—664(A)

Optical Society of America reports
Annual report of the Editor of Publications—651
Annual report of the Secretary of the Optical Society of America, Incorporated for the calendar year 1947 —652
Annual report of the Treasurer of the Optical Society of America—654

Optical testing
Automatic presentation, recording, and analysis device for vision experimentation, H. Richard Blackwell and Benjamin S. Pritchard—1097(A)
Centering of optical systems, A. L. Ingalls and K. Pestrecov—343
Coefficients of reflection in the ultraviolet of magnesium carbonate and oxide, Frank Benford, Sally Schwarz, and Gwen P. Lloyd—964
Differential adjustment method of refining optical systems, Waldemar M. Stempel—935
Infra-red pupillometer, M. Koomen, R. Tousey, and H. A. Knoll—719
Method of calculating the permissible size of appearance defects for visual instruments, D. C. Harper and W. T. Sherwood—669(A)
Optical determination of thin films on reflecting bases in transparent environments, Arthur B. Winterbottom —1074
Optical properties of Ni, Co, Fe, Mn, and Cd, F. Bueche —806
Optical properties of zinc fluoride phosphors, Gorton R. Fonda and Frank J. Studer—1007
Performance of an optical system as the sum of the contributions of its construction elements, M. Herzberger.—324

Optics, general
Absolute sensitivity of existing heat detectors, R. Clark Jones—1099(A)
Aerial photographic equipment and applications to reconnaissance, Amrom H. Katz—604
Algebraic theory of the primary aberrations of the symmetrical optical system, H. A. Buchdahl—14
Aspheric surfaces in optical systems for television projection, David S. Grey—667(A)
Athermalization of optical systems, David S. Grey—542
Atmospheric transmissometer: Its calibration and applications, C. A. Douglas—667(A)
Behavior of an interferometer in a gravitational field. II. Application to a planetary orbit, Herbert E. Ives —413
$CaSiO_3$:(Pb+Mn) phosphor, John B. Merrill and James H. Schulman—471
Centering of optical systems, A. L. Ingalls and K. Pestrecov—343
Color correction in color printing, Arthur C. Hardy and F. L. Wurzburg, Jr—300
Color of unstained wood, Parry Moon and Domina Eberle Spencer—405
Comparative survey of some possible systems of polarized headlights, B. H. Billings and E. H. Land—819
Continuously variable interference filters, A. F. Turner and O. A. Ullrich—662(A)
Control of photographic printing: improvement in terminology and further analysis of results, Loyd A. Jones and C. N. Nelson—897
Diffraction theory of lens errors. F. Zernike—661(A)
Electroformed precision prisms. Benjamin Goldberg— 409
Empirical relationships between the partial dispersions of the ordinary types of optical glasses. D. H. Rank—885
Focal plane diffraction doubling in the Amici roof prism, A. I. Mahan and E. E. Price—667(A)

Formation of optical images by x-rays, Paul Kirkpatrick and A. V. Baez—766
Foundation of optics, Hans Mueller—661(A)
Gratings made by photographing interference fringes, Robert E. Hopkins and Franklin R. Clapper—661(A)
Image contrast control with phase microscopy, Oscar W. Richards—668(A)
Image error theory for finite aperture and field. I. The image of a point; geometry of the wave surface, Max Herzberger—736
In defense of Beer's law, Arthur C. Hardy and F. Mansfield Young—854
Infra-red properties of polar crystals, Elias Burstein —1101(A)
Infra-red pupillometer, M. Koomen, R. Tousey, and H. A. Knoll—719
Interference fringes near a critical angle boundary, P. J. Leurgans, A. F. Turner, and O. A. Ullrich—1104(A)
Investigation of the visibility of physical defects in optical instruments, Harold H. Bloen—669(A)
Irradiance distribution in a Lloyd mirror interference Pattern, Robert N. Wolfe and Fred C. Eisen—706
Lead selenide photo-conductive cells, J. Starkiewicz —481(L)
Light wave of artificial mercury as the ultimate standard of length, William F. Meggers—7
Low temperature radiation pyrometry, J. C. Mouzon and C. A. Dyer—1099(A)
Measurements of the physical properties of infra-red optical materials, Lewis S. Combes and Stanley S. Ballard—1101(A)
Measurement of the velocity of light by signals sent in one direction, Herbert E. Ives—897
Method of calculating the allowable number of Newton rings for telescope optics, D. C. Harper and J. H. McLeod—669(A)
Method of calculating the permissible size of appearance defects for visual instruments, D. C. Harper and W. T. Sherwood—669(A)
Method for evaluating the intensity of focused stray light from concave diffraction gratings, F. S. Johnson and R. Tousey—1103(A)
Micro-interferometer study of diffraction gratings. David Richardson and Robert B. Tackaberry—662 (A)
Molding optical elements of thallium bromide iodide (KRS5), J. C. Evans and M. D. Clark—664(A)
New contributions to the optics of intensely light-scattering materials. Part I. Paul Kubelka—448; Erratum—1085
New spectrophotometer employing a glass Féry prism, Wm. C. Miller—1102(A)
Observations of anticoronae on Mt. Washington, David L. Arenberg—481(L)
On the inelastic deformation and crystal orientation of thallium halides, Alexander Smakula and Myron W. Klein—1101(A)
Optical characteristics of hyperbolic paraboloidal mirrors, Robert A. Woodson—667(A)
Optical determination of thin films on reflecting bases in transparent environments, Arthur B. Winterbottom —1074
Optimum band width for two-layer antireflection films, Robert B. Muchmore—20
Out-of-focus diffraction patterns, L. Ivan Epstein—1103(A)
Performance of an optical system as the sum of the contributions of its construction elements, M. Herzberger —324
Pharmacological properties of blood sera and drugs treated with various x-rays, David I. Macht and Marcus Ostro—663(A)
Phase microscopy with critical illumination, Harold Osterberg—1099(A)
Photoelectric determination of interference maxima, George R. Harrison and James C. Anderson—1105(A)
Plano-interferometer, David Richardson—1104(A)
Preconstruction of triplet, M. Herzberger—1104(A)
Projection screens for home television receivers, R. R. Law and I. G. Maloff—497
Reduction of sphero-chromatic aberration in catadioptric systems, Robert E. Stephens—733
Reflection and transmission of light by any system of parallel isotropic films, A. W. Crook—954
Refractive index of optical glass at low temperature, Fred A. Molby—1102(A)
Resolving power of a coated objective, Harold Osterberg and J. Ernest Wilkins, Jr.—668(A)
Rotating two dimensionally patterned gratings, Marcel J. E. Golay—1099(A)
Scattered and rescattered sunlight, A. Hammad—611
Schmidt system tolerances, Robert A. Woodson—1102(A)
Some considerations of the effect of radiation on the performance of liquid fuel rockets, S. S. Penner and S. Weinbaum—599; Erratum—840(L)
Temperature coefficient of the refractive index of water, J. B. Hawkes and R. W. Astheimer—804
Xerography—a new principle of photography and graphic reproduction, R. M. Schaffert and C. D. Oughton—991

Optics, geometrical

Differential adjustment method of refining optical systems, Waldemar M. Stempel—935
Image error theory for finite aperture and field. I. The image of a point; geometry of the wave surface, Max Herzberger—736
Lens design and tolerance analysis methods and results, Paul C. Foote and Robert A. Woodson—590
Optical characteristics of hyperbolic paraboloidal mirrors, Robert A. Woodson—667(A)

Optics, physical

Electro- and magneto-optical shutters for aerial cameras, Roy C. Gunter, Jr.—419(L)
On the theory of imperfect diffraction gratings, U. Fano —921
Optical properties of Ni, Co, Fe, Mn, and Cd, F. Bueche—806

Optics, physical (continued)
Optical properties of zinc fluoride phosphors, Gorton R. Fonda and Frank J. Studer—1007
Syntheses of spectral-distribution curves, W. L. Brewer and F. R. Holly, Jr.—858

Photoelectricity
Determination of the depolarization factors of highly polarized Raman lines, A. E. Douglas and D. H. Rank—281
Electrical response of the human retina to lights of various wave-lengths, Lorrin A. Riggs and E. Parker Johnson—662(A)
Photoelectric determination of interference maxima, George R. Harrison and James C. Anderson—1105(A)
Photoelectric method for preparing printing plates, Arthur C. Hardy and F. L. Wurzburg, Jr.—295
Survey of near infra-red communication systems, W. S. Huxford and John R. Platt—253

Photography, including cameras
Absolute sensitivity measurements on single-grain-layer photographic plates for different wave-lengths, J. H. Webb—312
Aerial photographic equipment and applications to reconnaissance, Amrom H. Katz—604
Applications of the photographic pressure effect, K. B. Mather—1066
Cinema-spectrograph for photographing rapid spectral sequences, Robert C. Herman and Shirleigh Silverman—209
Comments regarding "a new one-step photographic process" by Edwin H. Land—Lloyd E. Varden—69(L)
Control of photographic printing: Improvement in terminology and further analysis of results, Loyd A. Jones and C. N. Nelson—897
Curved field lens and camera, Robert E. Hopkins, John C. Evans, and Donald Feder—1102(A)
Effect of high index glasses on the field characteristics of photographic objectives, G. R. Aklin—841
Effect of light-absorption on the shape of the photographic, H. and D. Curve, J. H. Webb—27
Electro- and magneto-optical shutters for aerial cameras, Roy C. Gunter, Jr.—419(L)
Gratings made by photographing interference fringes, Robert E. Hopkins and Franklin R. Clapper—661(A)
Lenses of extremely wide angle for airplane mapping, Irvine C. Gardner and Francis E. Washer—421
Mechanism of latent image formation in a photographic emulsion by mechanical pressure, K. B. Mather—1066
Photographic granularity and graininess. IV. Visual acuity thresholds; dynamic *versus* static assumptions, Loyd A. Jones and George C. Higgins—398
Photographic reciprocity-law failure for radiations of different wave-length, M. Biltz and J. H. Webb—561
Photographic sharpness and resolving power. I. The design and performance of an apochromatic resolving-power camera objective, Fred H. Perrin and H. Orlo Hoadley—1040
Reply to Lloyd E. Varden's "comments regarding 'a new one-step photographic process,'" Edwin H. Land—70(L)
Sunlight and skylight as determinants of photographic exposure. I. Luminous density as determined by solar altitude and atmospheric conditions, Loyd A. Jones and H. R. Condit—123
Test on the process of photographing the trajectory of a rapidly moving distant light source, R. E. Nusbaum and J. S. Beggs—740(L)
Xerography—a new principle of photography and graphic reproduction, R. M. Schaffert and C. D. Oughton—991

Photometry
Brightness and altitude of the luminosity of the night sky, E. O. Hulburt—1096(A)
Calibration of a photo-multiplier photometer, J. R. DeVore—692
Daytime zenith sky brightness at 18,000- to 38,000-foot altitudes, D. M. Packer and C. Lock—1097(A)
On the inadequacy of the measurement of emission characteristics of fluorescent substances without spectral resolution, Z. Bodó—815(L)
Optical and electrical alterations to a Michigan microphotometer, H. H. Grossman, E. W. Peterson, J. L. Saunderson, and V. J. Caldecourt—1104(A)
Photometer for measurement of sky brightness near the sun, John W. Evans—1083
Photometry and colorimetry of railroad fuses, W. E. Knowles Middleton—660(A)
Quantitative spectrochemical determination of barium, strontium, and calcium, Werner Hartmann and Betty E. Prescott—539
Recording photometer and its use in studies of cathode-ray screen displays, Ferdinand Hamburger, Jr. and Ellwood J. King—875
Three-line method of obtaining characteristic curves for heterochromous photometry, Milton Green—1105(A)
Visibility on cathode-ray tube screens: the effects of light adaptation, R. M. Hanes and S. B. Williams—363
Whose absorption law?, Fred H. Perrin—72(L)

Polarization
Absorption spectra with polarized infra-red radiation, Norman Wright—663(A)
Comparative survey of some possible systems of polarized headlights, B. H. Billings and E. H. Land—819
Determination of the depolarization of factors of highly polarized Raman lines, A. E. Douglas and D. H. Rank—281
Improvement of Savert's polariscope, M. Richartz—623
Intensity and polarization of Brillouin spectra, D. H. Rank, J. S. McCartney, and G. J. Szasz—287
Light scattering in optical glass, D. H. Rank and A. E. Douglas—966
Optical compensators for measurement of elliptical polarization, H. G. Jerrard—35
Polarization of infra-red radiation, A. Elliott, E. J. Ambrose, and R. Temple—212

Polarization techniques in the infra-red, W. L. Hyde —663(A)
Transmitting polarizer for infra-red radiation, N. Wright—69(L)

Pyrometry

Low temperature radiation pyrometry, J. C. Mouzon and C. A. Dyer—1099(A)

Radiation

Infra-red chopped-radiation analyzer, G. Kivenson, R. T. Steinback, and Myrtle Rider—1086
Infra-red sensitivity of superconducting bolometers, Nelson Fuson—845
Irradiance distribution in a Lloyd mirror interference pattern, Robert N. Wolfe and Fred C. Eisen—706
Low temperature radiation pyrometry, J. C. Mouzon and C. A. Dyer—1099(A)
Photographic reciprocity-law failure for radiations of different wave-length, M. Biltz and J. H. Webb—561
Some considerations of the effect of radiation on the performance of liquid fuel rockets, S. S. Penner and S. Weinbaum—599; Erratum—840
Stray radiation in Littrow-type spectrometers which employ collimating mirrors, A. E. Martin—70(L)
Sunlight and skylight as determinants of photographic exposure. I. Luminous density as determined by solar altitude and atmospheric conditions, Loyd A. Jones and H. R. Condit—123
Table of Planckian radiation, Parry Moon—291
Transmitting polarizer for infra-red radiation, N. Wright—69(L)

Refraction

Paraxial differential transfer coefficients of a lens system, Marc G. Dreyfus—703
Preparation of aspherical refracting optical surfaces by an evaporation technique, L. G. Schulz—432
Refractive index of optical glass at low temperature, Fred A. Molby—1102(A)
Refractive indices of two thallium bromide-iodide crystals for visible and infra-red radiant energy, Leroy W. Tilton, Earle K. Plyler, and Robert E. Stephens —663(A)
Temperature coefficient of the refractive index of water, J. B. Hawkes and R. W. Astheimer—804

Spectrographic analysis

Air interrupter type spectrographic light source, J. H. Enns and R. A. Wolfe—1102(A)
Calibration method for infra-red prism spectrometers, D. S. McKinney and R. A. Friedel—222
Coefficients of reflection in the ultraviolet of magnesium carbonate and oxide, Frank Benford, Sally Schwarz, and Gwen P. Lloyd—964
Color variations in glasses containing iron, John W. Forrest, Norbert J. Kreidl, and Tyler G. Pett—554
Combination spark-arc source unit for spectrochemistry, M. F. Hasler and J. W. Kemp—1103(A)
Condensed arc source unit for spectrochemical analysis, D. A. Sinclair—547
Criteria for high precision analyses with d.c. arc excitation, Velmer A. Fassel—1102(A)
Detection of lead in air with the aid of a Geiger-Müller counter, O. G. Koppius—1100(A)
Evaluation of the elementary causes of deviations in spectrochemical analysis, Joseph Geffner—665(A)
Industrial application of Geiger-Müller counters to the analysis of phosphorus in steels, Ford R. Bryan and George A. Nahstoll—510
Infra-red absorption analyses used in control of a pilot plant triptane process, D. L. Fry—1098(A)
Instrumentation for direct-reading spectrochemistry, M. F. Hasler, J. W. Kemp, and D. R. Procter—1103(A)
Investigation of the use of Geiger-Müller photoelectron counters in the spectrographic analysis of phosphorus in steel, Richard Hanau and Ralph A. Wolfe—377
Method of spectrographic analysis of impurities in materials for oxide coating of thermionic cathodes, T. J. Organ and S. L. Parsons—191
Quantitative spectrochemical determination of barium, strontium, and calcium, Werner Hartmann and Betty E. Prescott—539
Quantitative spectrographic analysis of the rare earth elements. I. Determination of samarium in neodymium II. Determination of europium in samarium, Velmer A. Fassel and Harley A. Wilhelm—666(A), 518
Quantometer, a direct reading instrument for spectrochemical analysis, M. F. Hasler, R. W. Lindhurst, and J. W. Kemp—789
Rapid mobile analyzer for minute amounts of lead in air, Henry Aughey—1100(A)
Spectrochemical determination of hafnium-zirconium ratios, Cyrus Feldman—1100(A)
Spectrochemical determination of the major constituents of minerals and rocks, erratum, Aslak Kvalheim—479
Spectrochemical method for the determination of uranium, L. T. Steadman—1100(A)
Spectrographic analysis of alumina in silica brick, P. R. Irish—1104(A)
Spectrographic analysis of vitallium alloys, Y. T. Sihvonen, D. L. Fry, R. E. Nusbaum, and R. R. Baumgartner—1100(A)
Spectrographic determination of fluorine in organic substances, Charles E. Rankin—1104(A)
Stainless steel analysis with the direct reading spectrometer, Jacob H. Jurmain and John Sterner—1101(A)
Wide range analysis for zinc using spectrographic line widths, E. John Eastmond and Bernice E. Williams —800

Spectroscopy; spectrometry; spectrophotometry

Absorption and excitation of luminescent zinc silicate, Frank J. Studer and D. A. Larson—665(A)
Absorption spectra with polarized infra-red radiation, Norman Wright—663(A)
Air interrupter type spectrographic light source, J. H. Enns and R. A. Wolfe—1102(A)

Spectroscopy; spectrometry; spectrophotometry (continued)
Application of spectrophotometry in the textile industry: testing dyestuff shipments, E. P. Mersereau and J. L. Barach—658(A)
Application of spectrophotometry in a textile plant, Frederick T. Simon—659(A)
Calibration method for infra-red prism spectrometers, D. S. McKinney and R. A. Friedel—222
Cinema-spectrograph for photographing rapid spectral sequences, Robert C. Herman and Shireligh Silverman —209
Colorimetric behaviors of dye mixture, David L. MacAdam—659(A)
Combination spark-arc source unit for spectrochemistry, M. F. Hasler and J. W. Kemp—1102(A)
Comparison of direct colorimetry of titanium pigments with their indirect colorimetry based on spectrophotometry and a standard observer, Deane B. Judd —1093(A)
Construction and performance of a double beam infrared spectrometer, John U. White and Max D. Liston —1098(A)
Criteria for high precision analyses with d.c. arc excitation, Velmer A. Fassel—1102(A)
Detection and control system for a double beam infrared spectrometer, Max D. Liston and John U. White —1098(A)
Determination of the depolarization factors of highly polarized Raman lines, A. E. Douglas and D. H. Rank—281
Double activation of zinc fluoride phosphors, Gorton R. Fonda and Frank J. Studer—665(A)
Emission spectra of zinc cadmium sulfides, Frank J. Studer and D. A. Larson—480(L)
Evaluation of the elementary causes of deviations in spectrochemical analysis, Joseph Geffner—665(A)
Flame spectrum of acetylene from 1 to 5 microns, Curtis J. Humphreys and Earle K. Plyler—1094(A)
Industrial application of Geiger-Müller counters to the analysis of phosphorus in steels, Ford R. Bryan and George A. Nahstoll—510
Infra-red absorption analyses used in control of a pilot plant triptane process, D. L. Fry—1098(A)
Infra-red absorption of atmospheric gases, M. V. Migeotte and R. M. Chapman—1094(A)
Infra-red absorption spectra of some benzene derivatives, Earle K. Plyler—1095(A)
Infra-red instrument for industrial product control, N. C. Jamison, T. R. Kohler, and O. G. Koppius—1099(A)
Infra-red spectra of alcohols, N. W. Young—1095(A)
Infra-red spectra of normal propane, 1-deuteropropane, and 2-deuteropropane, H. L. McMurry, V. Thornton, and F. E. Condon—1095(A)
Instrumentation for direct-reading spectrochemistry, M. F. Hasler, J. W. Kemp, and D. R. Procter—1103(A)
Intensity and polarization of Brillouin spectra, D. H. Rank, J. S. McCartney, and G. J. Szasz—287
Investigation of the use of Geiger-Müller photoelectron counters in the spectrographic analysis of phosphorus in steel, Richard Hanau and Ralph A. Wolfe—377
Measurement of strongly reflecting transmission samples with the commercial recording spectrophotometer, W. E. Knowles Middleton—74(L)
Method for automatically plotting spectral energy distribution of luminescent materials, Frank J. Studer —467
Method for calculating the dominant wave-length of a dichroic amber glass for any thickness, J. H. Widmyer —658(A)
Method of spectrographic analysis of impurities in materials for oxide coating of thermionic cathodes, T. J. Organ and S. L. Parsons—191
Micro-interferometer study of diffraction gratings, David Richardson and Robert B. Tackaberry—662(A)
New principle in interferometer design, Edson R. Peck —66(L)
Nomographs for spectral band width of the Beckman DU spectrophotometer, H. M. Haendler—417(L)
Non-adaptability of the I.C.I. system to some near-whites which show absorption in the far blue region of the spectrum, A. E. Jacobsen—442
Orientation of insoluble dyes in cellulose, Henry Hemmendinger—659(A)
Photoelectric color-difference meter, Richard S. Hunter —661(A)
Photometry and colorimetry of railroad fuses, W. E. Knowles Middleton—660(A)
Polarization of infra-red radiation, A. Elliott, E. J. Ambrose, and R. Temple—212
Practical applications of a replica grating spectrograph installation, J. T. Rozsa—666(A)
Preliminary investigation of the spectra of uranium isotopes, J. Rand McNally, Jr.—1100(A)
Quantitative spectrochemical determination of barium, strontium, and calcium, Werner Hartmann and Betty E. Prescott—539
Quantitative spectrographic analysis of the rare earth elements. I. Determination of samarium in neodymium. II. Determination of europium in samarium, Velmer A. Fassel and Harley A. Wilhelm—518
Rapid scanning infra-red spectrometer for emission spectra, Shirleigh Silverman—664(A)
Recent infra-red work at Cambridge, G. B. B. M. Sutherland—1100(A)
Refractive indices of two thallium bromide-iodide crystals for visible and infra-red radiant energy, Leroy W. Tilton, Earle K. Plyler, and Robert E. Stephens —663(A)
Rotating two dimensionally patterned gratings, Marcel J. E. Golay—1099(A)
Some spectral characteristics of mercury arcs for use in study of the Raman effect, D. H. Rank and J. S. McCartney—279
Some techniques and accessories to facilitate the application of a G.E. recording spectrophotometer, E. E. Richardson—657(A)
Spectral response of a cadmium sulfide crystal, Curtis J. Humphreys—664(A)

Spectrochemical determination of hafnium-zirconium ratios, Cryus Feldman—1100(A)
Spectrochemical determination of the major constituents of minerals and rocks, erratum, Aslak Kvalheim—479
Spectrochemical method for the determination of uranium, L. T. Steadman—1100(A)
Spectrographic analysis of alumina in silica brick, P. R. Irish—1104(A)
Spectrographic analysis of vitallium alloys, Y. T. Sihvonen, D. L. Fry, R. E. Nusbaum, and R. R. Baumgartner—1100(A)
Spectrographic determination of fluorine in organic substances, Charles W. Rankin—1104(A)
Spectrometry with a thallium bromide iodide prism, Earle K. Plyler—664(A)
Spectrophotometric method for determination of lead, George L. Reymann, Kenneth H. Smith, and N. F. Barr—660(A)
Spectrophotometric studies of living human skin, Seibert Q. Duntley—660(A)
Spectrophotometric study of the color of rosin, Robert H. Osborn and Westcott C. Kenyon—660(A)
Spectrophotometry of living human skin as a research tool in medicine, Edward A. Edwards—660(A)
Stainless steel analysis with the direct reading spectrometer, Jacob H. Jurmain and John Sterner—1101(A)
Standards of reflectance, Harry J. Keegan—658(A)
Stray radiation in Littrow-type spectrometers which employ collimating mirrors, A. E. Martin—70(L)
Ultraviolet absorption spectra and the structures of the isomeric amidones, L. A. Strait, W. D. Kumler, P. P. T. Sah, E. L. Alpen, and F. N. H. Chang—1098(A)
Wave-lengths emitted by mercury 198, William F. Meggers—665(A)

Transmission

Measurement of strongly reflecting transmission samples with the commercial recording spectrophotometer, W. E. Knowles Middleton—74(L)
Principles of optical communication systems—general properties of non-image forming projectors and receivers, Hartland S. Snyder and John R. Platt—269
Reflection and transmission interference filters. Part II. Experimental, comparison with theory, results, L. N. Hadley and D. M. Dennison—483
Errata to Part I—546
Reflection and transmission of light by any system of parallel isotropic films, A. W. Crook—954
Spectrometry with a thallium bromide iodide prism, Earle K. Plyler—664(A)
Transmission filters for the ultraviolet, Michael Kasha —929
Transmission of powder films in the infra-red, R. L. Henry—775

Ultraviolet

Achromatic ultraviolet microscope objective, L. V. Foster and E. M. Thiel—689
Coefficients of reflection in the ultraviolet of magnesium carbonate and oxide, Frank Benford, Sally Schwarz, and Gwen P. Lloyd—964
Fluorescence of uranium trioxide hydrates, Dwayne T. Vier, Melvin L. Schultz, and Jacob Bigeleisen—811
Measurement of fluorescence spectra, S. Sambrusky and G. Wolfsohn—739(L)
Note on ultraviolet absorption of zinc oxide phosphors, F. H. Nicoll—417(L)
Short wave-length cut-off filters for the ultraviolet, Arnold M. Bass—977
Transmission filters for the ultraviolet, Michael Kasha —929
Ultraviolet absorption spectra of biological compounds at low temperatures, R. L. Sinsheimer, J. E. Scott, and J. R. Loofbourow—1105(A)
Ultraviolet absorption spectra and the structures of the isomeric amidones, L. A. Strait, W. D. Kumler, P. P. T. Sah, E. L. Alpen, and F. N. H. Chang—1098(A)
Ultraviolet phase microscopy, A. H. Bennett, D. L. Woernley, and A. J. Kavanagh—739(L)

Vision, visibility; visual phenomena

Applicability of Judd's color tolerance formula in the case of titanium pigments, Arthur C. Hardy—650(L)
Aspheric surfaces in optical systems for television projection, David S. Grey—667(A)
Atmospheric transmissometer: its calibration and applications, C. A. Douglas—667(A)
Automatic presentation, recording, and analysis device for vision experimentation, H. Richard Blackwell and Benjamin S. Pritchard—1097(A)
Bezold-Brücke phenomenon and the Hering theory of vision, Deane B. Judd—1095(A)
Brightness and altitude of the luminosity of the night sky, E. O. Hulburt—1096(A)
Case of unilateral deuteranopia, Louise L. Sloan and Lorraine Wollach—502
Comparative study of five tests of color vision, Alphonse Chapanis—626
Comparison of color systems with respect to uniform visual spacing, Robert W. Burnham—1093(A)
Comparison of computed and experimental detection ranges of objects viewed with telescopic systems from aboard ship, H. S. Coleman and W. S. Verplanck—250
Computation of distortion of an "out-of-focus" image, K. Pestrecov—669(A)
Daytime zenith sky brightness at 18,000- to 38,000-foot altitudes, D. M. Packer and C. Lock—1097(A)
Effect of spectral quality of light on visual performance and fatigue, Ernst Simonson and Josef Brozek—830
Effects of illumination level on visual performance and fatigue, Ernst Simonson and Josef Brozek—384
Illuminant-stable color vision test, I, Ellis Freeman —532
Illuminant-stable color vision test, II. Experimental-statistical evaluation, Ellis Freeman and M. A. Zaccaria—971
Image contrast control with phase microscopy, Oscar W. Richards—668(A)

Vision, visibility; visual phenomena (continued)
Investigation of the visibility of physical defects in optical instruments, Harold H. Bloem—669(A)
Loss in resolving power caused by primary astigmatism, coma, and spherical aberration in telescopic systems, Howard S. Coleman and Samuel W. Harding—217
Method of calculating the permissible size of appearance defects for visual instruments, D. C. Harper and W. T. Sherwood—669(A)
New determination of the Young-Helmholtz primaries, George Szekeres—350
Photographic granularity and graininess. IV. Visual acutiy thresholds; dynamic *versus* static assumptions, Loyd A. Jones and George Higgins—398
Principles of optical communication systems—general properties of non-image forming projectors and receivers, Hartland S. Snyder and John R. Platt—269
Quanta explanation of vision and the brightness impression for various times of observation and visual angles, M. A. Bouman and H. A. van der Velden—231
Recommended footcandle levels for prolonged critical seeing, Matthew Luckiesh—712
Reduction of apparent contrast by the atmosphere, Seibert Q. Duntley—179
Relations between visual sensitivity and viewing distance, H. Richard Blackwell—1097(A)
Size, shape, and contrast in detection of targets by daylight vision. II. Frequency of seeing and the quantum theory of cone vision, Edward S. Lamar, Selig Hecht, Charles D. Hendley, and Simon Shaler—741
Standard luminosity filter, Kasson S. Gibson—1096(A)
Standard response functions for protanopic and deuteranopic vision, Yves Le Grand—815(L)
Study of methods of visual threshold determination, H. Richard Blackwell—1097(A)
Test of ocular tremor and the scanning theory of visual acuity, Brian O'Brien and E. Dickerman O'Brien—1096(A)
Two-quanta hypothesis as a general explanation for the behavior of threshold values and visual acuity for the several receptors of the human eye, M. A. Bouman and H. A. van der Velden—570
Variation in sensitivity among cones in the human fovea, and the Hecht theory of visual acuity, Brian O'Brien and E. Dickerman O'Brien—1096(A)
Visibility on cathode-ray tube screens: the effects of light adaptation, R. M. Hanes and S. B. Williams—363
Visibility on cathode-ray tube screens: signals on a P7 screen seen at different intervals after excitation, A. L. Sweet and N. R. Bartlett—329
Visibility of distant objects, Seibert Q. Duntley—237
Visibility of stars in the daylight sky, R. Tousey and E. O. Hulburt—886
Visual acuity as measured with various orientations of a parallel-line test object, G. C. Higgins and K. Stultz—756
Visual performance and the surround, Parry Moon and Domina Eberle Spencer—650(L)
Visual sensitivities to combined chromaticity and luminance difference, W. R. J. Brown and D. L. MacAdam—1093(A)